MICHIGAN STATE UNIVERSITY LIBRARIES
3 1293 01046 3457

THESIS

This is to certify that the

dissertation entitled

Identification of an Isotopic and Hydrochemical Anomaly in the Discharge Area of the Fox Hills Aquifer, South-Central North Dakota: Evidence for Pleistocene Subglacial Recharge?

presented by

Catherine Anne Carlson

has been accepted towards fulfillment
of the requirements for

Ph.D. degree in Geological Sciences

Major professor

Date Nov 1, 1994

MSU is an Affirmative Action/Equal Opportunity Institution

O-12771

LIBRARY
Michigan State
University

PLACE IN RETURN BOX to remove this checkout from your record.
TO AVOID FINES return on or before date due.

DATE DUE	DATE DUE	DATE DUE
~~IL[illegible]7324906~~		
JUL 1 1998		

MSU Is An Affirmative Action/Equal Opportunity Institution
c:\circ\datedue.pm3-p.1

IDENTIFICATION OF AN ISOTOPIC AND HYDROCHEMICAL ANOMALY IN THE DISCHARGE AREA OF THE FOX HILLS AQUIFER, SOUTH-CENTRAL NORTH DAKOTA: EVIDENCE FOR PLEISTOCENE SUBGLACIAL RECHARGE?

By

Catherine Anne Carlson

A DISSERTATION

Submitted to
Michigan State University
in partial fullfillment of the requirements
for the degree of

DOCTOR OF PHILOSOPHY

Department of Geological Sciences

1994

ABSTRACT

IDENTIFICATION OF AN ISOTOPIC AND HYDROCHEMICAL ANOMALY IN THE DISCHARGE AREA OF THE FOX HILLS AQUIFER, SOUTH-CENTRAL NORTH DAKOTA: EVIDENCE FOR PLEISTOCENE SUBGLACIAL RECHARGE?

By

Catherine Anne Carlson

Various researchers have suggested that groundwater flow patterns of certain aquifers may have been altered during the Pleistocene because glacial ice blocked the aquifers' regional discharge areas and subglacial water was available for recharge. In particular, it has been suggested that the Northern Great Plains Aquifer System (NGPAS) may have experienced changes in its flow system, including temporary recharge of meltwater in the discharge area, when Pleistocene glaciers overrode the regional discharge area. The Fox Hills aquifer is the stratigraphically highest regional aquifer in the NGPAS and, therefore, is the aquifer most likely to be influenced by glaciation. Hydrogeologic, hydrogeochemical, isotopic, and modeling approaches were combined to investigate the effect of glaciation on the Fox Hills aquifer.

Sodium-bicarbonate-sulfate type water in the discharge area of the Fox Hills aquifer of south-central North Dakota is a water chemistry anomaly, since upgradient water is of the sodium-bicarbonate-chloride type. The chloride distribution in the aquifer suggests that a freshwater source contributed about 90% of the present water in the discharge area. It is unlikely that local recharge

under present climatic conditions could explain this increase in water volume. Water chemistry data indicate that leakage from the underlying high-chloride Dakota aquifer is not the source of the freshwater recharge. Stable isotope data suggest that water in the discharge area was precipitated in a cooler (than modern) climate, such as was prevalent during the Pleistocene. D-excess values suggest that at least two paleowaters are present in the discharge area--a low-chloride, high d-excess water and a high-chloride, low d-excess water. The low-chloride, high d-excess water is coincident with the water chemistry anomaly. Two ice sheet margins, each representing a number of pulses, have been documented in the study area. It is speculated that the discharge area was temporarily recharged with local precipitation during the Pleistocene due to the hydraulic gradient imposed by an overriding ice sheet. Stable isotope data suggest that proglacial lakes were not significant sources of water to the discharge area.

Copyright by
CATHERINE ANNE CARLSON
1994

In Memory of Emma K. Lange

ACKNOWLEDGMENTS

This dissertation would not have been possible without the support and guidance of Grahame J. Larson--committee chair, advisor, mentor, and friend. I deeply appreciate his advice, encouragement, professional assistance, and his generosity with his time and knowledge. I gratefully acknowledge my committee members who each made unique and necessary contributions to this work: Grahame J. Larson, Roger B. Wallace, Nancy O. Jannik (Winona State University), Nathaniel E. Ostrom, James A. Clark (Calvin College), and Duncan Sibley (defense substitute).

Financial support for this research was generously provided by NASA Space Grant Fellowship, North Dakota Space Grant College, University of North Dakota; Lucille Drake Pringle Endowed Fellowship, Department of Geological Sciences, Michigan State University; Association of Ground Water Scientists and Engineers Graduate Student Research Fellowship; Grant-in-Aid of Research, Sigma Xi, The Scientific Research Society; and College of Natural Science Graduate Continuing Fellowship, Michigan State University.

I extend heartfelt thanks to Claire Carlson and Diane Smith, whose love sustained me during this adventure.

TABLE OF CONTENTS

LIST OF TABLES xi

LIST OF FIGURES xii

INTRODUCTION 1

Statement of the Problem 1

The Test Aquifer 2

Investigative Techniques 3

Geology 3

Hydrogeology 3

Hydrogeochemistry 5

Stable Isotopes 5

Paleohydrologic Responses 5

Potential Significance 6

CHAPTER 1: GEOLOGY 7

Literature Review 7

The Williston Basin: Formation and Structure 7

Subsurface Stratigraphy 9

Hydrostratigraphic Units 12

Glacial History 14

Data Analysis and Interpretation 20
Fox Hills Formation Subcrop Map 20
Fox Hills Formation Sandstone (Aquifer) Isopach Map 20
Extent of Glacial Deposits 23
Summary 23
CHAPTER 2: HYDROGEOLOGY 28
Literature Review 28
Dakota Aquifer 28
Fox Hills Aquifer 29
Hell Creek Aquifers 33
Glacial Deposit Aquifers 34
Data Analysis and Interpretation 35
Conceptual Physical System 35
Mathematical Statement 35
Parameter Values 37
2-D Finite Difference Model 40
Simulation Results 40
Interpretation 42
Summary 44
CHAPTER 3: HYDROGEOCHEMISTRY 46
Literature Review 46
Fox Hills Aquifer 46

Dakota Aquifer 47
Data Analysis and Interpretation 48
Graphical Analysis 48
Hydrochemical Facies 50
Chloride Distribution 52
Average Linear Velocity from ^{36}Cl 55
Summary 56
CHAPTER 4: STABLE ISOTOPE HYDROLOGY 59
Literature Review 59
Atmospheric Waters 59
Lake Waters 60
Ice and Snow 61
Ground Water 61
Paleowaters 62
Data Collection 63
Data Analysis and Interpretation 65
Summary 75
CHAPTER 5. POSSIBLE PALEOHYDROLOGIC RESPONSES TO PLEISTOCENE GLACIATION 77
Literature Review 77
Glacial Meltwater Recharge Hypothesis 77
Hydrology of Glaciers 79
Data Analysis and Interpretation 83

Simulation 1: present conditions 84
Simulation 2: Lake McKenzie 84
Simulation 3: blocked discharge area 87
Simulation 4: subglacial recharge 91
Interpretation 101
Summary 101
SUMMARY AND CONCLUSIONS 104
Upgradient Aquifer Water 104
Local Precipitation/Recharge 104
Local Precipitation during the Pleisotocene 105
Leakage from Proglacial Lakes 106
Leakage from Adjacent Aquifers 107
Basal Meltwater 107
Conclusion and Recommendation 108
Appendix A. Geologic data 110
Appendix B. Hydrogeologic data 117
Appendix C. Hydrogeochemical data 122
Appendix D. Isotope data 130
Appendix E. Paleohydrologic modeling data 131
LIST OF REFERENCES 147

LIST OF TABLES

Table 1. Stable isotope data from the discharge area of the Fox Hills aquifer ... 72

Table 2. Estimation of subglacial recharge rates ... 99

Table 3. Geologic data derived from drill logs ... 110

Table 4. Water-level data for the Fox Hills aquifer ... 117

Table 5. Input data for simulation of water levels in the Fox Hills aquifer ... 118

Table 6. Hydrochemistry data for the Fox Hills aquifer ... 122

Table 7. Isotopic analyses of collected water samples ... 130

Table 8. Input data for simulation of water levels in the Fox Hills aquifer ... 131

Table 9. Lake McKenzie simulation input data ... 135

Table 10. Input data for simulation of Verone ice sheet blocking the discharge area ... 139

Table 11. Input data for simulation of Verone ice sheet recharging the discharge area ... 143

LIST OF FIGURES

Figure 1. Location of study area in North Dakota 4

Figure 2. Location and extent of the Williston basin (adapted from Gerhard et al., 1982; Gerhard and Anderson, 1988) 8

Figure 3. Stratigraphic column for the Williston basin (adapted from Carlson, 1982) 11

Figure 4. Generalized bedrock geologic map of North Dakota (Bluemle, 1988) 15

Figure 5. Regional glacial history (Bluemle, 1984): a) pre-glacial drainage, b) limits of Dunn and Verone glaciations 16

Figure 5 (con't). c) limit of Napoleon glaciation, d) limit of Phase D glaciation... 17

Figure 6. Subcrop map of the Fox Hills Formation 21

Figure 7. Major glacial aquifers of the study area (adapted from Randich, 1979; Ackerman, 1980) 22

Figure 8. Fox Hills Formation sandstone thickness map 24

Figure 9. Extent of glacial deposits in the study area 25

Figure 10. Fox Hills aquifer water levels in southwestern North Dakota (adapted from Lobmeyer, 1985) 31

Figure 11. Conceptual model of the Fox Hills aquifer 36

Figure 12. Water-level map of the Fox Hills aquifer 38

Figure 13. Transmissivity map of the Fox Hills aquifer 39

Figure 14. Finite-difference grid used for simulation of the Fox Hills aquifer 41

Figure 15. Simulated water levels in the Fox Hills aquifer 43

Figure 16. Piper diagram of Fox Hills aquifer water in southwestern North Dakota 49

Figure 17. Hydrochemical facies map of the Fox Hills aquifer in southwestern North Dakota 51

Figure 18. Chloride distribution in the Fox Hills aquifer 54

Figure 19. Location of stable isotope water samples 64

Figure 20. δD-$\delta^{18}O$ relationship of the Fox Hills aquifer water samples 66

Figure 21. Deuterium excess-$\delta^{18}O$ relationship of the Fox Hills aquifer water samples 68

Figure 22. δD-$\delta^{18}O$ relationship by d-excess groupings 69

Figure 23. Deuterium-excess values plotted with the chloride distribution 70

Figure 24. Mixing line of modern and paleowater 74

Figure 25. Inferred groundwater flow directions during Pleistocene glaciation (Downey, 1986) 80

Figure 26. Schematic diagram of glacier hydrology (Lawson, 1993) 82

Figure 27. Finite-difference grid for Fox Hills aquifer simulation 85

Figure 28. Simulated water levels in the Fox Hills aquifer 86

Figure 29. Finite-difference grid for simulating the influence of proglacial Lake McKenzie 88

Figure 30. Simulated water levels, taking into account Lake McKenzie 89

Figure 31. Finite-difference grid for simulation of the Verone ice sheet partially blocking the discharge area 90

Figure 32. Simulated water levels, taking into account the partially blocked discharge area 92

Figure 33. Schematic diagram of a glacier advancing over an escarpment (after Bluemle, 1977) 93

Figure 34. Linked cavity drainage system (Kamb, 1977): a) map view, b) cross-section 94

Figure 35. Modified transmissivity distribution 95

Figure 36. Finite-difference grid for simulation of the Verone ice sheet contributing recharge 97

Figure 37. Simulated water levels, taking into account recharge from the Verone ice sheet 100

INTRODUCTION

Statement of the Problem

Various researchers have suggested that groundwater flow patterns of certain aquifers may have been altered during the Pleistocene because glacial ice blocked the aquifers' regional discharge areas, subglacial meltwater was available for recharge, and adjacent geologic materials were compressed under the weight of overriding ice sheets. Ice sheets tend to move toward topographically low areas, which often are regional discharge areas. Groundwater discharge becomes blocked by the overriding ice sheet, resulting in altered and possibly reversed groundwater flow patterns; hence, temporary recharge of an aquifer may occur in the discharge area if a hydrologic connection between subglacial water and ground water is established.

The purpose of this study is to investigate the response of a regional aquifer system to Pleistocene glaciation and, in particular, the possibility of temporary recharge in the discharge area. This investigation involves identifying potential water sources for the discharge area of a regional aquifer as a set of multiple-working hypotheses. The potential sources/multiple-working hypotheses are:

a) upgradient aquifer water

b) local precipitation/recharge

c) local precipitation during the Pleistocene

d) leakage from proglacial lakes

e) leakage from adjacent aquifers/aquitards

f) subglacial meltwater

or a combination of (a) through (f). Each working hypothesis will be tested in this study as a means of identifying the source(s) of the water in the discharge area.

The Test Aquifer

Prior to choosing a regional aquifer with which to investigate the paleohydrological response of continental glaciation, criteria for choosing an aquifer are outlined in terms of the characteristics of an "ideal" test aquifer. First, an ideal test aquifer should have support in the literature for the possibility of glacial influences during the Pleistocene. Second, it should be of regional extent, with a discharge area that has been overridden, ideally, by a single glacial advance while the main portion of the aquifer remained ice free. Third, it should crop out in the discharge area, thereby allowing a direct hydrologic connection between the subglacial water and the aquifer. Fourth, the water chemistry should exhibit the presence of a separate freshwater body in the discharge area, representing the recharged glacial meltwater.

Because the Fox Hills aquifer of south-central North Dakota meets the above criteria, it is uniquely suited for this investigation. The Fox Hills aquifer is part of the Northern Great Plains Aquifer System (NGPAS) and Downey (1986) suggests that groundwater flow patterns may have been altered in the system due to Pleistocene glaciation. He also suggests that the regional discharge area of the system may have been temporarily recharged with meltwater--the first criterion. Since the Fox Hills aquifer is the stratigraphically highest regional aquifer in the system, it is also the aquifer most likely to be influenced by

glaciation in this region. Although, two glacial advances (rather than one) have been documented in the Fox Hills aquifer discharge area in south-central North Dakota, the second criterion is met, though not completely. These ice sheets covered only the discharge area, allowing normal flow patterns to continue in the main portion of the aquifer. The Fox Hills aquifer also meets the third criterion, because the aquifer crops out in its discharge area in south-central North Dakota. Furthermore, the water chemistry in the discharge area is not representative of the upgradient water chemistry--the fourth criterion.

The study area is located in south-central North Dakota, west of the Missouri River, and includes Sioux, Grant, and Morton counties (Figure 1). Information for Emmons County (east of the Missouri River and adjacent to Sioux County) and Corson County, South Dakota (south of Sioux County) are included where it aids understanding of the hydrogeologic system.

Investigative Techniques

Hydrogeologic, hydrogeochemical, isotopic and modeling approaches are combined to investigate the effect of glaciation on the Fox Hills aquifer.

Geology. The geologic investigation presented in Chapter 1 sets the stage for subsequent investigative techniques and includes (1) mapping the Fox Hills Formation subcrop, (2) mapping the sandstone thickness of the Fox Hills Formation, and (3) estimating the extent of glacial deposits using drill logs.

Hydrogeology. The hydrogeologic investigation presented in Chapter 2 includes (1) mapping the water-levels in the Fox Hills aquifer, (2) mapping the distribution of aquifer transmissivity, and (3) simulating present flow conditions in Sioux, Grant, and Morton counties using a 2-dimensional finite difference

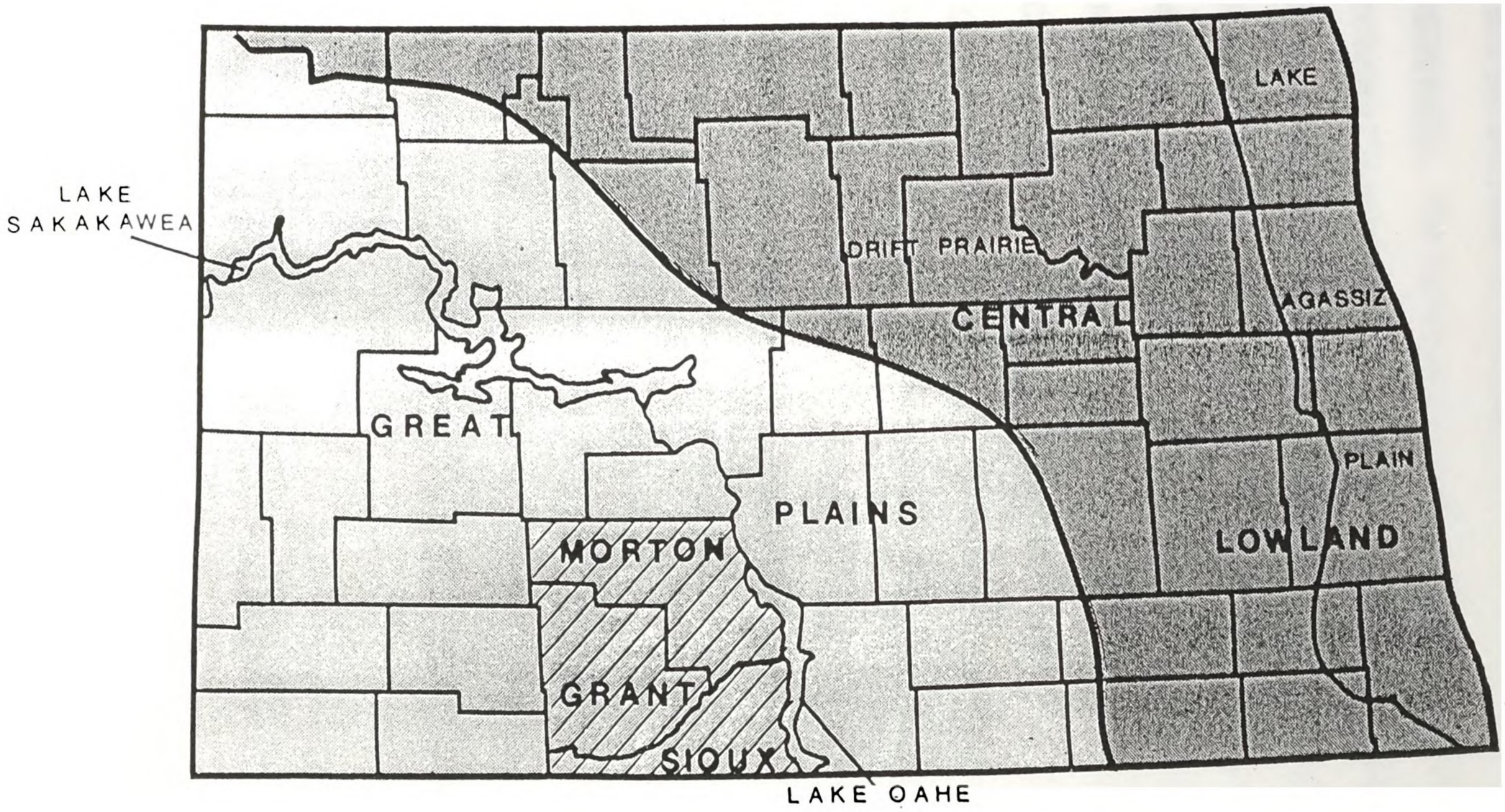

Figure 1. Location of study area in North Dakota.

groundwater flow model to assess possible recharge to the discharge area. Hypotheses (b) and (e) are tested in Chapter 2.

Hydrogeochemistry. The hydrogeochemical investigation is presented in Chapter 3 and includes (1) graphically analyzing water chemistry data using the Piper trilinear diagram method, (2) mapping the hydrochemical facies distribution in southwestern North Dakota and discussing the chemical evolution of the water types, (3) mapping the chloride distribution in southwestern North Dakota and discussing possible origins for different zones, and (4) calculating average linear velocity from ^{36}Cl data. Hypotheses (a), (b) and (e) are tested in Chapter 3.

Stable Isotopes. The stable isotope investigation presented in Chapter 4 includes (1) plotting the groundwater data on a δD-$\delta^{18}O$ graph and comparing their distribution with the North American and local (Oakes, North Dakota) meteoric water lines to assess the influence of fractionating processes (e.g., evaporation), (2) calculating the deuterium excess of the samples to indicate the presence of paleowaters in the discharge area, (3) plotting the deuterium-excess values on the chloride distribution map to indicate the geographical distribution of different recharge waters, and (4) calculating the mean annual air temperature of the samples to indicate past climatic conditions. Hypotheses (b) through (d), and (f) are tested in Chapter 4.

Paleohydrologic Responses. Investigation of the paleohydrologic responses of the Fox Hills aquifer to Pleistocene glaciation is presented in Chapter 5 and includes (1) simulating the influence of proglacial lakes on the flow regime in Sioux, Morton, and Grant counties using a 2-dimensional finite difference groundwater flow model, (2) simulating the hydrologic response of the Fox Hills aquifer to a discharge area partially blocked by glacial ice, (3) estimating the amount of leakage that could have occurred beneath the Laurentide ice sheet in Sioux and Morton counties, and (4) simulating the

hydrologic response of the Fox Hills aquifer to recharge under the glacial ice. Hypotheses (c), (d), and (f) are addressed in Chapter 5.

Potential Significance

The results of this study have the potential to increase our understanding of the influence of continental glaciation on groundwater flow patterns and to explain water chemistry anomalies in some aquifers. Continental ice sheets extended over much of the northern hemisphere during the Pleistocene and may have significantly altered groundwater flow paths and recharge locations of regional bedrock aquifers at several locations. Thus, present conceptual models of groundwater flow systems that do not take into account the potential influence of ice sheets may result in misinterpretation of a system's dynamics and poor prediction of its future behavior.

CHAPTER 1: GEOLOGY

Literature Review

Since the Fox Hills aquifer is situated in the Williston basin, the basin's formation and structure are discussed. In addition, the basin's subsurface stratigraphy is outlined to provide a framework for understanding the hydrostratigraphy of the upper units. Near-surface hydrostratigraphic units and the area's glacial history are then presented as a basis for all further discussions.

The Williston Basin: Formation and Structure. The Williston basin is a Phanerozoic sedimentary basin that extends across North Dakota, South Dakota, eastern Montana, southern Saskatchewan, and southwestern Manitoba (Figure 2). The center of the 130,000 km^2 basin is located in northwestern North Dakota, where sediment thickness is approximately 5 km (Anna, 1986). Initial subsidence of the basin occurred by Early Ordovician and was apparently unrelated to tectonic activity in North America (LeFever et al., 1987), although this is not generally agreed on (Gerhard et al., 1982). The basin may have originated as a craton-margin or a continental-shelf basin changing to an intracratonic basin in response to the Cordilleran orogen and crustal accretion to the west (Gerhard and Anderson, 1988). The eastern boundary of the basin, or hingeline, coincides with the boundary between the Churchill (Trans-Hudson) and Superior provinces (Gerhard and Anderson, 1988). Figure 2 shows the Sioux Arch, Black Hills Uplift, Cedar Creek Anticline, and Bowdoin Dome, bounding structures of the Williston basin (Gerhard and Anderson, 1988).

Thomas (1974, 1979) studied the regularity of surface lineaments in the Williston basin. He mapped lineaments using both surface and subsurface data

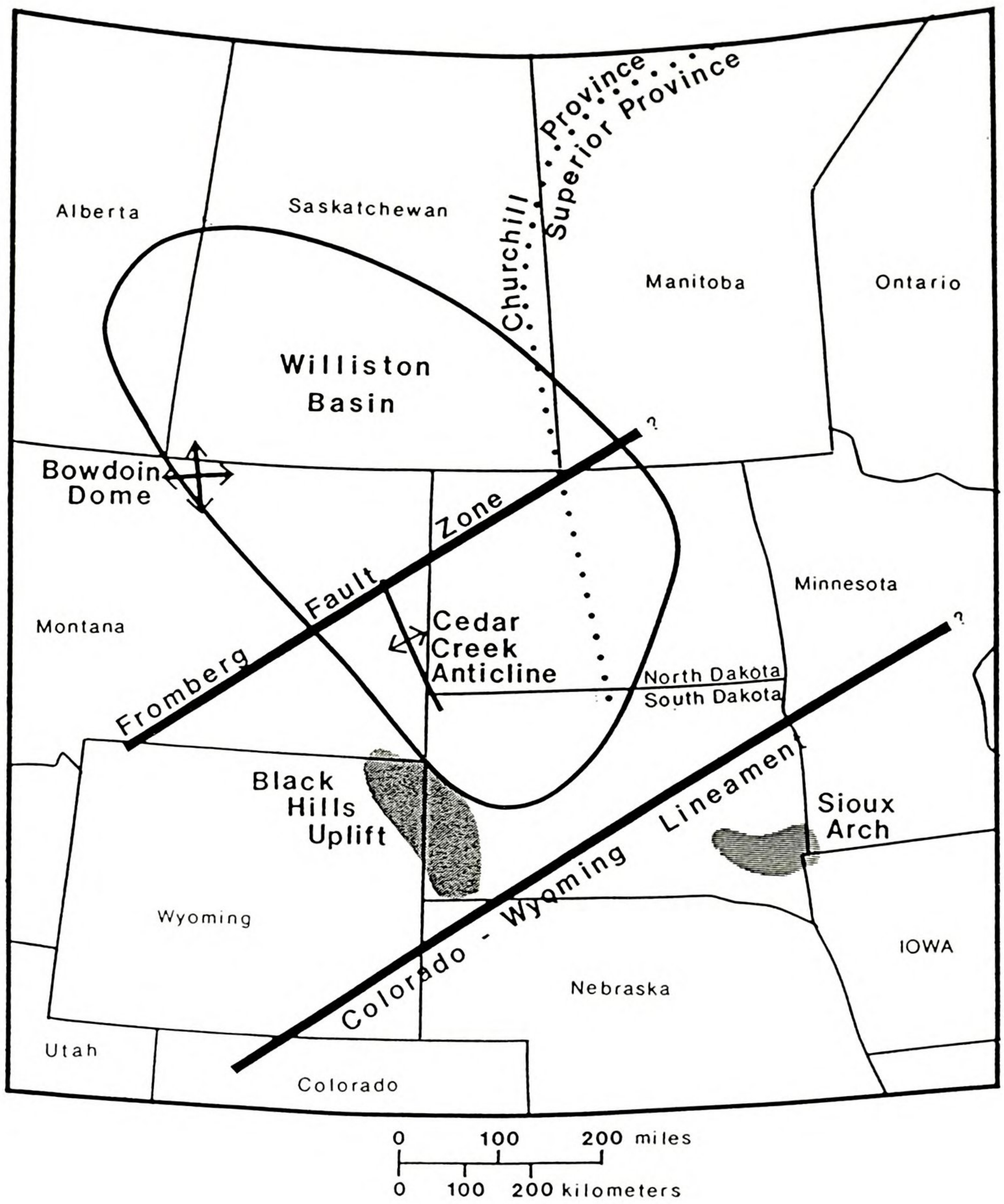

Figure 2. Location and extent of the Williston basin
(adapted from Gerhard et al., 1982; Gerhard and Anderson, 1988).

and identified two main directions of lineament trends--NE and NW. Thomas interpreted the lineaments as representing zones of weakness bounding Precambrian basement blocks. Recent work has indicated that two perpendicular sets of lineaments are imprinted on the Rocky Mountains and adjacent parts of the Great Plains. The main system trends N30-40W/N50-60E and a secondary system trends N5-15E/N75-85W (Maughan and Perry, 1986). Gerhard et al. (1982) suggest that the basement blocks in the central Rockies, the Black Hills, and the Williston basin were formed by left-lateral shearing along the Fromberg and Colorado-Wyoming lineaments (shear zones; Figure 2). These authors also suggest that subsequent stresses from orogenic activity of the North American plate produced periodic vertical motion along basement zones of weakness.

This recurrent movement of the basement blocks throughout the Phanerozoic Eon influenced sedimentation in the basin (Shurr, 1979; Anna, 1986) by controlling the physical characteristics of sediment and facies distribution. Recurrent movement of basement blocks also deformed overlying sediments by faulting and folding. Movement occurred primarily along the NE/NW system of lineaments, but the N/E system also produced important Laramide structures (Maughan and Perry, 1986).

Subsurface Stratigraphy. Crystalline rocks of Precambrian age form the basement in the Williston basin. The basin lies between the Superior and Wyoming provinces of Archean age. The Superior province belonged to a subducting plate during early Proterozoic convergence, and the Wyoming province belonged to the overriding plate (Hoffman, 1989). The Trans-Hudson orogen between the two provinces consists of juvenile Proterozoic crust including island arcs and obducted oceanic crust (Hoffman, 1989).

The sedimentary rocks of the Williston basin depict a history of repeated marine transgressions and regressions. The North American sedimentary-rock record has been divided into six cratonic sequences, with each sequence representing a major transgressive-regressive cycle bounded by craton-wide unconformities (Sloss, 1963). All six sequences (Sauk, Tippecanoe, Kaskaskia, Absaroka, Zuni, and Tejas) are present in the Williston basin (Figure 3).

The Sauk Sequence is represented by the Deadwood Formation of Upper Cambrian to Lower Ordovician age formed during a marine transgression from the west. The onlap depositional sequence consists of a basal sandstone overlain by shale and carbonate and an upper sandstone (Carlson, 1982; 1983; Bluemle, 1984).

A second marine transgression is recorded by the Tippecanoe Sequence of Middle Ordovician to Silurian age. The Williston basin began to be a slightly negative (topographically) area over which an extensive epicontinental sea invaded from the south and east. Initially clastics (Winnipeg Group) were deposited, followed by carbonates and minor amounts of evaporites and shales (Carlson, 1982; 1983; Bluemle, 1984).

The Kaskaskia Sequence consists of shallow-water carbonates and thin shales deposited by a transgressive sea from the north and west during Devonian time, and fine-grained clastics (Baaken Formation), carbonates and evaporites (Madison Group), and clastics and carbonates (Big Snowy Group) deposited in a second transgressive sea during Mississippian time (Carlson, 1982; 1983; Bluemle, 1984).

Deposits from an early Pennsylvanian transgression marks the beginning of the Absaroka Sequence. Clastics, carbonates, and evaporites were deposited through Triassic time (Carlson, 1982; 1983; Bluemle, 1984).

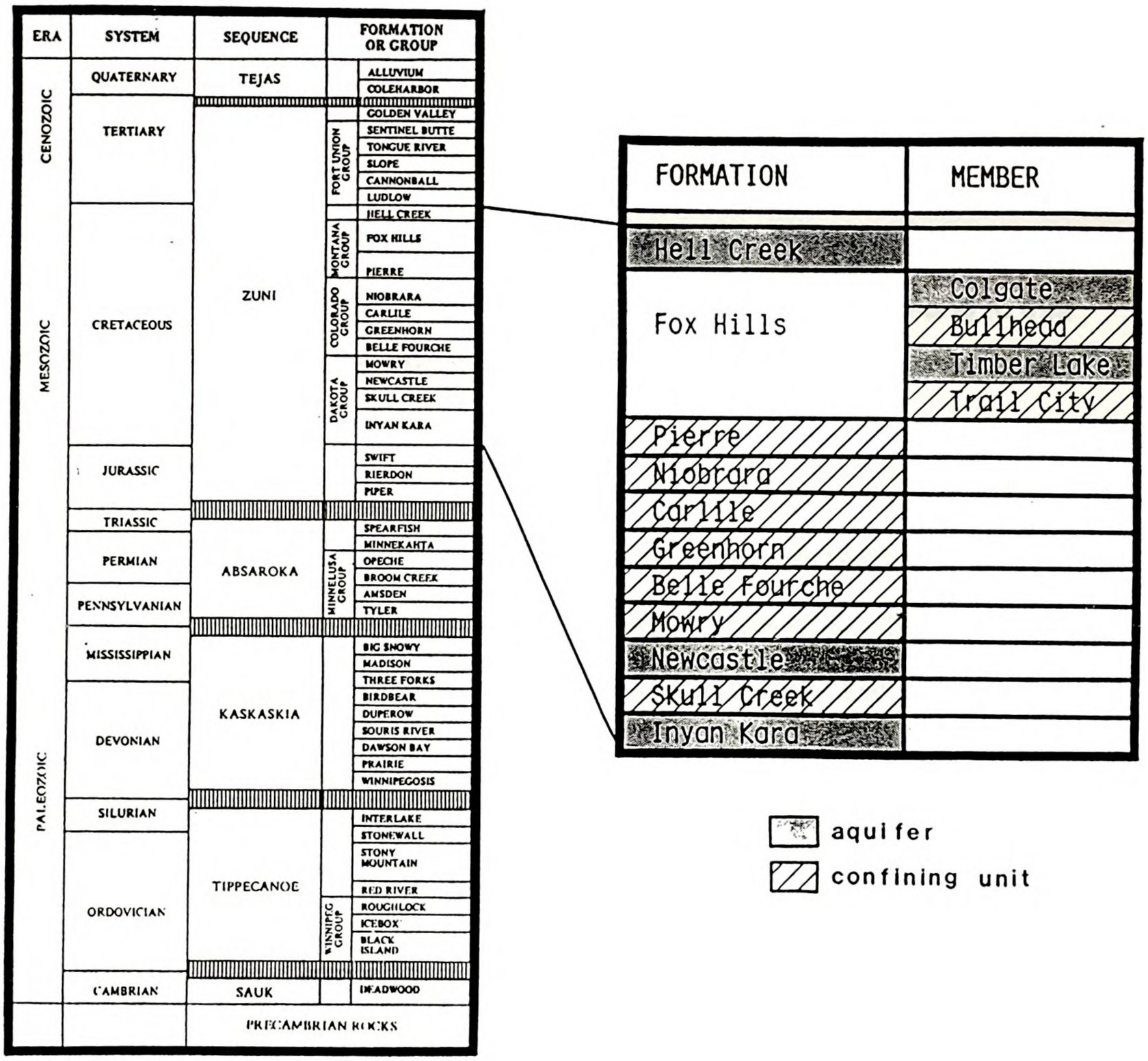

Figure 3. Stratigraphic column for the Williston basin (adapted from Carlson, 1982).

The Zuni Sequence consists primarily of clastics. A marine transgression from the west deposited redbeds, evaporites, and carbonates during Middle Jurassic time. Following a Late Jurassic-Early Cretaceous regression, Early Cretaceous seas invaded, resulting in the non-marine to marine Inyan Kara Formation. Thick deposits of marine shale formed before the sea regressed, leaving behind the fine sands of the marine Fox Hills Formation and non-marine Hell Creek Formation, and the lignite-bearing Fort Union Group (Carlson, 1982; 1983; Bluemle, 1984).

The Tejas Sequence consists largely of fluvial, lacustrine, and glacial deposits. No marine deposits are found in North Dakota that belong to this sequence (Carlson, 1982; 1983; Bluemle, 1984).

Hydrostratigraphic Units. The Lower Cretaceous Inyan Kara Group (Figure 3) comprises a regional aquifer (Dakota aquifer) that is found at depths from 670 m (2,200 ft) in southeastern Emmons County to 1490 m (4,900 ft) in northwestern Morton County. The Inyan Kara consists of sandstone (15 to 53 m thick; 50 to 175 ft thick) and shale, and is of variable thickness. The lower unit, the Lakota Formation, is comprised of non-marine sandstones and mudstones, which are overlain by marine shale (Fuson Formation) and marine sandstone and shale (Fall River Formation). The contact between the Inyan Kara and Skull Creek Formations is gradational. The Skull Creek Formation is a marine shale, 23 to 84 m (75 to 275 ft) thick (Armstrong, 1978; Carlson, 1982, 1983; Bluemle, 1984; Downey, 1986).

The Newcastle Formation consists of a muddy sandstone with localized zones of clean sandstone up to 18 m (60 ft) thick. This formation is absent in parts of Sioux, Morton, and Grant counties. In Emmons County the Newcastle Formation contains very fine grained sandstone (Carlson, 1982, 1983; Bluemle, 1984).

The remaining Cretaceous sediments below the Fox Hills Formation (Figure 3) consist of marine shales, some of which are calcareous and/or contain bentonitic beds. These marine formations include the Mowry, Belle Fourche, Greenhorn, Carlile, Niobrara, and Pierre formations, collectively ranging from 488 to 838 m (1,600 to 2,750 ft) in thickness (Carlson, 1982, 1983; Bluemle, 1984).

The Pierre Formation crops out in southeastern Sioux County and southwestern Emmons County, as well as, subcrops along preglacial and interglacial valleys. It consists of dark-gray to black siliceous shale, siltstone, and thin layers of bentonite. The formation is generally considered impermeable; however, locally the Pierre Formation yields water from shallow (about 1 m) fracture zones (Armstrong, 1978; Carlson, 1982, 1983; Bluemle, 1984).

The Upper Cretaceous Fox Hills Formation is a marine-to brackish-water deposit of sandstone and shale, variously subdivided into three or four members. For the purpose of this study a four-member division will be used following Carlson (1983; Figure 3). The lowest member is the Trail City which consists of silty to sandy shale that conformably overlies the Pierre Formation with a gradational contact. The Trail City Member is only a meter (few ft) thick. The Timber Lake Member is predominantly sandstone that thins westward from about 53 to 15 m (175 to 50 ft). The Bullhead Member consists of interbedded sand and shale generally 30 m (100 ft) thick. The Colgate Member consists of a well indurated white sandstone up to 18 m (60 ft) thick (Carlson, 1982, 1983; Bluemle, 1984).

The Fox Hills Formation crops out along the Cannonball River in southeastern Morton County, throughout much of central Emmons County, and in eastern Sioux County. It also subcrops in most of the remainder of Emmons

County. The formation is absent in parts of central and southeastern Emmons County and southeastern Sioux County, where it has been eroded (Figure 4). The formation dips to the northwest and reaches depths in excess of 457 m (1500 ft) in northwest Morton County. The Fox Hills aquifer is comprised of the Colgate Member in Sioux, Morton, and Grant counties and the Colgate and Timber Lake members in Emmons County (Armstrong, 1978; Randich, 1979; Ackerman, 1980; Carlson, 1982, 1983; Bluemle, 1984).

The Late Cretaceous Hell Creek Formation conformably and gradationally overlies the Fox Hills Formation. It is generally accepted that the Pierre, Fox Hills, and Hell Creek formations were deposited concurrently. The Pierre represents a deeper water marine environment, the Fox Hills a transitional environment, and the Hell Creek a continental environment. The Hell Creek Formation consists of sandstone, siltstone, mudstone, carbonaceous shale, and lignite. Although the Hell Creek Formation is predominantly a non-marine deposit, a thin marine tongue of the formation occurs in Sioux, Morton, and western Emmons counties. The sandstones typically contain bentonitic beds less than 2 m (6 ft) thick that occur in the upper section of the formation. The formation is present in western Emmons County and on some butte tops in central Emmons County. It also crops out in central Sioux County, eastern Grant County, and southeastern Morton County. The formation dips to the northwest and reaches a depth of nearly 366 m (1200 ft) in northwest Morton County. The sandstone units, which serve as local aquifers, are generally not laterally extensive (Ackerman, 1980; Carlson, 1982, 1983; Bluemle, 1984).

Glacial History. Prior to Pleistocene glaciation, south-central North Dakota's land surface was drained to the northeast by the ancestral Cannonball River system (Figure 5a; Bluemle, 1984). When glacial ice advanced from the northeast, this drainage was blocked and diverted southward along the margin of

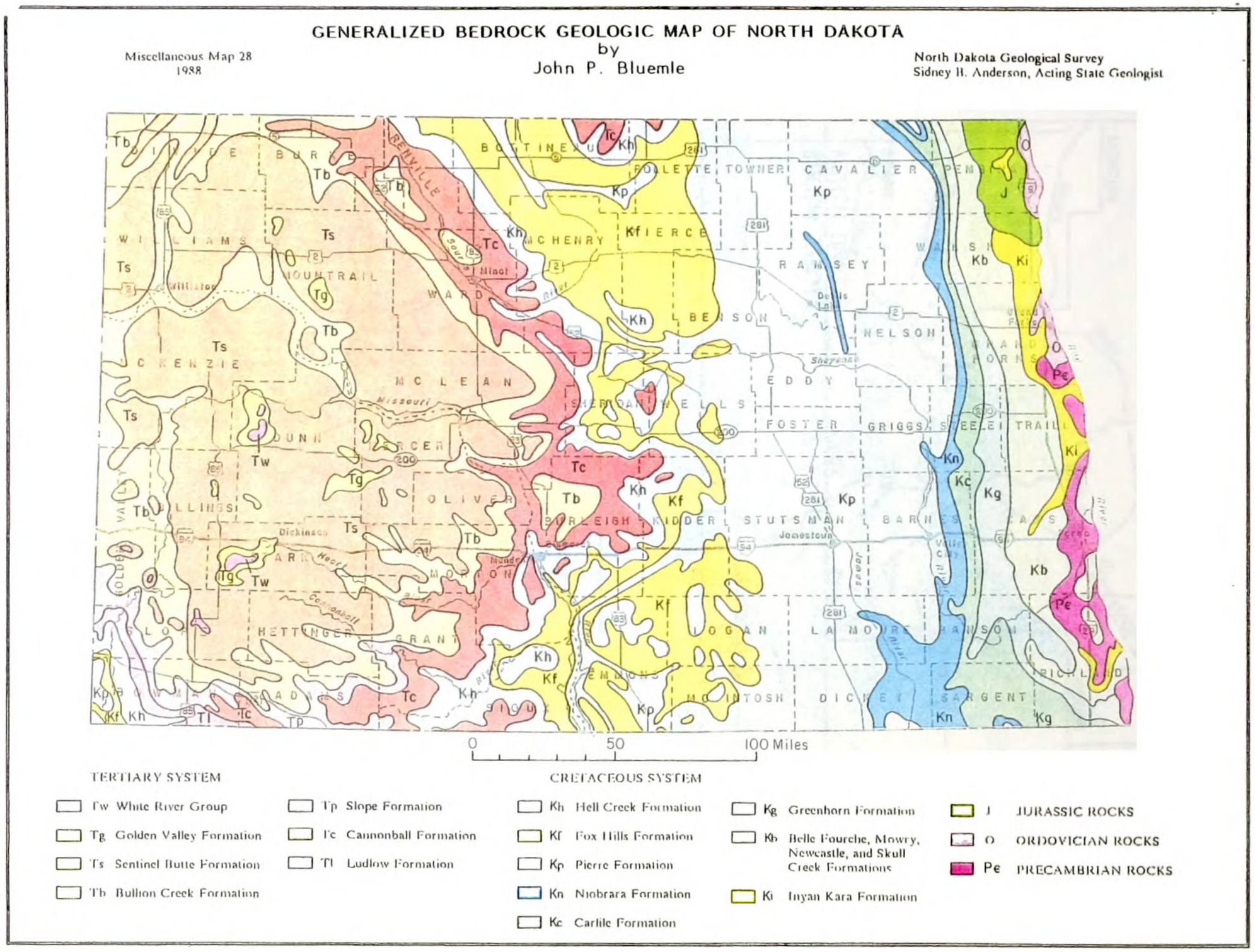

Figure 4. Generalized bedrock geologic map of North Dakota (Bluemle, 1988).

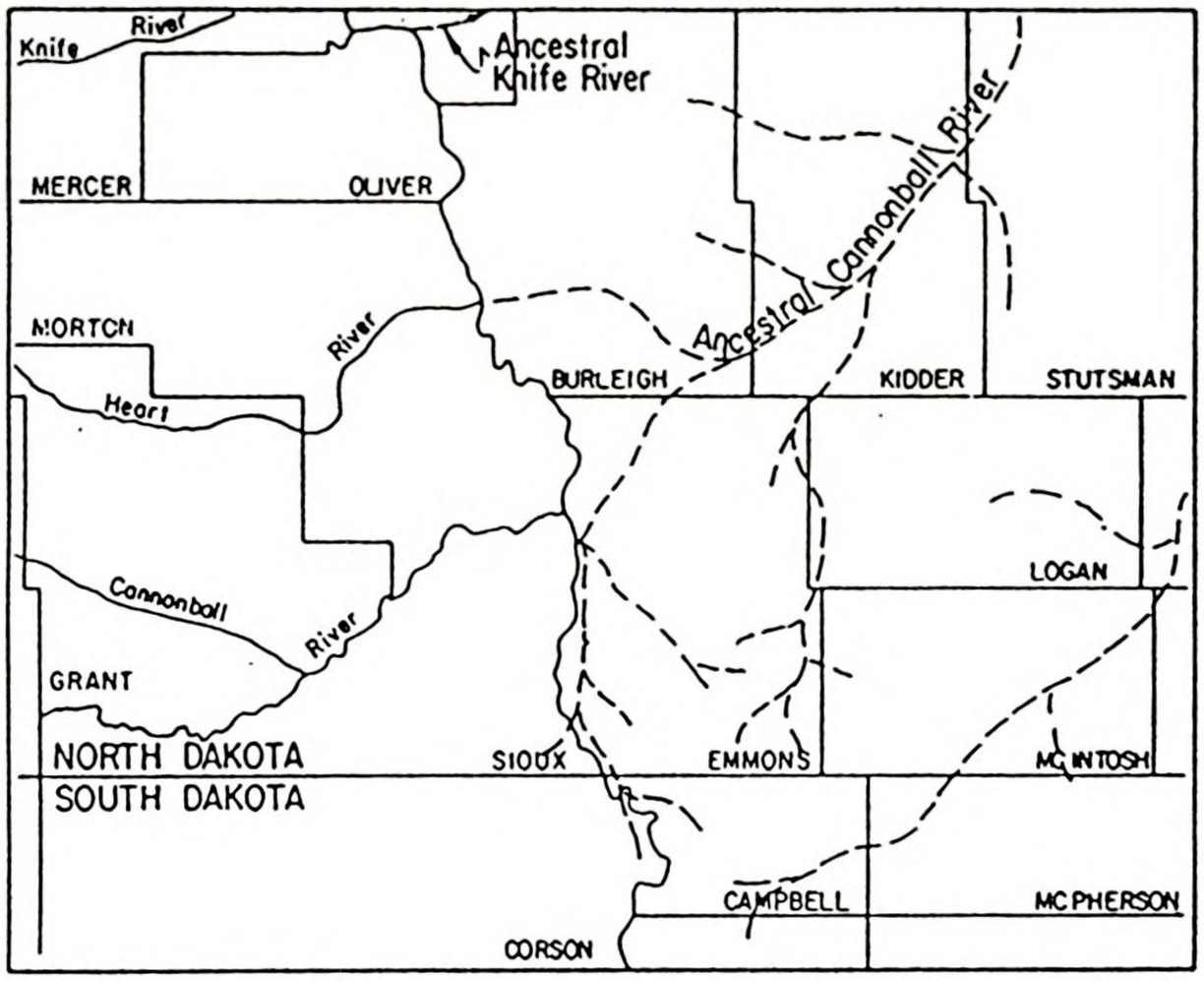

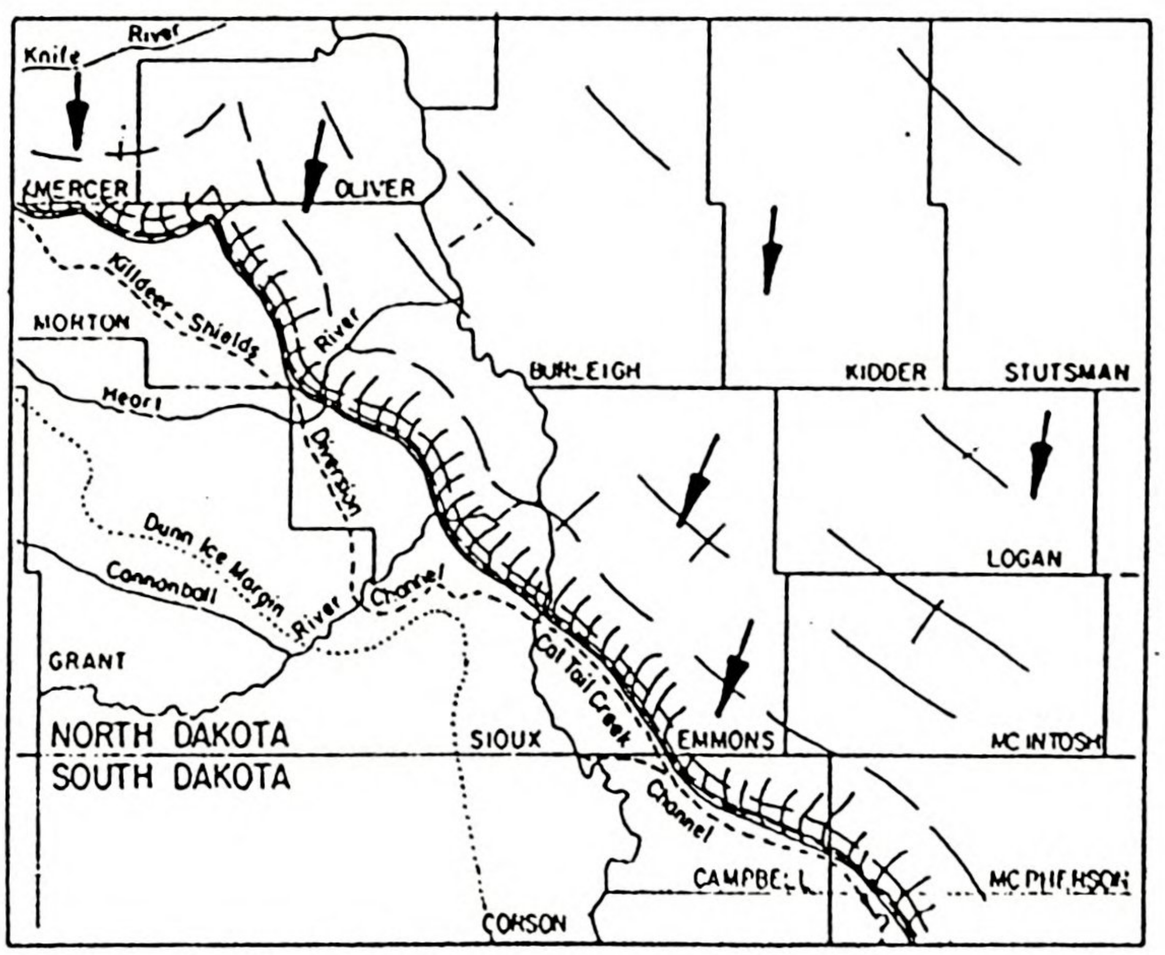

Figure 5. Regional glacial history (Bluemle, 1984):
a) pre-glacial drainage, b) limits of Dunn and Verone glaciations

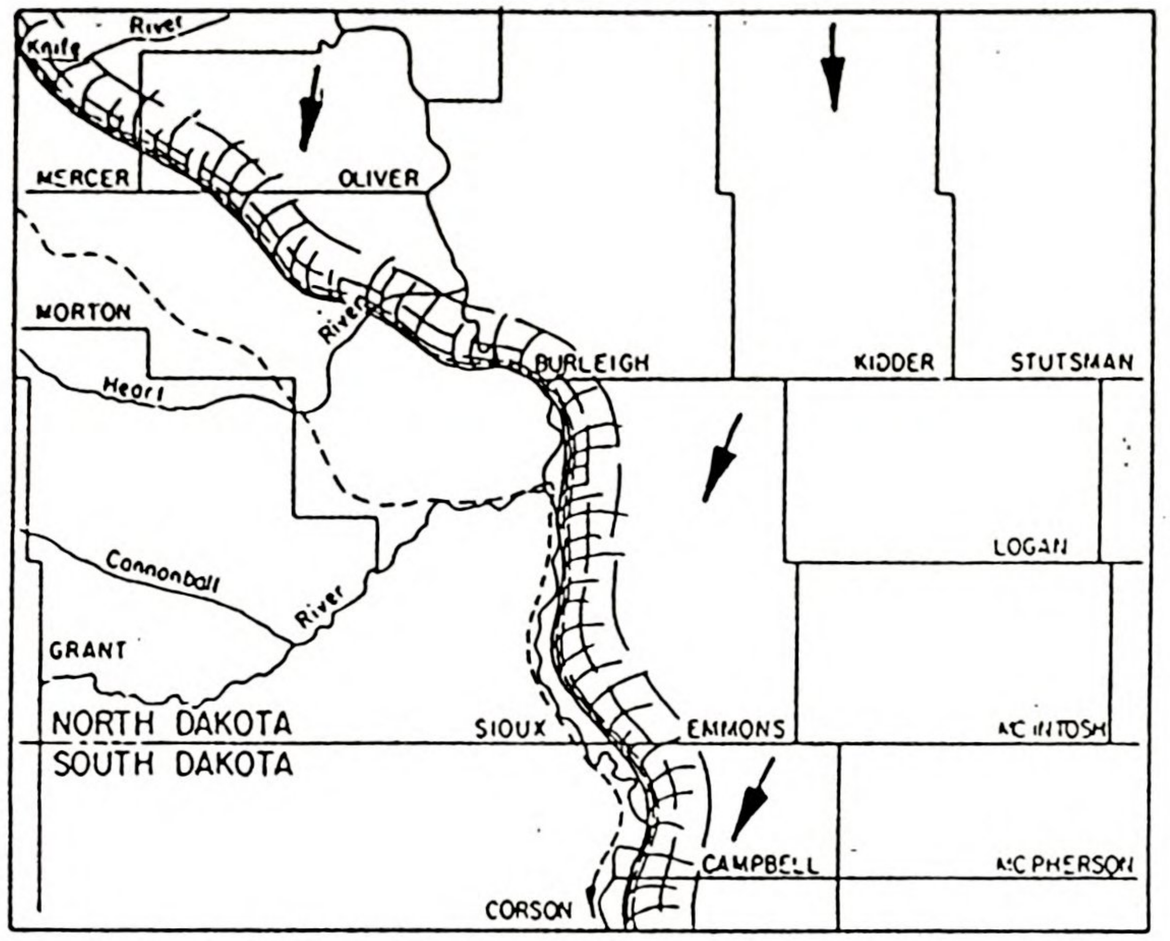

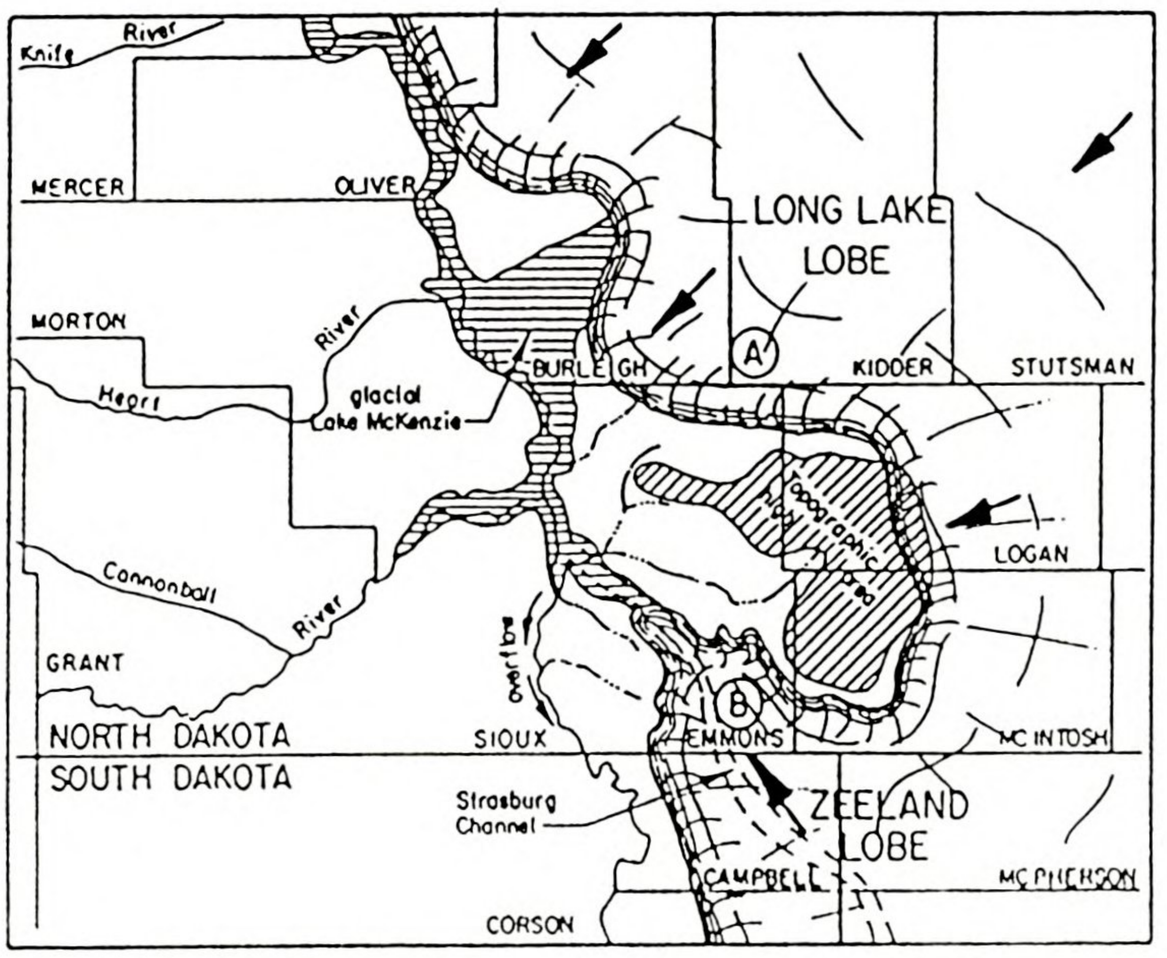

Figure 5 (con't). c) limit of Napoleon glaciation, d) limit of Phase D glaciation.

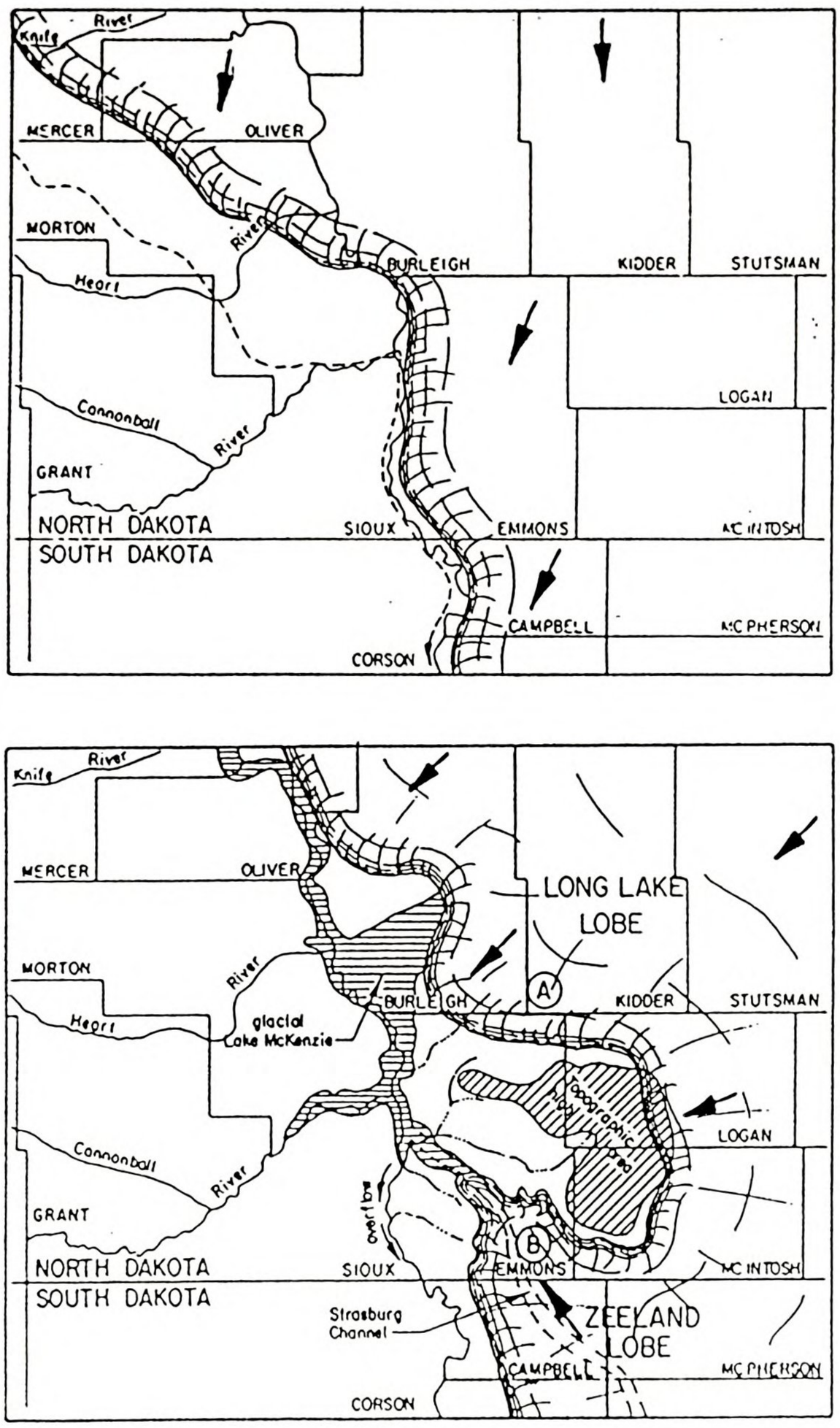

Figure 5 (con't). c) limit of Napoleon glaciation, d) limit of Phase D glaciation.

the glacier. The oldest recognized ice margin in North Dakota has been designated the Dunn Ice Margin (Figure 5b, dotted line) and may represent several glacial advances that are collectively called the Dunn Glaciation or Phase A (Clayton, 1969; Clayton and Moran, 1982; Bluemle, 1984). The Dunn Glaciation is presumed to be pre-Wisconsinan in age and to have had a northeastern source (Clayton and Moran, 1982; Bluemle, 1984).

The second recognizable ice margin in south-central North Dakota is designated the Verone Ice Margin (Figure 5b). It had a northern source and may be either late pre-Wisconsinan or Early Wisconsinan in age (Clayton and Moran, 1982; Bluemle, 1984). The Verone Glaciation may represent a composite of several glacial pulses (Bluemle, 1984). Drainage from Montana, Wyoming, Alberta, and Saskatchewan was diverted southeastward through a major trench, the Killdeer-Shields Diversion Channel. This trench, situated along the Verone Ice Margin, joined the Missouri River 25 km (14 miles) north of the South Dakota border either following the modern Missouri River or continuing southeastward along the Cat Tail Creek Channel (Figure 5b; Clayton and Moran, 1982; Bluemle, 1984). Interbedded lake and fluvial sediments indicate the formation of proglacial lakes during the Verone Glaciation, also known as Phase B (Clayton and Moran, 1982; Bluemle, 1984).

Following the Verone Glaciation, a long period of erosion occurred that removed much of the glacial sediment and resulted in the re-establishment of a northeastward drainage system along the ancestral Cannonball River (Bluemle, 1984). The next documented glacial advance, the Napoleon Glaciation or Phase C, most likely occurred during Early Wisconsinan time (though it could have occurred pre-Wisconsinan or Late Wisconsinan) and had a northern source (Clayton and Moran, 1982; Bluemle, 1984). The Napoleon Ice Margin generally coincides with the Missouri River in south-central North Dakota (Figure

5c), crossing the river in southeastern Morton County. Bickley (1972) suggests that the Napoleon ice was clean, producing thin deposits. Westward drainage east of the Missouri River was probably established at this time, although subsequent glaciations enhanced it (Bluemle, 1984).

Following the retreat of the Napoleon Glaciation, a long period of erosion occurred that removed most of the glacial sediment and exposed bedrock over much of Emmons County (Bluemle, 1984). The first recognizable Late Wisconsinan ice margin in North Dakota (Phase D) is dated at 25 ka to 20 ka (Clayton and Moran, 1982). The ice sheet was most likely in its wasting stage when it reached south-central North Dakota, as it split into two lobes (Figure 5d) on encountering a gentle topographic high in Logan and McIntosh counties (Bluemle, 1984). Drainage was probably first diverted southeastward along the Strasburg Channel until it was blocked by the advancing ice sheet, resulting in a proglacial lake, Lake McKenzie (Bluemle, 1984). Another glacial lake formed when ice blocked the Missouri River in north-central South Dakota (Bickley, 1972). Lake Standing Rock may have occupied southeastern Sioux and southwestern Emmons Counties during Late Wisconsinan time (Bluemle, 1984).

Clayton and Moran (1982) have suggested the following ages for the first four recognized glacial events in North Dakota: Dunn Glaciation, pre-Wisconsinan; Verone Glaciation, late pre-Wisconsinan to Early Wisconsinan; Napolean Glaciation, pre-Wisconsinan, Early Wisconsinan, or Late Wisconsinan; and Phase D, Late Wisconsinan, 25 ka to 20 ka years ago. These ages may be compared to the ages of four periods of loess deposition in the Missouri and Mississippi river valleys recently identified by Forman et al. (1992) using thermoluminescence and ^{14}C. Periods of loess deposition have been associated with advances of the Laurentide Ice Sheet into the headwaters of the

Missouri and Mississippi rivers (Johnson and Follmer, 1989) and may span all or part of a glacial/deglacial cycle (Ruhe, 1983).

The four periods of loess deposition are ca. 135±20 ka (Illinoian), 85-70 ka (Early Wisconsinan), 45-30 ka (Middle Wisconsinan), and 25-12 ka (Late Wisconsinan). The inferred ages of glaciation parallel the deglaciation record of the Laurentide Ice Sheet determined from chronologic and stratigraphic studies in the Hudson Bay Lowlands (Forman et al., 1992). Four periods of deglaciation culminating at ca. 130, 64, 35, and 8 ka have been identified. Although the ages of the inferred Laurentide glaciations cannot be applied to the North Dakota glacial events without further study, they do provide a frame of reference.

Data Analysis and Interpretation

Fox Hills Formation Subcrop Map. Lithologic logs for 294 test holes drilled in Sioux, Grant, and Morton counties by the North Dakota State Water Commission (Randich, 1975; Ackerman, 1977) were examined to prepare a subcrop map of the Fox Hills Formation. The resulting map (Figure 6; Appendix A) shows the Fox Hills Formation subcropping further west than is suggested by published geologic maps of the area (Carlson, 1982; 1983). The Fox Hills Formation subcrops along ancestral bedrock valleys buried by glacial deposits and identified by the glacial aquifers which occupy them. The Shields, Little Heart, Elm Creek, and St. James glacial aquifers (Figure 7) directly overlie the Fox Hills Formation in Sioux, Grant, and Morton counties.

Fox Hills Formation Sandstone (Aquifer) Isopach Map. Lithologic logs for 42 test holes drilled by the North Dakota State Water Commission in Sioux, Grant, Morton counties (Randich, 1975; Ackerman, 1977) were examined to prepare a sandstone isopach map of the Fox Hills Formation. Many of the test

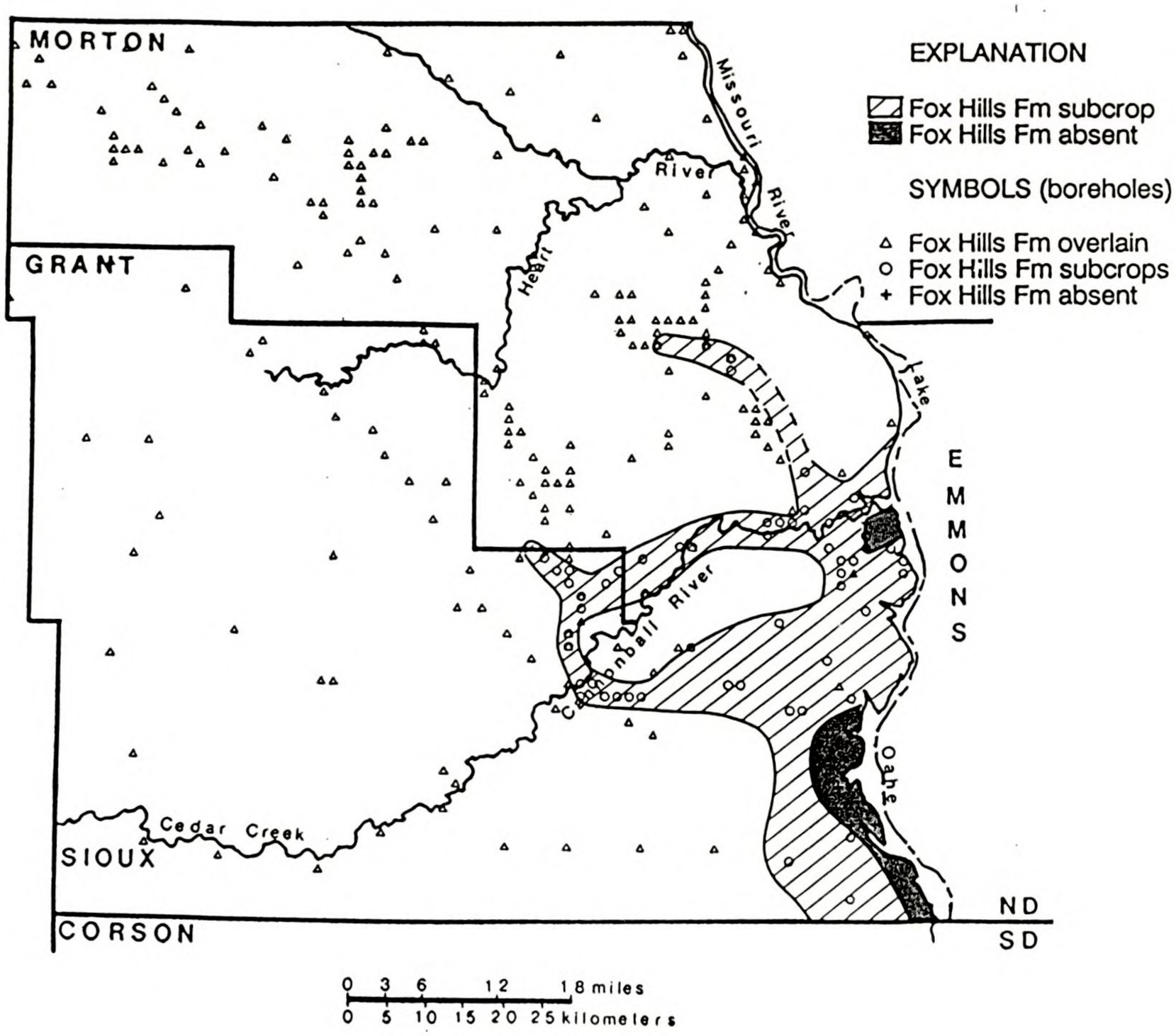

Figure 6. Subcrop map of the Fox Hills Formation.

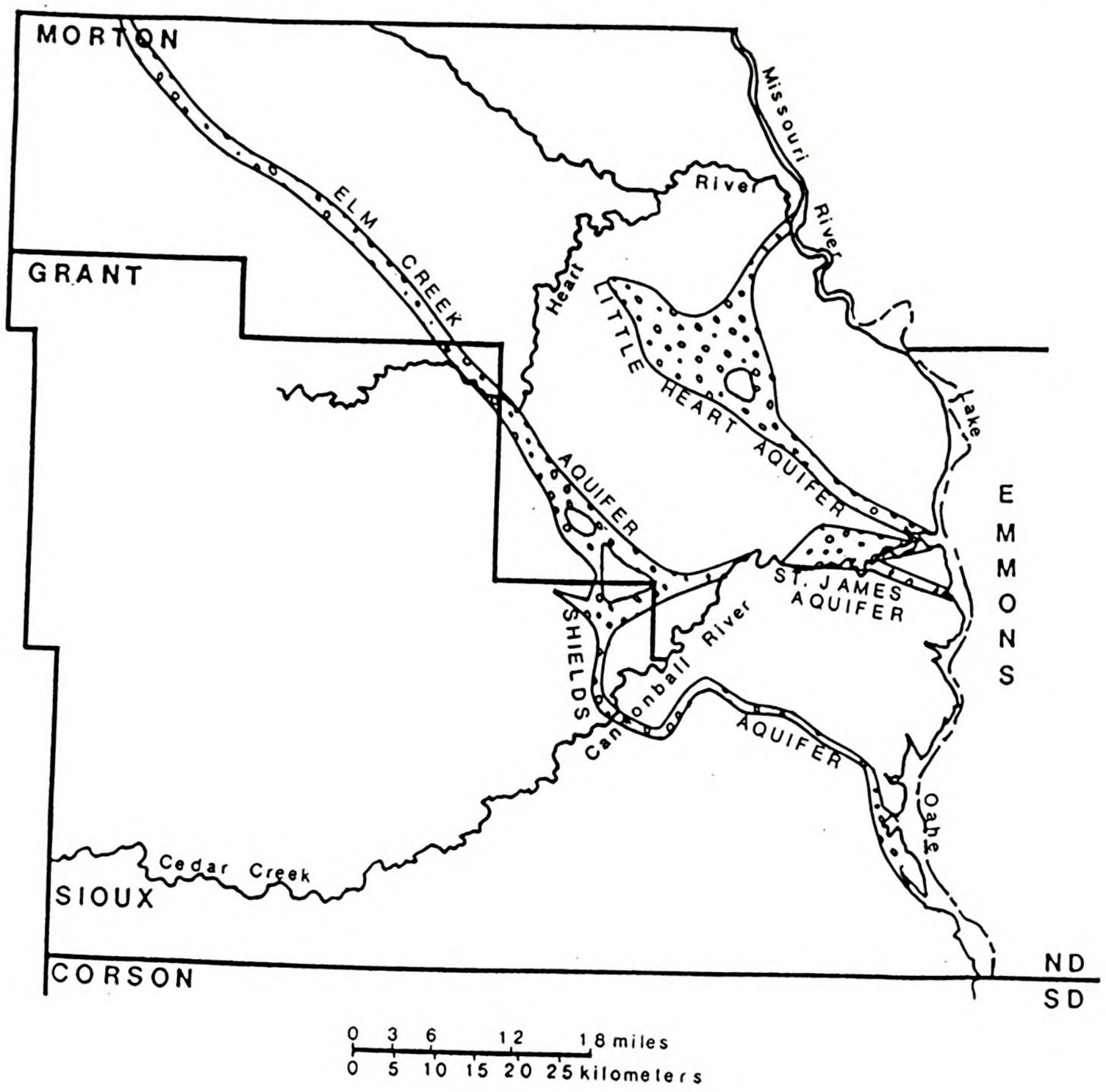

Figure 7. Major glacial aquifers of the study area
(adapted from Randich, 1979; Ackerman, 1980).

holes have qualitative geophysical logs (primarily potential and resistance) that aided in identifying and determining the thickness of permeable sandstone units (Appendix A). A map was produced using the drill log data as input to SURFER, a contouring program. The kriging method was used to calculate sandstone thicknesses for a 26 x 26 grid covering the three county study area. The resulting map is shown as Figure 8. Sandstone thicknesses range from 0 to 41.8 m.

Extent of Glacial Deposits. Lithologic logs for 294 test holes drilled in Sioux, Grant, and Morton counties by the North Dakota State Water Commission (Randich, 1975; Ackerman, 1977) were examined to determine the extent of glacial deposits in the study area. The resulting map (Figure 9; Appendix A) shows that glacial deposits occur west of the Killdeer-Shields Diversion Channel (Verone Glaciation) in southeastern Sioux and Grant counties. These western deposits are attributed to the Dunn Glaciation based on location. The remainder of the glacial deposits in Sioux and Grant counties were deposited during the Dunn and Verone Glaciations and Phase D (Lake Standing Rock sediments), while those in Morton County were deposited during the Dunn, Verone, and Napolean glaciations and Phase D (Lake McKenzie sediments).

Summary

The Upper Cretaceous Fox Hills aquifer is situated in the Williston basin, a Phanerozoic sedimentary basin that extends across North Dakota, South Dakota, eastern Montana, southern Saskatchewan, and southwestern Manitoba. The Fox Hills Formation is a marine-to brackish-water deposit of sandstone and shale. It crops out along the Cannonball River valley in southeastern Morton County and along the Missouri River

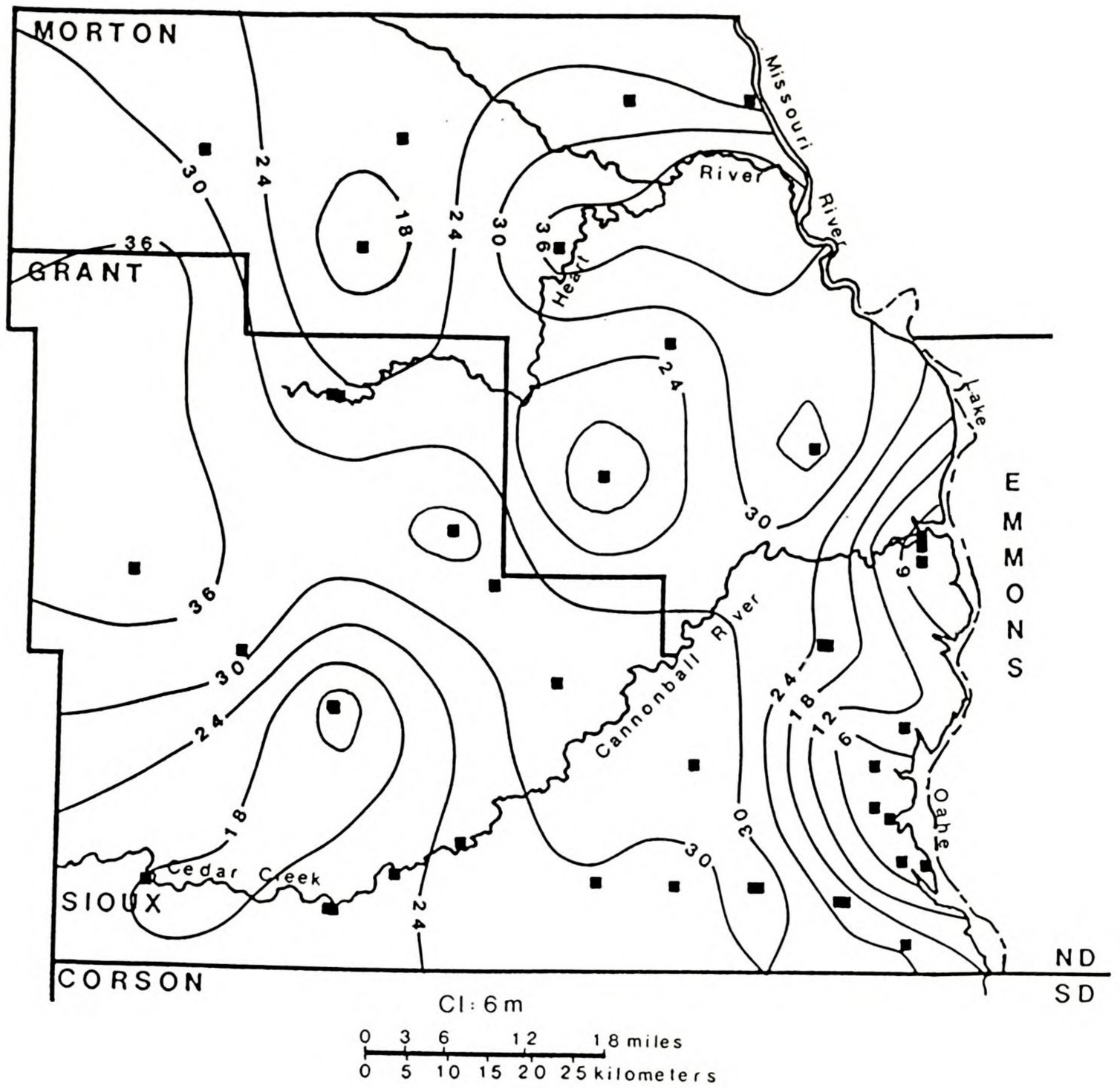

Figure 8. Fox Hills Formation sandstone thickness map.

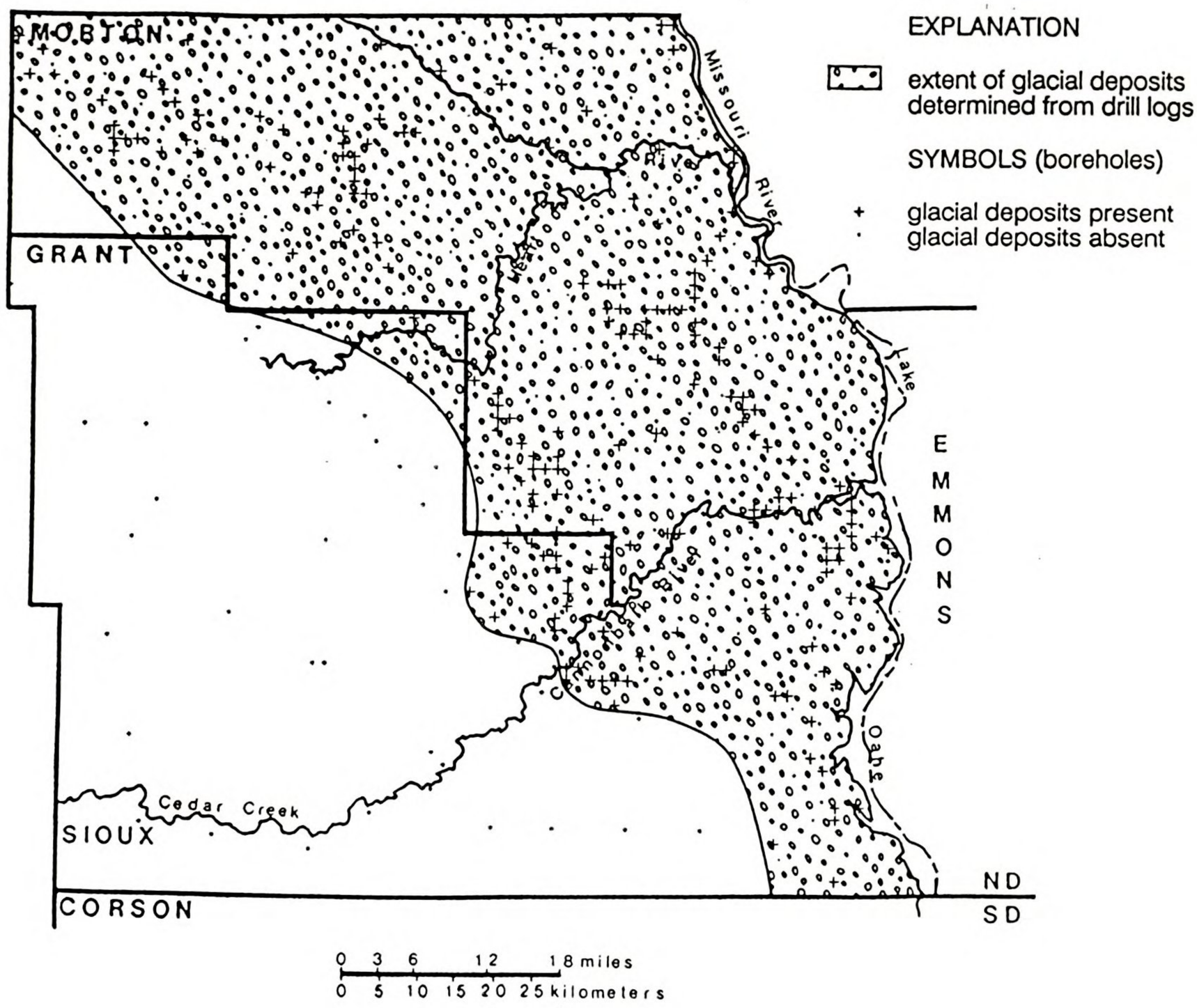

Figure 9. Extent of glacial deposits in the study area.

valley in eastern Sioux and western Emmons counties. The formation is absent in parts of southeastern Sioux and western Emmons counties, where it has been eroded.

The first regional aquifer below the Fox Hills Formation occurs in the Lower Cretaceous Inyan Kara Group (Dakota aquifer). Conformably underlying the Fox Hills Formation is the Pierre Formation, which is generally considered impermeable. The Late Cretaceous Hell Creek Formation conformably overlies the Fox Hills Formation. Its sandstone units serve as local aquifers that are generally not laterally extensive.

Four glacial advances are recognized in south-central North Dakota. The Dunn and Verone glaciations crossed the present Missouri River overriding outcrops of the Fox Hills Formation in Emmons, Sioux, and Morton counties. The Napoleon Glaciation extended across the present Missouri River in southeastern Morton County overriding outcrops of the Fox Hills Formation in Emmons County. The Late Wisconsinan, Phase D, glaciation overrode outcrops of the Fox Hills Formation in south-central Emmons county and blocked the Strasburg Channel forming Lake McKenzie, which covered Fox Hills Formation outcrops in Morton, Sioux, and Emmons counties. A southern ice advance across the Missouri River trench formed Lake Standing Rock, inundating outcrops of the Fox Hills Formation in Sioux and Emmons Counties.

Lithologic logs for 294 test holes drilled in Sioux, Grant, and Morton counties by the North Dakota State Water Commission were examined to prepare a subcrop map of the Fox Hills Formation and to determine the extent of glacial deposits in the study area. The Fox Hills Formation subcrops along ancestral bedrock valleys buried by glacial deposits and extends further west than is suggested by published geologic maps of the area. Lithologic logs for 42 test holes drilled by the North Dakota State Water Commission in Sioux, Grant,

Morton counties were examined to prepare a sandstone isopach map of the Fox Hills Formation.

CHAPTER 2: HYDROGEOLOGY

Literature Review

The hydrogeology of the Fox Hills aquifer and adjacent aquifers will be reviewed. The underlying Dakota aquifer will be discussed first, then the Fox Hills aquifer, and finally the overlying Hell Creek aquifers and glacial deposit aquifers.

Dakota Aquifer. The water-bearing sandstones of the Inyan Kara Group form the lower part of the Dakota aquifer. The hydraulic conductivity and transmissivity of the Inyan Kara ranges from 6 to 18 m/d and 500 to 1200 m^2/d, respectively, in south-central North Dakota (Butler, 1984). The porosity of the Inyan Kara sandstones vary from 30 to 35 percent in eastern North Dakota to less than 20 percent basinward. The potentiometric surface of the lower Dakota aquifer shows a potential high is located in south-central North Dakota, with head values ranging from 549 to 671 m (1800 to 2200 ft).

The Newcastle Formation forms the upper part of the Dakota aquifer in eastern North Dakota. Distribution of the Newcastle Formation is erratic in Sioux, Grant, and Morton counties (Carlson, 1982; 1983). Where present, sandstones may be up to 18 m (60 ft) thick. In Emmons County, the Newcastle sandstones are very fine grained, resulting in low yields (Armstrong, 1978).

A three-dimensional flow model of the Dakota aquifer in North Dakota indicates that leakage into and out of the Dakota is necessary to achieve a reasonable simulation of observed head values (Butler, 1984). Butler's flow model indicates leakage into the Dakota aquifer through the upper confining layer occurs in the western third of the state, while the model indicates leakage out of the aquifer through the upper confining layer for the eastern two-thirds.

The modeled vertical hydraulic conductivity for the upper confining layer varied from 1.5×10^{-10} to 2.4×10^{-8} m/s, with the lower value predominating in the lower Missouri River valley of south-central North Dakota. The vertical hydraulic conductivity of the confining layer in south-central North Dakota is six orders of magnitude smaller than the hydraulic conductivity of the Dakota aquifer. The model simulated heads within a standard deviation of 15 m. In south-central North Dakota, calculated head values differed from observed heads by up to 15 m along the Missouri River to as much as 55 m just west of the river.

Bredehoeft, et al. (1983) used four different conceptual models to simulate groundwater flow in the Dakota aquifer in South Dakota. The results of their simulations indicate that prior to development most of the recharge to and discharge from the Dakota aquifer occurred as leakage through confining layers. The hydraulic conductivity of the Dakota aquifer was assigned as 1.7 m/d. All models yielded similar values for the vertical hydraulic conductivity of the overlying confining layer--1.5×10^{-11} and 6.1×10^{-11} m/s. These values are within one order of magnitude of the vertical hydraulic conductivity value determined by Butler (1984) from the North Dakota model. The steady-state upward leakage through the confining layer was calculated to vary from 0 to $<1.5 \times 10^{-11}$ m/s (<0.47 mm/yr) in north-central South Dakota. The hydraulic conductivity values for the upper confining layer computed by the regional flow models were significantly higher than those determined from in situ and laboratory tests, suggesting that much of the flow through the confining layer occurs as fracture flow (Bredehoeft, et al., 1983).

Fox Hills Aquifer. In eastern Montana and western North Dakota, the sandstones of the Fox Hills and lower Hell Creek formations form a continuous sandstone sequence that has been termed the Fox Hills-basal Hell Creek aquifer (Thorstenson et al., 1979). In south-central North Dakota, the

sandstones of the Fox Hills and Hell Creek formations are separated by siltstone and bentonitic shale and are thus treated as separate aquifers (Ackerman, 1980). The hydraulic conductivity of the Fox Hills aquifer varies widely with core sample values ranging from 3.6×10^{-5} to 33 m/d (Randich, 1979; Ackerman, 1980). The geometric mean of ten samples in Morton County was 0.20 m/d (Ackerman, 1980). The mean for Sioux and Grant counties was 0.57 m/d (Randich, 1979). Hydraulic conductivity values determined from flow and recovery tests in Mercer and Oliver counties (north of Morton County) range from <0.04 to 4.8 m/d with a mean of 0.6 m/d (Croft and Wesolowski, 1970).

Transmissivities calculated from slug tests in Sioux and Grant counties range from 1.7 to 12.5 m^2/d with a mean of 5.2 m^2/d (Randich, 1979). Transmissivities estimated from sandstone thickness and hydraulic conductivity values for Emmons and Morton counties range from 2 to 40 m^2/d (Armstrong, 1978; Ackerman, 1980). Porosity values range from 35 to 53 percent in Sioux, Grant, and Morton counties (Randich, 1979; Ackerman, 1980).

The Fox Hills aquifer is recharged along the Cedar Creek anticline in southeastern Montana and southwestern North Dakota where the aquifer crops out, and by leakage from overlying aquifers in southwestern North Dakota. Groundwater flow is generally to the east and northeast (Figure 10). Two regional discharge areas occur in western North Dakota. The Missouri River valley is the main regional sink for the Fox Hills and overlying aquifers (Downey, 1986). The
Little Missouri River valley also serves as a regional discharge area, although of lesser regional extent (Hamilton, 1970).

The main discharge area occurs along the Missouri and Cannonball river valleys in Sioux and Morton counties, where the Fox Hills aquifer crops out and contributes discharge to surface flow (Randich, 1979; Ackerman, 1980).

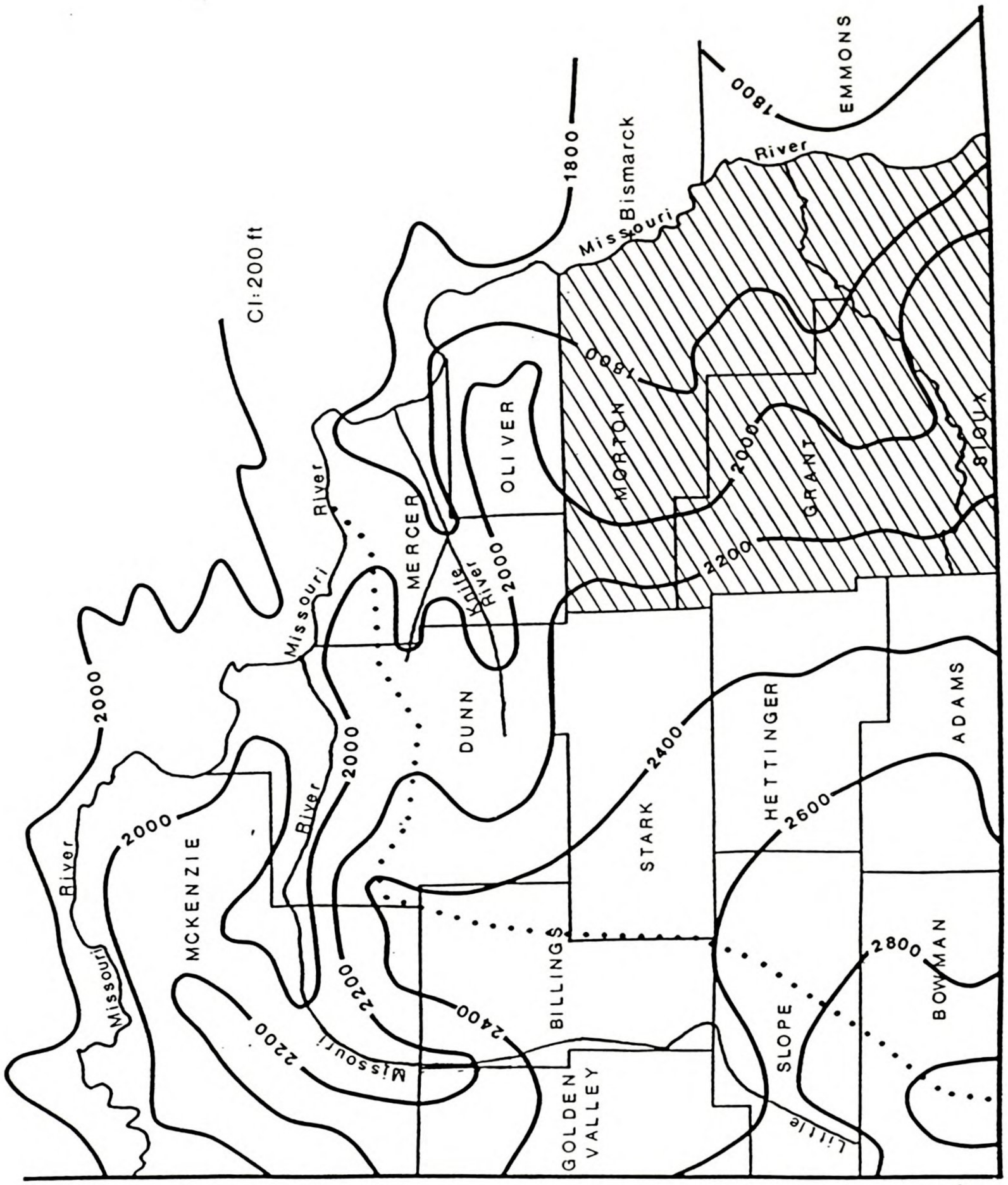

Figure 10. Fox Hills aquifer water levels in southwestern North Dakota (adapted from Lobmeyer, 1985).

Discharge also occurs by upward leakage into overlying aquifers along the Missouri and Knife river valleys in Dunn, McKenzie, Mercer, and Oliver counties (Croft, 1973; Klausing, 1979b; Croft, 1985b; Lobmeyer, 1985). East of the Missouri River, groundwater in the Fox Hills aquifer flows westward (Figure 10) toward the Missouri River/Lake Oahe (Lake Oahe lies behind Oahe Dam on the Missouri River and extends from the North Dakota/South Dakota border to just south of Bismarck).

In Morton County, groundwater flow in the Fox Hills aquifer is primarily lateral, with little water gained or lost via interaquifer leakage (Ackerman, 1980). Flow is generally to the east except along the Cannonball River where it deviates south toward the river. In the southeastern corner of the county, glacial drift aquifers directly overlie the Fox Hills aquifer. Head differences in these units indicate a general trend toward upward discharge into the glacial deposits from the Fox Hills aquifer (Ackerman, 1980).

Groundwater flow in the Fox Hills aquifer in Sioux and Grant counties is primarily northeasterly except along the Cannonball River, where groundwater discharges to the river. In areas where the Fox Hills and Hell Creek aquifers are separated by less than 20 m of bentonitic shale or siltstone, the water levels in the Hell Creek aquifers are generally about 3 m higher than those in the Fox Hills aquifer (Randich, 1979). In areas where thicker units separate the aquifers, the water levels in the Fox Hills aquifer are generally 15 to 30 m below those in the perched and semiperched Hell Creek aquifers, indicating that the Fox Hills aquifer probably receives some recharge from the overlying Hell Creek aquifers (Randich, 1979). However, low annual precipitation (40 cm) and high potential evaporation (90 cm) results in a low rate of recharge, with most occurring from March to early June (Howells, 1982).

In Emmons County, the Fox Hills Formation has been severely eroded south of Beaver Creek, limiting the aquifer to the Timber Lake Member. North of Beaver Creek, both the Timber Lake and Colgate members may be present and yield water to wells if saturated (Armstrong, 1978). Recharge to the Fox Hills aquifer occurs primarily from infiltration of precipitation and snowmelt. Groundwater generally flows to low-lying areas and eventually to Lake Oahe. Discharge also moves laterally into valley deposits (Armstrong, 1978).

Hell Creek Aquifers. In western North Dakota a sandstone unit at the base of the Hell Creek Formation is in hydraulic connection with the Fox Hills aquifer forming the Fox Hills-basal Hell Creek aquifer. However, in south-central North Dakota, 8 to 27 m of siltstone and bentonitic shale separate the sandstones of the Hell Creek and Fox Hills formations. In this region, sandstone beds in the Hell Creek Formation are generally discontinuous and not laterally extensive (Randich, 1979; Ackerman, 1980).

The hydraulic conductivity of core samples from the Hell Creek aquifers in Grant and Sioux counties average 5.5×10^{-3} m/d (Randich, 1979) and in Morton County 0.2 m/d (Ackerman, 1980). Transmissivities determined from slug tests in Sioux and Grant counties range from 1.4 to 7.3 m^2/d with an average of 3.2 m^2/d. Porosities range from 25 to 47 percent in Grant, Sioux, and Morton counties (Randich, 1979; Ackerman, 1980).

Groundwater movement in the Hell Creek aquifers of Morton County is generally lateral and to the east (Ackerman, 1980). Discharge occurs in the valleys of the Heart, Cannonball, and Missouri rivers and as leakage into glacial-drift aquifers (Ackerman, 1980). In Grant and Sioux counties, groundwater generally flows toward the northeast except along the outcrop where the flow mimics the surface topography (Randich, 1979). Water levels in the lower sandstones are generally within 3 m of the water levels in the Fox Hills aquifer,

while stratigraphically higher sandstones may have water levels 15 to 30 m above those in the Fox Hills aquifer (Randich, 1979). Thick sequences of silty and clayey material separate the more permeable beds, restricting recharge. In a climate where potential evaporation greatly exceeds precipitation, perched and semiperched water tables form, resulting in large differences in water levels of the adjacent aquifers (Howells, 1982). The Hell Creek Formation is generally unsaturated in Emmons County (Armstrong, 1978).

Glacial Deposit Aquifers. The most important glacial deposit aquifers in Sioux, Morton, and Grant counties are associated with buried bedrock valleys. The principal aquifers in the study area are the Shields Aquifer and the Little Heart Aquifer (Figure 7).

The Shields Aquifer occupies the southern extent of the Killdeer-Shields Diversion Channel, which coincides with the Verone ice-margin southwest of the Missouri River (Randich, 1979; Ackerman, 1980; Bluemle, 1984). The aquifer consists of several sand and gravel beds, with the most permeable materials along the central axis of the buried valley and at the valley bottom (Randich, 1979; Ackerman, 1980). Recharge enters the aquifer from hydraulically connected adjacent aquifers and as infiltration of precipitation. The aquifer discharges to streams, Lake Oahe, and an adjacent glacial aquifer.

The Little Heart aquifer occupies both a buried-valley system and a glacial lake basin (Ackerman, 1980). The aquifer material consists of sand and gravel beds, with the most permeable material along the axis of the valleys and near the valley bottoms. Recharge enters the aquifer from adjacent aquifers and as infiltration of precipitation and stream water. The aquifer discharges to small streams, Lake Oahe, and the Missouri River.

Data Analysis and Interpretation

A finite difference groundwater flow model was used to simulate present flow conditions in Sioux, Grant, and Morton counties.

Conceptual Physical System. The Fox Hills aquifer is comprised of two sandstone members that dip northwestward toward the center of the Williston Basin. Along the Missouri and Cannonball river valleys in Sioux, Grant, and Morton counties the Fox Hills Formation subcrops beneath glacial and alluvial deposits (Figure 4). Along the Missouri River valley in Emmons County, the formation is eroded isolating the Fox Hills aquifer in the study area from the aquifer in Emmons County. The Fox Hills aquifer is confined by the underlying marine Pierre Formation and overlying siltstone and bentonitic shale units of the Hell Creek Formation and glacial till.

The conceptual model of the Fox Hills aquifer in the study area is shown in Figure 11. Essentially horizontal flow is assumed to occur in the aquifer with possible recharge/discharge occurring along the upper and lower boundaries. Thus, vertical components of flow are considered negligible. The aquifer is modelled in two dimensions in the horizontal plane. Prescribed head boundaries are assigned to all four model boundaries. This allows water to enter and leave the modelled region by throughflow. Any additional gains or losses to the system are attributed to recharge or discharge through the upper or lower boundaries.

Mathematical Statement. The governing partial differential equation for the conceptual model is

$$d(T\, dh/ dx)/ dx + d(T\, dh/ dy)/ dy + R = 0,$$

where T is the transmissivity,

h is the head in the aquifer,

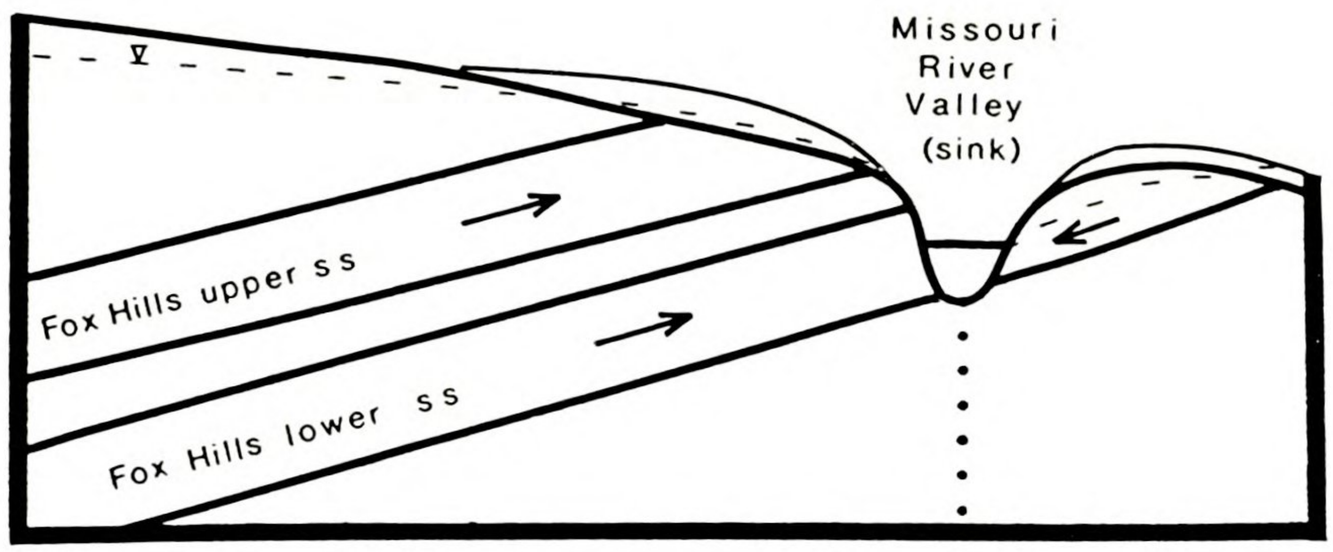

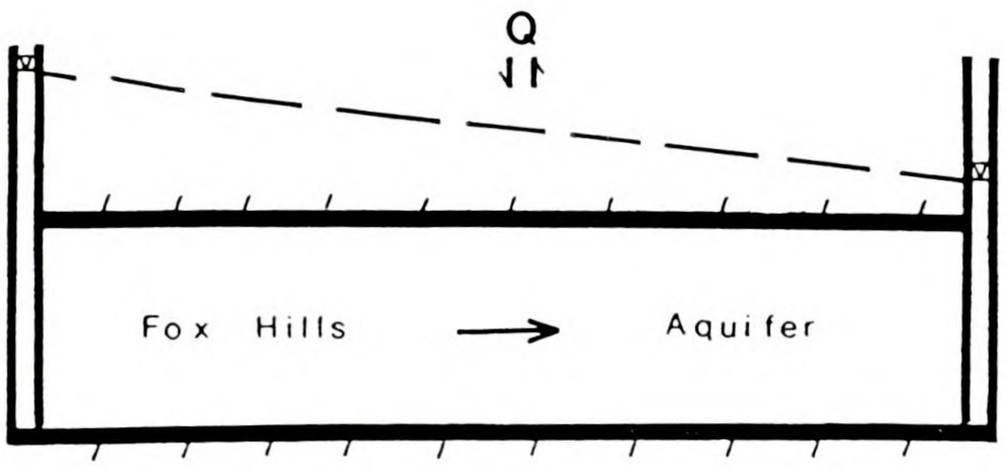

Figure 11. Conceptual model of the Fox Hills aquifer.

R is a source/sink term, and

x,y refer to the location in the horizontal plane.

This equation describes horizontal flow in a 2-D, confined, heterogeneous, isotropic aquifer with a sink/source under steady-state conditions. The prescribed head boundaries are described as

$$N:\ h(x,y_{max}) = h_{map}(x,y_{max}),$$

$$S:\ h(x,y_{min}) = h_{map}(x,y_{min}),$$

$$E:\ h(x_{max},y) = h_{map}(x_{max},y),$$

$$W:\ h(x_{min},y) = h_{map}(x_{min},y),$$

where h_{map} refers to water levels for the specified grid nodes on a contour map of present water levels in the Fox Hills aquifer.

Parameter Values. Maps of the water-level distribution and the distribution of transmissivity values were constructed for use in the simulation.

A map of the water levels in the Fox Hills aquifer of Sioux, Grant, and Morton counties was constructed using published water-level data from 44 wells (Croft, 1970; Trapp, 1971; Randich, 1975; Ackerman, 1977; Appendix B) and the contouring computer program SURFER. The kriging method was used to calculate water-levels for a 26 x 26 grid covering the three county study area. The resulting map (Figure 12) shows the general flow direction to be toward the east. Bending equipotential lines along the Cannonball River/Cedar Creek and Heart River valleys indicate discharge from the Fox Hills aquifer is occurring in these regions.

Transmissivity values (T=Kb) were estimated using the sandstone thicknesses (b), determined from 42 drill logs (Chapter 1), and a constant hydraulic conductivity value (K) of 0.57 m/d. The 42 calculated transmissivity values were then contoured with SURFER using the kriging method for the same 26 x 26 grid as above. The resulting map is shown as Figure 13.

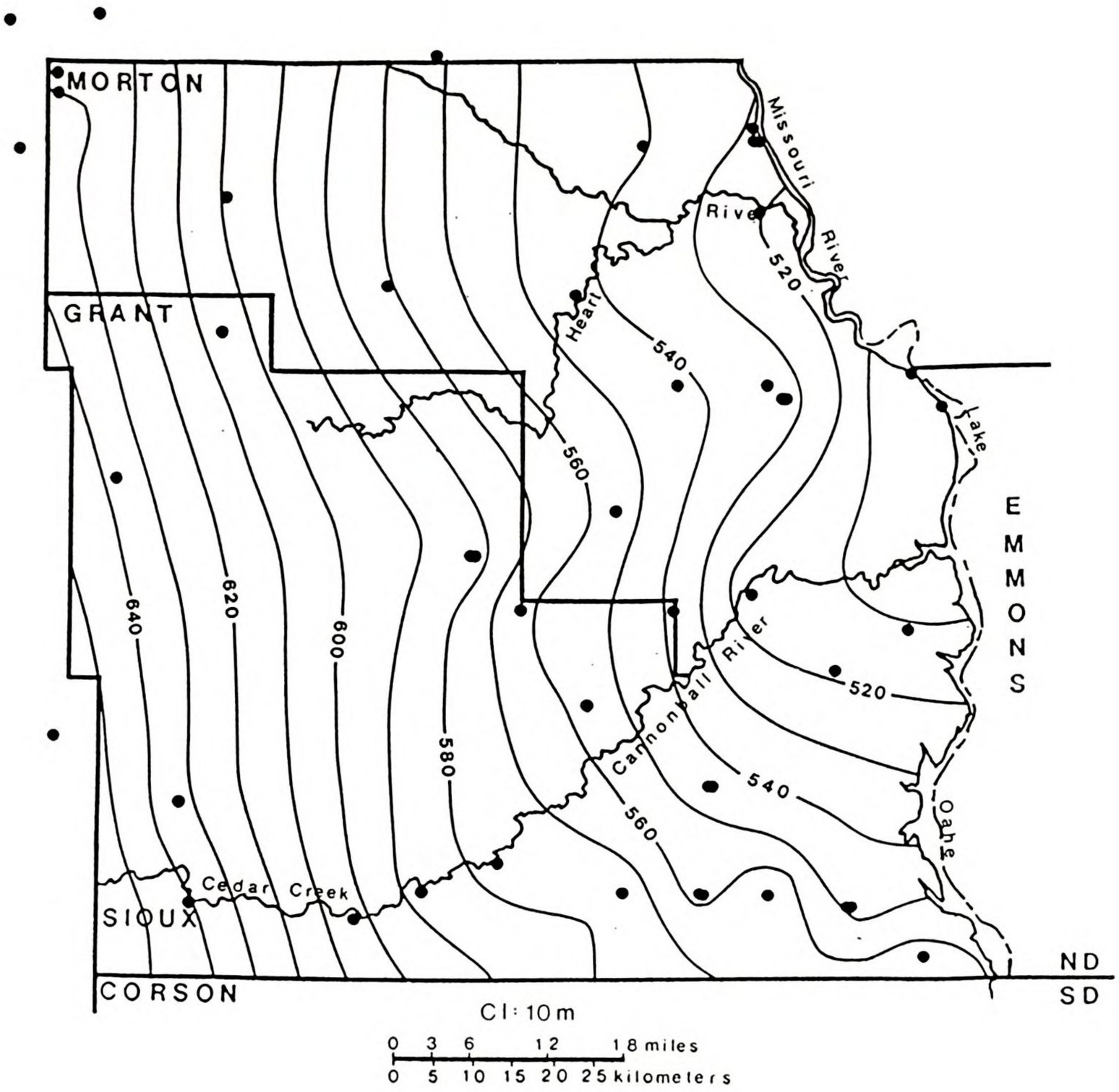

Figure 12. Water-level map of the Fox Hills aquifer.

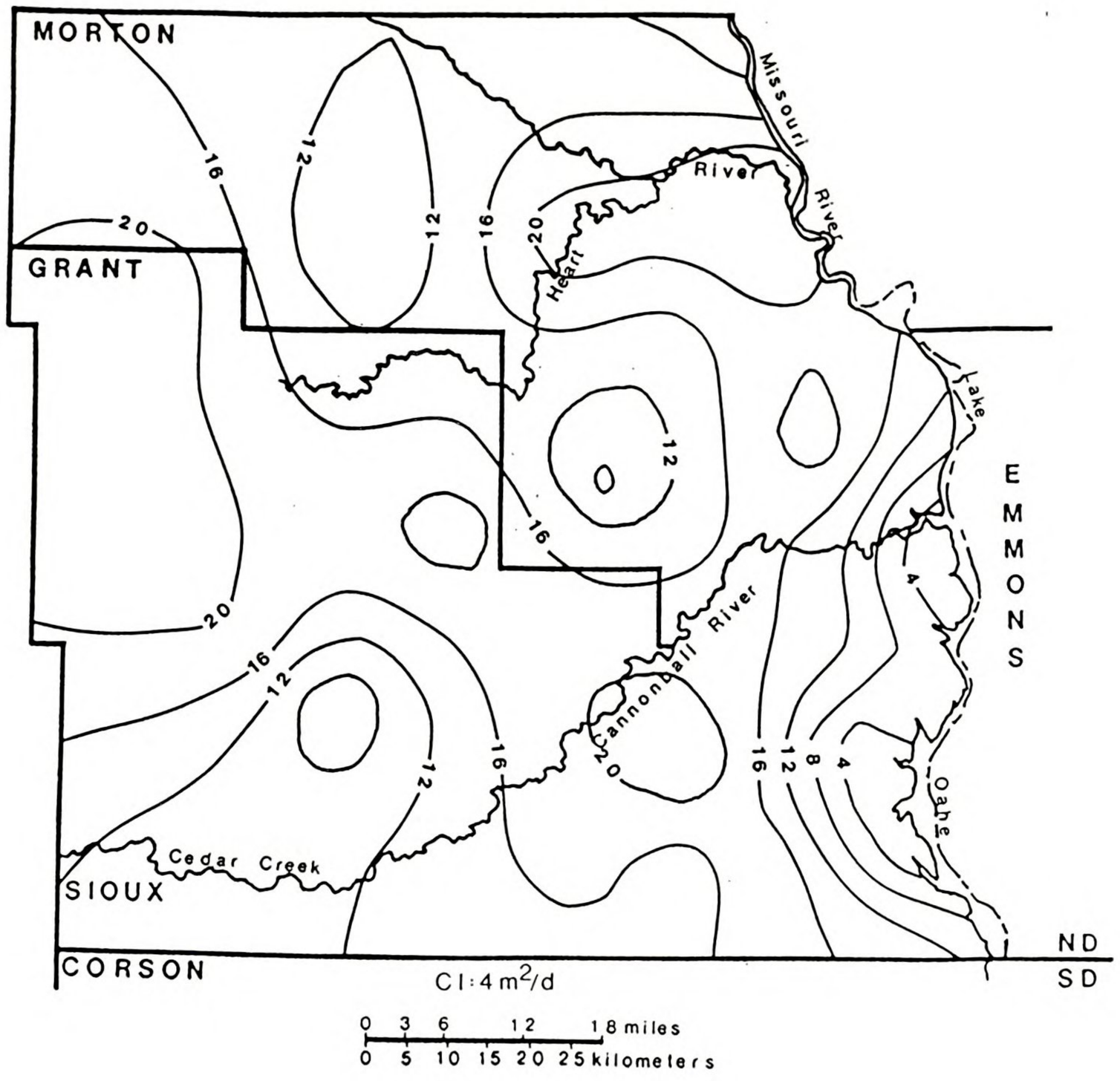

Figure 13. Transmissivity map of the Fox Hills aquifer.

2-D Finite Difference Model. A 2-D IADI finite difference computer code, SAM4 (Kinzelbach, 1986), was used for the simulation. This code uses the iterative alternating implicit procedure which combines equation solving and iterative procedures. SAM4 requires essentially horizontal flow in the model aquifer and allows for cell specific recharge and discharge. The Fox Hills aquifer was modeled as a steady-state (S=0) confined aquifer on a 26 x 22 grid system (Dx= Dy) that coincides with the lower 22 rows of the water-level and transmissivity maps presented above (Figure 14). Prescribed head boundaries were used on all sides of the model area. The upper boundary of the grid follows an east-west streamline. The water-level grid (map) was used to assign the prescribed and "initial" heads for each cell; the transmissivity grid (map) to assign transmissivity values. An iteration error limit of 0.05 m was chosen. Recharge/discharge was used to calibrate the model to the present water-level grid map by trial and error.

Simulation Results. The first simulation was run without any recharge or discharge to the system. Simulated water levels were much higher (20-30 m) than observed levels, indicating that water is discharged from the Fox Hills aquifer in the modeled region. The Cannonball and Missouri river valleys, where the Fox Hills Formation crops out, are considered to be the major discharge areas for the aquifer (Randich, 1979; Ackerman, 1980). Attempts to simulate the observed water levels by discharging water along the Fox Hills Formation subcrop were unsatisfactory, indicating that discharge must occur over a larger region. Extending the discharge area westward along the Cannonball River/Cedar Creek valley improved the simulation.

Groundwater flow in the Fox Hills aquifer in Morton County is considered to be lateral with only small amounts of leakage into or out of the aquifer (Ackerman, 1980). However, the water-level map indicates that discharge is

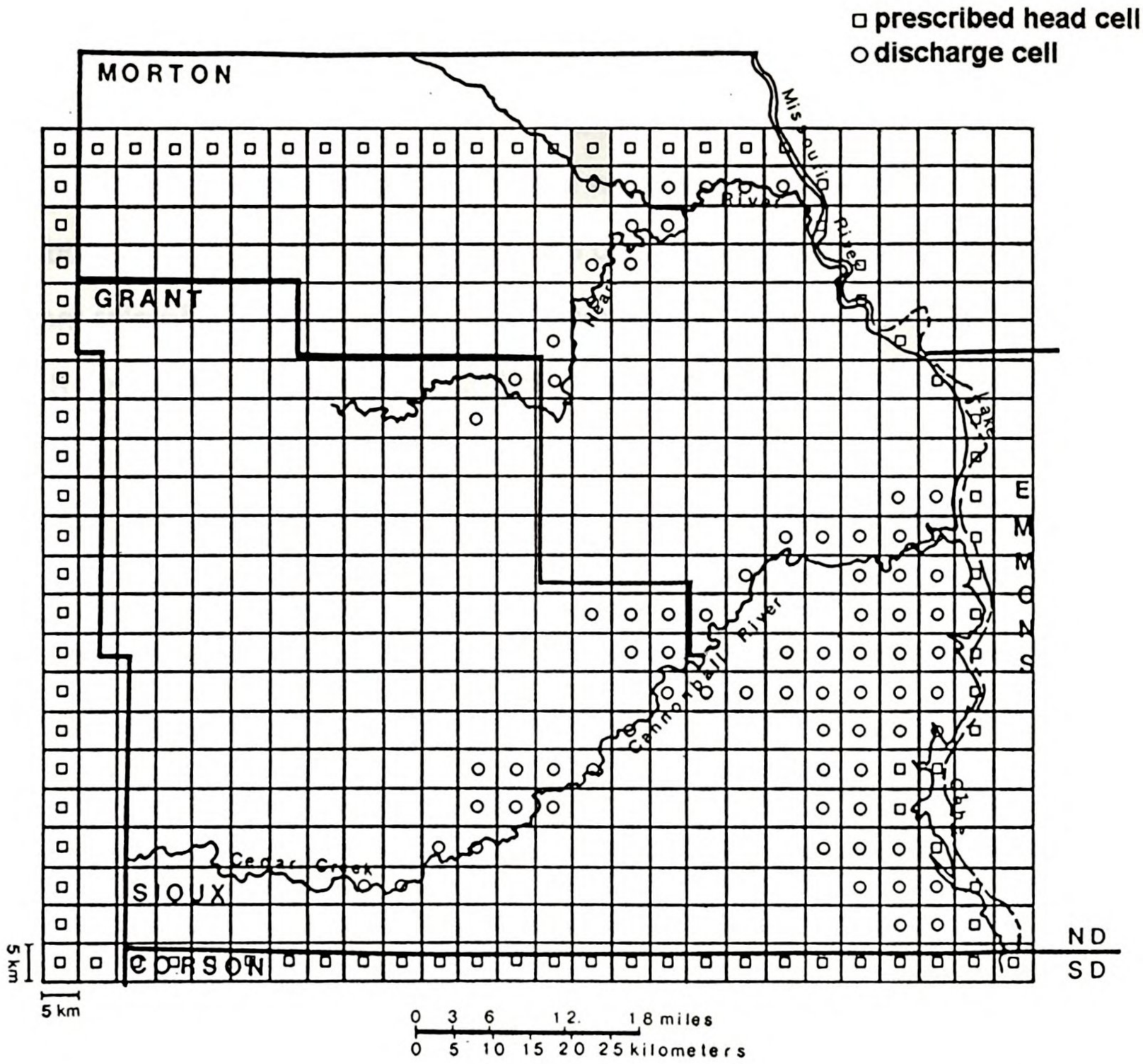

Figure 14. Finite-difference grid used for simulation of the Fox Hills aquifer.

occurring along the Heart River valley (Figures 10 and 12). These differences may be reconciled if the Fox Hills aquifer is in hydraulic connection with Hell Creek aquifers in the Heart River valley. The Heart River valley is a major discharge area for the Hell Creek aquifers (Ackerman, 1980). The possibility of a hydraulic connection between the two aquifer systems is recognized in the literature (Ackerman, 1980). Modeling discharge along the Heart River valley improved the overall simulation.

A satisfactory simulation of present water levels in the Fox Hills aquifer was obtained (Figure 15) when water was discharged from the aquifer at a constant rate of 0.5 mm/yr along the Cannonball River/Cedar Creek valley, the Heart River valley, and the Missouri River valley (where the Fox Hills Formation crops out).

No recharge was introduced to the system. The mean deviation from the present water levels for the 438 variable head cells was 1.3 m, i.e. the simulated water levels were 1.3 m higher than the observed values. The standard deviation (spread around the mean) was 4.9 m.

Interpretation. The Fox Hills aquifer water-level map shows that the discharge area of Sioux and Morton counties should receive its water from upgradient in the aquifer via throughflow and that discharge from the aquifer occurs along the Missouri, Cannonball, and Heart river valleys. Water-levels in the aquifer were satisfactorily simulated assuming water is discharged at a rate of 0.5 mm/yr in the 3 major river valleys. The simulation results support the hypothsis, suggested in the literature, that only minimal recharge enters the aquifer in the discharge area. Water-levels in the aquifer were simulated with a mean and standard deviation of 1.3 m and 4.9 m, respectively, without adding recharge to the system.

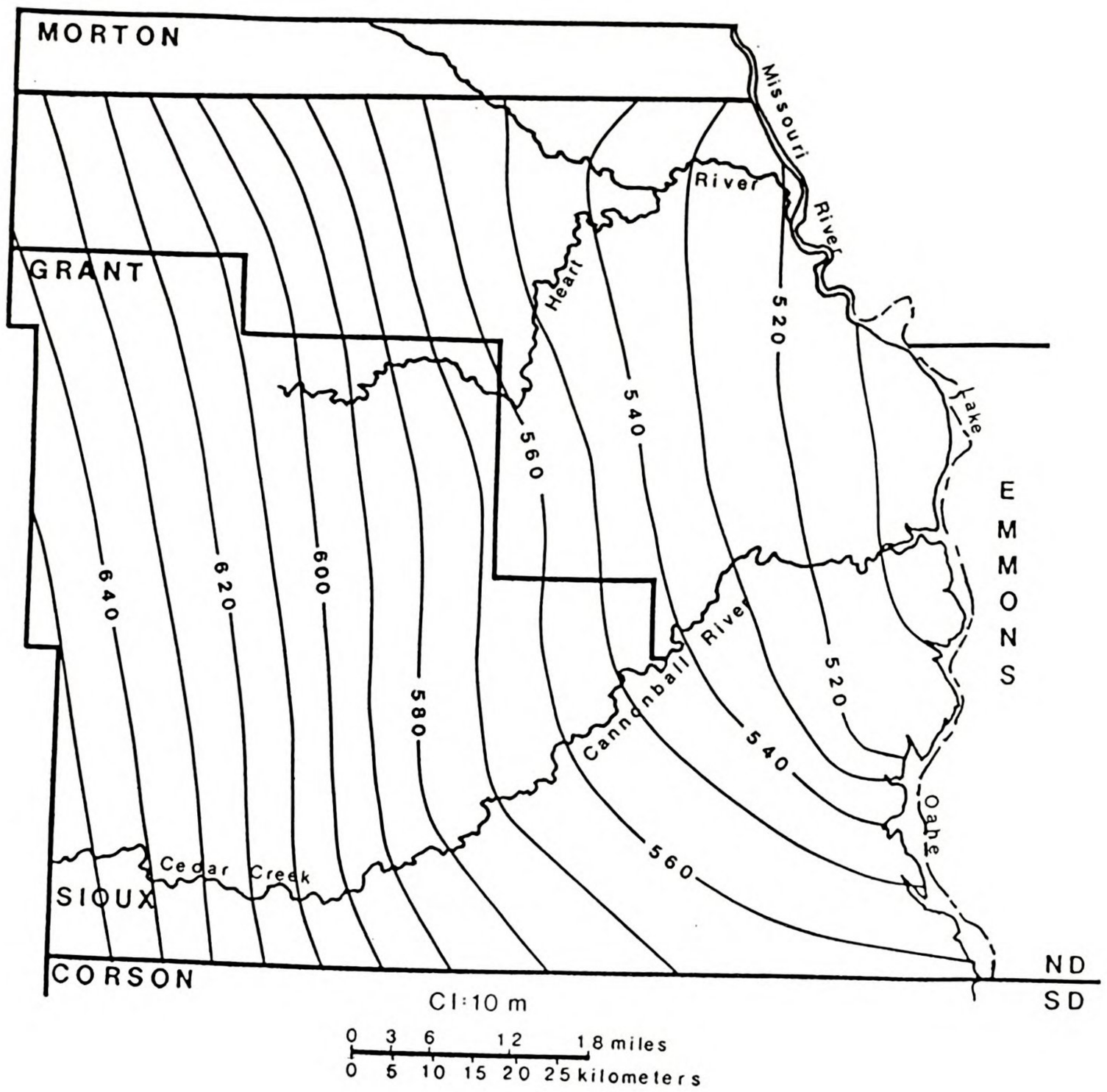

Figure 15. Simulated water levels in the Fox Hills aquifer.

The hydrogeologic investigation supports hypothesis (a), i.e., upgradient aquifer water is a source of water for the discharge area of the Fox Hills aquifer. Hypothesis (b), i.e., local precipitation is a potential source of water to the discharge area, is not supported by the steady-state, 2-D simulation. This is consistent with Howells (1982) assessment that a low rate of recharge results because of the combination of low annual precipitation and high potential evaporation. Hypothesis (e), i.e., leakage from adjacent hydrologic units into the discharge area, is also not supported by the steady-state, 2-D simulation. Although Randich (1979) observed that in some areas of Morton County the water levels in the Fox Hills aquifer are generally 15 to 30 m below those in the Hell Creek aquifers and suggested that the Fox Hills aquifer probably receives some recharge from the overlying Hell Creek aquifers, Howells (1982) noted that thick sequences of silty and clayey material separate the more permeable beds in Sioux and Corson counties, restricting recharge. Thus the simulation results, i.e., minimal recharge to the system, are consistent with Howells assessment.

Summary

The Fox Hills aquifer is recharged along the Cedar Creek anticline in southeastern Montana and southwestern North Dakota where the aquifer crops out, and by leakage from overlying aquifers in southwestern North Dakota. Groundwater flow is generally to the east and northeast with the main discharge area along the Missouri and Cannonball rivers in Sioux and Morton counties. East of the Missouri River, groundwater in the Fox Hills aquifer flows westward toward the Missouri River/Lake Oahe. Low annual precipitation and high potential evaporation results in a low rate of recharge, with most occurring from March to early June.

A 2-dimensional finite difference groundwater flow model was used to simulate present flow conditions in Sioux, Grant, and Morton counties. Maps of the water-level distribution and the distribution of transmissivity values were constructed for use in the simulation. The water-level map shows the general flow direction to be toward the east. Bending equipotential lines along the Cannonball River/Cedar Creek and Heart River valleys indicate discharge from the Fox Hills aquifer is occurring in these regions. A satisfactory simulation of present water levels in the Fox Hills aquifer was obtained using Kinzelbach's (1986) 2-D IADI finite difference model when water was discharged from the aquifer at a constant rate of 0.5 mm/yr along the Cannonball River/Cedar Creek valley, the Heart River valley, and the Missouri River valley (where the Fox Hills Formation crops out). The mean deviation from the present water levels for the 438 variable head cells was 1.3 m. The standard deviation (the spread around the mean) was 4.9 m. The simulation results suggest that only minimal recharge enters the aquifer in the discharge area.

The hydrogeologic investigation supports hypothesis (a), that upgradient water is the source of water in the discharge area of the Fox Hills aquifer in Sioux, Grant, and Morton counties. Hypotheses (b) and (e), local precipitation/recharge and leakage from adjacent aquifers, are not supported by the hydrogeologic investigation. These results are consistent with Howells (1982) assessment that a low rate of recharge results because of the combination of low annual precipitation and high potential evaporation and that thick sequences of silty and clayey material separate the more permeable beds, restricting recharge.

CHAPTER 3: HYDROGEOCHEMISTRY

Literature Review

Previous studies of the water chemistry of the Fox Hills aquifer will be reviewed, followed by a discussion of the water chemistry of the Dakota aquifer.

Fox Hills Aquifer. Several studies have been conducted on the water chemistry of the Fox Hills aquifer (Groenewold et al., 1979; Thorstenson et al., 1979). Thorstenson et al. examined the hydrochemistry of the Fox Hills aquifer in southwestern North Dakota and northwestern South Dakota. They found that the water chemistry changes significantly downgradient in the aquifer. For example, in the recharge area, the water contains primarily sodium, bicarbonate, and sulfate ions and traces of H_2S and CH_4. Downgradient, the water chemistry changes to contain primarily sodium, bicarbonate, and chloride ions, and more CH_4 is present. They also found that helium concentrations in the discharge area increased several orders of magnitude above atmospheric saturation levels. Thorstenson et al. concluded that most of the chemistry changes described above could be explained reasonably by processes occurring within the aquifer (i.e., sulfate reduction in the presence of lignite resulting in pyrite formation) and Ca-Mg/Na exchange. The authors attributed the downgradient increases in chloride and helium to leakage from the Pierre Formation or underlying formations. Using available hydrodynamic data, they estimated that the water in the aquifer was moving at a rate of 0.85 m/yr with the water in the discharge area approximately 250 ka.

Groenewold et al. (1979) studied the hydrochemistry of the Fox Hills aquifer in southwestern North Dakota and also concluded that sulfate reduction in the presence of lignite and Ca-Mg/Na exchange were responsible for the

downgradient change in water chemistry. However, they noted that lignite is rare in the aquifer, limiting the reaction. They suggest that sulfate reduction in the aquifer may be controlled by the rate of diffusion into the aquifer of dissolved organic matter from the overlying confining layer or by the rate of sulfate diffusing out of the aquifer into the sulfate-deficient confining layer. Groenewold et al. attributed the downgradient increases in chloride concentration to diffusion from the Pierre Formation. In addition to studying the geochemistry, Groenewold et al. determined ^{14}C ages for waters from 6 locations, which ranged from <10 ka to 27 ka. The oldest ages were determined for wells in Dunn County (Figure 10), which they interpreted as indicating that the water in the Fox Hills aquifer west of the Missouri River is generally younger than 30 ka (however, Dunn County is bisected by a N-S groundwater divide, and it is likely that downward leakage of relatively recent water may have occurred in this area). They concluded that since no glacial advances have extended west of the Missouri River in the last 30 ka, the effects of glaciation on the chemical evolution of water presently in the Fox Hills aquifer would be minimal. They also analyzed two samples for $\delta^{18}O$ from wells in Dunn County that produced values of -17 and -17.4, but provided no explanation for the light values.

Chlorine-36/Cl ratios for seven water samples from the Fox Hills aquifer in southwestern North Dakota have been reported by Davis and Bentley (1982) and Bentley et al. (1986). Since the ratios tend to decrease rapidly along the flow path from 258×10^{-15} to 7×10^{-15} as chloride concentrations increase, Bentley et al. (1986) have suggested that upward leakage from the Dakota aquifer (Newcastle Formation) may be replacing the water in the Fox Hills aquifer.

Dakota Aquifer. The upper part of the Dakota aquifer (Newcastle Formation) in North Dakota yields sodium chloride type water with chloride

concentrations in the range of 5,000 mg/L (Howells, 1982; Peter, 1984). The lower part of the Dakota aquifer (Inyan Kara) in south-central North Dakota yields saline to very saline water. Howells (1982) observed a pronounced chemistry change in Corson County, SD (directly south of Sioux County). He noted that near the Missouri River, the aquifer yielded sodium-calcium-magnesium-chloride-sulfate type water with a total dissolved solids (TDS) content of 2,500 mg/L. Ten miles west of the river, the TDS content is greater than 5,000 mg/L and the water is of the sodium-chloride type. Twenty miles west of the river, the TDS content is greater than 10,000 mg/L. In Emmons County, east of the Missouri River, the lower part of the Dakota aquifer yields sodium-sulfate type water (Armstrong, 1978).

Data Analysis and Interpretation

Graphical Analysis. Major ion chemistry data were obtained for 248 wells in the Fox Hills aquifer of southwestern North Dakota from published county reports (Croft, 1970; Trapp, 1971; Croft, 1974; Randich, 1975; Ackerman, 1977; Klausing, 1979a; Anna, 1980; Croft, 1985a). The data were converted to percent equivalents per million (% epm) and plotted on a Piper trilinear diagram (Zaporozec, 1972; Figure 16; Appendix C).

Sodium is the dominant cation throughout the aquifer comprising over 90% epm of the cations in 236 of the 248 samples. Two samples having <90% epm sodium were from wells in western Bowman County, where the Fox Hills Formation crops out in the recharge area. Ten additional samples with <90% epm sodium were from wells in Sioux, Morton, and Grant counties, at or near the formation subcrop in the discharge area.

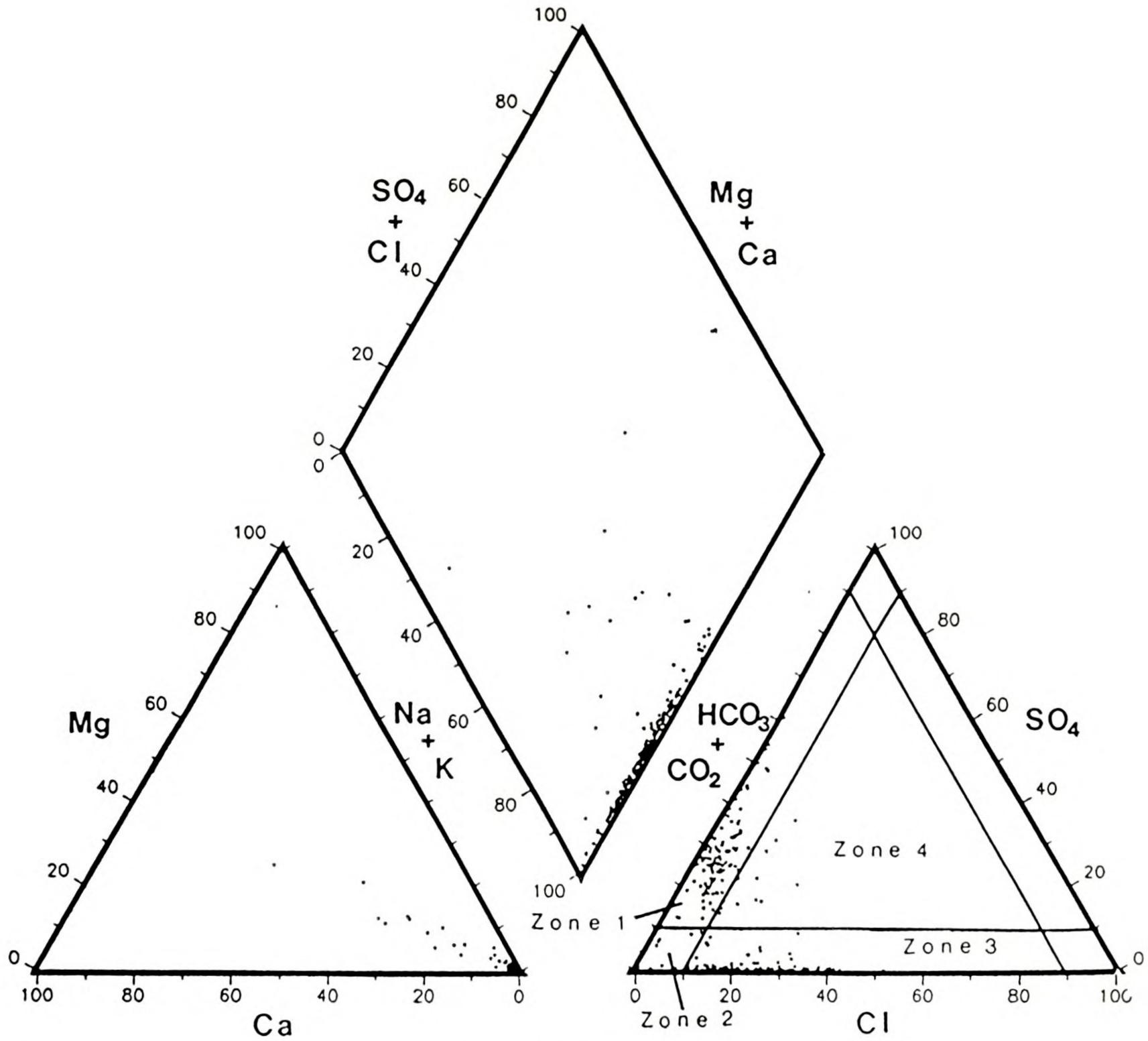

Figure 16. Piper diagram of Fox Hills aquifer water in southwestern North Dakota.

The anion chemistry data were more variable. When plotted, the data fell within four distinct zones on the Piper anion triangle (Figure 16). The majority of the samples (52%) fell in zone III, representing bicarbonate-chloride and chloride-bicarbonate chemistries (>90% epm). The next largest group of samples (38%) fell in zone I, representing bicarbonate-sulfate and sulfate-bicarbonate chemistries (>90% epm). Only 6% of the samples fell in zone IV (bicarbonate-sulfate-chloride) and 4% in zone II (bicarbonate, >90% epm).

Hydrochemical Facies. The distribution of anion facies in southwestern North Dakota is shown in Figure 17. Zone I type waters occur along the recharge area west of the Little Missouri River valley and within the Little Missouri River valley discharge area. Zone I type waters also occur along the Missouri River discharge area in Sioux, Morton, and Grant Counties, primarily where the Fox Hills Formation crops out. Zone III type waters dominate the remainder of the area with zone IV type waters fringing the zone I-zone III contact. Zone II type waters occur locally and may represent areas of significant downward leakage from overlying aquifers.

Recharge to the Fox Hills aquifer in southwest North Dakota occurs as leakage from the overlying Hell Creek-lower Ludlow aquifer. The Hell Creek Formation contains beds of lignite which serve as an energy source for sulfate-reducing bacteria (Anna, 1981). Sulfate reduction in the Fox Hills aquifer may be controlled by the rate of diffusion of dissolved organic matter from the overlying confining layer (Groenewold et al. 1979). Consequently, sulfate concentrations in the Fox Hills aquifer decrease in the downgradient direction. Paralleling the sulfate decrease is an increase in chloride concentrations, possibly due to diffusion from the Pierre Formation (as discussed below). The result of these processes is a shift from a sodium-bicarbonate-sulfate type water (zone I) to a sodium-bicarbonate-chloride type water (zone III) in the downgradient direction.

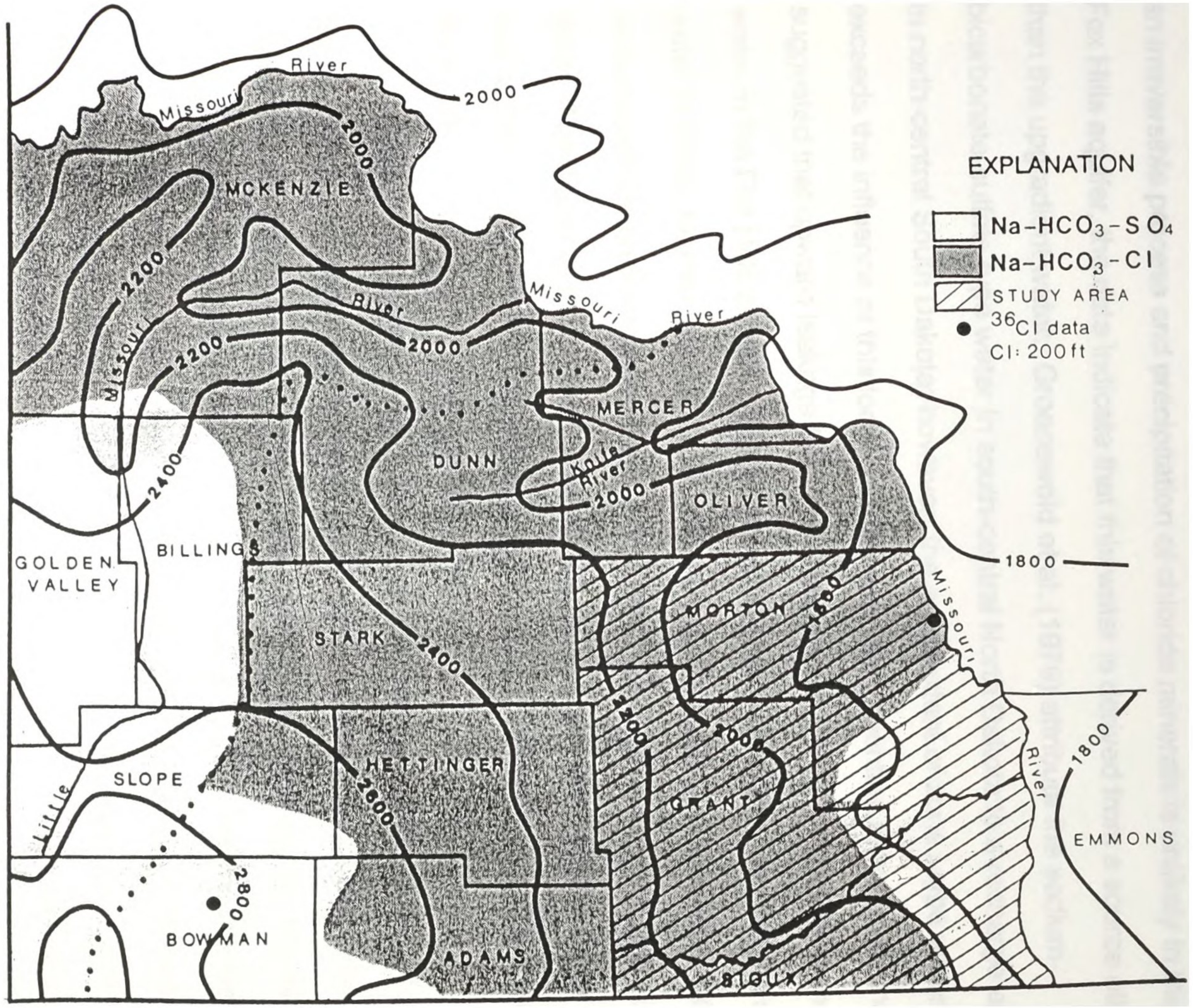

Figure 17. Hydrochemical facies map of the Fox Hills aquifer in southwestern North Dakota.

Sodium-bicarbonate-sulfate type water in the Fox Hills aquifer in Sioux, Morton, and Grant counties is a water chemistry anomaly because upgradient waters are of the sodium-bicarbonate-chloride type. Since sulfate reduction is an irreversible process and precipitation of chloride minerals is unlikely in the Fox Hills aquifer, the data indicate that this water is derived from a source other than the upgradient water. Groenewold et al. (1979) attribute the sodium-bicarbonate-sulfate type water in south-central North Dakota to a recharge area in north-central South Dakota; however, the areal extent of zone I type waters exceeds the influence of this local groundwater high. Bentley et al. (1986) have suggested that upward leakage from the Dakota aquifer may be replacing the water in the Fox Hills aquifer. This hypothesis does not hold for the anomalous water in Sioux, Morton, and Grant counties because the Dakota aquifer yields sodium-chloride type water in south-central North Dakota west of the Missouri River. The shape of the sodium-bicarbonate-sulfate type anomaly is similar to that of the Fox Hills Formation subcrop, suggesting that the freshwater entered the Fox Hills aquifer along the formation subcrop.

Chloride Distribution. Chloride concentrations in the Fox Hills aquifer generally increase from the recharge area along the Cedar Creek Anticline toward the Missouri River discharge area. Formations overlying the Fox Hills aquifer are generally of non-marine origin, and any chloride minerals formed during the deposition of the Fox Hills Formation (littoral) should be flushed out of the aquifer (Thorstenson et al., 1979). Thus, the marine Pierre Formation or underlying formations are the logical source of chloride. Thorstenson et al. (1979) and Groenewold et al. (1979) both suggest that the chloride concentration increases in the Fox Hills aquifer are due to input from the Pierre Formation, while Bentley et al. (1986) suggest that Dakota aquifer water is leaking into and replacing the Fox Hills aquifer water. In southwestern North

Dakota, the hydraulic head in the Dakota aquifer is generally lower than that in the Fox Hills aquifer. Thus, upward leakage from the Dakota aquifer does not occur throughout most of the region and the increase in chloride concentrations in the Fox Hills aquifer cannot be attributed to leakage from the Dakota aquifer. The observed chloride concentrations in the main body of the Fox Hills aquifer are best explained as input from the Pierre Formation.

Figure 18 is a map of the Fox Hills aquifer chloride distribution in south-central North Dakota. A low-chloride (<1 meq/L) zone occurs just west of the Missouri River, principally in the Fox Hills Formation subcrop/outcrop area. This low-chloride zone coincides with the sodium-bicarbonate-sulfate type water anomaly identified in Sioux, Grant, and Morton counties. The chloride concentrations can therefore be used to estimate the relative volume of freshwater input to the discharge area. To dilute the upgradient water (>9 meq/L Cl) to <1 meq/L Cl would require approximately 9 parts freshwater to 1 part upgradient water. In the southeastern corner of Grant County, the chloride concentrations drop from >6 meq/L to < 1 meq/L in a 6 km stretch along the groundwater flow path. In order to bring about this decrease in chloride concentration (by mixing with fresh water), a 500% increase in the volume of water would be required as the water moves downgradient through this region. Such an increase in the water volume would require recharge on the order of 4.3 to 8.5 mm/yr, only in the narrow band with chloride concentrations in the range of 1 to 6 meq/L. Neither the literature or water-level maps of the aquifer suggest any unusual conditions that are restricted to this region. It is unlikely that local recharge under present climatic conditions could explain this increase in water volume. A climatic regime capable of providing large volumes of recharge to the discharge area, as opposed to a narrow band in the discharge area, occurred

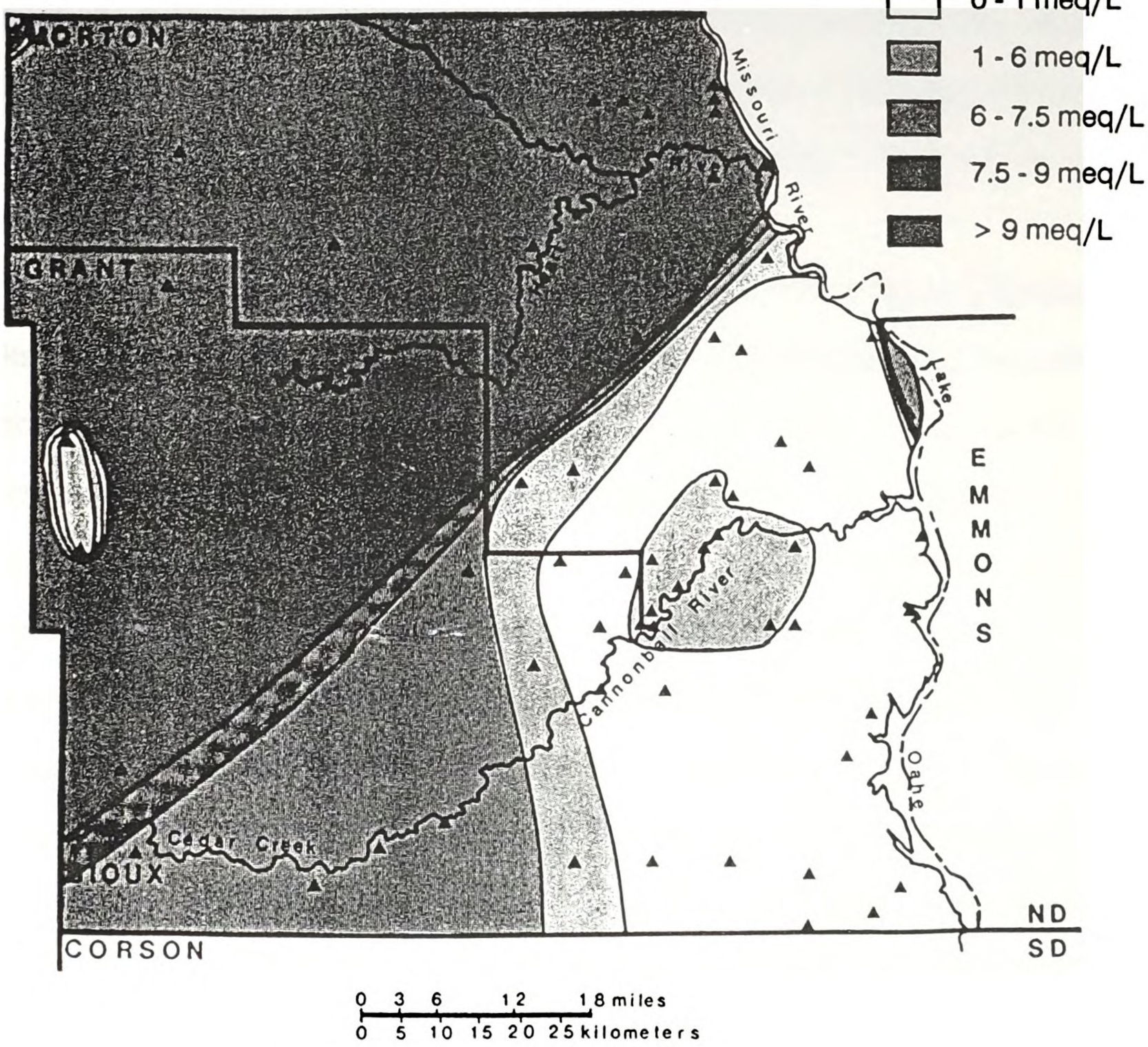

Figure 18. Chloride distribution in the Fox Hills aquifer.

during the Pleistocene when ice sheets advanced west of the Missouri River valley (Chapter 5).

Chloride concentrations are relatively constant in the low-chloride zone suggesting a near constant residence time for the water as chloride concentration would normally increase with age due to diffusion from the Pierre Formation. A rapid recharge event would be necessary to explain the observed narrow range of concentrations in the low-chloride zone. Recharge induced by an overriding ice sheet during the Pleistocene could account for the observed chloride distribution.

Average Linear Velocity from ^{36}Cl. Chloride generally lacks sources and sinks in shallow groundwater systems due to its high solubility and minimal geochemical interaction. This, along with a half-life of 3.01×10^5 a, makes ^{36}Cl ideally suited for dating old (50 ka to 1 Ma) ground water (Bentley et al., 1986). To calculate the age of ground water using ^{36}Cl, the initial ^{36}Cl concentration of the water and the secular equilibrium $^{36}Cl/Cl$ ratio for the aquifer must be known. The secular equilibrium ratio may be determined from field data, provided secular equilibrium has been reached in a distal portion of the aquifer or the secular equilibrium ratio may be calculated using chemical and hydrologic data. Bentley et al. (1986) calculated a typical ratio for ground water in a sandstone aquifer of 4.7×10^{-15}. The initial $^{36}Cl/Cl$ ratio may be estimated using field data from the recharge area or from a published map for the United States. If chloride concentrations increase along the flow path, the additional source of chloride must be accounted for in the calculation of the ^{36}Cl age. For the case of cross-aquifer leakage or diffusion of salt from aquitards, the following equation is employed (Bentley et al., 1986):

$$t = - \lambda^{-1} \ln [C\, C_o^{-1} (R - R_{se}) (R_o - R_{se})^{-1}]$$

where λ is the ^{36}Cl decay constant (2.3×10^{-6} a^{-1})

C is the measured chloride concentration

C_o is the initial chloride concentration

R is the measured ^{36}Cl ratio

R_o is the initial ratio, and

R_{se} is the secular equilibrium ratio.

The travel time from the recharge area to the Missouri River discharge area was estimated using published $^{36}Cl/Cl$ ratios for the Fox Hills aquifer (Davis and Bentley, 1982), the associated chloride concentrations (Croft, 1974; Ackerman, 1977), and a secular equilibrium ratio of 4.7×10^{-15}. Two wells approximately 206 km apart and along a flow line (Figure 17) have ratios of 258×10^{-15} and 10.2×10^{-15} and concentrations of 36 and 560 mg/L, respectively. The calculated travel time is 450k years, yielding an average linear velocity of 0.43 m/yr. This velocity is close to Thorstenson et al.'s (1979) estimate of 0.85 m/yr. Groenewold et al. (1979) report an age of 15 to 20 ka for the upgradient well based on ^{14}C. Thus, the age of the water at the downgradient well is about 465 ka.

Summary

Groenewold et al. (1979) and Thorstenson et al. (1979) studied the hydrochemistry of the Fox Hills aquifer in southwestern North Dakota and observed that water in the recharge area contains primarily sodium, bicarbonate, and sulfate ions, while downgradient water contains primarily sodium, bicarbonate, and chloride ions. They concluded that sulfate reduction in the presence of lignite and Ca-Mg/Na exchange were occurring in the aquifer. The authors attributed the downgradient increases in chloride to leakage from the Pierre Formation or underlying formations. Bentley et al. (1986) have suggested

that the increase in chloride concentrations is due to upward leakage from the Dakota aquifer (Newcastle Formation), which may be replacing the water in the Fox Hills aquifer.

Major ion chemistry data were obtained for 248 wells in the Fox Hills aquifer of southwestern North Dakota from published county reports. Sodium is the dominant cation throughout the aquifer comprising over 90% epm of the cations in 236 of the 248 samples. The anion chemistry data were more variable. Bicarbonate-sulfate and sulfate-bicarbonate (>90% epm) type waters occur in the recharge area along the North Dakota-Montana border and in the discharge area west of the Missouri River in Sioux, Morton, and Grant Counties (primarily where the Fox Hills Formation crops out). Bicarbonate-chloride and chloride-bicarbonate (>90% epm) type waters dominate the remainder of the area. Sulfate reduction and chloride diffusion explain the shift from a sodium-bicarbonate-sulfate type water to a sodium-bicarbonate-chloride type water in the downgradient direction. However, sodium-bicarbonate-sulfate type water in the Fox Hills aquifer in Sioux, Morton, and Grant counties is a water chemistry anomaly suggesting that freshwater recharged the aquifer in it the discharge area. Leakage from the underlying Dakota aquifer cannot explain the anomalous water chemistry in the Fox Hills aquifer because the Dakota aquifer yields sodium-chloride type water in south-central North Dakota west of the Missouri River. The shape of the sodium-bicarbonate-sulfate type anomaly is similar to that of the Fox Hills Formation subcrop, suggesting that the freshwater entered the Fox Hills aquifer along the formation subcrop.

A low-chloride (<1 meq/L) zone occurs just west of the Missouri River, principally in the Fox Hills Formation subcrop/outcrop area. This low-chloride zone coincides with the sodium-bicarbonate-sulfate type water anomaly identified in Sioux, Grant, and Morton counties. To dilute the upgradient water

(>9 meq/L Cl) to <1 meq/L Cl would require approximately 9 parts freshwater to 1 part upgradient water. In the southeastern corner of Grant County, where the chloride concentrations drop from >6 meq/L to < 1 meq/L in a 6 km stretch along the groundwater flow path, a 500% increase in the volume of water would be required as the water moves downgradient through this region. Such an increase in the water volume would require recharge on the order of 4.3 to 8.5 mm/yr, only in the narrow band with chloride concentrations in the range of 1 to 6 meq/L. Neither the literature or water-level maps of the aquifer suggest any unusual conditions that are restricted to this region. It is unlikely that local recharge under present climatic conditions could explain this increase in water volume.

Chloride concentrations are relatively constant in the low-chloride zone suggesting a near constant residence time for the water as chloride concentration would normally increase with age due to diffusion from the Pierre Formation. A rapid recharge event would be necessary to explain the observed narrow range of concentrations in the low-chloride zone.

The travel time from the recharge area to the Missouri River discharge area was estimated using published $^{36}Cl/Cl$ ratios for the Fox Hills aquifer, the associated chloride, and a secular equilibrium ratio of 4.7×10^{-15}. The calculated travel time is 450k years, yielding an average linear velocity of 0.43 m/yr.

The hydrogeochemical investigation does not support hypothesis (a), that upgradient aquifer water is a significant source of the water in the discharge area of the Fox Hills aquifer in Sioux, Grant, and Morton counties. In addition, hypotheses (b) and (e), local precipitation/recharge and leakage from adjacent aquifers, are not supported by the hydrochemical investigation and this is consistent with the results of the hydrogeological investigation (Chapter 2).

CHAPTER 4: STABLE ISOTOPE HYDROLOGY

Literature Review

Stable isotopes of hydrogen and oxygen are useful tracers in hydrogeological investigations. Incorporated into the water molecules themselves, the stable isotopes, deuterium (D) and oxygen-18 (^{18}O), are generally considered conservative in low-temperature environments (IAEA, 1983).

Isotopic concentrations of water samples are compared to an internationally agreed upon standard, Standard Mean Ocean Water (SMOW), and expressed as the deviations (d per mil) from SMOW (IAEA, 1983):

$$\delta \text{ per mil} = (R_{sample}/R_{SMOW} - 1)\ 10^3$$

where R is the ratio of the rare to common isotope. Positive δ values indicate excess with respect to the standard; negative values, depletion.

Atmospheric Waters. Craig (1961) found that the $\delta^{18}O$ and δD values in precipitation and fresh waters generally plot along a straight line ($\delta D = 8\ \delta^{18}O + 10$). This line is referred to as the global meteoric water line. The International Atomic Energy Agency (IAEA), in association with the World Meteorological Organization, established a worldwide network of 144 stations to survey hydrogen and oxygen isotope concentrations in precipitation. The relationship between $\delta^{18}O$ and δD for these stations ($\delta D = (8.08 \pm 0.8)\ \delta^{18}O + (9.57 \pm 0.62)$) is similar to the global meteoric water line of Craig (1961; Yurtsever and Gat, 1981). The isotope composition for continental stations in North America is described by the relationship (Yurtsever and Gat, 1981):

$$\delta D = (7.95 \pm 0.22)\ \delta^{18}O + (6.03 \pm 3.08).$$

A recent study by the North Dakota State Water Commission determined the following local meteoric water line for Oakes, North Dakota (approximately 200 km east of the study area) based on 19 precipitation samples collected from April 2, 1989 to April 16, 1990 (Shaver, personal communication):

$$\delta D = (7.83 \pm 0.38)\ \delta^{18}O + (6.99 \pm 5.53).$$

This local meteoric water line for North Dakota is similar to the North America continental meteoric water line.

Dansgaard (1964) related the degree of depletion to geographic and climatological parameters such as latitude, altitude, distance from the coast, the amount of precipitation, and temperature. Temperature was found to be the major parameter determining the isotopic composition of precipitation, which is expressed by the following empirical equations (Dansgaard, 1964):

$$\delta^{18}O = 0.695\ T_a - 13.6 \text{ per mil, and}$$

$$\delta D = 5.6\ T_a - 100 \text{ per mil,}$$

where T_a is the local mean annual air temperature.

Dansgaard's (1964) conclusion was supported by a subsequent study (Yurtsever and Gat, 1981) that was conducted on a larger sample data base and employed multiple linear regression techniques. Yurtsever and Gat show that the mean isotopic composition of precipitation is described primarily by average monthly temperature. Correlation to other geographical parameters was found to be not significant. Although Yurtsever and Gat assert that these findings reflect the situation on a global scale, these authors also indicate that the amount effect or evaporation effect may be important factors on a regional scale (Yurtsever and Gat, 1981).

Lake Waters. Lakes, as well as other surface waters, are subject to evaporation even with short exposure time. This evaporation results in an enrichment of the isotope content of the water body (Fontes, 1980) and a

diversion of the data from the meteoric water line. The $\delta^{18}O$-δD relationship for evaporating water bodies is linear with a slope less than 8, generally 2 to 5 (Fontes, 1980). Hwang (1982) collected surface water samples from 14 sloughs in Oliver County, North Dakota (approximately 75 km north of the study area) during the period from 1978 to 1980. The $\delta^{18}O$-δD relationship for these samples is:

$$\delta D = 5.55\ \delta^{18}O - 26.45,$$

clearly showing that evaporation is affecting the stable isotope composition of the slough waters.

Ice and Snow. The d-values of local snow and rain falling on an ice sheet reflect the local temperature and altitude effect. Snowmelt and rain, with relatively high d-values, percolating through lighter snow and ice causes a homogenization of the D and ^{18}O contents for long residence times, with a general increase in the d-value of the solid phase (Moser and Stichler, 1980; Arnason, 1981). Oxygen-isotope profiles of deep ice cores from polar ice sheets can provide information on paleoclimates. Dansgaard and Tauber (1969) estimated the mean $\delta^{18}O$ content of the Laurentide ice sheet to be -30 per mil based on the location of the ice sheet divide, altitude effect, and a cooler climate. Neglecting isotopic enrichment, the expected $\delta^{18}O$ content of subglacial meltwater would be about -30 per mil.

Ground Water. The stable isotope content of ground water is generally expected to reflect the average local climatic condition of the aquifer's recharge area (Fontes, 1981). Preferential seasonal recharge gives more relative weight to recharge waters of cold or humid periods. This has been observed for the Oakes aquifer (Shaver, personal communication) of North Dakota (approximately 200 km east of the study area), where the average $\delta^{18}O$ value of 29 water samples (-12.9) is similar to the weighted mean precipitation for

November through mid-June (-12.7). Snowmelt and spring rain are assumed to be the source of recharge to the Oakes aquifer (Shaver, personal communication). High evaporation rates in an aquifer's recharge area also affect the isotopic composition of groundwater. The New Rockford aquifer, Wells County, North Dakota exhibits a δD-$\delta^{18}O$ relationship of

$$\delta D = 6.1\ \delta^{18}O - 24.5,$$

based on 26 groundwater samples (Patch and Knell, 1988) indicating that evaporation of precipitation/surface water occured prior to recharge.

The climate dependence of the isotopic composition of groundwater results in a relatively constant stable isotope content within an aquifer. Variations within an aquifer may occur due to isotope exchange with the aquifer matrix, mixing of waters of different origins, and large climatic changes (Gat, 1981). Water and aquifer materials are generally in isotopic disequilibrium. Isotope exchange moves the system toward equilibrium. Only oxygen isotopes are affected by this process, since the hydrogen content of geologic materials is generally too low to induce significant isotope exchange (Panichi and Gonfiantini, 1981). The extent of oxygen isotope exchange depends on (1) the relative proportions of oxygen in the water aquifer matrix, (2) the initial ^{18}O contents, (3) the specific water-mineral fractionation factors, and (4) the time and surface of contact. This exchange process usually is negligible at normal temperatures due to the temperature dependence of water-mineral fractionation factors (Panichi and Gonfiantini, 1981).

Paleowaters. Atmospheric waters precipitated in the past, generally over 10,000 years ago, are referred to as paleowaters. Paleowaters, such as Pleistocene waters associated with glacial events, often originated in a different climatic regime. These climate changes are recorded in the stable isotope

composition of the ground water. Paleoclimate signatures may be assigned based on differences in $\delta^{18}O$ and δD, deuterium excess, or both (Fontes, 1980).

Deuterium excess is defined by Dansgaard (1964) as

$$d \equiv \delta D - 8\,\delta^{18}O.$$

Merlivat and Jouzel (1979) determined that the deuterium excess, or d-excess, is primarily a function of the initial relative humidity (h) over the area of vapor production. They calculated d-excess values of ocean-derived vapor for various relative humidities, e.g., for h = 0.8, d = 10.7, and for h = 0.9, d = 5.4. A continuous d-excess profile obtained from an East Antarctic ice core shows d-excess values 4.5 per mil lower for the coldest part of the last ice age (circa 18 ka) than for the past 7.5 ka (Jouzel et al., 1982). This shift in d-excess is attributed to a change in relative humidity over the source area for Antarctic precipitation (Jouzel et al., 1982). Jouzel et al. (1982) also observed an apparent time-lag of 2,500 yr for ^{18}O following the decrease in d-excess.

Data Collection

Eleven water samples were collected from North Dakota State Water Commission (NDSWC) wells in Sioux, Grant, and Morton counties for ^{18}O and D analyses (Figure 19). The samples were collected from the screened interval without prior purging. Robin and Gilham (1987) have suggested that depth-discrete sampling without prior purging may, in some cases, be preferrable. They found that a continual flow of ground water through the screened interval can be maintained indicating that water in the screened interval would be representative of the natural ground water. Kearl et al. (1992) observed horizontal laminar flow in the screened interval in the same direction as local groundwater flow using a borescope, supporting Robin and Gilham's results and

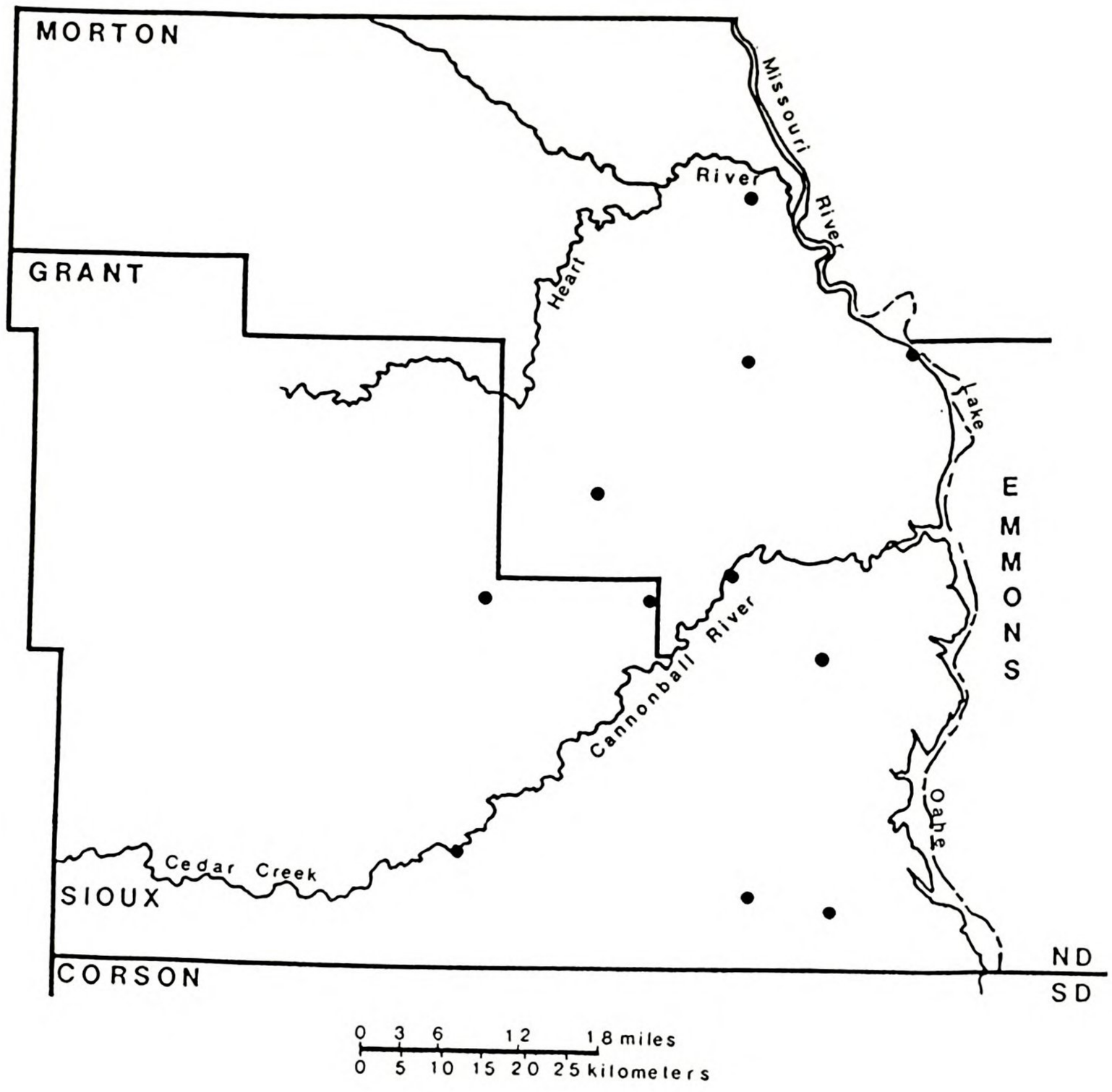

Figure 19. Location of stable isotope water samples.

indicating that water in the overlying casing does not mix with the water in the screen. Kearl et al. conclude that diffusion of gases into or out of the ground water is the only mechanism that could influence water chemistry in the screened interval. The thickness of the diffusive boundary layer is calculated using (Kearl et al., 1992):

$$\delta \sim 2(D_{AB}t)^{½}$$

where δ is the diffusive boundary layer

D_{AB} is the binary diffusivity coefficient of gas A in solute B; 10^{-5} cm^2/sec, and

t is time, taken as the diameter of the borehole divided by the groundwater flow velocity.

The maximum thickness of the diffusive boundary layer for a 3.175 cm well with a wellbore flow velocity of 0.43 m/yr (average linear velocity for the Fox Hills aquifer) is 9.65 cm. The well screens in the NDSWC wells are generally 2 to 7.4 m long, allowing samples to be taken well below the bottom of the casing; that is, in fresh formation water and, therefore, without fear of drawing stagnant water into the sampler. No artificial filter packs have been used in these monitoring wells that might influence the chemistry of the water in the screened interval.

Data Analysis and Interpretation

The water samples were analyzed at the Environmental Isotope Laboratory, University of Waterloo. The data are plotted on a $\delta^{18}O$-δD graph (see Figure 20) and a best-fit line was determined with slope 8.58 and intercept 15.2 (correlation coefficient = 0.9158). The slope and intercept are considerably greater than the values estimated for meteoric waters in North America

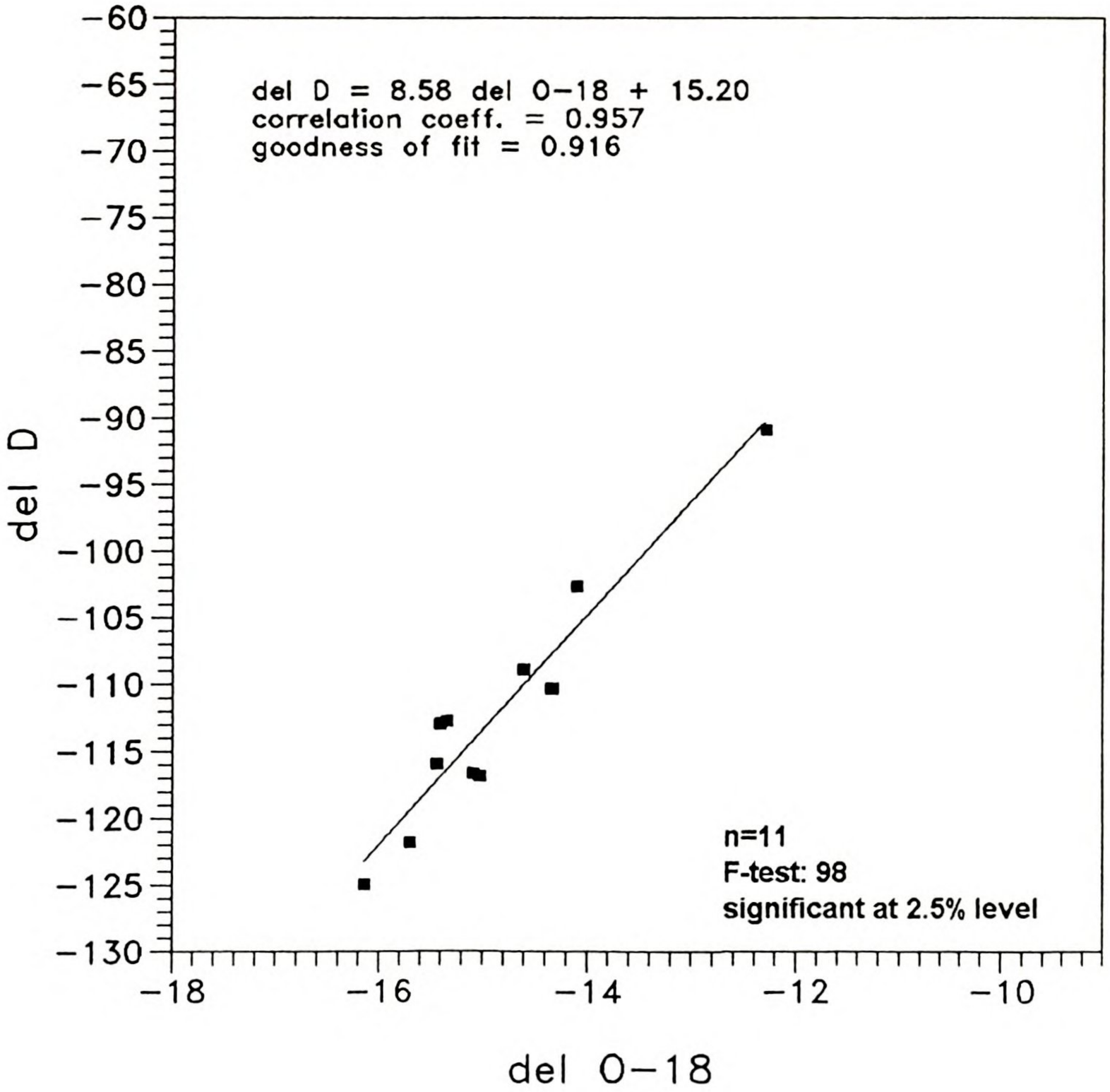

Figure 20. δD-$\delta^{18}O$ relationship of the Fox Hills aquifer water samples.

(7.95±0.22 and 6.03±3.08, respectively) and at Oakes, North Dakota (7.83±0.38 and 6.99±5.53, respectively). A plot of d-excess versus $\delta^{18}O$ (Figure 21) shows that the samples fall within three distinct groupings defined by d-excess values of approximately 4, 7.5, and 10. However, the $\delta^{18}O$ values show no correlation with d-excess. This suggests that three paleowaters are present in the study area that were precipitated under similar climatic conditions. Replotting the data on $\delta^{18}O$-δD graphs according to the d-excess groupings (Figure 22) produces slopes between 7.92 and 8.06 and intercepts between 4.91 and 9.57, with correlation coefficients of 0.9977 to 0.9998 (significant at the 2.5% level, based on F-tests). These values are consistent with both the North American meteoric water line and the local (Oakes, North Dakota) meteoric water line. The slopes indicate that the ground waters are of meteoric origin and unaffected by fractionating processes. Thus, evaporation prior to recharge (e.g. proglacial lakes) is not indicated by the stable isotope data.

Plotting d-excess values on a map of the chloride distribution (Figure 23) shows that all but one of the samples with d-excess values in the 7.5 and 10 groupings fall within the low-chloride zone identified in Chapter 3. All but one of the samples outside the low-chloride zone have d-excess values around 4. This suggests that two different paleowaters are present in the discharge area--a low-chloride, high d-excess water and a high-chloride, low d-excess water. The t test was used to test whether the means of the two waters are the same (Davis, 1986). The results (t=1.88 with 9 degrees of freedom) indicate that the two waters are different at the 10% significance level (α=0.10). Equality of variances, a requirement for the t test, was confirmed by the F test (1.31 for 4/5 degrees of freedom). One sample in the high chloride zone along the Missouri River has a d-excess value of 10.1; one sample in the low chloride zone has a d-

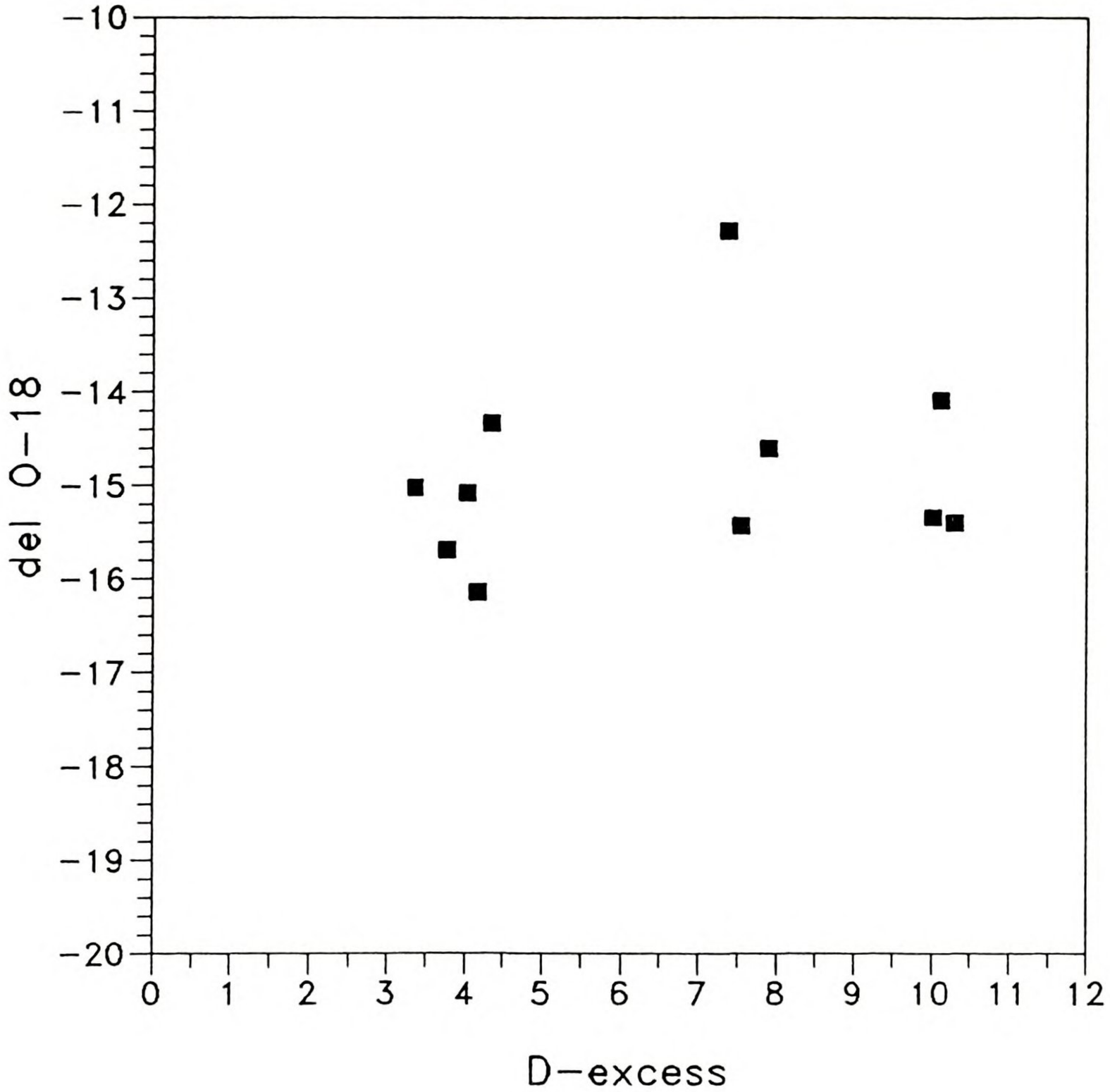

Figure 21. Deuterium excess-$\delta^{18}O$ relationship of the Fox Hills aquifer water samples.

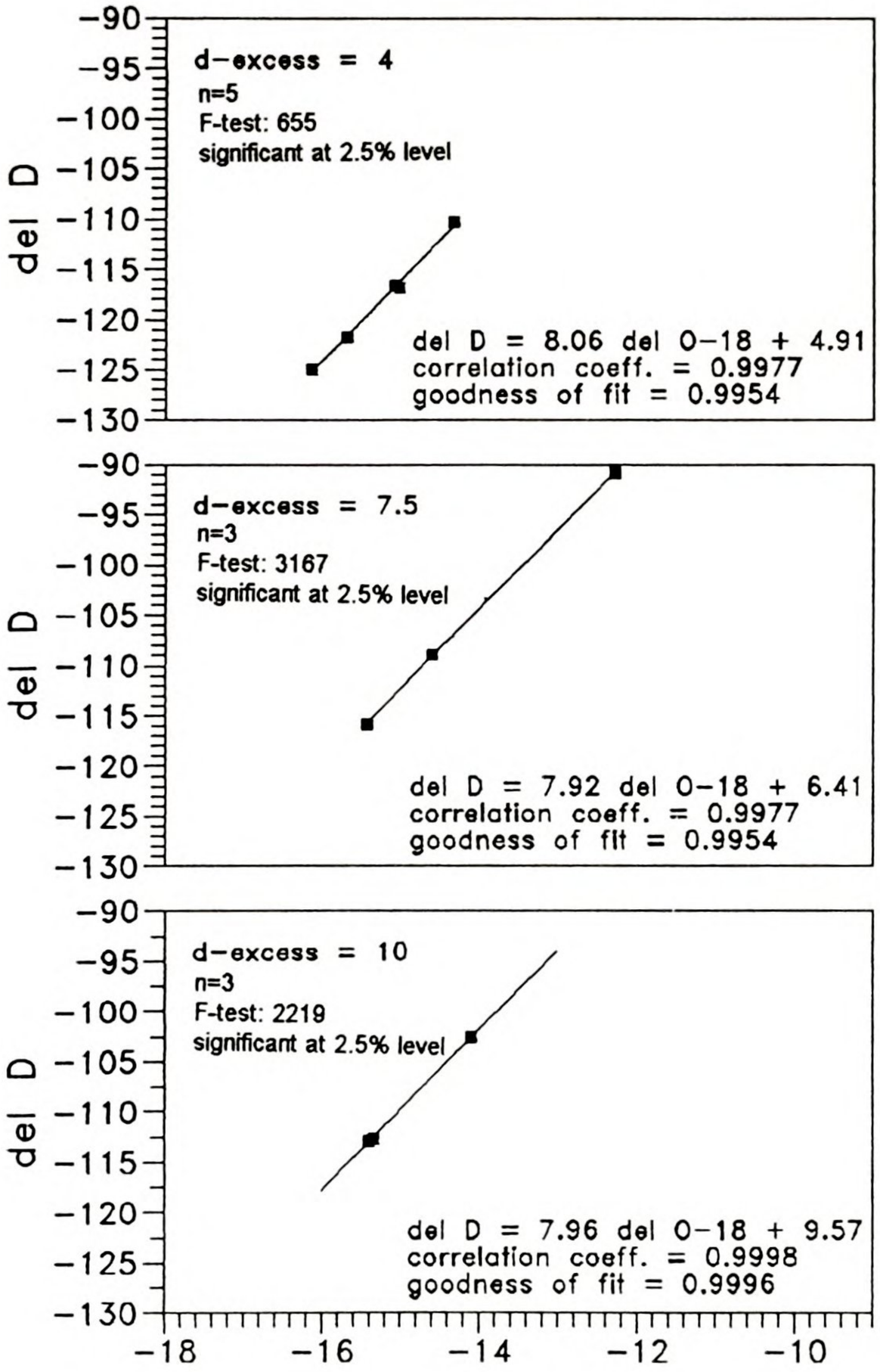

Figure 22. δD-$\delta^{18}O$ relationship by d-excess groupings.

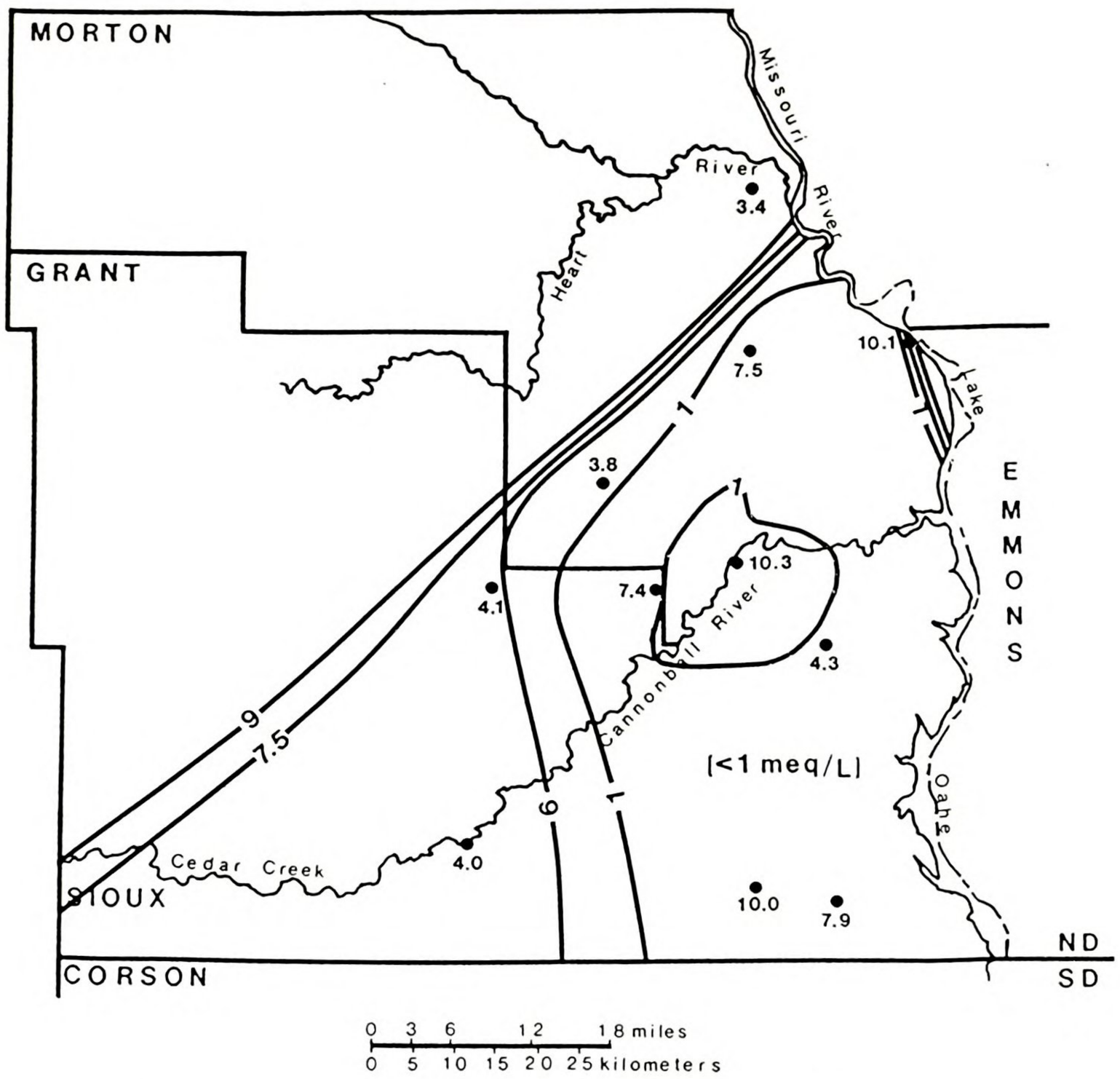

Figure 23. Deuterium-excess values plotted with the chloride distribution.

excess value of 4. As noted above, the d-excess values for the water in the low-chloride zone fall into two grouping, one around 7.5 and the other around 10. One could speculate that this suggests that more than one recharge event provided the low-chloride water in the discharge area, although at this time there is insufficient data to test the hypothesis.

The expected values of $\delta^{18}O$ and δD for precipitation in Sioux and Morton counties were calculated using mean annual temperature and Dansgaard's (1964) temperature equations. For a mean annual temperature of 6.2°C (Fort Yates, Sioux County), $\delta^{18}O$ and δD would be -9.3 and -65.3 per mil, respectively. These values are consistent with the stable isotope distribution map for North America (Drever, 1982).

The groundwater samples collected from the Fox Hills aquifer are considerably lighter than modern precipitation, indicating that recharge occurred under cooler climatic conditions. However, the samples are not as light as would be expected for glacial ice. Mean annual temperature of each sample was calculated using Dansgaard's (1964) temperature equation and the respective $\delta^{18}O$ values (see Table 1). The sample temperatures were 6.9 to 9.9°C cooler (-16.1 to -14.1 $\delta^{18}O$) than modern precipitation (-9.3 $\delta^{18}O$) for all but one sample, which yielded a temperature 4°C cooler (-12.3 $\delta^{18}O$) than modern. It was collected at a location where the Fox Hills subcrops below a glacial valley aquifer that receives its recharge via infiltration and Hell Creek aquifer discharge. Water levels in the Fox Hills and the glacial aquifer are within a meter of each other. Two explanations for this isotopic value are offered: mixing of aquifer waters and preferential seasonal recharge.

First, waters may be mixing between the Fox Hills and glacial aquifers. To test the mixing hypothesis, the isotopic composition for modern precipitation was plotted on a $\delta^{18}O$-δD graph along with the Fox Hills aquifer values (Figure

Table 1. Stable isotope data from the discharge area of the Fox Hills aquifer.

Location			del O-18	del D	Temp	delta Temp	D-excess
T	R	Sec	(per mil)	(per mil)	(C)	(C)	(per mil)
129N	081W	01BAB	-14.6	-108.9	-1.4	7.6	7.9
130N	082W	36BBC	-15.34	-112.7	-2.5	8.7	10.02
130N	085W	17DAA	-15.08	-116.6	-2.1	8.3	4.04
133N	080W	31CCD1	-14.33	-110.3	-1.1	7.3	4.34
133N	083W	12ADA1	-12.28	-90.85	1.9	4.3	7.39
133N	085W	12AAD	-16.14	-124.95	-3.7	9.9	4.17
134N	082W	36DCD	-15.4	-112.9	-2.6	8.8	10.3
135N	083W	32CBB1	-15.69	-121.75	-3.0	9.2	3.77
136N	079W	05CCC	-14.09	-102.6	-0.7	6.9	10.12
136N	081W	07DDC1	-15.43	-115.9	-2.6	8.8	7.54
138N	081W	09ABB1	-15.02	-116.8	-2.0	8.2	3.36
Reported del O-18 and del D values may be average of 2 replicates							
Raw data is in Appendix D							
Temperature determined from: Temp = (13.6 - del O-18) / 0.695							
delta Temperature determined from: delta Temp = 6.2 - Temp							
Deuterium excess determined from: D-excess = del D - 8 del O-18							

24). The resulting best-fit line could represent a mixing line, supporting the conjecture that light water in the Fox Hills aquifer may have been mixed with heavier glacial aquifer water.

A second explanation for the -12.3 ($\delta^{18}O$) sample is that the Fox Hills aquifer is receiving seasonal recharge (late winter through spring) via the glacial aquifer. The $\delta^{18}O$ value of -12.3 is similar to that observed for the Oakes (glacial) aquifer (-12.9), which receives seasonal recharge (Shaver, personal communication). Assuming the -12.3 $\delta^{18}O$ to be modern recharge, the Fox Hills aquifer water samples exhibit temperatures 2.6 to 5.6°C cooler than modern.

A global circulation model and energy balance model have been used to simulate temperature changes over the past 18,000 years (Hyde et al., 1989). These models suggest that the mean annual temperature at 43°N latitude was about 4 to 7.5°C cooler than modern during the last glacial maximum 18,000 years ago. Earlier glacial advances may have occurred under similar climatic conditions. Thus the Fox Hills aquifer water isotopic composition may represent recharge during the Pleistocene when ice sheets advanced into the aquifer's discharge area.

The meltwater from Pleistocene subglacial ice would be expected to have $\delta^{18}O$ values of around -30 per mil, as stated above. The observed $\delta^{18}O$ values are considerably heavier than this. The average $\delta^{18}O$ value for the samples, excluding the sample that may represent modern preferential recharge, is -15.1. Mixing of two waters with end points of -12.3, for local precipitation recharge, and -30, for subglacial ice meltwater, would produce a water with $\delta^{18}O$ = -15.1 for an 84% and 16% contribution, respectively. If the $\delta^{18}O$ value of the local precipitation recharge was lower than -12.3 during the Pleistocene, an even smaller contribution would come from subglacial meltwater.

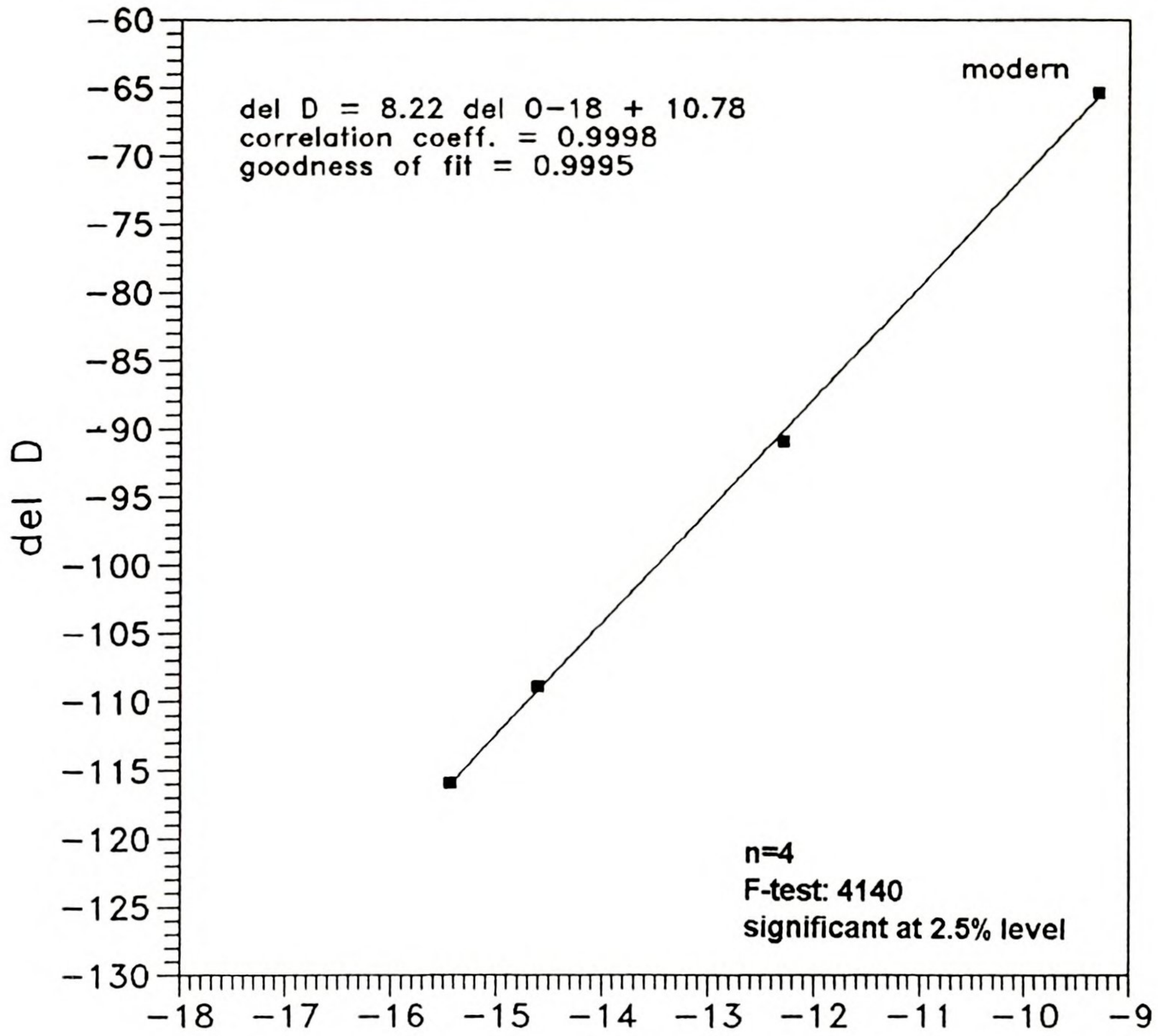

Figure 24. Mixing line of modern and paleowater.

Summary

Stable isotopes of hydrogen and oxygen are useful tracers in hydrogeological investigations because they are generally considered conservative in low-temperature environments. The stable isotope content of ground water is generally expected to reflect the average local climatic condition of the aquifer's recharge area. Paleowaters may be identified based on differences in $\delta^{18}O$ and δD, deuterium excess, or both.

Eleven water samples were collected from North Dakota State Water Commission wells in Sioux, Grant, and Morton counties for ^{18}O and D analyses. The samples fall within three distinct groupings defined by d-excess values of approximately 4, 7.5, and 10. However, the $\delta^{18}O$ values show no correlation with d-excess suggesting that, although three paleowaters are present in the study area, they were precipitated under similar climatic conditions. The slopes of the $\delta^{18}O$-δD graphs, plotted according to the d-excess groupings, are consistent with both the North American meteoric water line and the local (Oakes, North Dakota) meteoric water line. The slopes indicate that the ground waters are of meteoric origin and unaffected by fractionating processes. Thus, evaporation prior to recharge (e.g. proglacial lakes) is not indicated by the stable isotope data.

Two different paleowaters are present in the discharge area--a low-chloride, high d-excess (7.5 and 10) water and a high-chloride, low d-excess (4) water. All samples outside the low-chloride zone have d-excess values about 4, suggesting a single source for these waters. The d-excess values for the water in the low-chloride zone fall into two grouping, one around 7.5 and the other around 10, possibly related to more than one recharge event.

Calculated temperatures for the samples using $\delta^{18}O$ were 6.9 to 9.9°C cooler (-16.1 to -14.1 $\delta^{18}O$) than modern precipitation (-9.3 $\delta^{18}O$) for all but one

sample, which yielded a temperature 4°C cooler (-12.3 $\delta^{18}O$) than modern. Assuming the -12.3 $\delta^{18}O$ sample to be modern recharge, the Fox Hills aquifer water samples exhibit temperatures 2.6 to 5.6°C cooler than modern.

A global circulation model and energy balance model suggest that the mean annual temperature at 43°N latitude was about 4 to 7.5°C cooler than modern during the last glacial maximum 18,000 years ago. Earlier glacial advances may have occurred under similar climatic conditions.

The stable isotope investigation supports hypothesis (c), that the water in the discharge area of the Fox Hills aquifer in Sioux, Grant, and Morton counties is derived from local precipitation recharged during the Pleistocene. Hypotheses (b) and (e), local precipitation/recharge and leakage from adjacent aquifers, are not supported by the isotope data and this is consistent with the results of the hydrogeological and hydrogeochemical investigations. In addition, hypothesis (d) and (f), leakage from proglacial lakes and subglacial meltwater as the major source of the anomalous water body, are not supported by the stable isotope investigation.

CHAPTER 5: POSSIBLE PALEOHYDROLOGIC RESPONSES TO PLEISTOCENE GLACIATION

Literature Review

Various researchers have suggested that groundwater flow patterns in certain aquifers may have been altered during the Pleistocene because glacial ice blocked their regional discharge areas, glacial meltwater was available for recharge, and some geologic materials were compressed under the weight of overriding ice sheets. The development of the glacial meltwater recharge hypothesis is discussed below. An examination of the hydrology of glaciers is then presented to expand the meltwater hypothesis to include snowmelt and rain transported via the englacial drainage system.

Glacial Meltwater Recharge Hypothesis. One of the earliest presentations of the glacial meltwater recharge hypothesis is the glacial-artesian model proposed by McGinnis (1968) to explain the origin of Mississippi Valley-type zinc-lead deposits. He notes that since ice sheets tend to move toward topographically low areas they also tend to override and block regional groundwater discharge areas. McGinnis suggests that a hydrologic connection between the base of the ice sheet and groundwater in the discharge area might develop, resulting in altered groundwater flow patterns and recharge of the aquifer with meltwater.

Early studies, such as McGinnis's, attempted to explain groundwater chemistry anomalies. Gilkeson et al. (1981) studied the hydrochemistry of the Cambrian-Ordovician aquifer in northeastern Illinois and identified an anomalously high enrichment of ^{34}S. They postulate that the anomalous water was glacial basal meltwater injected into the aquifer due to the pressures

induced by the glacial ice overburden. Siegel (1983) also examined the problem of anomalous water chemistry in the Cambrian-Ordovician aquifer, though on a larger, regional scale. He presents a simple numerical model of glacial recharge to the aquifer system that indicates flow paths could be reversed due to glaciation. Filley and Parizek (1983) and Filley (1985) extended Siegel's work by investigating the potential impact of the Wisconsinan Lake Michigan Lobe on the Cambrian-Ordovician aquifer and two adjacent aquifers in northern Illinois using a more sophisticated numerical model. The results of their model indicate that rates and directions of groundwater flow may have been significantly altered. During glacial advance, groundwater flow was reversed locally resulting in the convergence of waters of consolidation (forced out of adjacent shale units) with waters transported from the upgradient recharge area. During ice sheet equilibrium, basal glacial water percolated into the groundwater system. Their results supported Gilkeson et al.'s explanation of the anomalous water. Recently, Siegel (1991) investigated a water chemistry anomaly in the Cambrian-Ordovician aquifer of Iowa. He suggests that the anomalous water body entered the deep aquifer as vertical recharge of subglacial meltwater from the Wisconsinan Des Moines Lobe.

Recent studies have focused on the relationship of subglacial deformation and subglacial discharge as a means of determining glacier properties. Mooers (1990) presents a numerical model of the ice-margin thermal regime of the Rainy Lobe in Minnesota. He calculates that subglacial meltwater production exceeded the amount that could refreeze to the base of the ice sheet. Tunnel valleys and eskers, which would indicate the presence of subglacial streams, are rare along the portion of the ice margin studied by Mooers (1990). Thus, Moors concludes that the excess water entered a subglacial aquifer as recharge and then discharged beyond the ice margin. Another significant contribution is that

of Boulton and Dobbie (1993). They develop a theory of subglacial consolidation that addresses the discharge of excess meltwater (i.e., through channels, as a thin film, and/or by groundwater flow). Boulton and Dobbie indicate that the subglacial drainage pathway is determined by the permeability of the underlying geologic material and the water potential gradient. If the glacier overlies an aquifer of high permeability and a water potential below that of the ice, all the meltwater will enter the aquifer. They suggest that many such aquifers have been overridden by Pleistocene ice sheets. However, if the glacier overlies a less permeable material, at least some of the meltwater will pond on the surface of the substratum and discharge by channel flow or sheet flow. They applied the theory to both one-dimensional and two-dimensional cases of subglacial groundwater flow depending on whether the ice sheet was separated from the aquifer by a low permeability zone (e.g. till) or directly overrode the aquifer, respectively. Boulton and Dobbie satisfactorily tested the theory (both models) using data from field sites in The Netherlands and England.

As noted in the Introduction, the literature supports the possibility that the Fox Hills aquifer was influenced by Pleistocene glaciation. In the USGS Regional Aquifer System Analysis (RASA) report on the hydrogeology of the NGPAS, Downey (1986) suggests the possibility of meltwater recharge and altered groundwater flow patterns due to glaciation. He notes that during Pleistocene glaciation, the regional discharge area along, and east of, the Missouri River was covered by glacial ice that may have blocked discharge and redirected flow to the southeast (Figure 25). In addition, meltwater at the base of the glacier would have had significant potential for downward migration, i.e., temporary recharge may have occurred in the discharge area.

Hydrology of Glaciers. The studies presented thus far have assumed that the glacial meltwater recharge is derived from melting at the base of the ice

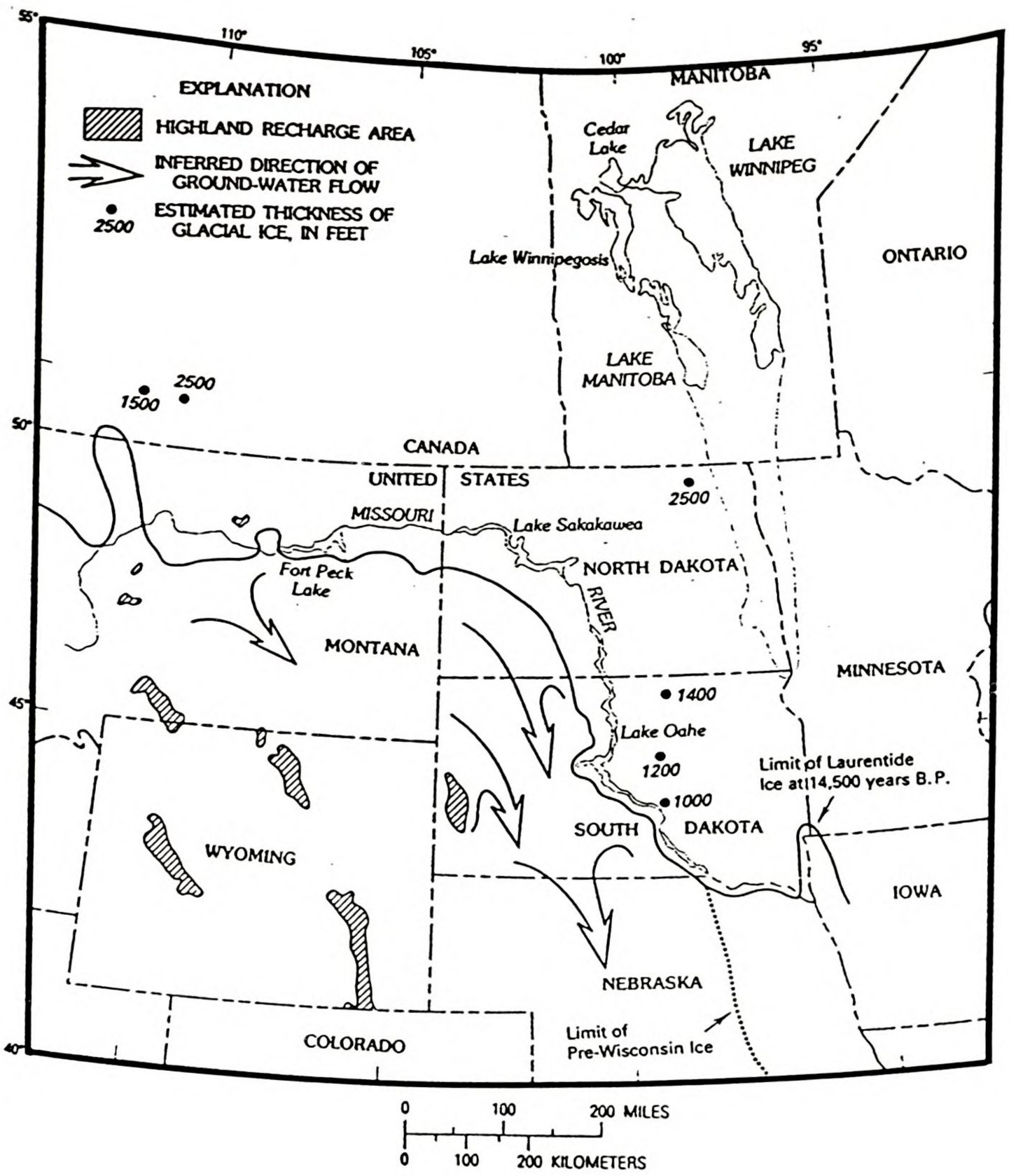

Figure 25. Inferred groundwater flow directions during Pleistocene glaciation (Downey, 1986).

sheet. Surface water, however, is the most important source of water in temperate glaciers (Shreve, 1972; Paterson, 1981). Paterson (1981) identifies various sources for the water at a glacier bed (Figure 26), including surface meltwater, rain, basal meltwater (geothermal and frictional), and meltwater from heat of deformation. Surface meltwater, produced by ablation processes, and rain commonly contribute several meters per unit area per year. Geothermal heat typically melts about 6 mm of ice from the base of the ice, as does frictional heat if the sliding velocity is about 20 m/a. Heat of deformation within the glacier contributes a small amount of water.

During the melt season, water associated with temperate glaciers is drained by a system that includes superglacial, englacial, and subglacial parts (Shreve, 1972). The superglacial drainage follows surface channels, similar to a river system, that eventually empty into moulins (vertical channels and cracks in the ice) and crevasses that are part of the englacial system. Shreve (1972) has likened the flow of water in the englacial system, which reaches from the ice surface to its bed, to that of groundwater flow through karst terrain. Via the englacial system, surface meltwater and rain may be transported to the glacier base (Figure 26).

Water at the base of a glacier (subglacial) may be discharged as sheetflow along the glacier's bed, flow in channels or linked cavities along the bed, groundwater flow through subglacial materials, or a combination of these (Kamb, 1987; Boulton and Dobbie, 1993). The character and geometry of the subglacial materials determine the rate of groundwater recharge. Where low permeability material, such as till, overlies a highly permeable aquifer, water drains vertically downward through the aquitard and into the aquifer. Flow in the aquifer is assumed to be horizontal toward the glacier toe. If the aquitard

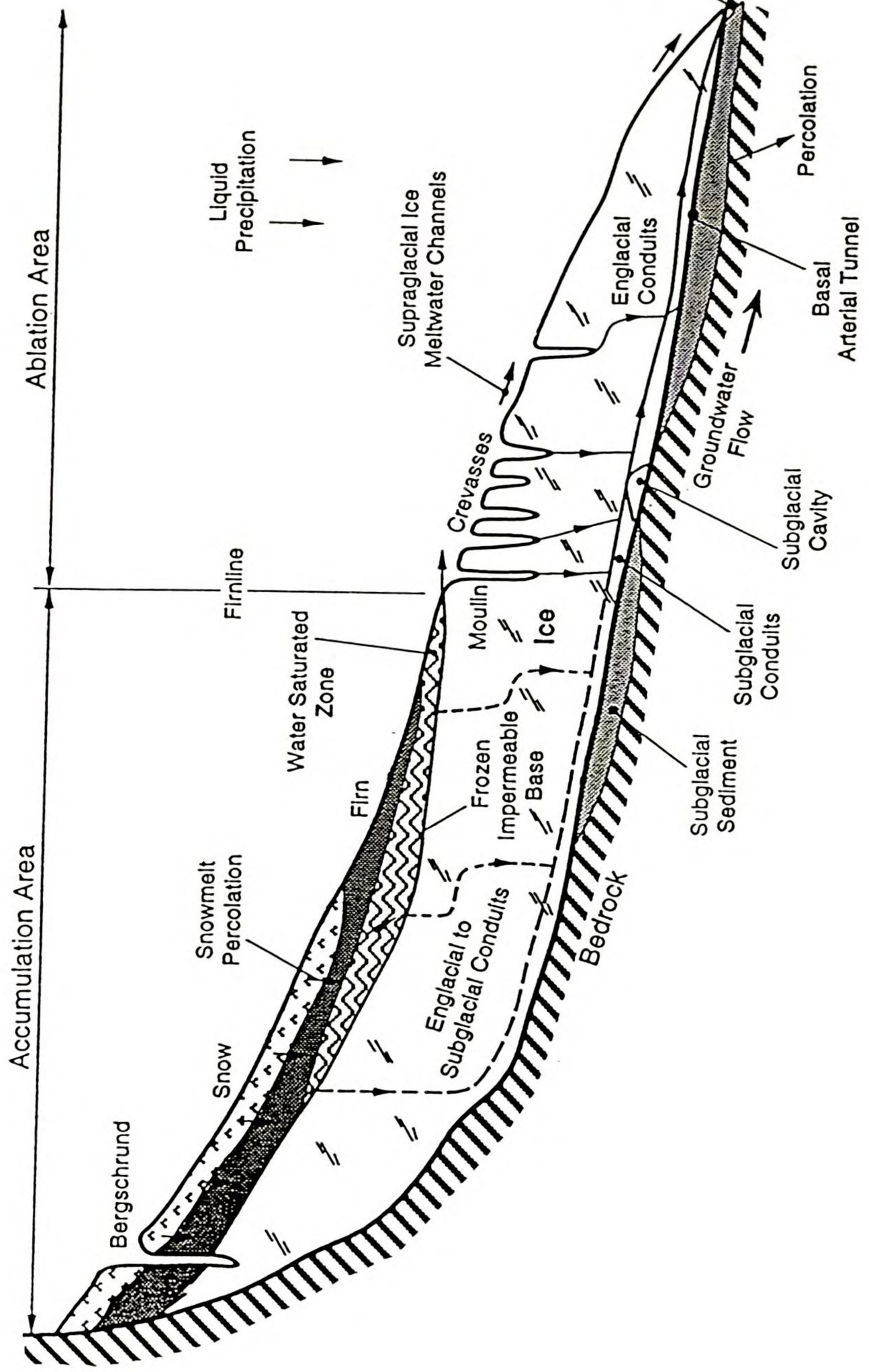

Figure 26. Schematic diagram of glacier hydrology (Lawson, 1993).

pinches out at the glacier terminus, the water will be discharged into the proglacial zone (Boulton and Dobbie, 1993).

Data Analysis and Interpretation

Modeling the response of an aquifer to Pleistocene glaciation is a speculative endeavor because of our limited knowledge of both the pre-glaciation aquifer system and the ice sheet configuration and hydraulics. Assumptions must be made that will directly influence the outcome of the simulation. Thus, attempts at simulating an aquifer's response to glaciation can only indicate the feasibility of various postulated ways in which the aquifer could have behaved under the specified conditions. The results of the simulations do not provide quantitative information on the physical/conceptual system.

With these limitations in mind, the hydrologic responses of the Fox Hills aquifer to glaciation-related stresses were simulated using a 2-D finite difference model, SAM4 (Kinzelbach, 1986), with an iteration error limit of 0.05 m. The simulations were first attempted assuming transient conditions; however, it became clear that the system reached equilibrium in a short time, 150-200 years. Since glacial episodes probably occurred on the order of a few thousand years, steady-state conditions were assumed for subsequent simulations. The governing equation and model grid are the same as those presented in Chapter 2, as are the assigned transmissivity and initial water-level values. A new set of boundary conditions are imposed on the model as discussed below. Four simulations were conducted. First, the model was run with new boundary conditions and without any additional stresses to test the validity of using the new boundary conditions. Second, Lake McKenzie was added as a constant head feature. Third, the discharge area was reduced in areal extent to mimic the

affect of the Verone ice sheet blocking discharge. Fourth, recharge was assigned to grid nodes where the Fox Hills Formation subcrop was overridden by the Verone ice sheet.

Simulation 1: present conditions. The present water-level distribution in the Fox Hills aquifer was simulated using prescribed head boundaries on the west and south edges of the modeled area, as before, but with no flow boundaries along the north and east edges of the modeled area (Figure 27). The northern boundary falls along a streamline and thus may be modeled as a no flow boundary. The eastern boundary falls along the Missouri River. As stated in Chapter 2 and shown in Figure 4, the Fox Hills Formation is eroded away along much of the Missouri River valley and, as the main discharge area for the aquifer, the Missouri River valley represents a hydrologic barrier. Thus the eastern boundary may be modeled as a no flow boundary. Discharge nodes were assigned as in the model in Chapter 2. The only difference between the two simulations is the north and east boundary conditions. The simulated head distribution (Figure 28) is similar to the observed head distribution. Groundwater movement is generally eastward toward the Missouri River valley with deviations toward the Cannonball and

Heart rivers valleys. The new boundary conditions are thus considered acceptable for the following simulations of stressed conditions.

Simulation 2: Lake McKenzie. The first recognizable Late Wisconsin glacial advance in North Dakota was most likely in its wasting stage when it reached the south-central portion of the state (Bluemle, 1984). Drainage was probably diverted southeastward along the Strasburg Channel until it was blocked by the advancing ice sheet, resulting in proglacial Lake McKenzie (Bluemle, 1984). In this simulation, it is assumed that Lake McKenzie is in direct communication with the Fox Hills aquifer, so that the maximum affect of the lake

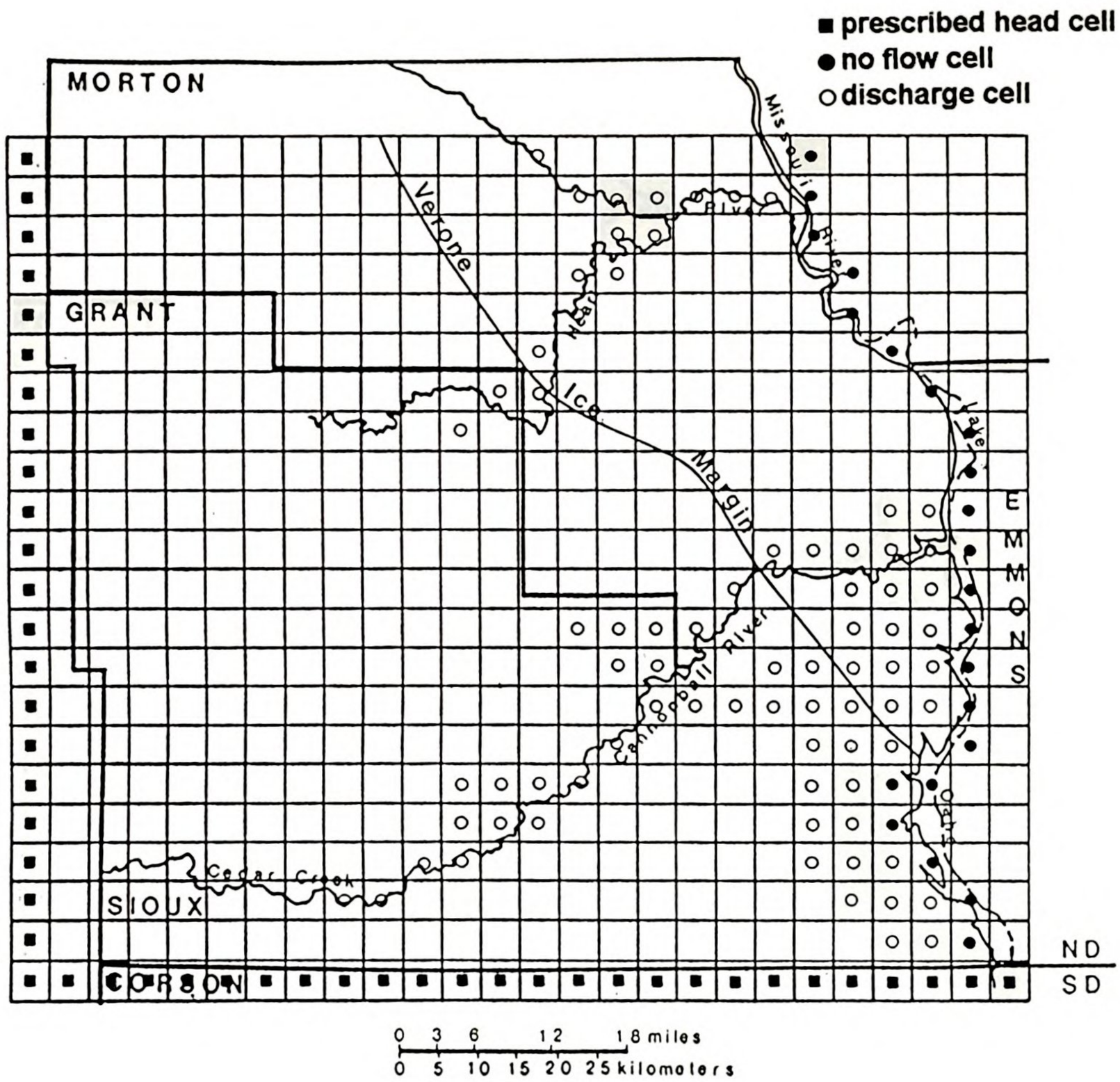

Figure 27. Finite-difference grid for Fox Hills aquifer simulation.

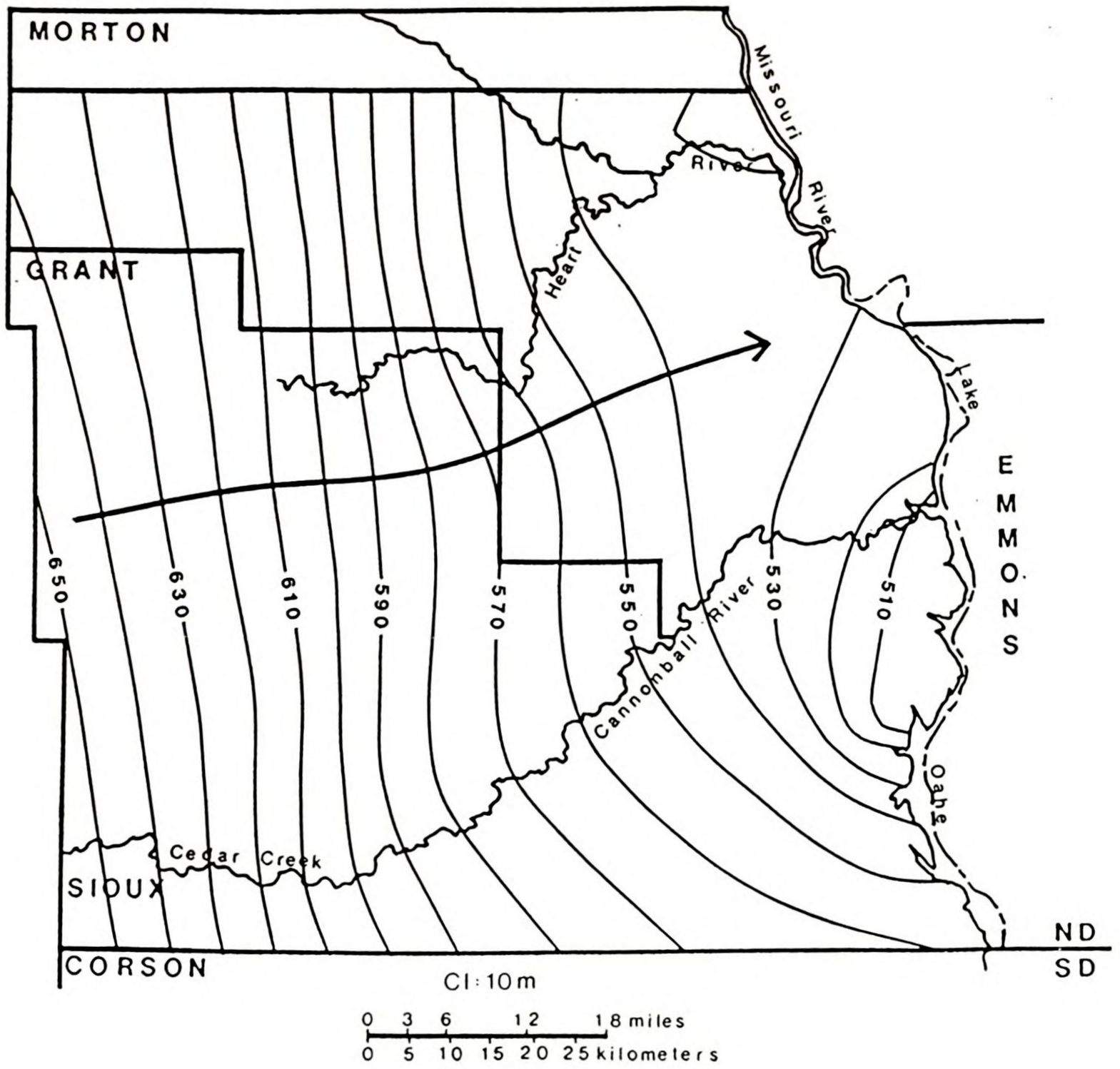

Figure 28. Simulated water levels in the Fox Hills aquifer.

on groundwater flow will be considered. Lake McKenzie was modeled by assigning constant head values to subcrop nodes within the lake boundary (Figure 29). A lake level of 549 m was assumed based on the present surface elevation along the postulated lake boundary. Discharge nodes were assigned as in simulation 1 with the exception that no discharge nodes were located within the lake boundary. The resulting head distribution (Figure 30) shows the water levels in the aquifer to be approximately 20 m higher than present conditions, however, groundwater flow is still toward the east. Any recharge to the aquifer from Lake McKenzie would be transported eastward toward the Missouri River valley where it would be discharged from the aquifer. Thus, leakage from Lake McKenzie can not explain the anomalous water chemistry in the study area.

Simulation 3: blocked discharge area. The age of the Verone glaciation is unknown, but has been inferred to be late pre-Wisconsin or Early Wisconsin (>65,000 a). Calculations of ice thickness (based on Mathews, 1974; Table 2) suggest that the ice sheet was less than 150 m thick in the study area and generally less than 100 m thick over the the present Fox Hills subcrop, with an ice overburden pressure less than 91 m equivalent water (ice thickness x 10/11) at the land surface. As water levels in the aquifer's recharge area in southwestern North Dakota are ≈300 m (1000 ft) higher than those postulated in the Verone ice sheet, the affect of the overridding glacier on flow in the aquifer should be localized.

The potential postulated for the ice sheet is greater than the water levels presently observed in the aquifer in the study area. Inferring similar aquifer water levels for the past, groundwater discharge would most likely have been blocked by the ice in the discharge area in North Dakota and diverted southward to the unobstructed discharge area in South Dakota. In this simulation, discharge only occurs from nodes along the Cannonball and Missouri river

on groundwater flow will be considered. Lake McKenzie was modeled by assigning constant head values to subcrop nodes within the lake boundary (Figure 29). A lake level of 549 m was assumed based on the present surface elevation along the postulated lake boundary. Discharge nodes were assigned as in simulation 1 with the exception that no discharge nodes were located within the lake boundary. The resulting head distribution (Figure 30) shows the water levels in the aquifer to be approximately 20 m higher than present conditions, however, groundwater flow is still toward the east. Any recharge to the aquifer from Lake McKenzie would be transported eastward toward the Missouri River valley where it would be discharged from the aquifer. Thus, leakage from Lake McKenzie can not explain the anomalous water chemistry in the study area.

Simulation 3: blocked discharge area. The age of the Verone glaciation is unknown, but has been inferred to be late pre-Wisconsin or Early Wisconsin (>65,000 a). Calculations of ice thickness (based on Mathews, 1974; Table 2) suggest that the ice sheet was less than 150 m thick in the study area and generally less than 100 m thick over the the present Fox Hills subcrop, with an ice overburden pressure less than 91 m equivalent water (ice thickness x 10/11) at the land surface. As water levels in the aquifer's recharge area in southwestern North Dakota are ≈300 m (1000 ft) higher than those postulated in the Verone ice sheet, the affect of the overridding glacier on flow in the aquifer should be localized.

The potential postulated for the ice sheet is greater than the water levels presently observed in the aquifer in the study area. Inferring similar aquifer water levels for the past, groundwater discharge would most likely have been blocked by the ice in the discharge area in North Dakota and diverted southward to the unobstructed discharge area in South Dakota. In this simulation, discharge only occurs from nodes along the Cannonball and Missouri river

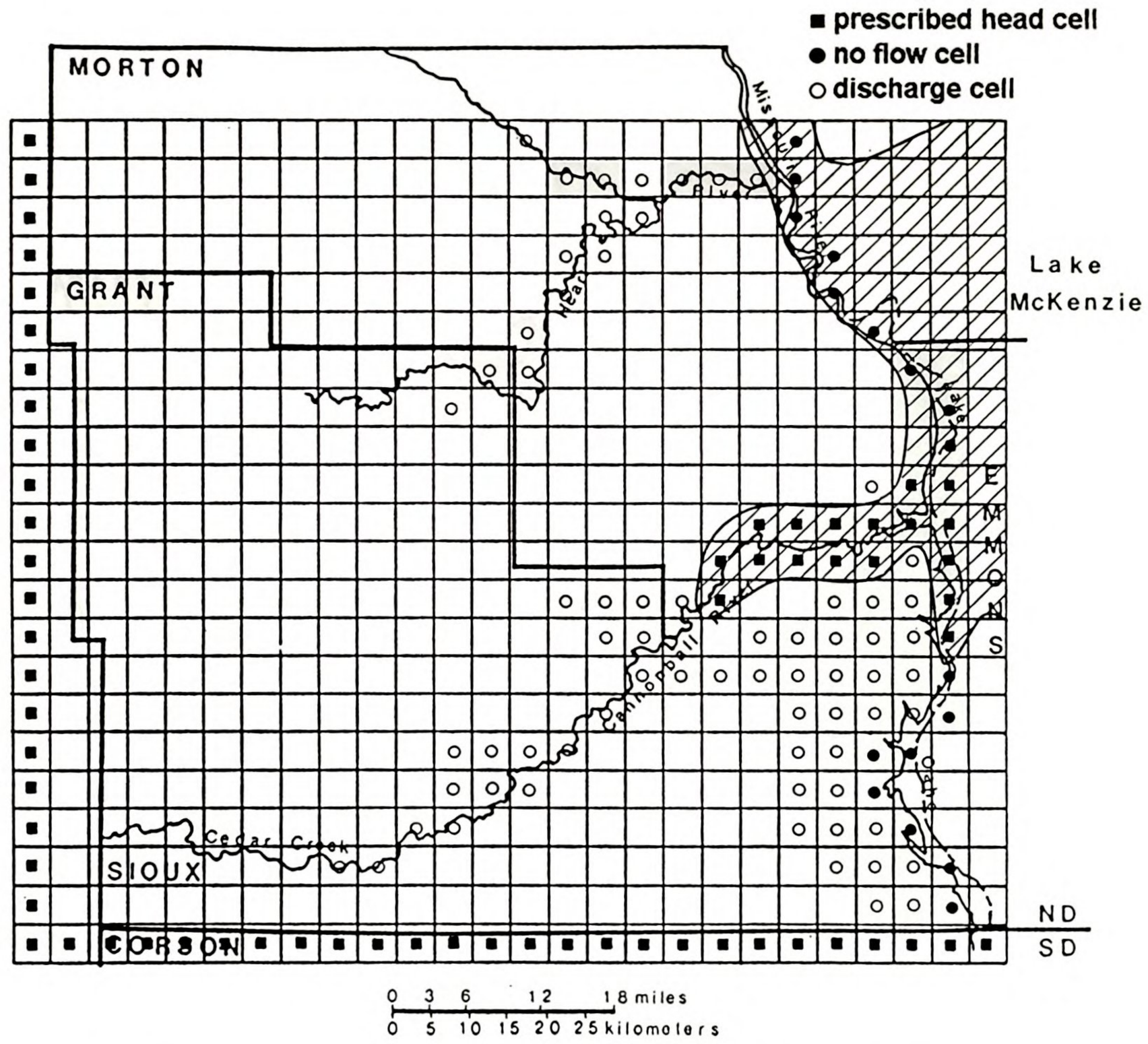

Figure 29. Finite-difference grid for simulating the influence of proglacial Lake McKenzie.

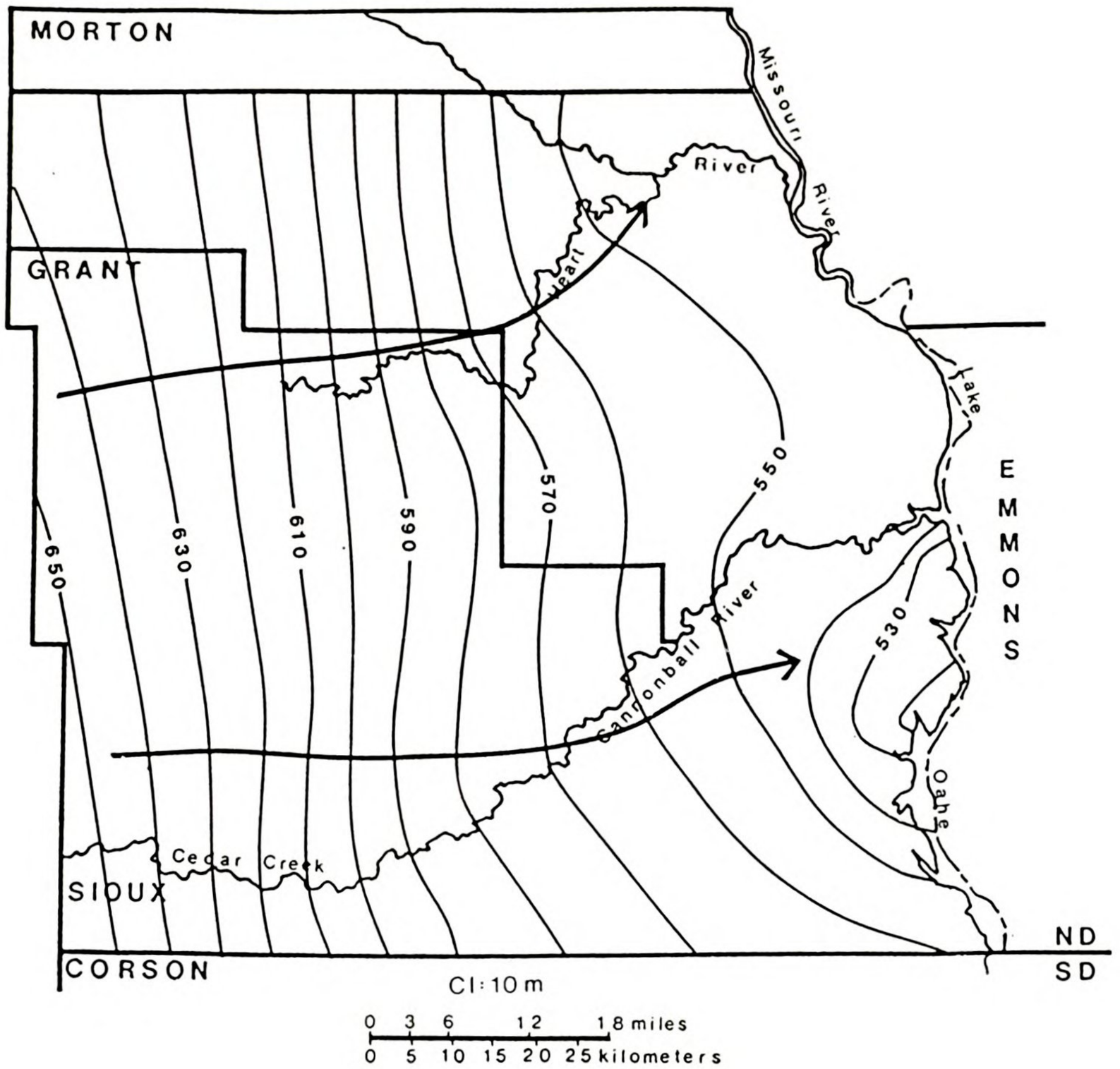

Figure 30. Simulated water levels, taking into account Lake McKenzie.

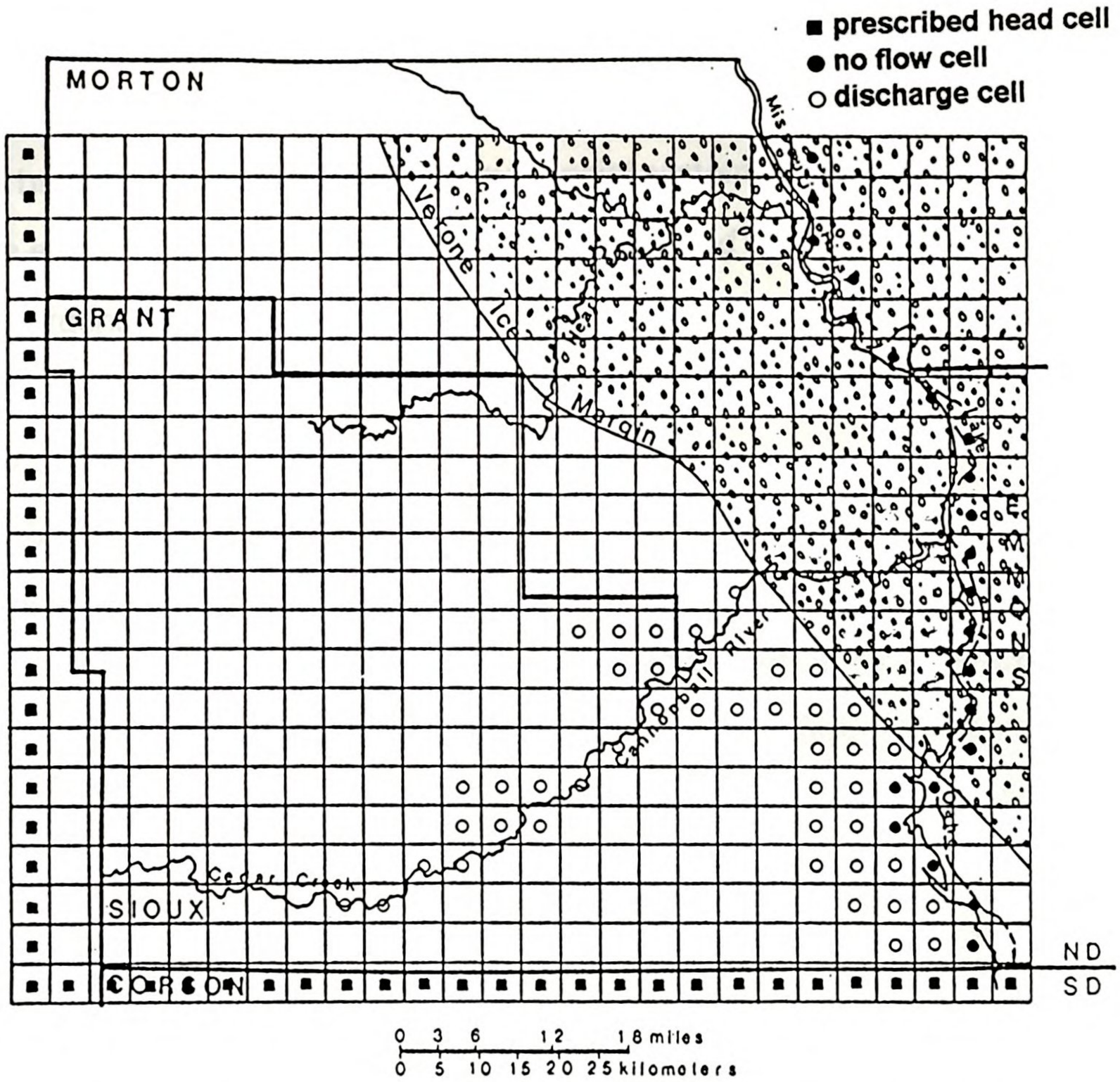

Figure 31. Finite-difference grid for simulation of the Verone ice sheet partially blocking the discharge area.

valleys south of the Verone Ice Margin (Figure 31). The simulated head distribution (Figure 32) shows groundwater flow diverted to the south toward the unobstructed discharge area in south-central North Dakota and north-central South Dakota. This is consistent with Downey's (1986) hypothesis that groundwater flow would have been diverted to the southeast during the Pleisotocene when the regional discharge areas were blocked by glacial ice.

Simulation 4: subglacial recharge. Large volumes of snowmelt and rain would have been transported to the subglacial system of the Verone ice sheet via the englacial system. This water would have had the potential to move downward into the underlying aquifer. Two possible hydrologic scenarios are postulated. The first assumes the water at the ice-bed contact to be unconfined; the second confined/pressurized.

Scenario a: As the Verone ice sheet advanced up the Missouri Slope and associated escarpments, it may have become compressed with resultant shearing in the ice, similar to the Late Wisconsin Lostwood ice advance that overrode the Missouri escarpment (Moran et al., 1976). Debris beneath the ice would have been carried to the ice surface along shear planes in the glacier as it moved onto uplands (Figure 33). As the stagnant ice melted, glacial sediment would have accumulated on top of the ice insulating the ice so that it took thousands of years to melt. During this time, the stagnant ice would have behaved as an unconfined aquifer. Rain and snowmelt would infiltrate into the fractured ice each year from spring through fall, establishing a water table of local meteoric water. A potential for downward water movement would have existed. Recharge of the underlying Fox Hills aquifer through the glacial debris may have occurred for thousands of years.

Scenario b: As the Verone ice sheet advanced over the Missouri Slope, cavities would have formed in the ice at the ice-bed interface (Figure 34).

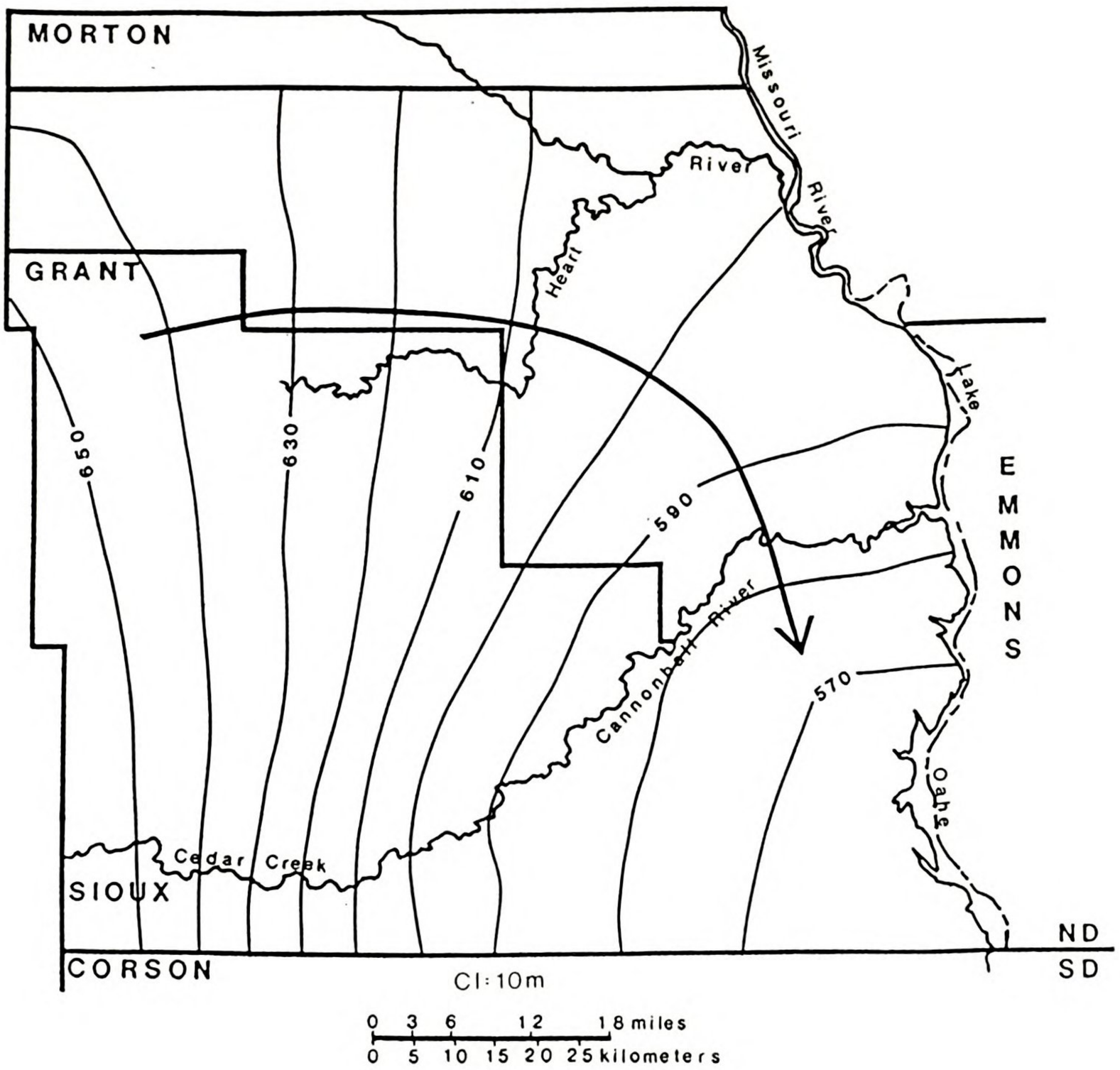

Figure 32. Simulated water levels, taking into account the partially blocked discharge area.

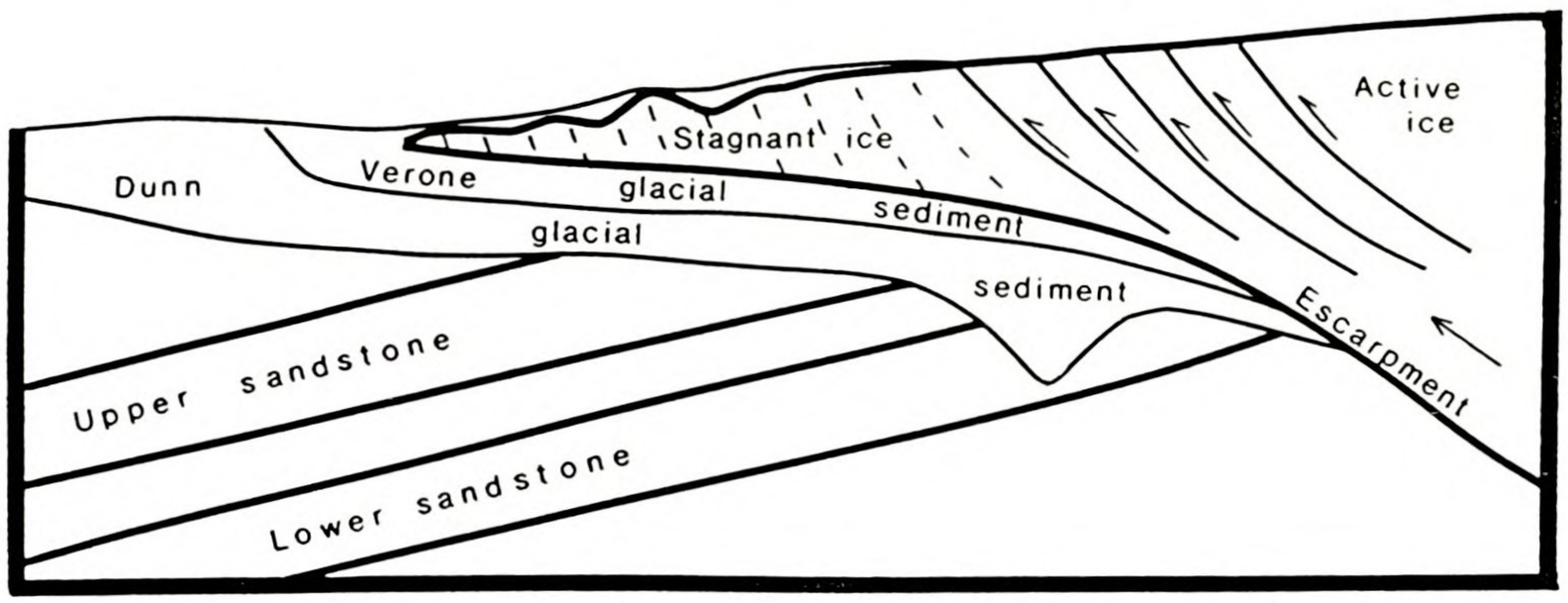

Figure 33. Schematic diagram of a glacier advancing over an escarpment (after Bluemle, 1977).

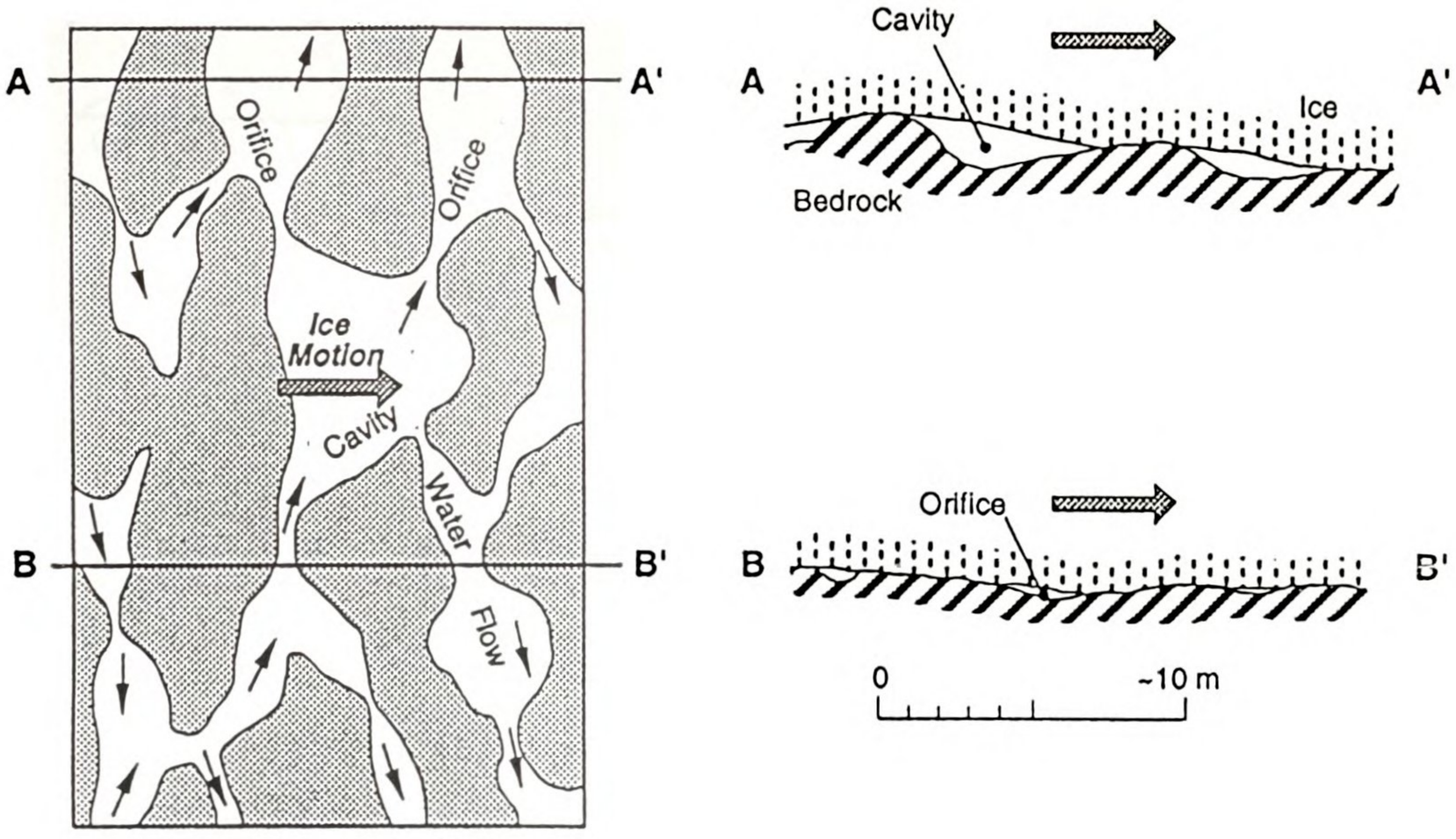

Figure 34. Linked cavity drainage system (Kamb, 1977): a) map view, b) cross-section.

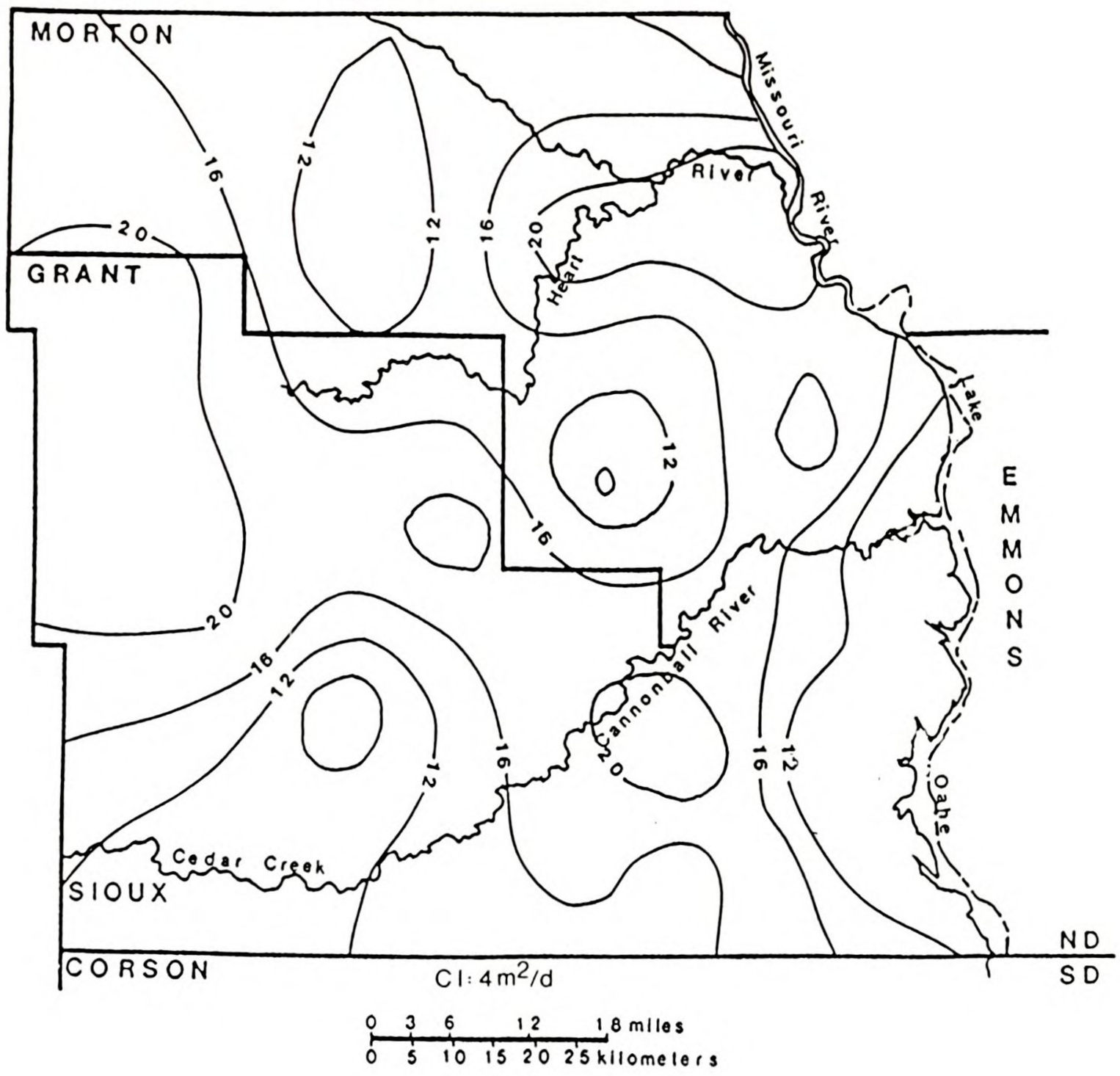

Figure 35. Modified transmissivity distribution.

During late spring through fall, snowmelt and rain moving from the ice surface through the englacial system would have entered the cavity system. In such a system, numerous small cavities are linked by orifices that restrict flow and induce water storage (Kamb, 1987). Increasing volumes of water from the surface results in increased water pressures in the cavity system. Water pressures in the cavity system are generally considered to be slightly less than the overburden pressure (Kamb, 1987). During winter, water in the linked cavity system would continue to be under pressure, although without a renewable water source (similar to a falling head permeameter). A potential for downward water movement through the glacial sediment at the bed would have existed. Recharge of the underlying Fox Hills aquifer may have occurred for the duration of the ice coverage. If the linked cavity system became unstable (i.e., too much available water), a conduit system would develop from the enlargement of the cavities. In this case, water would move quickly through the system with a low hydraulic head. Then as discharge declined in fall, the conduit system would close leaving the linked cavity system from late fall through spring.

Thus it is feasible that snowmelt and rain recharged the Fox Hills aquifer in its discharge area during the Verone glaciation. This hypothesis is tested by the fourth simulation.

It is assumed that the Verone Ice Margin was stable for a sufficient period of time such that steady-state conditions apply. It is also assumed that the Fox Hills Formation has been eroded along the Missouri River subcrop area since the Verone glaciation. For this reason, the sandstone thickness used in the model was modified along the subcrop such that the minimum thickness is 21 m (Figure 35) and the minimum transmissivity 12 m^2/d (0.57 m/d x 21 m). Previously identified discharge cells (simulation 3) were assigned a value of .5 mm/yr. Recharge cells were determined by identifying the subcrop discharge

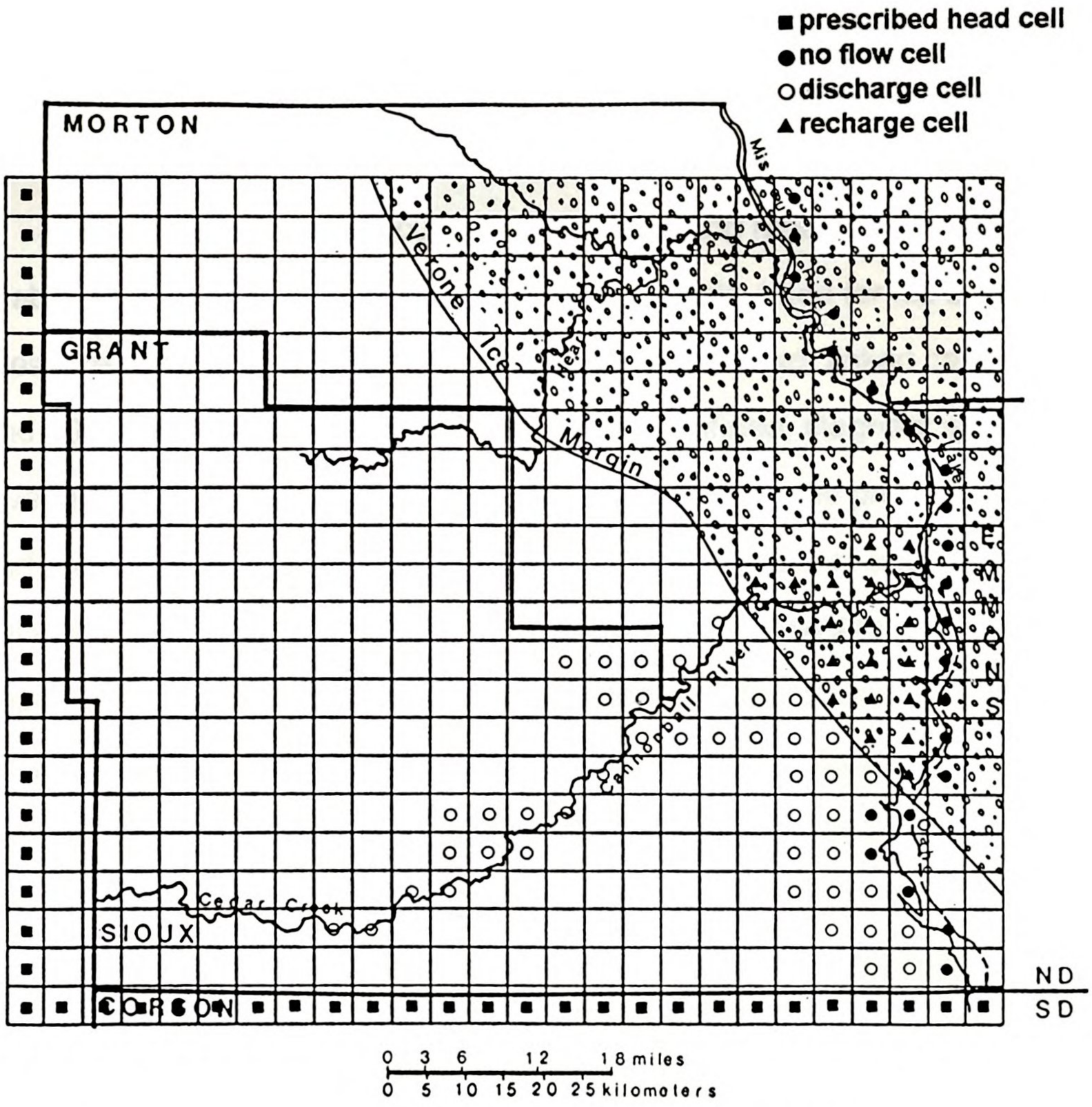

Figure 36. Finite-difference grid for simulation of the Verone ice sheet contributing recharge.

cells from the original simulation (Chapter 2) that would be overridden by the Verone ice sheet (Figure 36). Recharge was varied within specified limits (Table 2) to produce an acceptable water level distribution within the aquifer. An acceptable water-level distribution was defined as water levels in the aquifer less than the ice overburden pressure water equivalent head so that recharge rather than discharge would occur. The recharge values were constrained by the thickness of the ice and the inferred hydrogeologic system.

Ice thickness was calculated for nodes using Mathews (1974) equation (Table 2). Heads associated with the ice were calculated for ice overburden pressure water equivalent (maximum gradient; confined, linked cavity system) and 50% ice thickness (minimum gradient; unconfined, stagnant system). A level ground surface of 550 m was assumed based on the present upland surface elevation in the study area adjacent to the Missouri and Cannonball river valleys. A hydraulic conductivity of 10^{-6} m/d was assigned for the glacial till capping the aquifer assuming the till was derived from shale and siltstone. The thickness of the glacial till was estimated to be 30 m. Recharge values of 1.0 and 1.4 mm/yr were calculated (Table 2) and were used to constrain the possible recharge values input to the model.

Recharge of 1.4 mm/yr was too large to produce acceptable heads in the aquifer. The water levels in the aquifer beneath the recharge nodes were higher than the ice overburden water equivalent head. Recharge of 1.0 mm/yr did produce acceptable heads in the aquifer. The resulting head distribution (Figure 37) shows mounding of the water levels (below the ice overburden water equivalent head) in the aquifer beneath the overridden subcrop. A temporary groundwater divide separates ambient groundwater flow from the west and the newly recharged water in the east. No attempt was made to fit the eastern flow regime to the chloride distribution as that would imply that the simulation results

Table 2. Estimation of subglacial recharge rates.

Distance from Margin	Ice Thickness	Water Height in Ice Sheet		Water Elevation or Head			Recharge	
		water equivalent	50% ice thickness	ice max.	ice min.	Fox Hills aquifer	max.	min.
(m)	(m)	(m)	(m)	(m)	(m)	(m)	(mm/yr)	(mm/yr)
2500	36.5	33	18	583	568	504	1.0	0.8
7500	63.2	57	32	607	582	506	1.2	0.9
12500	81.6	74	41	624	591	509	1.4	1.0
17500	96.6	88	48	638	598	512	1.5	1.0
22500	109.5	100	55	650	605	514	1.7	1.1
						Total	6.8	4.8
						Average	1.4	1.0
Distance from margin estimated for Verone Ice Margin								
Ice thickness calculated following Mathews (1974): 0.73 x SQRT(distance from margin)								
Ice overburden water equivalent (max. water height) calculated as: (10/11) x ice thickness								
Free water surface in ice (min. water height) calculated as: 0.5 x ice thickness								
Water elevation in ice based on simplification that ground surface is level at 550m								
Water elevations in Fox Hills aquifer are approximate								
Recharge calculated as: q = (K'/b') (head in ice - head in aquifer)								
assuming K'/b' (confining layer hydraulic conductivity/thickness) = (1e-6 m/d) / (30 m)								

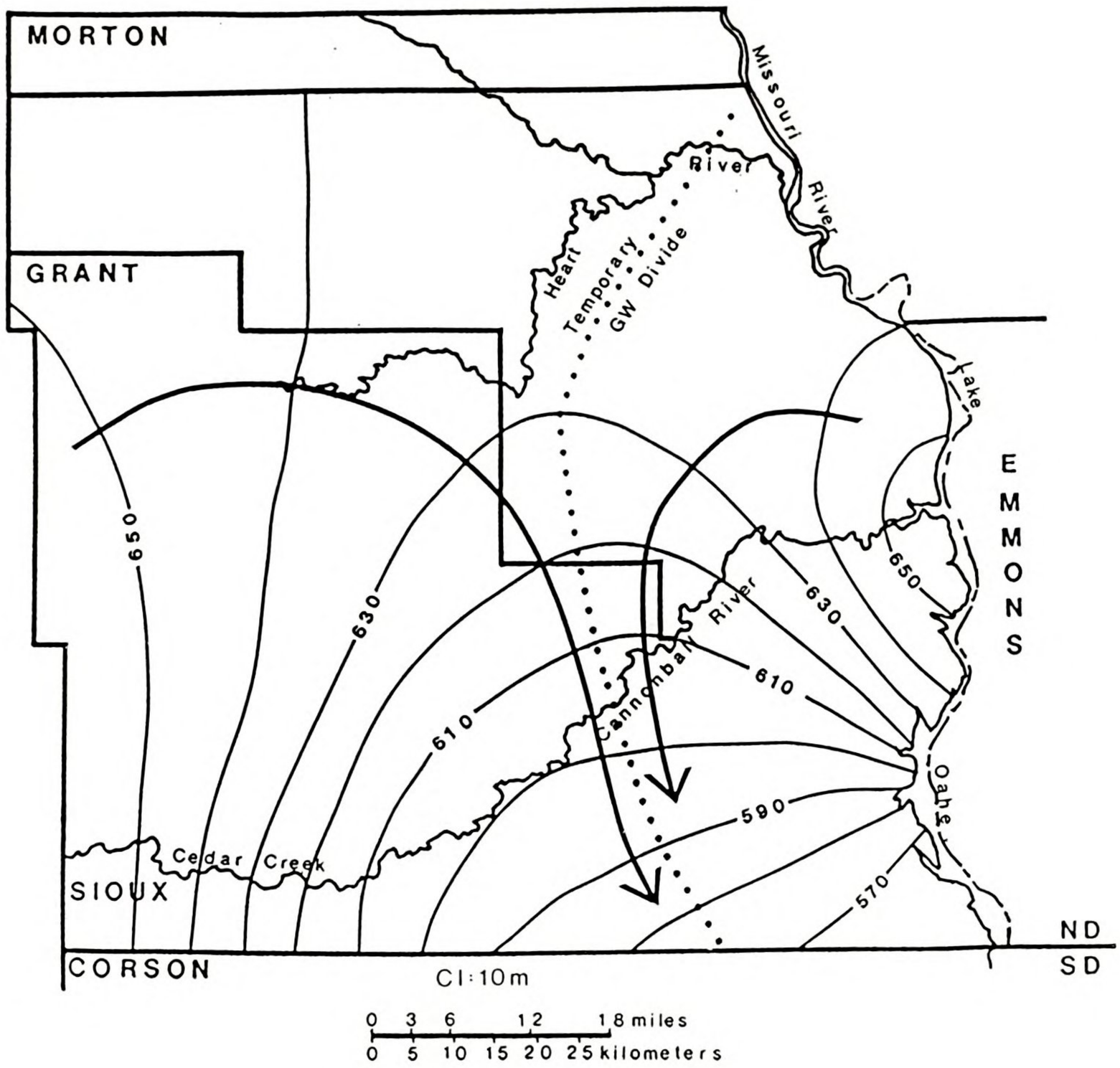

Figure 37. Simulated water levels, taking into account recharge from the Verone ice sheet.

provide quantitative information on the physical system. As stated above, the simulation merely shows that temporary recharge in the discharge area during glaciation is feasible. A more detailed model, with better defined northern and southern boundaries and ice sheet configuration, may allow for such "fitting" in the future. Though speculative, recharge of the Fox Hills aquifer by snowmelt and rain input under an ice sheet (2 ice sheets are known to have overridden the study area, only one was simulated) is presently the best explanation for the observed chemistry anomaly.

Interpretation. The above simulations show that partially blocking the discharge area of a regional aquifer could alter groundwater flow patterns as suggested in the literature. Temporary recharge in the blocked discharge area would provide fresh meltwater to the system. In some cases, this recharge might result in mounding of freshwater in the discharge area and, consequently, the formation of a temporary groundwater divide separating the ambient upgradient water from the newly recharged meltwater. Proglacial Lake McKenzie apparently would not have influenced the flow regime sufficiently to divert groundwater flow to the southeast or to input fresh water in the aquifer upgradient of the lake.

Summary

Various researchers have suggested that groundwater flow patterns in certain aquifers may have been altered during the Pleistocene because glacial ice blocked some regional discharge areas, subglacial meltwater was available for recharge, and some geologic materials were compressed under the weight of overriding ice sheets. Ice sheets tend to move toward topographically low areas, which are often regional discharge areas. Groundwater discharge becomes

blocked by the overriding ice sheet, resulting in altered groundwater flow patterns. If the glacier overlies an aquifer of high permeability with a water potential below that of the ice, all the meltwater would enter the aquifer, whereas, if the glacier overlies a less permeable material, at least some of the meltwater will pond on the surface of the substratum and discharge by channel flow or sheet flow.

Water at a glacier bed has various sources, including surface meltwater (produced by ablation processes), rain, basal meltwater, and meltwater from heat of deformation. Surface meltwater, combined with rain, however, is the most important source of water in temperate glaciers. During the melt season, surface meltwater and rain may be transported to the glacier base via the englacial system. Water at the base of a glacier (subglacial) may be discharged as sheetflow along the glacier's bed, flow in channels or linked cavities along the bed, groundwater flow through subglacial materials, or a combination of these. The character and geometry of the subglacial materials determine the rate of groundwater recharge. Flow in the aquifer is assumed to be horizontal toward the glacier toe.

A 2-dimensional finite difference groundwater flow model was used to simulate the response of the Fox Hills aquifer to continental glaciation as a means of assessing the feasibility of the glacial meltwater hypothesis. Compression of shale units was not considered. As stated above, modeling the response of an aquifer to Pleistocene glaciation is a speculative endeavor because of limited knowledge of both the preglaciation aquifer system and the ice sheet configuration and hydraulics. The Fox Hills simulations merely show that temporary recharge in the discharge area during glaciation is feasible. The simulations suggest that (1) proglacial Lake McKenzie probably would not have influenced the flow regime sufficiently to divert groundwater flow to the

southeast or to input fresh water in the aquifer upgradient of the lake, (2) partially blocking the discharge area of the Fox Hills aquifer could alter groundwater flow patterns as suggested in the literature and (3) temporary recharge in the blocked discharge area could result in mounding of freshwater in the discharge area and, consequently, the formation of a temporary groundwater divide separating the ambient upgradient water from the newly recharged meltwater. Though speculative, recharge of the Fox Hills aquifer by snowmelt and rain input under an ice sheet (two ice sheets are known to have overridden the study area, only one was simulated) is presently the best explanation for the observed chemistry anomaly.

SUMMARY AND CONCLUSIONS

Six working hypotheses/potential water sources were tested using hydrogeologic, hydrochemical, and stable isotopic methods. The results of these investigative techniques will be discussed with respect to each of the potential sources. The overall conclusion and recommendation follow.

Upgradient Aquifer Water

The water-level maps of Lobmeyer (1979) and this study show that the water in the discharge area of the Fox Hills aquifer should be ambient upgradient water transported from the aquifer's recharge area along the North Dakota-Montana border. However, the hydrochemical facies and the chloride distribution maps show that a separate water body is present in the discharge area and that this water could not have been derived from upgradient aquifer water. Thus, water in the discharge area does not have upgradient water as a significant source.

Local Precipitation/Recharge

The hydrochemical data indicate that the water in the discharge area is much lower in chloride than upgradient water, suggesting that mixing with freshwater has occurred. The chloride distribution in the aquifer suggests that the fresh water source contributed about 90% of the present water in the discharge area. In the southeastern corner of Grant County, the chloride concentrations drop from >6 meq/L to <1 meq/L in a 6 km stretch along the groundwater flow path. In order to bring about this decrease in the chloride

concentration (by mixing with fresh water), a 500% increase in the volume of water would be required as the water moves downgradient through this region. Such an increase in the water volume would require recharge on the order of 4.3 to 8.5 mm/yr, only in a narrow, 6 km, stretch of aquifer. Neither the literature nor the water-level maps of the aquifer suggest any unusual conditions that are restricted to this region. Thus, it is unlikely that local recharge under present climatic conditions could explain this increase in water volume. In addition, mean annual air temperatures calculated from the stable isotope data indicate that the water in the discharge area was precipitated in a cooler climate than modern. Thus, dilution with local precipitation does not explain the chemistry anomaly and modern local precipitation is not considered a significant source of water to the discharge area.

Local Precipitation during the Pleistocene

The hydrochemical and stable isotope data indicate that at least two paleowaters are present in the discharge area--a low-chloride, high d-excess water and a high-chloride, low d-excess water. Assuming that the -12.3 $\delta^{18}O$ sample represents modern recharge, the Fox Hills aquifer water samples exhibit temperatures 2.6 to 5.6 C cooler than modern. This suggests that the water in the discharge area was recharged during a cooler climatic condition, such as was prevalent during Pleistocene glaciation. A global circulation model and an energy balance model suggest that the mean annual temperature at 43 N latitude was about 4 to 7.5 C cooler than modern during the last glacial maximum 18,000 years ago. Earlier glacial advances may have occurred under similar climatic conditions. The possibility that local precipitation during the Pleistocene may have been the main source of recharge to the Fox Hills

discharge area is dependent on identifying a feasible recharge mechanism--one that is not operating today.

One can speculate that local precipitation falling on the ablation zone of a temperate ice sheet would be transported via the englacial system to the ice-bed contact. A significant potential for downward migration of this subglacial water would exist. If the ice sheet overrode permeable material, some of the subglacial water would discharge into the aquifer. The results of the simulation of the Verone glaciation, though speculative, support this hypothesis. Water levels in the Fox Hills aquifer where recharge occurred were raised sufficiently to produce a mounding affect with a resultant temporary groundwater divide separating ambient upgradient water from the newly recharged fresh water. Although the hydrochemistry and stable isotope data strongly indicate that a paleowater was recharged to the Fox Hills aquifer during cooler climatic conditions than modern, the mechanism of recharge is speculative.

Leakage from Proglacial Lakes

The presence of proglacial lakes would provide a significant potential for downward migration of water, and proglacial lakes are known to have existed in the study area during glacial advances. Lakes are subject to evaporation even with short exposure time; however, the stable isotope data indicate that minimal evaporation occurred prior to recharge. Thus, proglacial lakes are not considered a significant source of water to the discharge area. Although speculative, simulation of the Fox Hills aquifer with Lake McKenzie as a constant head feature supports this interpretation by showing that groundwater flow directions would not be significantly altered by the presence of the lake and that

any recharge from the lake would be transported eastward to the Missouri River valley discharge area.

Leakage from Adjacent Aquifers

The water levels in the Dakota aquifer (the first aquifer below the Fox Hills aquifer) in south-central North Dakota are higher than those in the Fox Hills aquifer, indicating a potential for leakage into the Fox Hills aquifer. However, based on hydrochemistry data, leakage from the Dakota aquifer into the Fox Hills aquifer would be expected to increase, not decrease, the chloride concentrations in the discharge area. Thus, leakage from the Dakota aquifer does not explain the low-chloride anomaly. The water levels in the overlying Hell Creek aquifers generally are higher than those in the Fox Hills aquifer, indicating a potential for leakage into the Fox Hills aquifer. However, the discontinuous sandstone beds within the Hell Creek Formation are typically perched or semiperched aquifers where downward migration of water is restricted. Thus, leakage from adjacent aquifers is not considered a significant source of recharge to the discharge area.

Basal Meltwater

Basal meltwater input under the glacier through the Fox Hills Formation subcrop would provide both a source and a feasible mechanism for temporary recharge in the discharge area of the Fox Hills aquifer. The subcrop is known to have been overridden by two glacial advances, the Dunn and Verone Glaciations, each of which may have consisted of more than one pulse. The

stable isotope values however, are heavier than expected for glacial ice. Assuming that the observed $\delta^{18}O$ values in the discharge area (average = -15.1) are the result of mixing modern local recharge (-12.3) and subglacial meltwater (-30), 84% of the ^{18}O is contributed by the modern local recharge and 16% by basal meltwater. If the $\delta^{18}O$ value of the local precipitation recharge was lower than -12.3 during the Pleistocene, an even smaller contribution would come from basal meltwater. Thus, basal meltwater is not the sole or main source of recharge to the aquifer. This is to be expected as surface meltwater, consisting of snowmelt and rain, is the most important source of water in temperate glaciers. Water at the bed of a glacier is thus primarily surface meltwater with smaller amounts of basal meltwater.

Conclusion and Recommendation

The results of this investigation point to only one main source for the anomalous water body in the discharge area of the Fox Hills aquifer in south-central North Dakota: local precipitation recharged during the Pleistocene. It is speculated that local precipitation was recharged in the discharge area due to the hydraulic gradient imposed by an overriding ice sheet.

Further testing of this hypothesis is advisable. Dating water in the Fox Hills aquifer along a flowline from recharge to discharge area would provide considerable insight into the dynamics of the aquifer system. Dating water from

the anomalous water body in the discharge area would provide time constraints on the recharge events and thereby further test the feasibility of the glacial meltwater recharge hypothesis proposed here.

APPENDICES

Appendix A. Geologic data.

Table 3. Geologic data derived from drill logs.

Location				Fox Hills Fm	Glacial Deposits	Sandstone
ID #	T	R	Sec			(m)
4521	129N	80W	23 ddd	subcrop	present	24.4
4520	129N	81W	01 bab	subcrop	present	21.3
8105	129N	87W	10 bbb	overlain	absent	
4490	129N	87W	10 bbc	overlain	absent	
4525	129N	88W	05 ddd	overlain	absent	
8081	130N	79W	19 ccb	absent	present	0.0
8077	130N	80W	03 abb	absent	present	0.0
8080	130N	80W	23 ddd	absent	present	0.0
8082	130N	80W	26 baa	subcrop	present	
8083	130N	82W	36 bbc	overlain	absent	36.9
4522	130N	83W	36 aaa	overlain	absent	20.7
4523	130N	84W	31 aaa	overlain	absent	
4489	130N	84W	36 aba	overlain	absent	29.6
8096	130N	85W	04 bbb	overlain	absent	
8097	130N	85W	17 add	overlain	absent	
4488	130N	85W	17 daa	overlain	absent	26.2
4524	130N	86W	28 ccc	overlain	absent	23.2
4492	130N	89W	32 dda	overlain	absent	17.4
8075	131N	80W	06 bcd	subcrop	present	
8642	131N	80W	16 ddd	absent	present	0.0
8079	131N	80W	33 baa	absent	present	0.0
8641	131N	81W	01 dad	subcrop	present	
8076	131N	81W	01 dda	subcrop	present	4.0
4519	131N	82W	18 dcd	overlain	absent	41.8
4413	131N	83W	11 bab	overlain	present	
4410	131N	84W	02 aaa	overlain	absent	
8094	131N	85W	32 aaa	overlain	absent	
8095	131N	85W	32 daa	overlain	absent	
4526	131N	89W	30 aaa	overlain	absent	
8640	132N	80W	16 ccc	subcrop	present	
8074	132N	80W	27 ddd	overlain	present	
8073	132N	80W	35 abb	subcrop	present	15.5
4418	132N	81W	29 bbb	subcrop	present	
4419	132N	81W	30 aac	subcrop	present	
4421	132N	81W	30 cdc	subcrop	absent	
4420	132N	81W	30 dbb	subcrop	present	
4415	132N	82W	09 ddd	overlain	absent	
4416	132N	82W	10 cbb	subcrop	present	
4417	132N	82W	10 cbc	subcrop	present	
8084	132N	82W	10 cdd	overlain	absent	

Table 3 (cont'd).

Location				Fox Hills Fm	Glacial Deposits
ID #	T	R	Sec		
4414	132N	82W	19 bdd	overlain	present
8090	132N	83W	10 dad	overlain	present
8091	132N	83W	29 ccc	subcrop	present
4409	132N	83W	30 bcb	subcrop	present
8092	132N	83W	31 baa	subcrop	present
8093	132N	83W	31 bbb	subcrop	present
4411	132N	83W	31 dba	subcrop	present
4412	132N	83W	33 aad	subcrop	present
8089	132N	83W	34 dda	subcrop	present
8088	132N	83W	35 ddc	subcrop	present
8087	132N	83W	36 ccc	subcrop	present
8648	132N	84W	01 ccd	overlain	present
4406	132N	84W	01 daa	subcrop	present
8645	132N	84W	01 ddc	subcrop	present
4398	132N	84W	06 ccc	overlain	present
8646	132N	84W	12 aaa	overlain	absent
8647	132N	84W	12 baa	subcrop	present
4407	132N	84W	12 ccd	subcrop	present
4518	132N	84W	16 daa	overlain	absent
4408	132N	84W	25 bab	overlain	absent
8104	132N	87W	26 ccb	overlain	absent
4491	132N	87W	27 ada	overlain	absent
4528	132N	88W	04 cbb	overlain	absent
4527	132N	90W	14 aab	overlain	absent
8635	133N	79W	02 cbb	subcrop	present
8068	133N	79W	06 bcb	subcrop	present
8072	133N	79W	07 dcd	overlain	present
8636	133N	79W	11 baa	subcrop	absent
8639	133N	79W	29 aba	subcrop	present
8069	133N	80W	01 ddd	subcrop	present
8070	133N	80W	12 ddd	subcrop	present
8071	133N	80W	13 dda	subcrop	present
8644	133N	80W	31 ccd	subcrop	present
8653	133N	83W	05 dcc	overlain	absent
4399	133N	83W	07 ccb	subcrop	present
8652	133N	83W	08 bbb	subcrop	present
8655	133N	83W	12 ada	subcrop	present
8654	133N	83W	14 bbb	subcrop	present
4400	133N	83W	17 cbb	subcrop	present
4401	133N	83W	17 daa	subcrop	present
4403	133N	83W	21 aaa	overlain	present
4402	133N	83W	21 abb	subcrop	present
4404	133N	83W	28 aab	subcrop	present
4405	133N	83W	28 dcd	subcrop	present
8649	133N	83W	33 ddc	overlain	present
8650	133N	84W	01 dcc	subcrop	present

Table 3 (cont'd).

Location				Fox Hills Fm	Glacial Deposits
ID #	T	R	Sec		
8651	133N	84W	03 dad	overlain	present
4397	133N	84W	30 aaa	overlain	present
4487	133N	85W	12 aad	overlain	absent
4396	133N	85W	26 ccc	overlain	absent
8103	133N	86W	06 bbb	overlain	absent
4484	133N	89W	04 dad	overlain	absent
8066	134N	79W	29 ddd	subcrop	present
8067	134N	79W	32 abb	subcrop	present
8931	134N	79W	32 ada	absent	present
8929	134N	79W	32 add	absent	present
8637	134N	79W	32 dad	subcrop	present
8928	134N	79W	32 ddd	subcrop	present
8634	134N	79W	34 cbb	subcrop	present
8638	134N	80W	35 ada	subcrop	absent
8085	134N	82W	36 cdc	overlain	absent
8086	134N	82W	36 dcd	overlain	absent
4517	134N	85W	03 bcc	overlain	absent
8098	134N	85W	06 bcc	overlain	absent
4516	134N	85W	21 bab	overlain	absent
4493	134N	89W	23 ccb	overlain	absent
8102	135N	86W	07 ddd	overlain	absent
4515	135N	86W	15 ddd	overlain	absent
4514	135N	86W	26 bbb	overlain	absent
4494	135N	89W	22 cdd	overlain	absent
4509	135N	90W	23 bbb	overlain	absent
8101	136N	85W	05 abb	overlain	present
8099	136N	85W	08 ddd	overlain	present
8100	136N	85W	09 bcd	overlain	present
4512	136N	87W	07 ddd	overlain	absent
4486	136N	87W	36 abd	overlain	absent
4513	136N	88W	13 aaa	overlain	absent
4485	137N	88W	21 ddc	overlain	present
4511	137N	89W	09 aba	overlain	absent
4510	137N	90W	30 aac	overlain	absent
4569	133N	82W	05 dba	subcrop	present
4572	134N	79W	07 bcb	subcrop	present
9296	134N	79W	17 adb	subcrop	present
9295	134N	79W	20 aab	absent	present
4571	134N	80W	16 daa	subcrop	present
9292	134N	80W	17 ccb	overlain	present
9293	134N	80W	19 daa	subcrop	present
9294	134N	80W	20 ccc	subcrop	present
8994	134N	80W	23 baa	subcrop	present
8993	134N	80W	23 bab	subcrop	present
8995	134N	81W	24 add	subcrop	present
8990	134N	81W	25 dab	subcrop	present

Table 3 (cont'd).

Location				Fox Hills Fm	Glacial Deposits
ID #	T	R	Sec		
4570	134N	82W	35 daa	subcrop	present
8989	134N	82W	36 bda	subcrop	present
4561	134N	83W	05 dcc	overlain	present
8965	134N	83W	06 abd	overlain	present
8964	134N	83W	06 bab	overlain	present
8966	134N	83W	06 bbc	overlain	present
4565	134N	83W	17 ccc	overlain	present
4566	134N	83W	17 ddb	overlain	present
4568	134N	83W	26 bba	overlain	present
4567	134N	83W	32 aaa	overlain	present
4562	134N	84W	01 cdc	overlain	present
4563	134N	84W	03 add	overlain	present
4564	134N	84W	11 ddd	overlain	present
8967	134N	84W	13 bbc	overlain	present
8968	134N	84W	13 cbb	overlain	present
8969	134N	84W	24 bbb	overlain	present
4769	135N	79W	10 aab	overlain	absent
4575	135N	80W	30 aab	overlain	present
4574	135N	80W	33 dda	subcrop	present
4573	135N	80W	36 aaa	overlain	absent
4576	135N	81W	02 ccd	overlain	present
8997	135N	81W	03 cbb	overlain	present
4577	135N	81W	11 aba	overlain	present
9289	135N	81W	11 ddd	overlain	present
9291	135N	81W	12 cdd	overlain	present
9290	135N	81W	14 aac	overlain	present
9328	135N	81W	24 ddd	overlain	present
8987	135N	82W	15 aaa	overlain	absent
8986	135N	82W	22 bcb	overlain	present
4560	135N	82W	30 cbb	overlain	present
4559	135N	83W	20 ccb	overlain	present
4768	135N	83W	32 cbb	overlain	present
4556	135N	84W	04 dcc	overlain	present
8978	135N	84W	09 ccd	overlain	present
8977	135N	84W	15 bba	overlain	present
8971	135N	84W	16 aaa	overlain	present
8982	135N	84W	16 aad	overlain	present
8972	135N	84W	16 abb	overlain	present
4557	135N	84W	21 ddd	overlain	present
4558	135N	84W	26 daa	overlain	present
8962	135N	84W	36 dcd	overlain	present
8963	135N	84W	36 dda	overlain	present
4770	136N	79W	05 ccc	overlain	absent
4590	136N	81W	06 bbb	overlain	present
9286	136N	81W	07 aaa	subcrop	present
4591	136N	81W	07 bbb	overlain	present

Table 3 (cont'd).

Location				Fox Hills Fm	Glacial Deposits
ID #	T	R	Sec		
4771	136N	81W	07 ddc	overlain	present
4592	136N	81W	16 bbb	overlain	present
4593	136N	81W	16 cdd	subcrop	present
9288	136N	81W	21 ccd	subcrop	present
4579	136N	81W	31 abb	overlain	present
4582	136N	82W	04 aaa	overlain	present
9305	136N	82W	07 ccc	overlain	present
4588	136N	82W	08 ddd	overlain	present
9000	136N	82W	09 aaa	subcrop	present
9001	136N	82W	09 abb	overlain	present
4580	136N	82W	22 daa	overlain	present
4586	136N	83W	01 ccc	overlain	present
4553	136N	84W	20 dba	overlain	absent
4554	136N	84W	30 daa	overlain	absent
4555	136N	84W	31 add	overlain	present
9011	137N	80W	08 cdc	overlain	present
9010	137N	80W	16 dbb	overlain	present
9007	137N	81W	10 baa	overlain	present
9006	137N	81W	16 aaa	overlain	present
9329	137N	81W	21 aca	overlain	present
9383	137N	81W	28 ccd	overlain	present
4589	137N	81W	31 ddd	overlain	present
9284	137N	81W	32 baa	overlain	present
9285	137N	81W	32 bbb	overlain	present
9003	137N	82W	20 daa	overlain	present
9002	137N	82W	21 ccc	overlain	present
4585	137N	82W	32 dcc	overlain	present
4584	137N	82W	33 dcc	overlain	present
4583	137N	82W	35 ccc	overlain	present
4581	137N	82W	36 ddd	overlain	present
4763	137N	83W	06 cdd	overlain	present
4552	137N	83W	07 bba	overlain	absent
4587	137N	83W	24 dda	overlain	present
4551	137N	85W	06 ccd	overlain	present
9304	137N	85W	17 cdb	overlain	present
4752	137N	86W	03 aad	overlain	present
4757	137N	87W	12 cda	overlain	present
2908	138N	80W	06 bcc	overlain	absent
2909	138N	80W	30 ccc	overlain	absent
4750	138N	81W	09 abb	overlain	absent
9014	138N	81W	12 dab	overlain	present
9012	138N	81W	24 dcd	overlain	present
9009	138N	81W	35 aba	overlain	present
9008	138N	81W	35 baa	overlain	present
9004	138N	82W	15 ddd	overlain	present
9005	138N	82W	25 ddc	overlain	present

Table 3 (cont'd).

Location				Fox Hills Fm	Glacial Deposits
ID #	T	R	Sec		
4761	138N	84W	27 ccc	overlain	absent
4762	138N	85W	26 cdd	overlain	absent
4656	138N	86W	02 bcb	overlain	present
4649	138N	86W	11 acc	overlain	present
4657	138N	86W	11 ddb	overlain	present
9303	138N	86W	13 ccc	overlain	present
4650	138N	86W	14 abc	overlain	present
9302	138N	86W	14 cbb	overlain	present
4547	138N	86W	17 cdd	overlain	present
4548	138N	86W	17 ddc	overlain	present
4546	138N	86W	18 dcd	overlain	present
4544	138N	86W	20 bab	overlain	present
4545	138N	86W	20 bbb	overlain	present
4550	138N	86W	35 bbc	overlain	present
4543	138N	87W	03 dbb	overlain	present
4766	139N	81W	09 aaa	overlain	absent
9326	139N	81W	25 cbb	overlain	present
9015	139N	81W	36 ccd	overlain	present
9013	139N	82W	25 bbd	overlain	present
4751	139N	83W	12 dba	overlain	present
4764	139N	83W	28 dad	overlain	present
4760	139N	84W	27 bbc	overlain	absent
4643	139N	85W	18 dcc	overlain	present
4641	139N	85W	18 dcd	overlain	present
4652	139N	85W	21 bac	overlain	present
4653	139N	85W	22 bcb	overlain	present
4651	139N	85W	30 aab	overlain	absent
4659	139N	86W	22 ccd	overlain	present
4660	139N	86W	22 ccd	overlain	present
4648	139N	86W	25 ddb	overlain	present
4661	139N	86W	27 baa	overlain	present
4658	139N	86W	27 bab	overlain	present
4655	139N	86W	34 acd	overlain	present
4654	139N	86W	34 adc	overlain	present
4647	139N	86W	35 bda	overlain	present
4644	139N	86W	35 cbc	overlain	present
4645	139N	86W	35 ccc	overlain	present
4755	139N	87W	16 cdb	overlain	present
4756	139N	87W	23 bbb	overlain	present
9331	139N	88W	06 ddd	overlain	present
9298	139N	88W	08 ccc	overlain	present
4540	139N	88W	15 ccc	overlain	present
4541	139N	88W	25 bad	overlain	present
4539	139N	88W	28 dda	overlain	present
4538	139N	88W	31 bbc	overlain	present
4753	139N	88W	34 bcc	overlain	present

Table 3 (cont'd).

Location				Fox Hills Fm	Glacial Deposits
ID #	T	R	Sec		
4535	139N	89W	08 ddc	overlain	present
9300	139N	89W	21 acc	overlain	present
9299	139N	89W	26 ccd	overlain	present
8955	139N	89W	27 acc	overlain	present
8958	139N	89W	27 bcd	overlain	present
8956	139N	89W	28 daa	overlain	present
8957	139N	89W	28 dba	overlain	present
8961	139N	89W	33 ddd	overlain	present
9016	140N	81W	06 ccc	overlain	present
9017	140N	81W	18 abd	overlain	present
9327	140N	82W	01 dad	overlain	present
4765	140N	83W	16 aaa	overlain	present
4759	140N	84W	35 ccc	overlain	present
4758	140N	85W	18 bbc	overlain	present
4640	140N	85W	25 bbc	overlain	present
4639	140N	85W	25 bcb	overlain	present
4754	140N	88W	16 adb	overlain	present
4536	140N	89W	15 dcc	overlain	present
4537	140N	89W	36 add	overlain	present
9297	140N	90W	18 cbc	overlain	present
4532	140N	90W	21 bbb	overlain	present
4531	140N	90W	21 bcb	overlain	present
4530	140N	90W	32 bdd	overlain	present
4533	140N	90W	34 aaa	overlain	present

Appendix B. Hydrogeologic data.

Table 4. Water-level data for the Fox Hills aquifer.

Location			Water Elevation	
T	R	Sec	(ft)	(m)
Hettinger & Stark counties				
132N	091W	28DDD	2179	664.2
139N	091W	11DCD	2082	634.6
Mercer & Oliver counties				
140N	085W	03DDD	1822	555.3
141N	089W	11BC	1984	604.7
141N	089W	20CB	2075	632.5
141N	090W	09BAC	2045	623.3
141N	090W	09DB	2065	629.4
141N	090W	19CCD	2076	632.8
Grant & Sioux counties				
129N	080W	23DDD	1859	566.6
129N	081W	01BAB	1778	541.9
129N	087W	10BBC	1975	602.0
130N	082W	36BBC	1878	572.4
130N	083W	36AAA	1815	553.2
130N	084W	36ABA	1900	579.1
130N	085W	17DAA	1888	575.5
130N	086W	28CCC1	1922	585.8
130N	089W	32DDA	2109	642.8
131N	082W	18DCD	1783	543.5
131N	089W	30AAA	2073	631.9
132N	084W	16DAA	1827	556.9
133N	080W	13DDA	1674	510.2
133N	080W	31CCD1	1703	519.1
133N	083W	12ADA1	1765	538.0
133N	085W	12AAD	1837	559.9
134N	082W	36DCD	1677	511.1
134N	085W	21BAB1	1923	586.1
135N	090W	23BBB1	2091	637.3
137N	088W	21DDC	1986	605.3
Morton County				
135N	079W	10AAB1	1627	495.9
135N	083W	32CBB1	1830	557.8
136N	079W	05CCC	1630	496.8
136N	081W	07DDC1	1760	536.4
136N	081W	16CDD	1766	538.3
136N	082W	07CCC1	1778	541.9
137N	083W	06CDD1	1774	540.7
137N	086W	03AAD1	1868	569.4
138N	081W	09ABB1	1699	517.9
139N	081W	04BDA2	1738	529.7
139N	081W	09AAA1	1738	529.7
139N	083W	12DBA1	1776	541.3
139N	088W	34BCC1	1962	598.0
140N	085W	03DDD	1822	555.3
140N	090W	17ACB	2034	620.0
140N	090W	20DBA1	2095	638.6

Table 5. Input data for simulation of water levels in the Fox Hills aquifer.

Water-level data from water-level map (m).

676	669	661	655	648	640	632	623	616	609	602	597	588	586	582	580	575	572	570	569	566	566	567	565	561	558
673	667	660	653	647	639	630	620	611	604	597	592	589	583	581	577	573	570	569	566	562	561	564	564	560	556
671	665	659	653	646	638	628	618	608	599	592	588	583	581	581	578	570	564	567	566	555	550	555	556	553	549
669	663	657	650	644	635	625	615	605	595	587	582	578	577	577	577	565	554	562	564	550	543	545	547	546	545
668	662	655	647	639	630	621	612	603	594	586	580	575	573	572	568	560	554	553	552	545	541	540	540	540	539
668	661	653	644	634	626	618	610	601	593	585	579	574	570	566	561	554	548	545	542	539	536	534	534	534	533
669	662	653	643	633	625	617	609	601	593	585	579	573	568	562	556	549	543	538	535	533	530	529	528	527	528
669	664	653	643	633	625	617	609	601	593	585	578	572	565	559	553	546	539	533	529	526	524	523	522	522	522
668	661	652	643	634	625	617	609	601	593	586	578	570	563	557	550	543	535	528	523	521	519	517	516	517	518
666	659	650	641	633	625	616	609	601	594	587	579	569	560	555	549	542	532	522	517	515	513	512	511	512	513
664	657	649	640	632	624	616	609	602	596	589	583	571	560	556	550	542	531	516	512	511	510	508	507	508	509
662	655	647	639	630	622	615	608	602	596	591	587	579	567	559	552	543	532	520	514	512	509	506	504	504	505
660	653	645	637	629	621	613	607	600	595	591	586	579	569	562	557	546	536	527	520	515	510	505	502	501	502
658	651	643	635	626	619	611	604	598	592	587	582	575	568	562	556	548	540	533	526	519	512	505	499	498	499
656	648	640	632	624	616	608	601	595	589	583	577	571	565	559	553	547	541	537	533	524	513	504	497	496	498
654	646	638	629	621	613	605	598	591	584	578	572	566	560	554	549	545	541	538	538	527	514	503	496	496	498
652	644	635	627	618	610	602	595	587	580	574	568	561	555	549	545	541	538	535	531	523	513	503	498	498	500
649	641	633	625	616	607	599	592	584	576	569	563	557	550	544	540	538	534	530	525	519	512	506	501	500	502
646	639	631	623	614	606	597	589	581	573	566	561	555	548	542	538	535	531	526	521	517	512	508	505	503	503
644	637	629	621	613	604	595	588	580	573	566	560	554	548	543	539	535	530	523	518	516	513	510	507	506	505
641	635	629	621	612	603	594	587	580	573	566	559	554	548	544	541	537	532	526	521	518	515	513	510	509	508
638	634	629	622	613	603	595	588	580	573	566	559	554	549	545	543	540	535	530	527	522	518	516	512	512	509

Table 5 (cont'd).

Transmissivity values from transmissivity map (m^2/d).

12.6	12.0	11.3	10.9	10.8	10.8	10.9	11.2	11.8	12.3	13.0	13.6	14.4	14.9	15.2	15.2	15.3	15.6	16.2	16.7	16.4	15.7	15.0	13.1	11.6	10.4
12.8	12.2	11.5	10.8	10.5	10.4	10.5	10.8	11.4	12.0	13.0	13.8	14.5	15.1	15.5	15.3	14.9	15.2	16.6	17.3	16.4	15.2	14.5	12.1	9.8	0.0
13.2	12.5	11.8	10.9	10.2	10.0	10.2	10.5	11.1	11.9	13.0	14.0	14.8	15.5	16.1	15.9	14.4	13.8	17.1	18.8	15.8	12.3	10.0	7.7	6.1	0.0
13.6	13.0	12.4	11.4	10.3	10.1	10.1	10.2	10.5	11.4	12.8	14.0	15.1	16.1	16.8	17.0	15.2	13.9	17.6	18.8	13.6	8.0	3.0	1.4	0.0	0.0
14.7	14.0	13.3	12.5	11.7	11.0	10.4	9.8	9.6	10.2	11.6	13.3	15.0	16.4	17.5	18.1	18.1	18.1	18.0	15.6	10.3	4.3	0.1	0.0	0.0	0.0
15.6	15.2	14.6	14.0	13.2	12.4	11.2	9.8	8.6	8.6	10.2	12.5	14.8	16.7	18.3	19.5	20.7	21.9	19.3	14.2	7.9	2.1	0.0	0.0	0.0	0.0
16.6	16.4	16.1	15.7	15.1	14.2	12.7	10.4	7.4	6.4	8.9	12.1	14.9	17.1	19.0	20.4	21.6	22.6	19.6	14.0	7.3	2.2	4.4	4.7	0.0	0.0
17.7	17.6	17.6	17.4	17.1	16.6	15.4	12.5	8.0	5.4	9.3	12.7	15.4	17.6	19.3	20.2	20.8	20.6	18.5	14.7	10.3	7.4	7.9	6.5	0.0	0.0
18.8	19.0	19.1	19.2	19.2	19.0	18.8	16.5	12.2	10.5	12.1	14.5	16.6	18.0	18.9	19.2	19.2	18.9	17.7	15.8	13.9	10.9	7.7	5.4	0.0	0.0
19.8	20.0	20.3	20.7	20.9	20.7	20.2	18.4	15.9	14.8	15.5	17.1	18.2	18.3	17.8	17.4	17.3	17.4	17.1	16.2	14.7	11.1	6.4	3.1	0.0	0.0
20.6	20.9	21.3	21.8	22.3	21.5	20.6	19.2	17.9	17.4	18.3	19.8	20.1	18.3	16.3	15.0	15.0	15.8	16.5	16.3	14.5	10.4	4.6	0.4	0.0	0.0
21.0	21.4	21.8	22.2	22.2	21.6	20.6	19.5	18.7	18.5	19.5	21.4	21.3	17.4	13.9	11.7	12.3	14.2	16.1	17.0	15.8	11.7	5.3	0.7	0.0	0.0
21.6	21.8	22.1	22.2	22.0	21.3	20.3	19.2	18.3	18.1	18.7	19.5	18.7	15.5	11.5	7.4	9.9	13.2	16.2	18.6	19.2	15.3	9.5	5.5	0.0	0.0
21.8	22.0	22.1	22.1	21.8	21.0	19.8	18.4	17.2	16.6	16.8	17.0	16.3	14.2	11.2	8.8	10.1	13.2	16.5	19.8	22.6	18.5	13.4	9.8	0.0	0.0
21.8	22.0	22.0	22.0	21.7	20.8	19.4	17.6	15.6	14.3	14.7	15.1	15.0	14.1	12.6	11.4	11.7	13.7	16.7	19.5	20.6	18.8	15.3	12.3	0.0	0.0
21.7	21.8	22.0	22.0	21.7	20.9	19.1	16.8	14.5	13.0	13.1	13.8	14.5	14.9	14.6	14.0	13.4	14.1	17.1	19.2	19.7	18.5	15.9	13.3	0.0	0.0
21.4	21.6	21.1	21.4	21.6	21.2	19.1	16.2	13.4	11.5	11.5	12.8	14.6	16.3	17.2	17.0	16.2	16.5	18.5	19.8	19.8	18.5	0.0	0.0	0.0	0.0
19.8	20.3	20.7	21.0	21.2	21.3	18.8	15.4	12.1	9.4	9.6	12.0	14.9	17.9	20.5	20.2	19.4	19.7	20.8	21.3	20.5	0.0	0.0	0.0	0.0	0.0
19.4	19.8	20.1	20.2	20.1	19.4	17.4	14.5	11.3	8.3	8.8	11.7	14.9	18.3	21.7	21.6	21.0	21.7	23.0	23.0	21.2	0.0	0.0	0.0	0.0	0.0
18.8	19.1	19.3	19.2	18.9	18.0	16.3	14.0	11.6	9.8	10.0	11.9	14.5	17.2	19.3	20.1	20.4	21.5	23.8	24.1	20.7	0.0	0.0	0.0	0.0	0.0
18.5	18.6	18.6	18.2	17.7	16.9	15.5	13.7	12.1	11.0	10.9	12.1	13.9	15.7	17.0	17.7	18.0	18.6	19.4	19.3	0.0	0.0	0.0	0.0	0.0	0.0
17.6	17.6	17.7	17.4	16.9	16.0	14.9	13.6	12.5	11.7	11.6	12.2	13.2	14.3	15.0	15.2	15.0	14.9	13.6	12.9	0.0	0.0	0.0	0.0	0.0	0.0

Table 5 (cont'd).

Storativity values (1E20 = and prescribed-head boundary; 0 = variable-head cell).

1E20	1E20	1E20	1E20	1E20	1E20	1E20	1E20	1E20	1E20	1E20	1E20	1E20	1E20	1E20	1E20	1E20	1E20	1E20	1E20	1E20	1E20	1E20	1E20
1E20	0	0	0	0	0	0	0	0	0	0	0	0	0	0	0	0	0	0	0	0	0	0	1E20	0
1E20	0	0	0	0	0	0	0	0	0	0	0	0	0	0	0	0	0	0	0	0	0	0	1E20	0
1E20	0	0	0	0	0	0	0	0	0	0	0	0	0	0	0	0	0	0	0	0	0	1E20	0	0
1E20	0	0	0	0	0	0	0	0	0	0	0	0	0	0	0	0	0	0	0	0	1E20	0	0	0
1E20	0	0	0	0	0	0	0	0	0	0	0	0	0	0	0	0	0	0	0	1E20	0	0	0	0
1E20	0	0	0	0	0	0	0	0	0	0	0	0	0	0	0	0	0	0	0	0	1E20

Table 5 (cont'd).

Discharge from the Fox Hills aquifer (mm/yr).

0	0	0	0	0	0	0	0	0	0	0	0	0	0	0	0	0	0	0	0	0	0	-.5	-.5	-.5	
0	0	0	0	0	0	0	0	0	0	0	0	0	0	0	0	0	0	0	0	0	0	-.5	-.5	-.5	0
0	0	0	0	0	0	0	0	-.5	-.5	0	0	0	0	0	0	0	0	0	0	0	-.5	-.5	-.5	-.5	0
0	0	0	0	0	0	0	0	0	0	-.5	-.5	0	0	0	0	0	0	0	0	-.5	-.5	-.5	-.5	0	0
0	0	0	0	0	0	0	0	0	0	0	-.5	-.5	0	0	0	0	0	0	0	-.5	-.5	-.5	0	0	0
0	0	0	0	0	0	0	0	0	0	0	0	-.5	-.5	-.5	0	0	0	0	0	-.5	-.5	-.5	0	0	0
0	0	0	0	0	0	0	0	0	0	0	-.5	0	0	0	-.5	0	0	0	0	-.5	-.5	-.5	-.5	0	0
0	0	0	0	0	0	0	0	0	0	0	0	0	0	0	0	-.5	-.5	-.5	-.5	-.5	-.5	-.5	-.5	0	0
0	0	0	0	0	0	0	0	0	0	0	0	0	0	0	-.5	-.5	0	0	-.5	-.5	-.5	-.5	-.5	0	0
0	0	0	0	0	0	0	0	0	0	0	0	0	0	-.5	-.5	-.5	-.5	0	0	0	-.5	-.5	-.5	0	0
0	0	0	0	0	0	0	0	0	0	0	0	0	0	0	0	0	0	-.5	0	0	-.5	-.5	-.5	0	0
0	0	0	0	0	0	0	0	0	0	0	0	0	0	0	0	0	0	0	-.5	-.5	-.5	-.5	-.5	0	0
0	0	0	0	0	0	0	0	0	0	0	0	0	0	0	0	0	0	0	0	0	0	-.5	-.5	0	0
0	0	0	0	0	0	0	0	0	0	0	0	0	0	0	0	0	0	0	0	0	0	0	0	0	0
0	0	0	0	0	0	0	0	0	0	0	-.5	0	0	0	0	0	0	0	0	0	0	0	0	0	0
0	0	0	0	0	0	0	0	0	0	0	0	-.5	0	0	0	0	0	0	0	0	0	0	0	0	0
0	0	0	0	0	0	0	0	0	0	0	0	0	-.5	0	0	0	0	0	0	0	0	0	0	0	0
0	0	0	0	0	0	0	0	0	0	0	0	0	0	-.5	-.5	0	0	0	0	0	0	0	0	0	0
0	0	0	0	0	0	0	0	0	0	0	0	0	0	-.5	-.5	0	0	0	0	0	0	0	0	0	0
0	0	0	0	0	0	0	0	0	0	0	0	0	0	0	0	0	0	0	0	0	0	0	0	0	0
0	0	0	0	0	0	0	0	0	0	0	-.5	-.5	0	0	0	0	0	0	0	0	0	0	0	0	0
0	0	0	0	0	0	0	0	0	0	-.5	0	0	0	0	0	0	0	0	0	0	0	0	0	0	0

Appendix C. Hydrogeochemical data.

Table 6. Hydrochemistry data for the Fox Hills aquifer.

Location			Concentration in Milligrams per Liter								Concentration in Milliequivalents per Liter								Percent Milliequivalents							
T	R	Sec	Ca	Mg	Na	K	HCO3	CO3	SO4	Cl	Ca	Mg	Na	K	HCO3	CO3	SO4	Cl	Ca	Mg	Na	K	HCO3	CO3	SO4	Cl
Adams & Bowman counties (Croft, 1974)																										
129N	096W	04DCB	5.3	0.2	397	1.2	735	32	120	55	0.26	0.02	17.27	0.03	12.05	1.07	2.50	1.55	1.50	0.09	98.2	0.17	70.2	6.21	14.56	9.04
129N	096W	12DBB	4.2	1.1	455	2.7	852	0	45	165	0.21	0.09	19.79	0.07	13.96	0.00	0.94	4.65	1.04	0.45	98.2	0.34	71.4	0.00	4.79	23.80
129N	096W	13ACA	2.5	1.2	464	1.2	877	0	6.6	194	0.12	0.10	20.18	0.03	14.37	0.00	0.14	5.47	0.61	0.48	98.8	0.15	71.9	0.00	0.69	27.39
129N	096W	13ADD	2.5	0.6	393	1.1	789	13	101	47	0.12	0.05	17.10	0.03	12.93	0.43	2.10	1.33	0.72	0.29	98.8	0.16	77.0	2.58	12.52	7.90
129N	096W	13BBB1	2.3	1.6	400	1.2	794	20	66	71	0.11	0.13	17.40	0.03	13.01	0.67	1.37	2.00	0.65	0.74	98.4	0.17	76.3	3.91	8.06	11.74
129N	096W	13BDD1	2.3	1.1	390	1.1	853	1	70	44	0.11	0.09	16.97	0.03	13.98	0.03	1.46	1.24	0.67	0.53	98.6	0.16	83.7	0.20	8.72	7.43
129N	098W	31ABB	0.6	3.3	376	1	708	13	194	24	0.03	0.27	16.36	0.03	11.60	0.43	4.04	0.68	0.18	1.63	98.0	0.15	69.3	2.59	24.11	4.04
129N	099W	04ABA2	1.9	0.9	400	1	685	27	214	29	0.09	0.07	17.40	0.03	11.23	0.90	4.46	0.82	0.54	0.42	98.9	0.15	64.5	5.17	25.61	4.70
129N	099W	04CBB	2.2	0.9	393	1	724	7	213	30	0.11	0.07	17.10	0.03	11.87	0.23	4.43	0.85	0.63	0.43	98.8	0.15	68.3	1.34	25.51	4.87
129N	102W	14CDD	2.6	0.9	391	1	676	27	212	22	0.13	0.07	17.01	0.03	11.08	0.90	4.41	0.62	0.75	0.43	98.7	0.15	65.1	5.29	25.94	3.65
129N	104W	34ADA	3.5	0.4	396	1.4	683	31	254	14	0.17	0.03	17.23	0.04	11.19	1.03	5.29	0.39	1.00	0.19	98.6	0.20	62.5	5.77	29.53	2.21
129N	104W	34ADD3	4.2	3.5	511	1	941	7	316	1.1	0.21	0.29	22.23	0.03	15.42	0.23	6.58	0.03	0.92	1.27	97.7	0.11	69.3	1.05	29.55	0.14
129N	105W	02CAA	1.8	0	308	0.8	581	15	180	1	0.09	0.00	13.40	0.02	9.52	0.50	3.75	0.03	0.66	0.00	99.2	0.15	69.0	3.62	27.16	0.20
130N	098W	04DBB	3.4	1.6	418	1.9	897	0	11	129	0.17	0.13	18.18	0.05	14.70	0.00	0.23	3.64	0.92	0.71	98.1	0.26	79.2	0.00	1.23	19.60
130N	098W	04DCC	2	1.5	438	1.1	892	4	4.1	138	0.10	0.12	19.05	0.03	14.62	0.13	0.09	3.89	0.52	0.64	98.7	0.15	78.0	0.71	0.46	20.78
130N	101W	25AAA	11	8.6	373	1.3	680	23	208	36	0.55	0.71	16.23	0.03	11.15	0.77	4.33	1.02	3.13	4.04	92.6	0.19	64.6	4.44	25.09	5.88
130N	104W	21BBA	2.5	1.7	461	0.8	658	56	387	4.1	0.12	0.14	20.05	0.02	10.78	1.87	8.06	0.12	0.61	0.69	98.6	0.10	51.8	8.96	38.69	0.56
130N	104W	26DCD	1.9	0.4	360	1	621	50	194	3.2	0.09	0.03	15.66	0.03	10.18	1.67	4.04	0.09	0.60	0.21	99.0	0.16	63.7	10.43	25.29	0.57
131N	094W	20CBC1	6.2	2.3	504	3	888	0	44	237	0.31	0.19	21.92	0.08	14.55	0.00	0.92	6.69	1.38	0.84	97.4	0.34	65.7	0.00	4.13	30.18
131N	100W	09CCD	2.1	1.7	416	1	783	0	212	44	0.10	0.14	18.10	0.03	12.83	0.00	4.41	1.24	0.57	0.76	98.5	0.14	69.4	0.00	23.87	6.71
131N	100W	23DBA	2.2	0.2	415	1	789	3	179	35	0.11	0.02	18.05	0.03	12.93	0.10	3.73	0.99	0.60	0.09	99.2	0.14	72.9	0.56	21.00	5.56
131N	100W	26ABA	3.6	2.4	435	1.7	782	45	93	120	0.18	0.20	18.92	0.04	12.82	1.50	1.94	3.39	0.93	1.02	97.8	0.22	65.3	7.64	9.86	17.24
131N	101W	18BCC1	3.4	0.6	503	1.3	774	38	400	7.8	0.17	0.05	21.88	0.03	12.69	1.27	8.33	0.22	0.77	0.22	98.9	0.15	56.4	5.63	37.01	0.98
131N	102W	02DDA	1.2	0	409	1.1	743	11	240	26	0.06	0.00	17.79	0.03	12.18	0.37	5.00	0.73	0.33	0.00	99.5	0.16	66.6	2.01	27.34	4.01
131N	102W	07DDD1	3.4	0.6	465	2.8	779	23	165	133	0.17	0.05	20.23	0.07	12.77	0.77	3.44	3.75	0.83	0.24	98.6	0.35	61.6	3.70	16.58	18.11
131N	102W	11CAB	1.2	0	403	1.1	688	36	231	22	0.06	0.00	17.53	0.03	11.28	1.20	4.81	0.62	0.34	0.00	99.5	0.16	63.0	6.70	26.86	3.47
131N	102W	11DAD	0	0	415	1	751	4	219	33	0.00	0.00	18.05	0.03	12.31	0.13	4.56	0.93	0.00	0.00	99.9	0.14	68.6	0.74	25.43	5.19
131N	102W	14AAB	1.5	0.4	410	1.1	667	47	200	36	0.07	0.03	17.84	0.03	10.93	1.57	4.16	1.02	0.42	0.18	99.2	0.16	61.8	8.86	23.55	5.74
131N	104W	28AAA2	3.3	1	366	1	663	25	209	3.6	0.16	0.08	15.92	0.03	10.87	0.83	4.35	0.10	1.02	0.51	98.3	0.16	67.3	5.16	26.94	0.63

Table 6 (cont'd).

Location			Concentration in Milligrams per Liter								Concentration in Milliequivalents per Liter								Percent Milliequivalents							
T	R	Sec	Ca	Mg	Na	K	HCO3	CO3	SO4	Cl	Ca	Mg	Na	K	HCO3	CO3	SO4	Cl	Ca	Mg	Na	K	HCO3	CO3	SO4	Cl
131N	105W	18DCC	3.1	0.2	444	1	701	36	322	7.2	0.15	0.02	19.31	0.03	11.49	1.20	6.70	0.20	0.79	0.08	99.0	0.13	58.6	6.12	34.21	1.04
131N	105W	21ACC	2.6	0.5	426	1	687	55	270	3.8	0.13	0.04	18.53	0.03	11.26	1.83	5.62	0.11	0.69	0.22	99.0	0.14	59.8	9.74	29.87	0.57
131N	105W	23CDD	1.9	0.2	435	1.1	767	45	242	7.5	0.09	0.02	18.92	0.03	12.57	1.50	5.04	0.21	0.50	0.09	99.3	0.15	65.1	7.76	26.08	1.10
131N	106W	03DAA	46	22	541	5.4	825	0	681	5.7	2.30	1.81	23.53	0.14	13.52	0.00	14.18	0.16	8.26	6.52	84.7	0.50	48.5	0.00	50.89	0.58
131N	106W	04DCC	32	15	149	4.5	390	0	138	11	1.60	1.23	6.48	0.12	6.39	0.00	2.87	0.31	16.94	13.09	68.8	1.22	66.8	0.00	30.01	3.24
132N	097W	07CAB1	5.2	1.5	451	1.7	877	0	175	54	0.26	0.12	19.62	0.04	14.37	0.00	3.64	1.52	1.29	0.62	97.9	0.22	73.6	0.00	18.65	7.80
132N	100W	35DDD	4.1	1.2	447	1.3	908	0	179	37	0.20	0.10	19.44	0.03	14.88	0.00	3.73	1.04	1.03	0.50	98.3	0.17	75.7	0.00	18.96	5.31
132N	104W	17CCC	2.6	2.3	423	1	676	54	289	5.2	0.13	0.19	18.40	0.03	11.08	1.80	6.02	0.15	0.69	1.01	98.2	0.14	58.2	9.45	31.60	0.77
132N	104W	21AAA	2.5	1.5	444	1.1	792	35	250	7.7	0.12	0.12	19.31	0.03	12.98	1.17	5.21	0.22	0.64	0.63	98.6	0.14	66.3	5.96	26.60	1.11
132N	105W	16BDB	3.4	2.8	425	1	736	35	259	3.2	0.17	0.23	18.49	0.03	12.06	1.17	5.39	0.09	0.90	1.22	97.7	0.14	64.5	6.23	28.82	0.48
132N	106W	26BDC	5.8	3.5	627	1.6	769	18	661	2.3	0.29	0.29	27.27	0.04	12.60	0.60	13.76	0.06	1.04	1.03	97.8	0.15	46.6	2.22	50.91	0.24
Dunn County (Klausing, 1979a)																										
141N	096W	29CCC	22	3.7	550	5.6	897	0	260	220	1.10	0.30	23.93	0.14	14.70	0.00	5.41	6.21	4.31	1.19	93.9	0.56	55.9	0.00	20.57	23.58
142N	091W	25DBB	7.6	8.5	584	1.7	1350	13	17	131	0.38	0.70	25.40	0.04	22.13	0.43	0.35	3.70	1.43	2.64	95.8	0.16	83.2	1.63	1.33	13.89
145N	092W	25ABB	4	0.7	590	2	1100	33	7	240	0.20	0.06	25.67	0.05	18.03	1.10	0.15	6.77	0.77	0.22	98.8	0.20	69.2	4.22	0.56	25.99
145N	095W	22DAD1	2.8	1.5	480	3.1	1060	0	12	106	0.14	0.12	20.88	0.08	17.37	0.00	0.25	2.99	0.66	0.58	98.4	0.37	84.3	0.00	1.21	14.51
146N	093W	03CDD	2	0.4	530	1.9	1150	0	8.4	180	0.10	0.03	23.06	0.05	18.85	0.00	0.17	5.08	0.43	0.14	99.2	0.21	78.2	0.00	0.73	21.07
146N	094W	05CBD	4.5	3.2	732	2.8	1660	0	10	206	0.22	0.26	31.84	0.07	27.21	0.00	0.21	5.81	0.69	0.81	98.3	0.22	81.9	0.00	0.63	17.49
146N	094W	08DAD	6.6	2.6	913	3.4	1980	21	10	274	0.33	0.21	39.72	0.09	32.45	0.70	0.21	7.73	0.82	0.53	98.4	0.22	79.0	1.70	0.51	18.81
146N	095W	03DCB	2	0.7	527	1.8	1160	0	0	154	0.10	0.06	22.92	0.05	19.01	0.00	0.00	4.34	0.43	0.25	99.1	0.20	81.4	0.00	0.00	18.60
147N	094W	26BCB	2.6	0.6	596	1.9	1230	0	1.7	214	0.13	0.05	25.93	0.05	20.16	0.00	0.04	6.04	0.50	0.19	99.1	0.19	76.9	0.00	0.13	23.01
147N	094W	34BAD	2.4	0.7	560	1.8	1190	0	3.7	181	0.12	0.06	24.36	0.05	19.50	0.00	0.08	5.11	0.49	0.23	99.1	0.19	79.0	0.00	0.31	20.68
147N	095W	12CAD	3.4	1	736	2.6	1560	0	100	129	0.17	0.08	32.02	0.07	25.57	0.00	2.08	3.64	0.52	0.25	99.0	0.21	81.7	0.00	6.65	11.63
147N	095W	13CCC2	1.8	0.4	522	1.9	1100	26	9.5	150	0.09	0.03	22.71	0.05	18.03	0.87	0.20	4.23	0.39	0.14	99.3	0.21	77.3	3.72	0.85	18.14
147N	095W	14AAA	3.2	2	745	2.5	1570	0	94	136	0.16	0.16	32.41	0.06	25.73	0.00	1.96	3.84	0.49	0.50	98.8	0.19	81.6	0.00	6.21	12.17
147N	095W	24AAC	2	0.2	519	1.6	1110	14	100	82	0.10	0.02	22.58	0.04	18.19	0.47	2.08	2.31	0.44	0.07	99.3	0.18	78.9	2.02	9.03	10.03
147N	095W	26BBB1	3.4	1.6	564	1.7	1170	0	19	189	0.17	0.13	24.53	0.04	19.18	0.00	0.40	5.33	0.68	0.53	98.6	0.17	77.0	0.00	1.59	21.41
147N	097W	20BAB	2.2	0.1	494	1.6	1140	0	0	109	0.11	0.01	21.49	0.04	18.68	0.00	0.00	3.07	0.51	0.04	99.3	0.19	85.9	0.00	0.00	14.13
148N	095W	22CCA	5.1	1.8	783	2.8	1560	0	30	292	0.25	0.15	34.06	0.07	25.57	0.00	0.62	8.24	0.74	0.43	98.6	0.21	74.3	0.00	1.81	23.92
148N	095W	31CCA	2.1	1.7	500	1.5	1130	6	14	124	0.10	0.14	21.75	0.04	18.52	0.20	0.29	3.50	0.48	0.63	98.7	0.17	82.3	0.89	1.29	15.54
148N	095W	32DBD	2.7	1.8	703	2.5	1690	0	0	139	0.13	0.15	30.58	0.06	27.70	0.00	0.00	3.92	0.44	0.48	98.9	0.21	87.6	0.00	0.00	12.40
148N	096W	09ABD	2.8	0	535	1.9	1200	2	11	138	0.14	0.00	23.27	0.05	19.67	0.07	0.23	3.89	0.60	0.00	99.2	0.21	82.4	0.28	0.96	16.32
148N	096W	11BB	4.3	5.2	771	2.2	1690	0	6.8	249	0.21	0.43	33.54	0.06	27.70	0.00	0.14	7.02	0.63	1.25	98.0	0.16	79.4	0.00	0.41	20.15
148N	097W	09DBD	2.6	1.6	552	2.3	1150	16	3.3	154	0.13	0.13	24.01	0.06	18.85	0.53	0.07	4.34	0.53	0.54	98.7	0.24	79.2	2.24	0.29	18.26
148N	097W	17DAA	2.6	0.6	587	2.6	1150	9	4.5	231	0.13	0.05	25.53	0.07	18.85	0.30	0.09	6.52	0.50	0.19	99.0	0.26	73.2	1.16	0.36	25.30
148N	097W	20CAD	1.6	0.7	556	1.7	1170	0	4.1	150	0.08	0.06	24.19	0.04	19.18	0.00	0.09	4.23	0.33	0.24	99.3	0.18	81.6	0.00	0.36	18.01
148N	097W	22CDC	1.9	0.4	512	1.5	1140	21	0	122	0.09	0.03	22.27	0.04	18.68	0.70	0.00	3.44	0.42	0.15	99.3	0.17	81.9	3.07	0.00	15.08

Table 6 (cont'd).

Location			Concentration in Milligrams per Liter								Concentration in Milliequivalents per Liter								Percent Milliequivalents							
T	R	Sec	Ca	Mg	Na	K	HCO3	CO3	SO4	Cl	Ca	Mg	Na	K	HCO3	CO3	SO4	Cl	Ca	Mg	Na	K	HCO3	CO3	SO4	Cl
148N	097W	30ADA	2.9	0.5	514	2.4	1140	10	4.9	119	0.14	0.04	22.36	0.06	18.68	0.33	0.10	3.36	0.64	0.18	98.9	0.27	83.1	1.48	0.45	14.94
148N	097W	33ABB	1.6	0.3	500	2.2	1150	0	5.9	120	0.08	0.02	21.75	0.06	18.85	0.00	0.12	3.39	0.36	0.11	99.3	0.26	84.3	0.00	0.55	15.14
Golden Valley, Billings & Slope counties (Anna, 1980)																										
133N	099W	02CBB	2.4	1.5	480	1	891	32	150	80	0.12	0.12	20.88	0.03	14.60	1.07	3.12	2.26	0.57	0.58	98.7	0.12	69.4	5.07	14.84	10.72
133N	099W	32BBA	2.3	2.6	450	1.2	830	30	180	64	0.11	0.21	19.58	0.03	13.60	1.00	3.75	1.81	0.58	1.07	98.2	0.15	67.5	4.96	18.59	8.96
133N	103W	23BDC	1.4	0.6	410	5.5	814	91	65	8.2	0.07	0.05	17.84	0.14	13.34	3.03	1.35	0.23	0.39	0.27	98.6	0.78	74.3	16.89	7.54	1.29
133N	105W	30CCC	5.9	1.8	610	1.5	700	28	720	9.8	0.29	0.15	26.54	0.04	11.47	0.93	14.99	0.28	1.09	0.55	98.2	0.14	41.5	3.37	54.17	1.00
133N	106W	13ADB2	4.1	5.1	570	1.8	678	25	660	8.1	0.20	0.42	24.80	0.05	11.11	0.83	13.74	0.23	0.80	1.65	97.4	0.18	42.9	3.22	53.02	0.88
133N	106W	34BAA	2.8	0.4	470	1.5	728	14	420	5.5	0.14	0.03	20.45	0.04	11.93	0.47	8.74	0.16	0.68	0.16	99.0	0.19	56.0	2.19	41.06	0.73
134N	104W	24DDD1	3.1	2.8	400	2.5	653	45	150	110	0.15	0.23	17.40	0.06	10.70	1.50	3.12	3.10	0.87	1.29	97.5	0.36	58.1	8.14	16.95	16.84
134N	105W	09BAA	1.9	2.3	330	0.8	527	28	230	23	0.09	0.19	14.36	0.02	8.64	0.93	4.79	0.65	0.65	1.29	97.9	0.14	57.6	6.22	31.91	4.32
134N	105W	26BAA	1.8	0.6	360	1.5	623	33	220	9	0.09	0.05	15.66	0.04	10.21	1.10	4.58	0.25	0.57	0.31	98.9	0.24	63.2	6.81	28.37	1.57
135N	102W	03CDB	2.3	1.6	420	1.8	712	29	220	66	0.11	0.13	18.27	0.05	11.67	0.97	4.58	1.86	0.62	0.71	98.4	0.25	61.2	5.07	24.01	9.76
135N	102W	19DAA	2.1	1.7	460	3.6	822	35	56	170	0.10	0.14	20.01	0.09	13.47	1.17	1.17	4.80	0.52	0.69	98.3	0.45	65.4	5.66	5.66	23.28
135N	104W	19CDD	2.1	2	360	1.2	630	22	200	14	0.10	0.16	15.66	0.03	10.33	0.73	4.16	0.39	0.66	1.03	98.1	0.19	66.1	4.69	26.66	2.53
136N	100W	31DDC1	4.7	0.6	470	3.5	742	87	220	57	0.23	0.05	20.45	0.09	12.16	2.90	4.58	1.61	1.13	0.24	98.2	0.43	57.2	13.65	21.56	7.57
136N	102W	11DAC	0.8	0	410	1.6	710	41	220	25	0.04	0.00	17.84	0.04	11.64	1.37	4.58	0.71	0.22	0.00	99.5	0.23	63.6	7.47	25.04	3.86
136N	102W	15ACC	2.1	1	420	1.3	730	30	140	88	0.10	0.08	18.27	0.03	11.96	1.00	2.91	2.48	0.57	0.44	98.8	0.18	65.2	5.45	15.87	13.52
136N	102W	20BBD	0.8	0.5	410	1.6	700	31	220	28	0.04	0.04	17.84	0.04	11.47	1.03	4.58	0.79	0.22	0.23	99.3	0.23	64.2	5.78	25.62	4.42
136N	102W	21DBD	1.2	0.7	400	1.6	730	34	220	22	0.06	0.06	17.40	0.04	11.96	1.13	4.58	0.62	0.34	0.33	99.1	0.23	65.4	6.19	25.03	3.39
136N	103W	14ADA	0.8	0.5	410	1.7	720	41	220	18	0.04	0.04	17.84	0.04	11.80	1.37	4.58	0.51	0.22	0.23	99.3	0.24	64.6	7.49	25.09	2.78
136N	103W	23ADB	1.6	0.5	400	1.4	690	46	220	21	0.08	0.04	17.40	0.04	11.31	1.53	4.58	0.59	0.45	0.23	99.1	0.20	62.8	8.51	25.43	3.29
136N	103W	24ABD	0.8	0.5	400	1.6	730	34	220	22	0.04	0.04	17.40	0.04	11.96	1.13	4.58	0.62	0.23	0.23	99.3	0.23	65.4	6.19	25.03	3.39
136N	104W	12BAD	2.4	2	390	3.5	593	32	300	25	0.12	0.16	16.97	0.09	9.72	1.07	6.25	0.71	0.69	0.95	97.8	0.52	54.8	6.01	35.21	3.98
137N	101W	29CCA	1.6	0.5	410	1.8	850	41	110	19	0.08	0.04	17.84	0.05	13.93	1.37	2.29	0.54	0.44	0.23	99.1	0.26	76.9	7.54	12.64	2.96
137N	101W	30ABC	0.8	0.2	390	1.7	750	32	170	23	0.04	0.02	16.97	0.04	12.29	1.07	3.54	0.65	0.23	0.10	99.4	0.25	70.1	6.08	20.17	3.70
137N	101W	30BBC	0.8	0	400	1.8	860	32	110	15	0.04	0.00	17.40	0.05	14.10	1.07	2.29	0.42	0.23	0.00	99.5	0.26	78.9	5.97	12.81	2.37
137N	102W	06CBD	0.8	1.2	420	1.8	750	31	240	7.5	0.04	0.10	18.27	0.05	12.29	1.03	5.00	0.21	0.22	0.53	99.0	0.25	66.3	5.57	26.96	1.14
137N	103W	12BAB	0.4	1.5	400	1.7	620	36	280	31	0.02	0.12	17.40	0.04	10.16	1.20	5.83	0.87	0.11	0.70	98.9	0.25	56.2	6.64	32.27	4.84
137N	105W	10ABB	5.9	1.1	500	1.4	770	21	370	18	0.29	0.09	21.75	0.04	12.62	0.70	7.70	0.51	1.33	0.41	98.1	0.16	58.6	3.25	35.78	2.36
138N	102W	34DDA	1.2	0.5	410	0.9	650	42	210	28	0.06	0.04	17.84	0.02	10.65	1.40	4.37	0.79	0.33	0.23	99.3	0.13	61.9	8.13	25.40	4.59
138N	103W	13BAA	2.2	2.1	400	1.1	605	36	270	30	0.11	0.17	17.40	0.03	9.92	1.20	5.62	0.85	0.62	0.98	98.2	0.16	56.4	6.82	31.97	4.81
138N	106N	25DDA	1.5	1.6	420	0.9	717	24	280	21	0.07	0.13	18.27	0.02	11.75	0.80	5.83	0.59	0.40	0.71	98.8	0.12	61.9	4.22	30.72	3.12
139N	102W	02DCA	0.8	0.7	420	1.6	730	40	220	39	0.04	0.06	18.27	0.04	11.96	1.33	4.58	1.10	0.22	0.31	99.2	0.22	63.0	7.02	24.13	5.80
139N	102W	14DBD	1.2	0	410	1.8	733	32	210	41	0.06	0.00	17.84	0.05	12.01	1.07	4.37	1.16	0.33	0.00	99.4	0.26	64.6	5.73	23.49	6.22
139N	102W	17CAC2	2	0.7	410	1.1	660	39	250	32	0.10	0.06	17.84	0.03	10.82	1.30	5.21	0.90	0.55	0.32	99.0	0.16	59.4	7.13	28.56	4.95
139N	105W	13BBC	3	0.9	440	1.3	760	27	270	24	0.15	0.07	19.14	0.03	12.46	0.90	5.62	0.68	0.77	0.38	98.7	0.17	63.4	4.58	28.60	3.44

Table 6 (cont'd).

Location			Concentration in Milligrams per Liter								Concentration in Milliequivalents per Liter								Percent Milliequivalents							
T	R	Sec	Ca	Mg	Na	K	HCO3	CO3	SO4	Cl	Ca	Mg	Na	K	HCO3	CO3	SO4	Cl	Ca	Mg	Na	K	HCO3	CO3	SO4	Cl
140N	100W	28CAB	1.6	2.2	410	2.3	794	31	160	34	0.08	0.18	17.84	0.06	13.01	1.03	3.33	0.96	0.44	1.00	98.2	0.32	71.0	5.63	18.17	5.23
140N	101W	35DAD	1.5	0.4	420	1.5	746	42	120	67	0.07	0.03	18.27	0.04	12.23	1.40	2.50	1.89	0.41	0.18	99.2	0.21	67.9	7.77	13.87	10.49
140N	102W	06DCC	1.4	0.1	430	1.1	680	40	260	37	0.07	0.01	18.71	0.03	11.15	1.33	5.41	1.04	0.37	0.04	99.4	0.15	58.9	7.04	28.59	5.51
140N	102W	10DDA	1.2	0.2	450	1.8	590	19	500	7	0.06	0.02	19.58	0.05	9.67	0.63	10.41	0.20	0.30	0.08	99.4	0.23	46.2	3.03	49.78	0.94
140N	102W	18DCC	2.6	1.6	420	1.2	670	26	260	44	0.13	0.13	18.27	0.03	10.98	0.87	5.41	1.24	0.70	0.71	98.4	0.17	59.4	4.68	29.26	6.71
140N	102W	22DBD	3.1	1.3	410	1.2	668	38	220	56	0.15	0.11	17.84	0.03	10.95	1.27	4.58	1.58	0.85	0.59	98.4	0.17	59.6	6.89	24.93	8.60
140N	102W	22DCD	3.1	0.6	410	1.1	680	30	220	48	0.15	0.05	17.84	0.03	11.15	1.00	4.58	1.35	0.86	0.27	98.7	0.16	61.6	5.53	25.33	7.49
140N	102W	26ACC	4	0	440	0	740	50	220	38	0.20	0.00	19.14	0.00	12.13	1.67	4.58	1.07	1.03	0.00	99.0	0.00	62.4	8.57	23.55	5.51
140N	102W	26BBB	3.2	1.5	400	0	580	22	220	38	0.16	0.12	17.40	0.00	9.51	0.73	4.58	1.07	0.90	0.70	98.4	0.00	59.8	4.61	28.82	6.75
140N	102W	26BCA	2.9	0.5	410	0.9	730	33	190	37	0.14	0.04	17.84	0.02	11.96	1.10	3.96	1.04	0.80	0.23	98.8	0.13	66.2	6.09	21.90	5.78
140N	102W	27ACB1	1.2	0.5	440	1.9	780	53	170	42	0.06	0.04	19.14	0.05	12.78	1.77	3.54	1.18	0.31	0.21	99.2	0.25	66.3	9.16	18.36	6.15
140N	102W	34AAD	1.2	0.5	400	1.7	710	38	240	31	0.06	0.04	17.40	0.04	11.64	1.27	5.00	0.87	0.34	0.23	99.2	0.25	62.0	6.75	26.61	4.66
140N	103W	02CDC	2.1	2.4	440	1.2	710	30	220	65	0.10	0.20	19.14	0.03	11.64	1.00	4.58	1.83	0.54	1.01	98.3	0.16	61.1	5.25	24.04	9.63
140N	104W	12ADB	1.6	1	430	1.7	666	23	300	38	0.08	0.08	18.71	0.04	10.92	0.77	6.25	1.07	0.42	0.43	98.9	0.23	57.5	4.03	32.87	5.64
140N	104W	15BBD	2	0.5	430	2.3	674	22	310	38	0.10	0.04	18.71	0.06	11.05	0.73	6.45	1.07	0.53	0.22	98.9	0.31	57.2	3.80	33.43	5.55
140N	105W	14ABA	4	0.5	450	1.8	708	35	320	37	0.20	0.04	19.58	0.05	11.60	1.17	6.66	1.04	1.00	0.21	98.6	0.23	56.7	5.70	32.54	5.10
140N	105W	30CCC1	13	19	570	3.3	728	39	640	31	0.65	1.56	24.80	0.08	11.93	1.30	13.32	0.87	2.39	5.77	91.5	0.31	43.5	4.74	48.58	3.19
140N	106W	25CBB1	3.6	1.5	530	1.3	790	18	430	23	0.18	0.12	23.06	0.03	12.95	0.60	8.95	0.65	0.77	0.53	98.6	0.14	55.9	2.59	38.67	2.80
141N	100W	30ACA	1.8	1.1	410	2.1	765	30	170	37	0.09	0.09	17.84	0.05	12.54	1.00	3.54	1.04	0.50	0.50	98.7	0.30	69.2	5.52	19.53	5.76
141N	101W	02AAC	0	0	440	2	890	0	150	40	0.00	0.00	19.14	0.05	14.59	0.00	3.12	1.13	0.00	0.00	99.7	0.27	77.4	0.00	16.58	5.99
141N	101W	21BCB	2.4	0.5	430	0	760	42	200	33	0.12	0.04	18.71	0.00	12.46	1.40	4.16	0.93	0.63	0.22	99.1	0.00	65.7	7.39	21.97	4.91
141N	101W	21CAC	1.6	0.2	410	2	740	42	190	38	0.08	0.02	17.84	0.05	12.13	1.40	3.96	1.07	0.44	0.09	99.2	0.28	65.4	7.54	21.32	5.78
142N	101W	33DBA	0.4	0	460	1.9	820	41	190	35	0.02	0.00	20.01	0.05	13.44	1.37	3.96	0.99	0.10	0.00	99.7	0.24	68.1	6.92	20.03	5.00
142N	102W	04BCB	3.2	0	570	2.8	1500	26	12	2	0.16	0.00	24.80	0.07	24.59	0.87	0.25	0.06	0.64	0.00	99.1	0.29	95.4	3.36	0.97	0.22
143N	102W	01BBD	0.8	0.2	470	1.8	870	29	140	48	0.04	0.02	20.45	0.05	14.26	0.97	2.91	1.35	0.19	0.08	99.5	0.22	73.1	4.96	14.95	6.95
143N	102W	29AAD	2.4	5	450	1.8	750	42	250	44	0.12	0.41	19.58	0.05	12.29	1.40	5.21	1.24	0.59	2.04	97.1	0.23	61.0	6.95	25.85	6.16
143N	105W	33BAB	3.5	0.6	450	1.3	834	26	190	40	0.17	0.05	19.58	0.03	13.67	0.87	3.96	1.13	0.88	0.25	98.7	0.17	69.7	4.42	20.16	5.75
144N	099W	14ABB	1.8	0.9	430	1.3	969	22	7	84	0.09	0.07	18.71	0.03	15.88	0.73	0.15	2.37	0.48	0.39	99.0	0.18	83.0	3.83	0.76	12.39
144N	100W	24BBD1	1.8	0.2	430	1.7	928	39	29	77	0.09	0.02	18.71	0.04	15.21	1.30	0.60	2.17	0.48	0.09	99.2	0.23	78.9	6.74	3.13	11.26
144N	102W	27DCC	1.6	0	470	2	890	34	160	56	0.08	0.00	20.45	0.05	14.59	1.13	3.33	1.58	0.39	0.00	99.4	0.25	70.7	5.49	16.15	7.66
144N	102W	29BBA	1.6	0	440	2	810	34	170	49	0.08	0.00	19.14	0.05	13.28	1.13	3.54	1.38	0.41	0.00	99.3	0.27	68.7	5.86	18.31	7.15
Hettinger & Stark counties (Trapp, 1971)																										
132N	091W	28DDD	4.3	1.6	554	2.6	1010	18	5.7	242	0.21	0.13	24.10	0.07	16.55	0.60	0.12	6.83	0.88	0.54	98.3	0.27	68.7	2.49	0.49	28.33
135N	097W	04DCA	3.8	1.6	566	2.4	1080	21	46	191	0.19	0.13	24.62	0.06	17.70	0.70	0.96	5.39	0.76	0.53	98.5	0.25	71.5	2.83	3.87	21.77
139N	095W	01DDA	2.4	0.5	600	1.9	1160	0	2.4	246	0.12	0.04	26.10	0.05	19.01	0.00	0.05	6.94	0.46	0.16	99.2	0.18	73.1	0.00	0.19	26.69
McKenzie County (Croft, 1985a)																										

Table 6 (cont'd).

Location			Concentration in Milligrams per Liter								Concentration in Milliequivalents per Liter								Percent Milliequivalents							
T	R	Sec	Ca	Mg	Na	K	HCO3	CO3	SO4	Cl	Ca	Mg	Na	K	HCO3	CO3	SO4	Cl	Ca	Mg	Na	K	HCO3	CO3	SO4	Cl
145N	098W	34DCA	2.9	0.2	460	1.2	980	24	2.9	86	0.14	0.02	20.01	0.03	16.06	0.80	0.06	2.43	0.72	0.08	99.1	0.15	83.0	4.13	0.31	12.54
145N	102W	15ABC	1.8	0.9	430	1.2	940	41	15	69	0.09	0.07	18.71	0.03	15.41	1.37	0.31	1.95	0.48	0.39	99.0	0.16	81.0	7.18	1.64	10.23
145N	102W	27CBB	1.8	0.6	440	1.3	890	36	85	64	0.09	0.05	19.14	0.03	14.59	1.20	1.77	1.81	0.47	0.26	99.1	0.17	75.3	6.20	9.14	9.32
146N	101W	30BDB2	2.4	1.7	430	1.2	980	26	1.2	53	0.12	0.14	18.71	0.03	16.06	0.87	0.02	1.50	0.63	0.74	98.5	0.16	87.1	4.70	0.14	8.10
146N	102W	27BCA	3.2	0	450	1.6	970	33	2.1	84	0.16	0.00	19.58	0.04	15.90	1.10	0.04	2.37	0.81	0.00	99.0	0.21	81.9	5.67	0.23	12.21
146N	103W	02BCC	4.2	0.6	480	1.6	1000	38	2.5	100	0.21	0.05	20.88	0.04	16.39	1.27	0.05	2.82	0.99	0.23	98.6	0.19	79.8	6.17	0.25	13.74
147N	100W	20DDB2	1.5	1.6	480	1.4	1100	0	0	99	0.07	0.13	20.88	0.04	18.03	0.00	0.00	2.79	0.35	0.62	98.9	0.17	86.6	0.00	0.00	13.41
148N	099W	05DBA	1.8	2.6	510	1.5	1110	8	2.5	140	0.09	0.21	22.19	0.04	18.19	0.27	0.05	3.95	0.40	0.95	98.5	0.17	81.0	1.19	0.23	17.58
148N	099W	36CAA	2.1	0.7	490	1.5	1100	23	2.1	110	0.10	0.06	21.32	0.04	18.03	0.77	0.04	3.10	0.49	0.27	99.1	0.18	82.2	3.49	0.20	14.14
148N	102W	15DDA1	1.6	0.7	490	2	990	43	4.5	120	0.08	0.06	21.32	0.05	16.23	1.43	0.09	3.39	0.37	0.27	99.1	0.24	76.8	6.78	0.44	16.01
148N	105W	26DDB	2.4	2.2	440	1	970	19	1.2	95	0.12	0.18	19.14	0.03	15.90	0.63	0.02	2.68	0.62	0.93	98.3	0.13	82.6	3.29	0.13	13.93
149N	094W	14BA	6.2	0.6	820	3.3	1230	0	550	180	0.31	0.05	35.67	0.08	20.16	0.00	11.45	5.08	0.86	0.14	98.8	0.23	54.9	0.00	31.21	13.84
149N	096W	27CBA	2.7	1.3	560	1.8	1200	21	7.4	170	0.13	0.11	24.36	0.05	19.67	0.70	0.15	4.80	0.55	0.43	98.8	0.19	77.7	2.76	0.61	18.94
149N	097W	29ADD	1.8	1.3	540	1.7	1210	0	3.7	150	0.09	0.11	23.49	0.04	19.83	0.00	0.08	4.23	0.38	0.45	99.0	0.18	82.2	0.00	0.32	17.53
149N	102W	31DAC	2	1.5	510	1.6	1110	0	2.1	160	0.10	0.12	22.19	0.04	18.19	0.00	0.04	4.51	0.44	0.55	98.8	0.18	80.0	0.00	0.19	19.84
150N	096W	26DCB	2.7	1.3	600	2	1250	0	6.6	220	0.13	0.11	26.10	0.05	20.49	0.00	0.14	6.21	0.51	0.41	98.9	0.19	76.4	0.00	0.51	23.13
150N	099W	22BBA1	2.1	1	530	1.8	1090	39	1.6	140	0.10	0.08	23.06	0.05	17.87	1.30	0.03	3.95	0.45	0.35	99.0	0.20	77.2	5.62	0.14	17.06
150N	104W	04BBB	2.3	3.3	530	1.6	1090	17	1.2	180	0.11	0.27	23.06	0.04	17.87	0.57	0.02	5.08	0.49	1.16	98.2	0.17	75.9	2.41	0.11	21.58
150N	104W	14BCA	4	5.1	860	3.2	2120	10	11	110	0.20	0.42	37.41	0.08	34.75	0.33	0.23	3.10	0.52	1.10	98.2	0.21	90.5	0.87	0.60	8.08
151N	104W	04AAA	1.8	2.6	540	1.8	1100	18	3.3	180	0.09	0.21	23.49	0.05	18.03	0.60	0.07	5.08	0.38	0.90	98.5	0.19	75.8	2.52	0.29	21.36
151N	104W	25DBD	2.5	1.5	530	1.6	1110	13	0.8	180	0.12	0.12	23.06	0.04	18.19	0.43	0.02	5.08	0.53	0.53	98.8	0.18	76.7	1.83	0.07	21.41
152N	098W	10CDD	3.4	2.6	650	2	1300	0	0.8	280	0.17	0.21	28.28	0.05	21.31	0.00	0.02	7.90	0.59	0.74	98.5	0.18	72.9	0.00	0.06	27.03
152N	098W	24CCC	3.4	2.8	770	2.7	1350	0	1.6	440	0.17	0.23	33.50	0.07	22.13	0.00	0.03	12.41	0.50	0.68	98.6	0.20	64.0	0.00	0.10	35.90
152N	099W	03ACB	2	1.7	630	2.1	1290	0	0	230	0.10	0.14	27.41	0.05	21.14	0.00	0.00	6.49	0.36	0.50	98.9	0.19	76.5	0.00	0.00	23.48
152N	099W	24BBB	0.8	2.2	610	1.9	1240	0	0.8	220	0.04	0.18	26.54	0.05	20.32	0.00	0.02	6.21	0.15	0.68	99.0	0.18	76.6	0.00	0.06	23.38
152N	101W	14CAD	2.7	4.3	770	2.6	1720	0	3.7	220	0.13	0.35	33.50	0.07	28.19	0.00	0.08	6.21	0.40	1.04	98.4	0.20	81.8	0.00	0.22	18.00
152N	103W	25CAB	1.6	5.1	540	1.7	1090	29	4.5	160	0.08	0.42	23.49	0.04	17.87	0.97	0.09	4.51	0.33	1.75	97.7	0.18	76.2	4.12	0.40	19.26
153N	094W	23CCC1	4.4	3.4	760	3.3	1270	28	8.6	420	0.22	0.28	33.06	0.08	20.82	0.93	0.18	11.85	0.65	0.83	98.3	0.25	61.6	2.76	0.53	35.08
153N	096W	03BCB	3.8	1.8	790	2.8	1530	0	0	380	0.19	0.15	34.37	0.07	25.08	0.00	0.00	10.72	0.55	0.43	98.8	0.21	70.1	0.00	0.00	29.95
153N	097W	02CDD	3.8	1.6	700	2.2	1320	0	0.8	320	0.19	0.13	30.45	0.06	21.63	0.00	0.02	9.03	0.62	0.43	98.8	0.18	70.5	0.00	0.05	29.43
153N	097W	35DCC	3.7	2.7	710	2.4	1310	0	1.6	330	0.18	0.22	30.89	0.06	21.47	0.00	0.03	9.31	0.59	0.71	98.5	0.20	69.7	0.00	0.11	30.21
Mercer & Oliver counties (Croft, 1970)																										
141N	089W	11BC	3.6	0.2	601	1.9	1280	0	3.3	189	0.18	0.02	26.14	0.05	20.98	0.00	0.07	5.33	0.68	0.06	99.1	0.18	79.5	0.00	0.26	20.21
142N	084W	24BBA	4.2	1.3	684	2.5	1170	38	4.6	343	0.21	0.11	29.75	0.06	19.18	1.27	0.10	9.68	0.70	0.35	98.7	0.21	63.5	4.19	0.32	32.02
142N	090W	25CB	5.2	0.5	810	20	1940	65	21	63	0.26	0.04	35.24	0.51	31.80	2.17	0.44	1.78	0.72	0.11	97.7	1.42	87.9	5.99	1.21	4.91
143N	090W	24BA	2.8	0.7	626	24	1520	0	11	108	0.14	0.06	27.23	0.61	24.91	0.00	0.23	3.05	0.50	0.21	97.1	2.19	88.4	0.00	0.81	10.81
144N	087W	20DDD	3.6	0.5	590	34	1070	50	3.3	267	0.18	0.04	25.67	0.87	17.54	1.67	0.07	7.53	0.67	0.15	95.9	3.25	65.4	6.22	0.26	28.10

Table 6 (cont'd).

Location			Concentration in Milligrams per Liter								Concentration in Milliequivalents per Liter								Percent Milliequivalents							
T	R	Sec	Ca	Mg	Na	K	HCO3	CO3	SO4	Cl	Ca	Mg	Na	K	HCO3	CO3	SO4	Cl	Ca	Mg	Na	K	HCO3	CO3	SO4	Cl
144N	089W	14CDD	4	0.5	601	1.9	1160	0	4.9	237	0.20	0.04	26.14	0.05	19.01	0.00	0.10	6.69	0.76	0.16	98.9	0.18	73.7	0.00	0.40	25.91
144N	090W	04BBA	4	0.2	614	10	1350	50	2.5	121	0.20	0.02	26.71	0.26	22.13	1.67	0.05	3.41	0.73	0.06	98.3	0.94	81.2	6.11	0.19	12.52
144N	090W	15DB	2.4	1.2	567	1.9	1120	38	2	185	0.12	0.10	24.66	0.05	18.36	1.27	0.04	5.22	0.48	0.40	98.9	0.19	73.8	5.09	0.17	20.97
144N	090W	24BD	3.6	0.7	626	20	1370	55	8.2	124	0.18	0.06	27.23	0.51	22.45	1.83	0.17	3.50	0.64	0.21	97.3	1.83	80.3	6.56	0.61	12.51
145N	085W	22CAC	4.5	1.7	587	2.1	1100	25	8.6	234	0.22	0.14	25.53	0.05	18.03	0.83	0.18	6.60	0.87	0.54	98.4	0.21	70.3	3.25	0.70	25.74
145N	085W	24DDA	4	0.4	623	2	1130	0	0.7	305	0.20	0.03	27.10	0.05	18.52	0.00	0.01	8.60	0.73	0.12	99.0	0.19	68.2	0.00	0.05	31.70
145N	087W	06CBB3	4	1.2	593	2.4	1200	22	2.1	201	0.20	0.10	25.80	0.06	19.67	0.73	0.04	5.67	0.76	0.38	98.6	0.23	75.3	2.81	0.17	21.71
145N	089W	25DBA	2.8	0.2	577	2.3	1060	58	3	206	0.14	0.02	25.10	0.06	17.37	1.93	0.06	5.81	0.55	0.06	99.2	0.23	69.0	7.68	0.25	23.08
146N	087W	08DDD2	3.4	0.6	583	2.1	1140	47	1.8	192	0.17	0.05	25.36	0.05	18.68	1.57	0.04	5.42	0.66	0.19	98.9	0.21	72.7	6.09	0.15	21.07
146N	087W	10DBC	3.3	1	571	2	1060	33	3.8	234	0.16	0.08	24.84	0.05	17.37	1.10	0.08	6.60	0.66	0.33	98.8	0.20	69.1	4.37	0.31	26.24
146N	090W	20CCC	3.2	1	571	1.9	1080	22	3.5	217	0.16	0.08	24.84	0.05	17.70	0.73	0.07	6.12	0.64	0.33	98.8	0.19	71.9	2.98	0.30	24.86
147N	085W	20BD3	4.6	0.6	653	2.3	1010	49	0.8	359	0.23	0.05	28.41	0.06	16.55	1.63	0.02	10.13	0.80	0.17	98.8	0.20	58.4	5.76	0.06	35.75
Morton County (Ackerman, 1977)																										
133N	82W	05ABC	5.8	0.9	590	2.2	1170	7	170	100	0.29	0.07	25.67	0.06	19.18	0.23	3.54	2.82	1.11	0.28	98.4	0.22	74.4	0.91	13.73	10.95
133N	82W	15ACD2	6.6	1.8	670	7.6	1130	0	530	42	0.33	0.15	29.15	0.19	18.52	0.00	11.03	1.18	1.10	0.50	97.7	0.65	60.2	0.00	35.90	3.85
133N	82W	29CDD1	3.3	4.4	560	2	1150	7	230	74	0.16	0.36	24.36	0.05	18.85	0.23	4.79	2.09	0.66	1.45	97.7	0.21	72.6	0.90	18.45	8.04
133N	82W	31DDA	4.3	1.6	530	1.9	1100	0	240	37	0.21	0.13	23.06	0.05	18.03	0.00	5.00	1.04	0.92	0.56	98.3	0.21	74.9	0.00	20.76	4.34
133N	82W	32BAD	4.9	1.2	570	2	1130	0	200	93	0.24	0.10	24.80	0.05	18.52	0.00	4.16	2.62	0.97	0.39	98.4	0.20	73.2	0.00	16.45	10.37
134N	081W	06DAB2	9.2	4.4	680	2.6	890	0	700	41	0.46	0.36	29.58	0.07	14.59	0.00	14.57	1.16	1.51	1.19	97.1	0.22	48.1	0.00	48.07	3.81
134N	081W	08DAD1	25	11	600	3.1	800	0	690	4.1	1.25	0.90	26.10	0.08	13.11	0.00	14.37	0.12	4.40	3.19	92.1	0.28	47.5	0.00	52.06	0.42
134N	081W	08DAD2	6.6	3.8	610	1.8	760	0	750	1.7	0.33	0.31	26.54	0.05	12.46	0.00	15.62	0.05	1.21	1.15	97.5	0.17	44.3	0.00	55.53	0.17
134N	081W	30BCD2	5	1.3	610	2.5	1100	0	320	69	0.25	0.11	26.54	0.06	18.03	0.00	6.66	1.95	0.93	0.40	98.4	0.24	67.7	0.00	25.01	7.31
134N	084W	03ADC	3.5	2.8	520	1.8	960	8	250	90	0.17	0.23	22.62	0.05	15.73	0.27	5.21	2.54	0.76	1.00	98.0	0.20	66.3	1.12	21.92	10.69
135N	079W	10AAB1	7	2.3	690	3.2	1110	36	4.9	420	0.35	0.19	30.02	0.08	18.19	1.20	0.10	11.85	1.14	0.62	98.0	0.27	58.0	3.83	0.33	37.80
135N	079W	10AAB2	7	2.6	650	3	1100	16	310	150	0.35	0.21	28.28	0.08	18.03	0.53	6.45	4.23	1.21	0.74	97.8	0.27	61.6	1.82	22.07	14.47
135N	080W	32DDA	5.9	2.8	430	1.9	800	0	300	0	0.29	0.23	18.71	0.05	13.11	0.00	6.25	0.00	1.53	1.19	97.0	0.25	67.7	0.00	32.27	0.00
135N	081W	24DDD	7.9	5	420	2.3	800	8	270	9.4	0.39	0.41	18.27	0.06	13.11	0.27	5.62	0.27	2.06	2.15	95.5	0.31	68.1	1.38	29.18	1.38
135N	083W	32CBB1	5.7	2.4	750	2	1160	28	470	160	0.28	0.20	32.63	0.05	19.01	0.93	9.79	4.51	0.86	0.60	98.4	0.15	55.5	2.73	28.57	13.18
136N	079W	05CCC	6.9	2.9	720	3.1	1210	6	140	340	0.34	0.24	31.32	0.08	19.83	0.20	2.91	9.59	1.08	0.75	97.9	0.25	60.9	0.61	8.96	29.48
136N	079W	07BAD1	3.7	1	490	1.5	630	0	550	3.9	0.18	0.08	21.32	0.04	10.33	0.00	11.45	0.11	0.85	0.38	98.6	0.18	47.2	0.00	52.32	0.50
136N	081W	07DDC1	2	3.4	400	1.3	380	29	130	7	0.10	0.28	17.40	0.03	6.23	0.97	2.71	0.20	0.56	1.57	97.7	0.19	61.7	9.57	26.80	1.96
136N	081W	16CDD	70	23	220	4	490	0	310	9.1	3.49	1.89	9.57	0.10	8.03	0.00	6.45	0.26	23.20	12.57	63.6	0.68	54.5	0.00	43.78	1.74
136N	082W	07CCC1	5	4.3	690	2.3	1200	12	0.4	380	0.25	0.35	30.02	0.06	19.67	0.40	0.01	10.72	0.81	1.15	97.8	0.19	63.9	1.30	0.03	34.81
137N	080W	07CAD	4.4	1.7	610	2	1010	0	380	87	0.22	0.14	26.54	0.05	16.55	0.00	7.91	2.45	0.81	0.52	98.5	0.19	61.5	0.00	29.39	9.12
137N	081W	28CBC2	39	15	230	2.7	520	0	230	0	1.95	1.23	10.01	0.07	8.52	0.00	4.79	0.00	14.68	9.31	75.5	0.52	64.0	0.00	35.97	0.00
137N	083W	06CDD1	4.8	1.1	740	2.7	1200	0	6.6	490	0.24	0.09	32.19	0.07	19.67	0.00	0.14	13.82	0.73	0.28	98.8	0.21	58.5	0.00	0.41	41.10
137N	086W	03AAD1	3.1	0.8	720	2.2	1210	34	4.7	330	0.15	0.07	31.32	0.06	19.83	1.13	0.10	9.31	0.49	0.21	99.1	0.18	65.3	3.73	0.32	30.65

Table 6 (cont'd).

Location			Concentration in Milligrams per Liter								Concentration in Milliequivalents per Liter								Percent Milliequivalents							
T	R	Sec	Ca	Mg	Na	K	HCO3	CO3	SO4	Cl	Ca	Mg	Na	K	HCO3	CO3	SO4	Cl	Ca	Mg	Na	K	HCO3	CO3	SO4	Cl
138N	080W	06BCA2	5.3	1.7	670	2	1150	0	7.8	360	0.26	0.14	29.15	0.05	18.85	0.00	0.16	10.16	0.89	0.47	98.5	0.17	64.6	0.00	0.56	34.82
138N	081W	09ABB1	6.5	1.5	900	3.1	1120	25	4.7	730	0.32	0.12	39.15	0.08	18.36	0.83	0.10	20.59	0.82	0.31	98.7	0.20	46.0	2.09	0.25	51.64
139N	081W	04BDA2	5.7	2.1	800	2.9	1290	0	11	510	0.28	0.17	34.80	0.07	21.14	0.00	0.23	14.39	0.81	0.49	98.5	0.21	59.1	0.00	0.64	40.23
139N	081W	09AAA1	6.2	2.1	850	3	1300	0	3.6	560	0.31	0.17	36.98	0.08	21.31	0.00	0.07	15.80	0.82	0.46	98.5	0.20	57.3	0.00	0.20	42.49
139N	081W	16BBC	1	1.3	800	2.2	1310	0	0.08	500	0.05	0.11	34.80	0.06	21.47	0.00	0.00	14.11	0.14	0.31	99.4	0.16	60.3	0.00	0.00	39.65
139N	081W	16CCB	7.6	8	780	2.8	1290	0	9.9	500	0.38	0.66	33.93	0.07	21.14	0.00	0.21	14.11	1.08	1.88	96.8	0.20	59.6	0.00	0.58	39.78
139N	082W	08BCC	5	0.9	690	3.5	1300	0	4.5	330	0.25	0.07	30.02	0.09	21.31	0.00	0.09	9.31	0.82	0.24	98.6	0.29	69.4	0.00	0.31	30.31
139N	082W	15ADA	4.9	1.9	750	2.2	1250	23	7.7	420	0.24	0.16	32.63	0.06	20.49	0.77	0.16	11.85	0.74	0.47	98.6	0.17	61.6	2.30	0.48	35.62
139N	083W	12DBA1	3.9	1.1	750	2.3	1220	45	4.4	370	0.19	0.09	32.63	0.06	20.00	1.50	0.09	10.44	0.59	0.27	99.0	0.18	62.4	4.68	0.29	32.59
139N	088W	34BCC1	3.7	0.2	720	2	1070	82	0.8	390	0.18	0.02	31.32	0.05	17.54	2.73	0.02	11.00	0.58	0.05	99.2	0.16	56.0	8.73	0.05	35.16
140N	085W	03DDD	2.9	3.2	640	3.2	1240	17	1.2	290	0.14	0.26	27.84	0.08	20.32	0.57	0.02	8.18	0.51	0.93	98.3	0.29	69.8	1.95	0.09	28.12
140N	090W	17ACB	3.9	1.8	730	2.3	1870	0	8.6	31	0.19	0.15	31.76	0.06	30.65	0.00	0.18	0.87	0.61	0.46	98.8	0.18	96.7	0.00	0.56	2.76
140N	090W	20DBA	5.8	1.3	760	2.3	2020	0	6.6	38	0.29	0.11	33.06	0.06	33.11	0.00	0.14	1.07	0.86	0.32	98.6	0.18	96.5	0.00	0.40	3.12
Sioux & Grant counties (Randich, 1975)																										
129N	079W	07CBD	51	12	310	5.3	580	0	390	0.4	2.54	0.99	13.49	0.14	9.51	0.00	8.12	0.01	14.84	5.75	78.6	0.79	53.9	0.00	46.04	0.06
129N	080W	23DDD	100	58	290	8.6	540	0	670	7.5	4.99	4.77	12.62	0.22	8.85	0.00	13.95	0.21	22.08	21.11	55.8	0.97	38.5	0.00	60.62	0.92
129N	081W	01BAB	11	2.6	610	5.1	900	17	600	13	0.55	0.21	26.54	0.13	14.75	0.57	12.49	0.37	2.00	0.78	96.7	0.48	52.4	2.01	44.34	1.30
129N	081W	25DCC	7.8	3.3	450	2.3	840	0	310	7.5	0.39	0.27	19.58	0.06	13.77	0.00	6.45	0.21	1.92	1.34	96.5	0.29	67.4	0.00	31.59	1.04
129N	087W	10BBC	3.2	0.7	480	1.4	910	0	21	220	0.16	0.06	20.88	0.04	14.91	0.00	0.44	6.21	0.76	0.27	98.8	0.17	69.2	0.00	2.03	28.79
130N	084W	36ABA	7.4	0.9	540	2	680	11	410	130	0.37	0.07	23.49	0.05	11.15	0.37	8.54	3.67	1.54	0.31	97.9	0.21	47.0	1.55	35.99	15.46
130N	085W	17DAA1	3.8	0.4	490	1.7	870	0	11	250	0.19	0.03	21.32	0.04	14.26	0.00	0.23	7.05	0.88	0.15	98.8	0.20	66.2	0.00	1.06	32.74
130N	086W	28CCC1	3.8	1.6	510	3.2	870	20	30	250	0.19	0.13	22.19	0.08	14.26	0.67	0.62	7.05	0.84	0.58	98.2	0.36	63.1	2.95	2.76	31.20
130N	089W	32DDA	3.3	1.2	480	1.4	890	0	9.4	220	0.16	0.10	20.88	0.04	14.59	0.00	0.20	6.21	0.78	0.47	98.6	0.17	69.5	0.00	0.93	29.57
131N	080W	02AD	76	28	680	7.5	1590	0	420	2.4	3.79	2.30	29.58	0.19	26.06	0.00	8.74	0.07	10.57	6.42	82.5	0.53	74.7	0.00	25.08	0.19
131N	080W	21AAC	40	18	190	5	550	0	120	7.5	2.00	1.48	8.27	0.13	9.01	0.00	2.50	0.21	16.82	12.47	69.6	1.08	76.9	0.00	21.31	1.80
131N	089W	30AAA	3.9	0.6	550	2.6	880	21	10	330	0.19	0.05	23.93	0.07	14.42	0.70	0.21	9.31	0.80	0.20	98.7	0.27	58.5	2.84	0.84	37.78
132N	082W	30ADB	24	5.8	230	1.7	580	0	110	5.6	1.20	0.48	10.01	0.04	9.51	0.00	2.29	0.16	10.22	4.07	85.3	0.37	79.5	0.00	19.16	1.32
132N	083W	29BBB	5	1.6	440	1.3	860	0	220	17	0.25	0.13	19.14	0.03	14.10	0.00	4.58	0.48	1.28	0.67	97.9	0.17	73.6	0.00	23.91	2.50
132N	084W	16DAA	3.6	1	430	3.8	870	0	17	170	0.18	0.08	18.71	0.10	14.26	0.00	0.35	4.80	0.94	0.43	98.1	0.51	73.5	0.00	1.82	24.71
133N	079W	27BD	59	34	480	8.1	920	0	560	6.2	2.94	2.80	20.88	0.21	15.08	0.00	11.66	0.17	10.97	10.43	77.8	0.77	56.0	0.00	43.32	0.65
133N	080W	31CCD1	63	25	65	5	440	0	27	3.5	3.14	2.06	2.83	0.13	7.21	0.00	0.56	0.10	38.55	25.22	34.7	1.57	91.6	0.00	7.14	1.25
133N	081W	35DCB	5.6	4.1	540	2.7	980	0	350	53	0.28	0.34	23.49	0.07	16.06	0.00	7.29	1.50	1.16	1.40	97.2	0.29	64.7	0.00	29.33	6.02
133N	083W	06CDD	3.6	1.2	330	1	640	0	190	0	0.18	0.10	14.36	0.03	10.49	0.00	3.96	0.00	1.23	0.67	97.9	0.17	72.6	0.00	27.38	0.00
133N	083W	12ADA1	4.7	1.6	540	2.5	950	19	330	24	0.23	0.13	23.49	0.06	15.57	0.63	6.87	0.68	0.98	0.55	98.2	0.27	65.6	2.67	28.93	2.85
133N	083W	34CBC2	77	24	260	3.7	780	0	200	29	3.84	1.97	11.31	0.09	12.78	0.00	4.16	0.82	22.31	11.46	65.7	0.55	72.0	0.00	23.44	4.60
133N	085W	12AAD	3.3	1	560	1.8	1130	0	6.2	220	0.16	0.08	24.36	0.05	18.52	0.00	0.13	6.21	0.67	0.33	98.8	0.19	74.5	0.00	0.52	24.97
134N	079W	26CC2	3	1.6	110	1.6	280	4	15	2.4	0.15	0.13	4.79	0.04	4.59	0.13	0.31	0.07	2.93	2.58	93.7	0.80	89.9	2.61	6.12	1.33

Table 6 (cont'd).

Location			Concentration in Milligrams per Liter								Concentration in Milliequivalents per Liter								Percent Milliequivalents							
T	R	Sec	Ca	Mg	Na	K	HCO3	CO3	SO4	Cl	Ca	Mg	Na	K	HCO3	CO3	SO4	Cl	Ca	Mg	Na	K	HCO3	CO3	SO4	Cl
134N	080W	31BBA2	1	1	500	0	1040	36	10	150	0.05	0.08	21.75	0.00	17.05	1.20	0.21	4.23	0.23	0.38	99.4	0.00	75.1	5.29	0.92	18.65
134N	082W	36DCD	9.1	3.8	650	3.4	1050	31	480	56	0.45	0.31	28.28	0.09	17.21	1.03	9.99	1.58	1.56	1.07	97.1	0.30	57.7	3.47	33.52	5.30
134N	090W	36CBC	2.6	1.3	520	1.5	1200	0	12	100	0.13	0.11	22.62	0.04	19.67	0.00	0.25	2.82	0.57	0.47	98.8	0.17	86.5	0.00	1.10	12.41
135N	090W	23BBB1	3.3	1	570	2.9	1080	56	20	170	0.16	0.08	24.80	0.07	17.70	1.87	0.42	4.80	0.66	0.33	98.7	0.30	71.4	7.53	1.68	19.35
137N	088W	21DDC	2.9	1.2	690	2.1	1250	9	1.6	340	0.14	0.10	30.02	0.05	20.49	0.30	0.03	9.59	0.48	0.33	99.0	0.18	67.4	0.99	0.11	31.54
(personal comm.)																										
130N	082W	36BBC	45	17	169	4.4	452	0	195	0	2.25	1.40	7.35	0.11	7.41	0.00	4.06	0.00	20.22	12.59	66.2	1.01	64.6	0.00	35.40	0.00
130N	083W	36AAA	39	13	530	5	763	0	620	4.1	1.95	1.07	23.06	0.13	12.51	0.00	12.91	0.12	7.43	4.08	88.0	0.49	49.0	0.00	50.56	0.45

Appendix D. Isotope data.

Table 7. Isotopic analyses of collected water samples.

Location			del O-18	del D
T	R	Sec	(per mil)	(per mil)
129N	081W	01BAB	-14.6	-109.4
				-108.4
130N	082W	36BBC	-15.34	-113.2
				-112.2
130N	085W	17DAA	-15.08	-116.6
133N	080W	31CCD1	-14.33	-110.3
133N	083W	12ADA1	-12.28	-90.85
133N	085W	12AAD	-16.14	-123.7
				-126.2
134N	082W	36DCD	-15.4	-112.9
135N	083W	32CBB1	-15.69	-121.2
				-122.3
136N	079W	05CCC	-14.09	-102.6
136N	081W	07DDC1	-15.43	-115.9
138N	081W	09ABB1	-15.03	-116.8
			-15.01	
Analytical Error: 0.2 per mil O-18; 1.0 per mil D				

Appendix E. Paleohydrologic modeling data.

Table 8. Input data for simulation of water levels in the Fox Hills aquifer.

Initial Heads (m).

676	669	661	655	648	640	632	623	616	609	602	597	588	586	582	580	575	572	570	569	566	566	567	565	561	558
673	667	660	653	647	639	630	620	611	604	597	592	589	583	581	577	573	570	569	566	562	561	564	564	560	556
671	665	659	653	646	638	628	618	608	599	592	588	583	581	581	578	570	564	567	566	555	550	555	556	553	549
669	663	657	650	644	635	625	615	605	595	587	582	578	577	577	577	565	554	562	564	550	543	545	547	546	545
668	662	655	647	639	630	621	612	603	594	586	580	575	573	572	568	560	554	553	552	545	541	540	540	540	539
668	661	653	644	634	626	618	610	601	593	585	579	574	570	566	561	554	548	545	542	539	536	534	534	534	533
669	662	653	643	633	625	617	609	601	593	585	579	573	568	562	556	549	543	538	535	533	530	529	528	527	528
669	664	653	643	633	625	617	609	601	593	585	578	572	565	559	553	546	539	533	529	526	524	523	522	522	522
668	661	652	643	634	625	617	609	601	593	586	578	570	563	557	550	543	535	528	523	521	519	517	516	517	518
666	659	650	641	633	625	616	609	601	594	587	579	569	560	555	549	542	532	522	517	515	513	512	511	512	513
664	657	649	640	632	624	616	609	602	596	589	583	571	560	556	550	542	531	516	512	511	510	508	507	508	509
662	655	647	639	630	622	615	608	602	596	591	587	579	567	559	552	543	532	520	514	512	509	506	504	504	505
660	653	645	637	629	621	613	607	600	595	591	586	579	569	562	557	546	536	527	520	515	510	505	502	501	502
658	651	643	635	626	619	611	604	598	592	587	582	575	568	562	556	548	540	533	526	519	512	505	499	498	499
656	648	640	632	624	616	608	601	595	589	583	577	571	565	559	553	547	541	537	533	524	513	504	497	496	498
654	646	638	629	621	613	605	598	591	584	578	572	566	560	554	549	545	541	538	538	527	514	503	496	496	498
652	644	635	627	618	610	602	595	587	580	574	568	561	555	549	545	541	538	535	531	523	513	503	498	498	500
649	641	633	625	616	607	599	592	584	576	569	563	557	550	544	540	538	534	530	525	519	512	506	501	500	502
646	639	631	623	614	606	597	589	581	573	566	561	555	548	542	538	535	531	526	521	517	512	508	505	503	503
644	637	629	621	613	604	595	588	580	573	566	560	554	548	543	539	535	530	523	518	516	513	510	507	506	505
641	635	629	621	612	603	594	587	580	573	566	559	554	548	544	541	537	532	526	521	518	515	513	510	509	508
638	634	629	622	613	603	595	588	580	573	566	559	554	549	545	543	540	535	530	527	522	518	516	512	512	509

Table 8 (cont'd).

Transmissivity values (m^2/d).

12.6	12.0	11.3	10.9	10.8	10.8	10.9	11.2	11.8	12.3	13.0	13.6	14.4	14.9	15.2	15.2	15.3	15.6	16.2	16.7	16.4	15.7	15.0	13.1	11.6	10.4
12.8	12.2	11.5	10.8	10.5	10.4	10.5	10.8	11.4	12.0	13.0	13.8	14.5	15.1	15.5	15.3	14.9	15.2	16.6	17.3	16.4	15.2	14.5	12.1	9.8	0
13.2	12.5	11.8	10.9	10.2	10.0	10.2	10.5	11.1	11.9	13.0	14.0	14.8	15.5	16.1	15.9	14.4	13.8	17.1	18.8	15.8	12.3	10.0	7.7	6.1	0
13.6	13.0	12.4	11.4	10.3	10.1	10.1	10.2	10.5	11.4	12.8	14.0	15.1	16.1	16.8	17.0	15.2	13.9	17.6	18.8	13.6	8.0	3.0	1.4	0	0
14.7	14.0	13.3	12.5	11.7	11.0	10.4	9.8	9.6	10.2	11.6	13.3	15.0	16.4	17.5	18.1	18.1	18.1	18.0	15.6	10.3	4.3	0.1	0.0	0	0
15.6	15.2	14.6	14.0	13.2	12.4	11.2	9.8	8.6	8.6	10.2	12.5	14.8	16.7	18.3	19.5	20.7	21.9	19.3	14.2	7.9	2.1	0.0	0	0	0
16.6	16.4	16.1	15.7	15.1	14.2	12.7	10.4	7.4	6.4	8.9	12.1	14.9	17.1	19.0	20.4	21.6	22.6	19.6	14.0	7.3	2.2	4.4	4.7	0	0
17.7	17.6	17.6	17.4	17.1	16.6	15.4	12.5	8.0	5.4	9.3	12.7	15.4	17.6	19.3	20.2	20.8	20.6	18.5	14.7	10.3	7.4	7.9	6.5	0	0
18.8	19.0	19.1	19.2	19.2	19.0	18.8	16.5	12.2	10.5	12.1	14.5	16.6	18.0	18.9	19.2	19.2	18.9	17.7	15.8	13.9	10.9	7.7	5.4	0	0
19.8	20.0	20.3	20.7	20.9	20.7	20.2	18.4	15.9	14.8	15.5	17.1	18.2	18.3	17.8	17.4	17.3	17.4	17.1	16.2	14.7	11.1	6.4	3.1	0	0
20.6	20.9	21.3	21.8	22.3	21.5	20.6	19.2	17.9	17.4	18.3	19.8	20.1	18.3	16.3	15.0	15.0	15.8	16.5	16.3	14.5	10.4	4.6	0.4	0	0
21.0	21.4	21.8	22.2	22.2	21.6	20.6	19.5	18.7	18.5	19.5	21.4	21.3	17.4	13.9	11.7	12.3	14.2	16.1	17.0	15.8	11.7	5.3	0.7	0	0
21.6	21.8	22.1	22.2	22.0	21.3	20.3	19.2	18.3	18.1	18.7	19.5	18.7	15.5	11.5	7.4	9.9	13.2	16.2	18.6	19.2	15.3	9.5	5.5	0	0
21.8	22.0	22.1	22.1	21.8	21.0	19.8	18.4	17.2	16.6	16.8	17.0	16.3	14.2	11.2	8.8	10.1	13.2	16.5	19.8	22.6	18.5	13.4	9.8	0	0
21.8	22.0	22.0	22.0	21.7	20.8	19.4	17.6	15.6	14.3	14.7	15.1	15.0	14.1	12.6	11.4	11.7	13.7	16.7	19.5	20.6	18.8	15.3	12.3	0	0
21.7	21.8	22.0	22.0	21.7	20.9	19.1	16.8	14.5	13.0	13.1	13.8	14.5	14.9	14.6	14.0	13.4	14.1	17.1	19.2	19.7	18.5	15.9	13.3	0	0
21.4	21.6	21.1	21.4	21.6	21.2	19.1	16.2	13.4	11.5	11.5	12.8	14.6	16.3	17.2	17.0	16.2	16.5	18.5	19.8	19.8	18.5	0	0	0	0
19.8	20.3	20.7	21.0	21.2	21.3	18.8	15.4	12.1	9.4	9.6	12.0	14.9	17.9	20.5	20.2	19.4	19.7	20.8	21.3	20.5	0	0	0	0	0
19.4	19.8	20.1	20.2	20.1	19.4	17.4	14.5	11.3	8.3	8.8	11.7	14.9	18.3	21.7	21.6	21.0	21.7	23.0	23.0	21.2	0	0	0	0	0
18.8	19.1	19.3	19.2	18.9	18.0	16.3	14.0	11.6	9.8	10.0	11.9	14.5	17.2	19.3	20.1	20.4	21.5	23.8	24.1	20.7	0	0	0	0	0
18.5	18.6	18.6	18.2	17.7	16.9	15.5	13.7	12.1	11.0	10.9	12.1	13.9	15.7	17.0	17.7	18.0	18.6	19.4	19.3	0	0	0	0	0	0
17.6	17.6	17.7	17.4	16.9	16.0	14.9	13.6	12.5	11.7	11.6	12.2	13.2	14.3	15.0	15.2	15.0	14.9	13.6	12.9	0	0	0	0	0	0

Table 8 (cont'd).

Storativity values (1E20 = prescribed-head boundary; 0 = variable-head cell).

1E20	1E20	1E20	1E20	1E20	1E20	1E20	1E20	1E20	1E20	1E20	1E20	1E20	1E20	1E20	1E20	1E20	1E20	1E20	1E20	1E20	1E20	1E20	1E20	1E20
1E20	0	0	0	0	0	0	0	0	0	0	0	0	0	0	0	0	0	0	0	0	0	0	0	0	0
1E20	0	0	0	0	0	0	0	0	0	0	0	0	0	0	0	0	0	0	0	0	0	0	0	0	0
1E20	0	0	0	0	0	0	0	0	0	0	0	0	0	0	0	0	0	0	0	0	0	0	0	0	0
1E20	0	0	0	0	0	0	0	0	0	0	0	0	0	0	0	0	0	0	0	0	0	0	0	0	0
1E20	0	0	0	0	0	0	0	0	0	0	0	0	0	0	0	0	0	0	0	0	0	0	0	0	0
1E20	0	0	0	0	0	0	0	0	0	0	0	0	0	0	0	0	0	0	0	0	0	0	0	0	0
1E20	0	0	0	0	0	0	0	0	0	0	0	0	0	0	0	0	0	0	0	0	0	0	0	0	0
1E20	0	0	0	0	0	0	0	0	0	0	0	0	0	0	0	0	0	0	0	0	0	0	0	0	0
1E20	0	0	0	0	0	0	0	0	0	0	0	0	0	0	0	0	0	0	0	0	0	0	0	0	0
1E20	0	0	0	0	0	0	0	0	0	0	0	0	0	0	0	0	0	0	0	0	0	0	0	0	0
1E20	0	0	0	0	0	0	0	0	0	0	0	0	0	0	0	0	0	0	0	0	0	0	0	0	0
1E20	0	0	0	0	0	0	0	0	0	0	0	0	0	0	0	0	0	0	0	0	0	0	0	0	0
1E20	0	0	0	0	0	0	0	0	0	0	0	0	0	0	0	0	0	0	0	0	0	0	0	0	0
1E20	0	0	0	0	0	0	0	0	0	0	0	0	0	0	0	0	0	0	0	0	0	0	0	0	0
1E20	0	0	0	0	0	0	0	0	0	0	0	0	0	0	0	0	0	0	0	0	0	0	0	0	0
1E20	0	0	0	0	0	0	0	0	0	0	0	0	0	0	0	0	0	0	0	0	0	0	0	0	0
1E20	0	0	0	0	0	0	0	0	0	0	0	0	0	0	0	0	0	0	0	0	0	0	0	0	0
1E20	0	0	0	0	0	0	0	0	0	0	0	0	0	0	0	0	0	0	0	0	0	0	0	0	0
1E20	0	0	0	0	0	0	0	0	0	0	0	0	0	0	0	0	0	0	0	0	0	0	0	0	0

Table 8 (cont'd).

Discharge from the Fox Hills aquifer (mm/yr).

0	0	0	0	0	0	0	0	0	0	0	0	0	0	0	0	0	0	0	0	0	0	-.5	-.5	-.5
0	0	0	0	0	0	0	0	0	0	0	0	0	0	0	0	0	0	0	0	0	0	-.5	-.5	-.5	0
0	0	0	0	0	0	0	0	-.5	-.5	0	0	0	0	0	0	0	0	0	0	0	-.5	-.5	-.5	-.5	0
0	0	0	0	0	0	0	0	0	0	-.5	-.5	0	0	0	0	0	0	0	0	-.5	-.5	-.5	-.5	0	0
0	0	0	0	0	0	0	0	0	0	0	-.5	-.5	0	0	0	0	0	0	0	-.5	-.5	-.5	0	0	0
0	0	0	0	0	0	0	0	0	0	0	0	-.5	-.5	-.5	0	0	0	0	0	-.5	-.5	-.5	0	0	0
0	0	0	0	0	0	0	0	0	0	0	-.5	0	0	0	-.5	0	0	0	0	-.5	-.5	-.5	-.5	0	0
0	0	0	0	0	0	0	0	0	0	0	0	0	0	0	0	-.5	-.5	-.5	-.5	-.5	-.5	-.5	-.5	0	0
0	0	0	0	0	0	0	0	0	0	0	0	0	0	0	-.5	-.5	0	0	-.5	-.5	-.5	-.5	-.5	0	0
0	0	0	0	0	0	0	0	0	0	0	0	0	0	-.5	-.5	-.5	-.5	0	0	0	-.5	-.5	-.5	0	0
0	0	0	0	0	0	0	0	0	0	0	0	0	0	0	0	0	0	-.5	0	0	-.5	-.5	-.5	0	0
0	0	0	0	0	0	0	0	0	0	0	0	0	0	0	0	0	0	0	-.5	-.5	-.5	-.5	-.5	0	0
0	0	0	0	0	0	0	0	0	0	0	0	0	0	0	0	0	0	0	0	0	0	-.5	-.5	0	0
0	0	0	0	0	0	0	0	0	0	0	0	0	0	0	0	0	0	0	0	0	0	0	0	0	0
0	0	0	0	0	0	0	0	0	0	0	-.5	0	0	0	0	0	0	0	0	0	0	0	0	0	0
0	0	0	0	0	0	0	0	0	0	0	0	-.5	0	0	0	0	0	0	0	0	0	0	0	0	0
0	0	0	0	0	0	0	0	0	0	0	0	0	-.5	0	0	0	0	0	0	0	0	0	0	0	0
0	0	0	0	0	0	0	0	0	0	0	0	0	0	-.5	-.5	0	0	0	0	0	0	0	0	0	0
0	0	0	0	0	0	0	0	0	0	0	0	0	0	-.5	-.5	0	0	0	0	0	0	0	0	0	0
0	0	0	0	0	0	0	0	0	0	0	-.5	-.5	0	0	0	0	0	0	0	0	0	0	0	0	0
0	0	0	0	0	0	0	0	0	0	-.5	0	0	0	0	0	0	0	0	0	0	0	0	0	0	0

Table 8 (cont'd).

Discharge from the Fox Hills aquifer (mm/yr).

0	0	0	0	0	0	0	0	0	0	0	0	0	0	0	0	0	0	0	0	0	0	-.5	-.5	-.5	
0	0	0	0	0	0	0	0	0	0	0	0	0	0	0	0	0	0	0	0	0	-.5	-.5	-.5	0	
0	0	0	0	0	0	0	0	-.5	-.5	0	0	0	0	0	0	0	0	0	0	0	-.5	-.5	-.5	-.5	0
0	0	0	0	0	0	0	0	0	0	-.5	-.5	0	0	0	0	0	0	0	0	-.5	-.5	-.5	-.5	0	0
0	0	0	0	0	0	0	0	0	0	0	-.5	-.5	0	0	0	0	0	0	0	-.5	-.5	-.5	0	0	0
0	0	0	0	0	0	0	0	0	0	0	0	-.5	-.5	-.5	0	0	0	0	0	-.5	-.5	-.5	0	0	0
0	0	0	0	0	0	0	0	0	0	0	-.5	0	0	0	-.5	0	0	0	0	-.5	-.5	-.5	-.5	0	0
0	0	0	0	0	0	0	0	0	0	0	0	0	0	0	0	-.5	-.5	-.5	-.5	-.5	-.5	-.5	-.5	0	0
0	0	0	0	0	0	0	0	0	0	0	0	0	0	0	-.5	-.5	0	0	-.5	-.5	-.5	-.5	-.5	0	0
0	0	0	0	0	0	0	0	0	0	0	0	0	0	-.5	-.5	-.5	-.5	0	0	0	-.5	-.5	-.5	0	0
0	0	0	0	0	0	0	0	0	0	0	0	0	0	0	0	0	0	-.5	0	0	-.5	-.5	-.5	0	0
0	0	0	0	0	0	0	0	0	0	0	0	0	0	0	0	0	0	0	-.5	-.5	-.5	-.5	-.5	0	0
0	0	0	0	0	0	0	0	0	0	0	0	0	0	0	0	0	0	0	0	0	0	-.5	-.5	0	0
0	0	0	0	0	0	0	0	0	0	0	0	0	0	0	0	0	0	0	0	0	0	0	0	0	0
0	0	0	0	0	0	0	0	0	0	0	-.5	0	0	0	0	0	0	0	0	0	0	0	0	0	0
0	0	0	0	0	0	0	0	0	0	0	0	-.5	0	0	0	0	0	0	0	0	0	0	0	0	0
0	0	0	0	0	0	0	0	0	0	0	0	0	-.5	0	0	0	0	0	0	0	0	0	0	0	0
0	0	0	0	0	0	0	0	0	0	0	0	0	0	-.5	-.5	0	0	0	0	0	0	0	0	0	0
0	0	0	0	0	0	0	0	0	0	0	0	0	0	0	-.5	-.5	0	0	0	0	0	0	0	0	0
0	0	0	0	0	0	0	0	0	0	0	-.5	-.5	0	0	0	0	0	0	0	0	0	0	0	0	0
0	0	0	0	0	0	0	0	0	0	-.5	0	0	0	0	0	0	0	0	0	0	0	0	0	0	0

Table 9. Lake McKenzie simulation input data.

Initial Heads (m).

676	669	661	655	648	640	632	623	616	609	602	597	588	586	582	580	575	572	570	569	566	566	567	565	561	558
673	667	660	653	647	639	630	620	611	604	597	592	589	583	581	577	573	570	569	566	562	561	564	564	560	556
671	665	659	653	646	638	628	618	608	599	592	588	583	581	581	578	570	564	567	566	555	550	555	556	553	549
669	663	657	650	644	635	625	615	605	595	587	582	578	577	577	577	565	554	562	564	550	543	545	547	546	545
668	662	655	647	639	630	621	612	603	594	586	580	575	573	572	568	560	554	553	552	545	541	540	540	540	539
668	661	653	644	634	626	618	610	601	593	585	579	574	570	566	561	554	548	545	542	539	536	534	534	534	533
669	662	653	643	633	625	617	609	601	593	585	579	573	568	562	556	549	543	538	535	533	530	529	528	527	549
669	664	653	643	633	625	617	609	601	593	585	578	572	565	559	553	546	539	533	529	526	524	523	522	549	549
668	661	652	643	634	625	617	609	601	593	586	578	570	563	557	550	543	535	528	523	521	519	517	516	549	549
666	659	650	641	633	625	616	609	601	594	587	579	569	560	555	549	542	532	549	517	515	513	512	511	549	549
664	657	649	640	632	624	616	609	602	596	589	583	571	560	556	550	542	531	549	549	549	549	549	507	549	549
662	655	647	639	630	622	615	608	602	596	591	587	579	567	559	552	543	532	520	549	549	549	549	549	549	549
660	653	645	637	629	621	613	607	600	595	591	586	579	569	562	557	546	536	527	520	515	510	505	549	549	549
658	651	643	635	626	619	611	604	598	592	587	582	575	568	562	556	548	540	533	526	519	512	505	499	549	549
656	648	640	632	624	616	608	601	595	589	583	577	571	565	559	553	547	541	537	533	524	513	504	497	496	498
654	646	638	629	621	613	605	598	591	584	578	572	566	560	554	549	545	541	538	538	527	514	503	496	496	498
652	644	635	627	618	610	602	595	587	580	574	568	561	555	549	545	541	538	535	531	523	513	503	498	498	500
649	641	633	625	616	607	599	592	584	576	569	563	557	550	544	540	538	534	530	525	519	512	506	501	500	502
646	639	631	623	614	606	597	589	581	573	566	561	555	548	542	538	535	531	526	521	517	512	508	505	503	503
644	637	629	621	613	604	595	588	580	573	566	560	554	548	543	539	535	530	523	518	516	513	510	507	506	505
641	635	629	621	612	603	594	587	580	573	566	559	554	548	544	541	537	532	526	521	518	515	513	510	509	508
638	634	629	622	613	603	595	588	580	573	566	559	554	549	545	543	540	535	530	527	522	518	516	512	512	509

Table 9 (cont'd).

Transmissivity values (m^2/d).

12.6	12.0	11.3	10.9	10.8	10.8	10.9	11.2	11.8	12.3	13.0	13.6	14.4	14.9	15.2	15.2	15.3	15.6	16.2	16.7	16.4	15.7	15.0	13.1	11.6	10.4
12.8	12.2	11.5	10.8	10.5	10.4	10.5	10.8	11.4	12.0	13.0	13.8	14.5	15.1	15.5	15.3	14.9	15.2	16.6	17.3	16.4	15.2	14.5	12.1	9.8	0
13.2	12.5	11.8	10.9	10.2	10.0	10.2	10.5	11.1	11.9	13.0	14.0	14.8	15.5	16.1	15.9	14.4	13.8	17.1	18.8	15.8	12.3	10.0	7.7	6.1	0
13.6	13.0	12.4	11.4	10.3	10.1	10.1	10.2	10.5	11.4	12.8	14.0	15.1	16.1	16.8	17.0	15.2	13.9	17.6	18.8	13.6	8.0	3.0	1.4	0	0
14.7	14.0	13.3	12.5	11.7	11.0	10.4	9.8	9.6	10.2	11.6	13.3	15.0	16.4	17.5	18.1	18.1	18.1	18.0	15.6	10.3	4.3	0.1	0.0	0	0
15.6	15.2	14.6	14.0	13.2	12.4	11.2	9.8	8.6	8.6	10.2	12.5	14.8	16.7	18.3	19.5	20.7	21.9	19.3	14.2	7.9	2.1	0.0	0	0	0
16.6	16.4	16.1	15.7	15.1	14.2	12.7	10.4	7.4	6.4	8.9	12.1	14.9	17.1	19.0	20.4	21.6	22.6	19.6	14.0	7.3	2.2	4.4	4.7	0	0
17.7	17.6	17.6	17.4	17.1	16.6	15.4	12.5	8.0	5.4	9.3	12.7	15.4	17.6	19.3	20.2	20.8	20.6	18.5	14.7	10.3	7.4	7.9	6.5	0	0
18.8	19.0	19.1	19.2	19.2	19.0	18.8	16.5	12.2	10.5	12.1	14.5	16.6	18.0	18.9	19.2	19.2	18.9	17.7	15.8	13.9	10.9	7.7	5.4	0	0
19.8	20.0	20.3	20.7	20.9	20.7	20.2	18.4	15.9	14.8	15.5	17.1	18.2	18.3	17.8	17.4	17.3	17.4	17.1	16.2	14.7	11.1	6.4	3.1	0	0
20.6	20.9	21.3	21.8	22.3	21.5	20.6	19.2	17.9	17.4	18.3	19.8	20.1	18.3	16.3	15.0	15.0	15.8	16.5	16.3	14.5	10.4	4.6	0.4	0	0
21.0	21.4	21.8	22.2	22.2	21.6	20.6	19.5	18.7	18.5	19.5	21.4	21.3	17.4	13.9	11.7	12.3	14.2	16.1	17.0	15.8	11.7	5.3	0.7	0	0
21.6	21.8	22.1	22.2	22.0	21.3	20.3	19.2	18.3	18.1	18.7	19.5	18.7	15.5	11.5	7.4	9.9	13.2	16.2	18.6	19.2	15.3	9.5	5.5	0	0
21.8	22.0	22.1	22.1	21.8	21.0	19.8	18.4	17.2	16.6	16.8	17.0	16.3	14.2	11.2	8.8	10.1	13.2	16.5	19.8	22.6	18.5	13.4	9.8	0	0
21.8	22.0	22.0	22.0	21.7	20.8	19.4	17.6	15.6	14.3	14.7	15.1	15.0	14.1	12.6	11.4	11.7	13.7	16.7	19.5	20.6	18.8	15.3	12.3	0	0
21.7	21.8	22.0	22.0	21.7	20.9	19.1	16.8	14.5	13.0	13.1	13.8	14.5	14.9	14.6	14.0	13.4	14.1	17.1	19.2	19.7	18.5	15.9	13.3	0	0
21.4	21.6	21.1	21.4	21.6	21.2	19.1	16.2	13.4	11.5	11.5	12.8	14.6	16.3	17.2	17.0	16.2	16.5	18.5	19.8	19.8	18.5	0	0	0	0
19.8	20.3	20.7	21.0	21.2	21.3	18.8	15.4	12.1	9.4	9.6	12.0	14.9	17.9	20.5	20.2	19.4	19.7	20.8	21.3	20.5	0	0	0	0	0
19.4	19.8	20.1	20.2	20.1	19.4	17.4	14.5	11.3	8.3	8.8	11.7	14.9	18.3	21.7	21.6	21.0	21.7	23.0	23.0	21.2	0	0	0	0	0
18.8	19.1	19.3	19.2	18.9	18.0	16.3	14.0	11.6	9.8	10.0	11.9	14.5	17.2	19.3	20.1	20.4	21.5	23.8	24.1	20.7	0	0	0	0	0
18.5	18.6	18.6	18.2	17.7	16.9	15.5	13.7	12.1	11.0	10.9	12.1	13.9	15.7	17.0	17.7	18.0	18.6	19.4	19.3	0	0	0	0	0	0
17.6	17.6	17.7	17.4	16.9	16.0	14.9	13.6	12.5	11.7	11.6	12.2	13.2	14.3	15.0	15.2	15.0	14.9	13.6	12.9	0	0	0	0	0	0

Table 9 (cont'd).

Storativity values (1E20 = prescribed-head boundary, 0 = variable-head cell).

1E20	1E20	1E20	1E20	1E20	1E20	1E20	1E20	1E20	1E20	1E20	1E20	1E20	1E20	1E20	1E20	1E20	1E20	1E20	1E20	1E20	1E20	1E20	1E20	1E20
1E20	0	0	0	0	0	0	0	0	0	0	0	0	0	0	0	0	0	0	0	0	0	0	0	0	0
1E20	0	0	0	0	0	0	0	0	0	0	0	0	0	0	0	0	0	0	0	0	0	0	0	0	0
1E20	0	0	0	0	0	0	0	0	0	0	0	0	0	0	0	0	0	0	0	0	0	0	0	0	0
1E20	0	0	0	0	0	0	0	0	0	0	0	0	0	0	0	0	0	0	0	0	0	0	0	0	0
1E20	0	0	0	0	0	0	0	0	0	0	0	0	0	0	0	0	0	0	0	0	0	0	0	0	0
1E20	0	0	0	0	0	0	0	0	0	0	0	0	0	0	0	0	0	0	0	0	0	0	0	0	0
1E20	0	0	0	0	0	0	0	0	0	0	0	0	0	0	0	0	0	0	0	0	0	0	0	0	0
1E20	0	0	0	0	0	0	0	0	0	0	0	0	0	0	0	0	0	0	0	0	0	0	0	1E20	0
1E20	0	0	0	0	0	0	0	0	0	0	0	0	0	0	0	0	0	1E20	0	0	0	0	0	1E20	0
1E20	0	0	0	0	0	0	0	0	0	0	0	0	0	0	0	0	0	1E20	1E20	1E20	1E20	1E20	0	1E20	0
1E20	0	0	0	0	0	0	0	0	0	0	0	0	0	0	0	0	0	0	1E20	1E20	1E20	1E20	1E20	1E20	0
1E20	0	0	0	0	0	0	0	0	0	0	0	0	0	0	0	0	0	0	0	0	0	0	1E20	1E20	0
1E20	0	0	0	0	0	0	0	0	0	0	0	0	0	0	0	0	0	0	0	0	0	0	0	1E20	0
1E20	0	0	0	0	0	0	0	0	0	0	0	0	0	0	0	0	0	0	0	0	0	0	0	0	0
1E20	0	0	0	0	0	0	0	0	0	0	0	0	0	0	0	0	0	0	0	0	0	0	0	0	0
1E20	0	0	0	0	0	0	0	0	0	0	0	0	0	0	0	0	0	0	0	0	0	0	0	0	0
1E20	0	0	0	0	0	0	0	0	0	0	0	0	0	0	0	0	0	0	0	0	0	0	0	0	0
1E20	0	0	0	0	0	0	0	0	0	0	0	0	0	0	0	0	0	0	0	0	0	0	0	0	0
1E20	0	0	0	0	0	0	0	0	0	0	0	0	0	0	0	0	0	0	0	0	0	0	0	0	0

Table 9 (cont'd).

Discharge from the Fox Hills aquifer (mm/yr).

0	0	0	0	0	0	0	0	0	0	0	0	0	0	0	0	0	0	0	0	0	0	-.5	-.5	-.5
0	0	0	0	0	0	0	0	0	0	0	0	0	0	0	0	0	0	0	0	0	-.5	-.5	-.5	0
0	0	0	0	0	0	0	0	-.5	-.5	0	0	0	0	0	0	0	0	0	0	-.5	-.5	-.5	-.5	0
0	0	0	0	0	0	0	0	0	0	-.5	-.5	0	0	0	0	0	0	0	-.5	-.5	-.5	-.5	0	0
0	0	0	0	0	0	0	0	0	0	0	-.5	-.5	0	0	0	0	0	0	-.5	-.5	-.5	0	0	0
0	0	0	0	0	0	0	0	0	0	0	0	-.5	-.5	-.5	0	0	0	0	-.5	-.5	-.5	0	0	0
0	0	0	0	0	0	0	0	0	0	0	-.5	0	0	0	-.5	0	0	0	-.5	-.5	-.5	-.5	0	0
0	0	0	0	0	0	0	0	0	0	0	0	0	0	0	0	-.5	-.5	-.5	-.5	-.5	-.5	-.5	0	0
0	0	0	0	0	0	0	0	0	0	0	0	0	0	0	-.5	-.5	0	0	-.5	-.5	-.5	-.5	0	0
0	0	0	0	0	0	0	0	0	0	0	0	0	0	-.5	-.5	-.5	-.5	0	0	0	-.5	-.5	0	0
0	0	0	0	0	0	0	0	0	0	0	0	0	0	0	0	0	0	-.5	0	0	-.5	-.5	0	0
0	0	0	0	0	0	0	0	0	0	0	0	0	0	0	0	0	0	0	-.5	-.5	-.5	-.5	0	0
0	0	0	0	0	0	0	0	0	0	0	0	0	0	0	0	0	0	0	0	0	-.5	-.5	0	0
0	0	0	0	0	0	0	0	0	0	0	0	0	0	0	0	0	0	0	0	0	0	0	0	0
0	0	0	0	0	0	0	0	0	0	0	-.5	0	0	0	0	0	0	0	0	0	0	0	0	0
0	0	0	0	0	0	0	0	0	0	0	0	-.5	0	0	0	0	0	0	0	0	0	0	0	0
0	0	0	0	0	0	0	0	0	0	0	0	0	-.5	0	0	0	0	0	0	0	0	0	0	0
0	0	0	0	0	0	0	0	0	0	0	0	0	0	-.5	-.5	0	0	0	0	0	0	0	0	0
0	0	0	0	0	0	0	0	0	0	0	-.5	-.5	0	0	0	0	0	0	0	0	0	0	0	0
0	0	0	0	0	0	0	0	0	0	-.5	0	0	0	0	0	0	0	0	0	0	0	0	0	0

Table 10. Input data for simulation of Verone ice sheet blocking the discharge area.

Initial heads (m)

676	669	661	655	648	640	632	623	616	609	602	597	588	586	582	580	575	572	570	569	566	566	567	565	561	558
673	667	660	653	647	639	630	620	611	604	597	592	589	583	581	577	573	570	569	566	562	561	564	564	560	556
671	665	659	653	646	638	628	618	608	599	592	588	583	581	581	578	570	564	567	566	555	550	555	556	553	549
669	663	657	650	644	635	625	615	605	595	587	582	578	577	577	577	565	554	562	564	550	543	545	547	546	545
668	662	655	647	639	630	621	612	603	594	586	580	575	573	572	568	560	554	553	552	545	541	540	540	540	539
668	661	653	644	634	626	618	610	601	593	585	579	574	570	566	561	554	548	545	542	539	536	534	534	534	533
669	662	653	643	633	625	617	609	601	593	585	579	573	568	562	556	549	543	538	535	533	530	529	528	527	528
669	664	653	643	633	625	617	609	601	593	585	578	572	565	559	553	546	539	533	529	526	524	523	522	522	522
668	661	652	643	634	625	617	609	601	593	586	578	570	563	557	550	543	535	528	523	521	519	517	516	517	518
666	659	650	641	633	625	616	609	601	594	587	579	569	560	555	549	542	532	522	517	515	513	512	511	512	513
664	657	649	640	632	624	616	609	602	596	589	583	571	560	556	550	542	531	516	512	511	510	508	507	508	509
662	655	647	639	630	622	615	608	602	596	591	587	579	567	559	552	543	532	520	514	512	509	506	504	504	505
660	653	645	637	629	621	613	607	600	595	591	586	579	569	562	557	546	536	527	520	515	510	505	502	501	502
658	651	643	635	626	619	611	604	598	592	587	582	575	568	562	556	548	540	533	526	519	512	505	499	498	499
656	648	640	632	624	616	608	601	595	589	583	577	571	565	559	553	547	541	537	533	524	513	504	497	496	498
654	646	638	629	621	613	605	598	591	584	578	572	566	560	554	549	545	541	538	538	527	514	503	496	496	498
652	644	635	627	618	610	602	595	587	580	574	568	561	555	549	545	541	538	535	531	523	513	503	498	498	500
649	641	633	625	616	607	599	592	584	576	569	563	557	550	544	540	538	534	530	525	519	512	506	501	500	502
646	639	631	623	614	606	597	589	581	573	566	561	555	548	542	538	535	531	526	521	517	512	508	505	503	503
644	637	629	621	613	604	595	588	580	573	566	560	554	548	543	539	535	530	523	518	516	513	510	507	506	505
641	635	629	621	612	603	594	587	580	573	566	559	554	548	544	541	537	532	526	521	518	515	513	510	509	508
638	634	629	622	613	603	595	588	580	573	566	559	554	549	545	543	540	535	530	527	522	518	516	512	512	509

Table 10 (cont'd).

Transmissivity values (m^2/d)

12.6	12.0	11.3	10.9	10.8	10.8	10.9	11.2	11.8	12.3	13.0	13.6	14.4	14.9	15.2	15.2	15.3	15.6	16.2	16.7	16.4	15.7	15.0	13.1	12.0	12.0
12.8	12.2	11.5	10.8	10.5	10.4	10.5	10.8	11.4	12.0	13.0	13.8	14.5	15.1	15.5	15.3	14.9	15.2	16.6	17.3	16.4	15.2	14.5	12.1	0	0
13.2	12.5	11.8	10.9	10.2	10.0	10.2	10.5	11.1	11.9	13.0	14.0	14.8	15.5	16.1	15.9	14.4	13.8	17.1	18.8	15.8	12.3	12.0	12.0	0	0
13.6	13.0	12.4	11.4	10.3	10.1	10.1	10.2	10.5	11.4	12.8	14.0	15.1	16.1	16.8	17.0	15.2	13.9	17.6	18.8	13.6	12.0	12.0	0	0	0
14.7	14.0	13.3	12.5	11.7	11.0	10.4	9.8	9.6	10.2	11.6	13.3	15.0	16.4	17.5	18.1	18.1	18.1	18.0	15.6	12.0	12.0	0	0	0	0
15.6	15.2	14.6	14.0	13.2	12.4	11.2	9.8	8.6	8.6	10.2	12.5	14.8	16.7	18.3	19.5	20.7	21.9	19.3	14.2	12.0	12.0	0	0	0	0
16.6	16.4	16.1	15.7	15.1	14.2	12.7	10.4	7.4	6.4	8.9	12.1	14.9	17.1	19.0	20.4	21.6	22.6	19.6	14.0	12.0	12.0	12.0	12.0	0	0
17.7	17.6	17.6	17.4	17.1	16.6	15.4	12.5	8.0	5.4	9.3	12.7	15.4	17.6	19.3	20.2	20.8	20.6	18.5	14.7	12.0	12.0	12.0	12.0	0	0
18.8	19.0	19.1	19.2	19.2	19.0	18.8	16.5	12.2	10.5	12.1	14.5	16.6	18.0	18.9	19.2	19.2	18.9	17.7	15.8	13.9	12.0	12.0	12.0	0	0
19.8	20.0	20.3	20.7	20.9	20.7	20.2	18.4	15.9	14.8	15.5	17.1	18.2	18.3	17.8	17.4	17.3	17.4	17.1	16.2	14.7	12.0	12.0	12.0	0	0
20.6	20.9	21.3	21.8	22.3	21.5	20.6	19.2	17.9	17.4	18.3	19.8	20.1	18.3	16.3	15.0	15.0	15.8	16.5	16.3	14.5	12.0	12.0	12.0	0	0
21.0	21.4	21.8	22.2	22.2	21.6	20.6	19.5	18.7	18.5	19.5	21.4	21.3	17.4	13.9	11.7	12.3	14.2	16.1	17.0	15.8	12.0	12.0	12.0	0	0
21.6	21.8	22.1	22.2	22.0	21.3	20.3	19.2	18.3	18.1	18.7	19.5	18.7	15.5	11.5	7.4	9.9	13.2	16.2	18.6	19.2	15.3	12.0	12.0	0	0
21.8	22.0	22.1	22.1	21.8	21.0	19.8	18.4	17.2	16.6	16.8	17.0	16.3	14.2	11.2	8.8	10.1	13.2	16.5	19.8	22.6	18.5	13.4	12.0	0	0
21.8	22.0	22.0	22.0	21.7	20.8	19.4	17.6	15.6	14.3	14.7	15.1	15.0	14.1	12.6	11.4	11.7	13.7	16.7	19.5	20.6	18.8	15.3	12.3	0	0
21.7	21.8	22.0	22.0	21.7	20.9	19.1	16.8	14.5	13.0	13.1	13.8	14.5	14.9	14.6	14.0	13.4	14.1	17.1	19.2	19.7	18.5	15.9	0	0	0
21.4	21.6	21.1	21.4	21.6	21.2	19.1	16.2	13.4	11.5	11.5	12.8	14.6	16.3	17.2	17.0	16.2	16.5	18.5	19.8	19.8	18.5	0	0	0	0
19.8	20.3	20.7	21.0	21.2	21.3	18.8	15.4	12.1	9.4	9.6	12.0	14.9	17.9	20.5	20.2	19.4	19.7	20.8	21.3	20.5	0	0	0	0	0
19.4	19.8	20.1	20.2	20.1	19.4	17.4	14.5	11.3	8.3	8.8	11.7	14.9	18.3	21.7	21.6	21.0	21.7	23.0	23.0	21.2	0	0	0	0	0
18.8	19.1	19.3	19.2	18.9	18.0	16.3	14.0	11.6	9.8	10.0	11.9	14.5	17.2	19.3	20.1	20.4	21.5	23.8	24.1	0	0	0	0	0	0
18.5	18.6	18.6	18.2	17.7	16.9	15.5	13.7	12.1	11.0	10.9	12.1	13.9	15.7	17.0	17.7	18.0	18.6	19.4	19.3	0	0	0	0	0	0
17.6	17.6	17.7	17.4	16.9	16.0	14.9	13.6	12.5	11.7	11.6	12.2	13.2	14.3	15.0	15.2	15.0	14.9	13.6	12.9	0	0	0	0	0	0

Table 10 (cont'd).

Storativity values (1E20 = prescribed-head boundary; 0 = variable-head cell).

1E20	1E20	1E20	1E20	1E20	1E20	1E20	1E20	1E20	1E20	1E20	1E20	1E20	1E20	1E20	1E20	1E20	1E20	1E20	1E20	1E20	1E20	1E20	1E20	1E20
1E20	0	0	0	0	0	0	0	0	0	0	0	0	0	0	0	0	0	0	0	0	0	0	0	0
1E20	0	0	0	0	0	0	0	0	0	0	0	0	0	0	0	0	0	0	0	0	0	0	0	0
1E20	0	0	0	0	0	0	0	0	0	0	0	0	0	0	0	0	0	0	0	0	0	0	0	0
1E20	0	0	0	0	0	0	0	0	0	0	0	0	0	0	0	0	0	0	0	0	0	0	0	0
1E20	0	0	0	0	0	0	0	0	0	0	0	0	0	0	0	0	0	0	0	0	0	0	0	0
1E20	0	0	0	0	0	0	0	0	0	0	0	0	0	0	0	0	0	0	0	0	0	0	0	0
1E20	0	0	0	0	0	0	0	0	0	0	0	0	0	0	0	0	0	0	0	0	0	0	0	0
1E20	0	0	0	0	0	0	0	0	0	0	0	0	0	0	0	0	0	0	0	0	0	0	0	0
1E20	0	0	0	0	0	0	0	0	0	0	0	0	0	0	0	0	0	0	0	0	0	0	0	0
1E20	0	0	0	0	0	0	0	0	0	0	0	0	0	0	0	0	0	0	0	0	0	0	0	0
1E20	0	0	0	0	0	0	0	0	0	0	0	0	0	0	0	0	0	0	0	0	0	0	0	0
1E20	0	0	0	0	0	0	0	0	0	0	0	0	0	0	0	0	0	0	0	0	0	0	0	0
1E20	0	0	0	0	0	0	0	0	0	0	0	0	0	0	0	0	0	0	0	0	0	0	0	0
1E20	0	0	0	0	0	0	0	0	0	0	0	0	0	0	0	0	0	0	0	0	0	0	0	0
1E20	0	0	0	0	0	0	0	0	0	0	0	0	0	0	0	0	0	0	0	0	0	0	0	0
1E20	0	0	0	0	0	0	0	0	0	0	0	0	0	0	0	0	0	0	0	0	0	0	0	0
1E20	0	0	0	0	0	0	0	0	0	0	0	0	0	0	0	0	0	0	0	0	0	0	0	0
1E20	0	0	0	0	0	0	0	0	0	0	0	0	0	0	0	0	0	0	0	0	0	0	0	0
1E20	0	0	0	0	0	0	0	0	0	0	0	0	0	0	0	0	0	0	0	0	0	0	0	0
1E20	0	0	0	0	0	0	0	0	0	0	0	0	0	0	0	0	0	0	0	0	0	0	0	0

Table 10 (cont'd).

Recharge/discharge values (+ recharge, - discharge) (mm/yr).

0	0	0	0	0	0	0	0	0	0	0	0	0	0	0	0	0	0	0	0	0	0	0	0	0
0	0	0	0	0	0	0	0	0	0	0	0	0	0	0	0	0	0	0	0	0	-.5	-.5	-.5	0
0	0	0	0	0	0	0	0	-.5	-.5	0	0	0	0	0	0	0	0	0	0	0	-.5	-.5	-.5	0
0	0	0	0	0	0	0	0	0	0	-.5	-.5	0	0	0	0	0	0	0	0	-.5	-.5	-.5	-.5	0
0	0	0	0	0	0	0	0	0	0	0	-.5	-.5	-.5	0	0	0	0	0	0	-.5	-.5	-.5	0	0
0	0	0	0	0	0	0	0	0	0	0	-.5	-.5	-.5	-.5	0	0	0	0	0	-.5	-.5	-.5	0	0
0	0	0	0	0	0	0	0	0	0	0	0	0	0	0	-.5	0	0	0	0	-.5	-.5	-.5	0	0
0	0	0	0	0	0	0	0	0	0	0	0	0	0	0	0	-.5	-.5	-.5	-.5	-.5	-.5	0	0	0
0	0	0	0	0	0	0	0	0	0	0	0	0	0	0	-.5	-.5	0	0	-.5	-.5	0	0	0	0
0	0	0	0	0	0	0	0	0	0	0	0	0	0	-.5	-.5	-.5	-.5	0	0	0	0	0	0	0
0	0	0	0	0	0	0	0	0	0	0	0	0	0	0	0	0	0	-.5	0	0	0	0	0	0
0	0	0	0	0	0	0	0	0	0	0	0	0	0	0	0	0	0	0	0	0	0	0	0	0
0	0	0	0	0	0	0	0	0	0	0	0	0	0	0	0	0	0	0	0	0	0	0	0	0
0	0	0	0	0	0	0	0	0	0	0	0	0	0	0	0	0	0	0	0	0	0	0	0	0
0	0	0	0	0	0	0	0	0	0	0	0	0	0	0	0	0	0	0	0	0	0	0	0	0
0	0	0	0	0	0	0	0	0	0	0	0	0	0	0	0	0	0	0	0	0	0	0	0	0
0	0	0	0	0	0	0	0	0	0	0	0	0	0	0	0	0	0	0	0	0	0	0	0	0
0	0	0	0	0	0	0	0	0	0	0	0	0	0	0	0	0	0	0	0	0	0	0	0	0
0	0	0	0	0	0	0	0	0	0	0	0	0	0	0	0	0	0	0	0	0	0	0	0	0
0	0	0	0	0	0	0	0	0	0	0	0	0	0	0	0	0	0	0	0	0	0	0	0	0
0	0	0	0	0	0	0	0	0	0	0	0	0	0	0	0	0	0	0	0	0	0	0	0	0
0	0	0	0	0	0	0	0	0	0	0	0	0	0	0	0	0	0	0	0	0	0	0	0	0
0	0	0	0	0	0	0	0	0	0	0	0	0	0	0	0	0	0	0	0	0	0	0	0	0

Table 11. Input data for simulation of Verone ice sheet recharging the discharge area.

Initial heads (m)

676	669	661	655	648	640	632	623	616	609	602	597	588	586	582	580	575	572	570	569	566	566	567	565	561	558
673	667	660	653	647	639	630	620	611	604	597	592	589	583	581	577	573	570	569	566	562	561	564	564	560	556
671	665	659	653	646	638	628	618	608	599	592	588	583	581	581	578	570	564	567	566	555	550	555	556	553	549
669	663	657	650	644	635	625	615	605	595	587	582	578	577	577	577	565	554	562	564	550	543	545	547	546	545
668	662	655	647	639	630	621	612	603	594	586	580	575	573	572	568	560	554	553	552	545	541	540	540	540	539
668	661	653	644	634	626	618	610	601	593	585	579	574	570	566	561	554	548	545	542	539	536	534	534	534	533
669	662	653	643	633	625	617	609	601	593	585	579	573	568	562	556	549	543	538	535	533	530	529	528	527	528
669	664	653	643	633	625	617	609	601	593	585	578	572	565	559	553	546	539	533	529	526	524	523	522	522	522
668	661	652	643	634	625	617	609	601	593	586	578	570	563	557	550	543	535	528	523	521	519	517	516	517	518
666	659	650	641	633	625	616	609	601	594	587	579	569	560	555	549	542	532	522	517	515	513	512	511	512	513
664	657	649	640	632	624	616	609	602	596	589	583	571	560	556	550	542	531	516	512	511	510	508	507	508	509
662	655	647	639	630	622	615	608	602	596	591	587	579	567	559	552	543	532	520	514	512	509	506	504	504	505
660	653	645	637	629	621	613	607	600	595	591	586	579	569	562	557	546	536	527	520	515	510	505	502	501	502
658	651	643	635	626	619	611	604	598	592	587	582	575	568	562	556	548	540	533	526	519	512	505	499	498	499
656	648	640	632	624	616	608	601	595	589	583	577	571	565	559	553	547	541	537	533	524	513	504	497	496	498
654	646	638	629	621	613	605	598	591	584	578	572	566	560	554	549	545	541	538	538	527	514	503	496	496	498
652	644	635	627	618	610	602	595	587	580	574	568	561	555	549	545	541	538	535	531	523	513	503	498	498	500
649	641	633	625	616	607	599	592	584	576	569	563	557	550	544	540	538	534	530	525	519	512	506	501	500	502
646	639	631	623	614	606	597	589	581	573	566	561	555	548	542	538	535	531	526	521	517	512	508	505	503	503
644	637	629	621	613	604	595	588	580	573	566	560	554	548	543	539	535	530	523	518	516	513	510	507	506	505
641	635	629	621	612	603	594	587	580	573	566	559	554	548	544	541	537	532	526	521	518	515	513	510	509	508
638	634	629	622	613	603	595	588	580	573	566	559	554	549	545	543	540	535	530	527	522	518	516	512	512	509

Table 11 (cont'd).

Transmissivity values (m^2/d)

12.6	12.0	11.3	10.9	10.8	10.8	10.9	11.2	11.8	12.3	13.0	13.6	14.4	14.9	15.2	15.2	15.3	15.6	16.2	16.7	16.4	15.7	15.0	13.1	12.0	12.0
12.8	12.2	11.5	10.8	10.5	10.4	10.5	10.8	11.4	12.0	13.0	13.8	14.5	15.1	15.5	15.3	14.9	15.2	16.6	17.3	16.4	15.2	14.5	12.1	0	0
13.2	12.5	11.8	10.9	10.2	10.0	10.2	10.5	11.1	11.9	13.0	14.0	14.8	15.5	16.1	15.9	14.4	13.8	17.1	18.8	15.8	12.3	12.0	12.0	0	0
13.6	13.0	12.4	11.4	10.3	10.1	10.1	10.2	10.5	11.4	12.8	14.0	15.1	16.1	16.8	17.0	15.2	13.9	17.6	18.8	13.6	12.0	12.0	0	0	0
14.7	14.0	13.3	12.5	11.7	11.0	10.4	9.8	9.6	10.2	11.6	13.3	15.0	16.4	17.5	18.1	18.1	18.1	18.0	15.6	12.0	12.0	0	0	0	0
15.6	15.2	14.6	14.0	13.2	12.4	11.2	9.8	8.6	8.6	10.2	12.5	14.8	16.7	18.3	19.5	20.7	21.9	19.3	14.2	12.0	12.0	0	0	0	0
16.6	16.4	16.1	15.7	15.1	14.2	12.7	10.4	7.4	6.4	8.9	12.1	14.9	17.1	19.0	20.4	21.6	22.6	19.6	14.0	12.0	12.0	12.0	12.0	0	0
17.7	17.6	17.6	17.4	17.1	16.6	15.4	12.5	8.0	5.4	9.3	12.7	15.4	17.6	19.3	20.2	20.8	20.6	18.5	14.7	12.0	12.0	12.0	12.0	0	0
18.8	19.0	19.1	19.2	19.2	19.0	18.8	16.5	12.2	10.5	12.1	14.5	16.6	18.0	18.9	19.2	19.2	18.9	17.7	15.8	13.9	12.0	12.0	12.0	0	0
19.8	20.0	20.3	20.7	20.9	20.7	20.2	18.4	15.9	14.8	15.5	17.1	18.2	18.3	17.8	17.4	17.3	17.4	17.1	16.2	14.7	12.0	12.0	12.0	0	0
20.6	20.9	21.3	21.8	22.3	21.5	20.6	19.2	17.9	17.4	18.3	19.8	20.1	18.3	16.3	15.0	15.0	15.8	16.5	16.3	14.5	12.0	12.0	12.0	0	0
21.0	21.4	21.8	22.2	22.2	21.6	20.6	19.5	18.7	18.5	19.5	21.4	21.3	17.4	13.9	11.7	12.3	14.2	16.1	17.0	15.8	12.0	12.0	12.0	0	0
21.6	21.8	22.1	22.2	22.0	21.3	20.3	19.2	18.3	18.1	18.7	19.5	18.7	15.5	11.5	7.4	9.9	13.2	16.2	18.6	19.2	15.3	12.0	12.0	0	0
21.8	22.0	22.1	22.1	21.8	21.0	19.8	18.4	17.2	16.6	16.8	17.0	16.3	14.2	11.2	8.8	10.1	13.2	16.5	19.8	22.6	18.5	13.4	12.0	0	0
21.8	22.0	22.0	22.0	21.7	20.8	19.4	17.6	15.6	14.3	14.7	15.1	15.0	14.1	12.6	11.4	11.7	13.7	16.7	19.5	20.6	18.8	15.3	12.3	0	0
21.7	21.8	22.0	22.0	21.7	20.9	19.1	16.8	14.5	13.0	13.1	13.8	14.5	14.9	14.6	14.0	13.4	14.1	17.1	19.2	19.7	18.5	15.9	0	0	0
21.4	21.6	21.1	21.4	21.6	21.2	19.1	16.2	13.4	11.5	11.5	12.8	14.5	16.3	17.2	17.0	16.2	16.5	18.5	19.8	19.8	18.5	0	0	0	0
19.8	20.3	20.7	21.0	21.2	21.3	18.8	15.4	12.1	9.4	9.6	12.0	14.9	17.9	20.5	20.2	19.4	19.7	20.8	21.3	20.5	0	0	0	0	0
19.4	19.8	20.1	20.2	20.1	19.4	17.4	14.5	11.3	8.3	8.8	11.7	14.9	18.3	21.7	21.6	21.0	21.7	23.0	23.0	21.2	0	0	0	0	0
18.8	19.1	19.3	19.2	18.9	18.0	16.3	14.0	11.6	9.8	10.0	11.9	14.5	17.2	19.3	20.1	20.4	21.5	23.8	24.1	0	0	0	0	0	0
18.5	18.6	18.6	18.2	17.7	16.9	15.5	13.7	12.1	11.0	10.9	12.1	13.9	15.7	17.0	17.7	18.0	18.6	19.4	19.3	0	0	0	0	0	0
17.6	17.6	17.7	17.4	16.9	16.0	14.9	13.6	12.5	11.7	11.6	12.2	13.2	14.3	15.0	15.2	15.0	14.9	13.6	12.9	0	0	0	0	0	0

Table 11 (cont'd).

Storativity values (1E20 = prescribed-head boundary; 0 = variable-head cell).

1E20	1E20	1E20	1E20	1E20	1E20	1E20	1E20	1E20	1E20	1E20	1E20	1E20	1E20	1E20	1E20	1E20	1E20	1E20	1E20	1E20	1E20	1E20	1E20	1E20
1E20	0	0	0	0	0	0	0	0	0	0	0	0	0	0	0	0	0	0	0	0	0	0	0	0	0
1E20	0	0	0	0	0	0	0	0	0	0	0	0	0	0	0	0	0	0	0	0	0	0	0	0	0
1E20	0	0	0	0	0	0	0	0	0	0	0	0	0	0	0	0	0	0	0	0	0	0	0	0	0
1E20	0	0	0	0	0	0	0	0	0	0	0	0	0	0	0	0	0	0	0	0	0	0	0	0	0
1E20	0	0	0	0	0	0	0	0	0	0	0	0	0	0	0	0	0	0	0	0	0	0	0	0	0
1E20	0	0	0	0	0	0	0	0	0	0	0	0	0	0	0	0	0	0	0	0	0	0	0	0	0
1E20	0	0	0	0	0	0	0	0	0	0	0	0	0	0	0	0	0	0	0	0	0	0	0	0	0
1E20	0	0	0	0	0	0	0	0	0	0	0	0	0	0	0	0	0	0	0	0	0	0	0	0	0
1E20	0	0	0	0	0	0	0	0	0	0	0	0	0	0	0	0	0	0	0	0	0	0	0	0	0
1E20	0	0	0	0	0	0	0	0	0	0	0	0	0	0	0	0	0	0	0	0	0	0	0	0	0
1E20	0	0	0	0	0	0	0	0	0	0	0	0	0	0	0	0	0	0	0	0	0	0	0	0	0
1E20	0	0	0	0	0	0	0	0	0	0	0	0	0	0	0	0	0	0	0	0	0	0	0	0	0
1E20	0	0	0	0	0	0	0	0	0	0	0	0	0	0	0	0	0	0	0	0	0	0	0	0	0
1E20	0	0	0	0	0	0	0	0	0	0	0	0	0	0	0	0	0	0	0	0	0	0	0	0	0
1E20	0	0	0	0	0	0	0	0	0	0	0	0	0	0	0	0	0	0	0	0	0	0	0	0	0
1E20	0	0	0	0	0	0	0	0	0	0	0	0	0	0	0	0	0	0	0	0	0	0	0	0	0
1E20	0	0	0	0	0	0	0	0	0	0	0	0	0	0	0	0	0	0	0	0	0	0	0	0	0
1E20	0	0	0	0	0	0	0	0	0	0	0	0	0	0	0	0	0	0	0	0	0	0	0	0	0
1E20	0	0	0	0	0	0	0	0	0	0	0	0	0	0	0	0	0	0	0	0	0	0	0	0	0
1E20	0	0	0	0	0	0	0	0	0	0	0	0	0	0	0	0	0	0	0	0	0	0	0	0	0

Table 11 (cont'd).

Recharge/discharge values (+ recharge, - discharge) (mm/yr).

0	0	0	0	0	0	0	0	0	0	0	0	0	0	0	0	0	0	0	0	0	0	0	0	0
0	0	0	0	0	0	0	0	0	0	0	0	0	0	0	0	0	0	0	0	0	-.5	-.5	-.5	0
0	0	0	0	0	0	0	0	-.5	-.5	0	0	0	0	0	0	0	0	0	0	0	-.5	-.5	-.5	0
0	0	0	0	0	0	0	0	0	0	-.5	-.5	0	0	0	0	0	0	0	0	-.5	-.5	-.5	-.5	0
0	0	0	0	0	0	0	0	0	0	0	-.5	-.5	-.5	0	0	0	0	0	0	-.5	-.5	-.5	0	0
0	0	0	0	0	0	0	0	0	0	0	-.5	-.5	-.5	-.5	0	0	0	0	0	-.5	-.5	-.5	0	0
0	0	0	0	0	0	0	0	0	0	0	0	0	0	0	-.5	0	0	0	0	-.5	-.5	-.5	1.0	0
0	0	0	0	0	0	0	0	0	0	0	0	0	0	0	0	-.5	-.5	-.5	-.5	-.5	-.5	1.0	1.0	0
0	0	0	0	0	0	0	0	0	0	0	0	0	0	0	-.5	-.5	0	0	-.5	-.5	1.0	1.0	1.0	0
0	0	0	0	0	0	0	0	0	0	0	0	0	0	-.5	-.5	-.5	-.5	0	0	0	1.0	1.0	1.0	0
0	0	0	0	0	0	0	0	0	0	0	0	0	0	0	0	0	0	-.5	0	0	1.0	1.0	1.0	0
0	0	0	0	0	0	0	0	0	0	0	0	0	0	0	0	0	0	0	1.0	1.0	1.0	1.0	1.0	0
0	0	0	0	0	0	0	0	0	0	0	0	0	0	0	0	0	0	0	0	0	0	1.0	1.0	0
0	0	0	0	0	0	0	0	0	0	0	0	0	0	0	0	0	0	0	0	0	0	0	0	0
0	0	0	0	0	0	0	0	0	0	0	0	0	0	0	0	0	0	0	0	0	0	0	0	0
0	0	0	0	0	0	0	0	0	0	0	0	0	0	0	0	0	0	0	0	0	0	0	0	0
0	0	0	0	0	0	0	0	0	0	0	0	0	0	0	0	0	0	0	0	0	0	0	0	0
0	0	0	0	0	0	0	0	0	0	0	0	0	0	0	0	0	0	0	0	0	0	0	0	0
0	0	0	0	0	0	0	0	0	0	0	0	0	0	0	0	0	0	0	0	0	0	0	0	0

LIST OF REFERENCES

LIST OF REFERENCES

Ackerman, D. J., 1977, Ground-water basic data for Morton County, North Dakota: North Dakota Geological Survey Bulletin 72--Part II, 592 p.

---, 1980, Ground water resources of Morton County, North Dakota: North Dakota Geological Survey Bulletin 72--Part III, 51 p.

Anna, L. O., 1980, Ground water data for Billings, Golden Valley, and Slope counties, North Dakota: North Dakota Geological Survey Bulletin 76--Part II, 241 p.

---, 1981, Ground-water resources of Billings, Golden Valley, and Slope counties, North Dakota: North Dakota Geological Survey Bulletin 76--Part III, 56 p.

---, 1986, Structural influences on Cretaceous sedimentation, Northern Great Plains, *in* Peterson, J. A., ed., Paleotectonics and sedimentation in the Rocky Mountain region, United States: American Association of Petroleum Geologists Memoir 41, p. 173-191.

Armstrong, C. A., 1978, Ground-water resources of Emmons County, North Dakota: North Dakota Geological Survey Bulletin 66--Part III, 43 p.

Arnason, B., 1981, Ice and snow hydrology, *in* Gat, J. R., and Gonfiantini, R., eds., Stable isotope hydrology: Deuterium and Oxygen-18 in the water cycle: Vienna, International Atomic Energy Agency Technical Report Series No. 210, p. 143-176.

Bentley, H. W., Phillips, F. M., and Davis, S. N., 1986, Chlorine-36 in the terrestrial environment, *in* Fritz, P., and Fontes, J. C., eds., Handbook of environmental isotope geochemistry: New York, Elsevier, v. 2, p. 427-480.

Bickley, W. B., Jr., 1972, Stratigraphy and history of the Sakakawea Sequence, south-central North Dakota [Ph.D. Dissertation]: University of North Dakota, Grand Forks, 183 p.

Bluemle, J. P., 1984, Geology of Emmons County, North Dakota: North Dakota Geological Survey Bulletin 66--Part I, 69 p.

---, 1988, Generalized bedrock geologic map of North Dakota: North Dakota Geological Survey Miscellaneous Map 28.

Boulton, G. S., and Dobbie, K. E., 1993, Consolidation of sediments by glaciers: relations between sediment geotechnics, soft-bed glacier dynamics and subglacial ground-water flow: Journal of Glaciology, v. 39, p. 26-44.

Bredehoeft, J. D., Neuzil, C. E., and Milly, P. C. D., 1983, Regional flow in the Dakota Aquifer: A study of the role of confining layers: U.S. Geological Survey Water-Supply Paper 2237, 45 p.

Butler, R. D., 1984, Hydrogeology of the Dakota Aquifer System, Williston Basin, North Dakota, *in* Jorgensen, D. G., and Signor, D. C., eds., Proceedings of the Geohydrology Dakota Aquifer Symposium: Worthington, OH, The National Water Well Association, p. 14-23.

Carlson, C. G., 1982, Geology of Grant and Sioux Counties, North Dakota: North Dakota Geological Survey Bulletin 67--Part I, 32 p.

---, 1983, Geology of Morton County, North Dakota: North Dakota Geological Survey Bulletin 72--Part I, 37 p.

Clayton, L., 1969, Preliminary geologic map of Dunn County, North Dakota: North Dakota Geological Survey Miscellaneous Map 11.

Clayton, L., and Moran, S. R., 1982, Chronology of Late Wisconsinan glaciation in middle North America: Quaternary Science Reviews, v. 1, p. 55-82.

Craig, H., 1961, Isotopic variations in meteoric waters: Science, v. 133, p. 1702-1703.

Croft, M. C., and Wesolowski, E. A., 1970, Transmissivity and storage coeffi cient of aquifers in the Fox Hills Sandstone and the Hell Creek Formation, Mercer`and Oliver counties, North Dakota: U.S. Geological Survey Professional Paper 700-B; p. 190-195.

Croft, M. G., 1970, Ground-water basic data, Mercer and Oliver counties, North Dakota: North Dakota Geological Survey Bulletin 56--Part II, 268 p.

---, 1973, Ground-water resources of Mercer and Oliver counties, North Dakota: North Dakota Geological Survey Bulletin 56--Part III, 81 p.

---, 1974, Ground-water basic data for Adams and Bowman counties, North Dakota: North Dakota Geological Survey Bulletin 65--Part II, 294 p.

---, 1985a, Ground-water data for McKenzie County, North Dakota: North Dakota Geological Survey Bulletin 80--Part II, 455 p.

---, 1985b, Ground-water resources of McKenzie County, North Dakota: North Dakota Geological Survey Bulletin 80--Part III, 57 p.

Dansgaard, W., 1964, Stable isotopes in precipitation: Tellus, v. 16, p. 436-468.

Dansgaard, W., and Tauber, H., 1969, Glacier Oxygen-18 content and Pleistocene ocean temperatures: Science, v. 166, p. 499-502.

Davis, S. N., and Bentley, H. W., 1982, Dating groundwater: a short review, *in* Currie, L. A., ed., Nuclear and chemical dating techniques: American Chemical Society, p. 187-222.

Downey, J. S., 1986, Geohydrology of bedrock aquifers in the Northern Great Plains in parts of Montana, North Dakota, South Dakota, and Wyoming: U.S. Geological Survey Professional Paper 1402-E, 87 p.

Drever, J. I., 1982, Geochemistry of natural waters: Englewood Cliffs, New Jersey, Prentice-Hall, 388 p.

Filley, T. H., 1985, The hydrogeological response to continental glaciation [MS Thesis]: The Pennsylvania State University, 209 p.

Filley, T. H., and Parizek, R. R., 1983, Dynamics of groundwater flow associated with a continental glacier: Geological Society of America Abstracts with Programs, v. 15, p. 572.

Fontes, J. C., 1980, Environmental isotopes in groundwater hydrology, *in* Fritz, P., and Fontes, J. C., eds., Handbook of environmental isotope geochemistry: New York, Elsevier, v. 1, p. 75-140.

---, 1981, Palaeowaters, *in* Gat, J. R., and Gonfiantini, R., eds., Stable isotope hydrology: Deuterium and Oxygen-18 in the water cycle: Vienna, International Atomic Energy Agency Technical Report Series No. 210, p. 273-302.

Forman, S. L., Bettis III, E. A., Kemmis, T. J., and Miller, B. B., 1992, Chronologic evidence for multiple periods of loess deposition during the Late Pleistocene in the Missouri and Mississippi River Valley, United States: Implications for the activity of the Laurentide Ice Sheet: Palaeogeography, Palaeoclimatology, Palaeoecology, v. 93, p. 71-83.

Gat, J. R., 1981, Groundwater, *in* Gat, J. R., and Gonfiantini, R., eds., Stable isotope hydrology: Deuterium and Oxygen-18 in the water cycle: Vienna, International Atomic Energy Agency Technical Report Series No. 210, p. 223-240.

Gerhard, L. C., and Anderson, S. B., 1988, Geology of the Williston basin (United States portion), *in* Sloss, L. L., ed., Sedimentary cover--North American craton; U.S: Boulder, Colorado, Geological Society of America, v. D-2, p. 221-241.

Gerhard, L. C., Anderson, S. B., LeFever, J. A., and Carlson, C. G., 1982, Geological development, origin, and energy mineral resources of Williston basin, North Dakota: American Association of Petroleum Geologists Bulletin, v. 66, p. 989-1020.

Gilkeson, R. H., Perry, E. C., Jr., and Cartwright, K., 1981, Isotopic and geologic studies to identify the sources of sulfate in groundwater containing high barium concentrations: Urbana-Champaign, University of Illinois, Water Resources Center, 39 p.

Groenewold, G. H., Cherry, J. A., Meyer, G. N., Hemish, L. A., Rehm, B. W., and Winczewski, L. M., 1979, Geology and geohydrology of the Knife River basin and adjacent areas of west-central North Dakota: North Dakota Geological Survey Report of Investigation 64, 402 p.

Hamilton, T. M., 1970, Groundwater flow in part of the Little Missouri River basin, North Dakota [Ph.D. Dissertation]: University of North Dakota, Grand Forks, ND, 179 p.

Hoffman, P. F., 1989, Precambrian geology and tectonic history of North America, *in* Bally, A. W., and Palmer, A. R., eds., The Geology of North America--An overview: Boulder, Colorado, Geological Society of America, v. A, p. 447-512.

Howells, L., 1982, Geohydrology of the Standing Rock Indian Reservation, North and South Dakota: U.S. Geological Survey, Hydrologic Investigations Atlas HA-644.

Hwang, W. J., 1982, Deuterium as a tracer in the groundwater study of a central North Dakota mining area [MS Thesis]: North Dakota State University, Fargo, 70 p.

Hyde, W. T., Crowley, T. J., Kim, K. Y., and North, G. R., 1989, Comparison of GCM and energy balance model simulations of seasonal temperature changes over the past 18,000 years: Journal of Climate, v. 2, p. 864-887.

IAEA, 1983, Stable isotopes of hydrogen and oxygen, *in* Isotope techniques in the hydrogeological assessment of potential sites for the disposal of high-level radioactive waste: Vienna, International Atomic Energy Agency Technical Report Series No. 228, p. 44-57.

Johnson, W. H., and Follmer, L. R., 1989, Source and origin of Roxana Silt and middle Wisconsinan midcontinent glacial activity: Quaternary Research, v. 31, p. 319-331.

Jouzel, J. J., Merlivat, L., and Lorius, C., 1982, Deuterium excess in an East Antarctic ice core suggests higher relative humidity at the oceanic surface during the last glacial maximum: Nature, v. 299, p. 688-691.

Kamb, B., 1987, Glacier surge mechanism based on linked cavity configuration of the basal water conduit system: Journal of Geophysical Research, v. 92, p. 9083-9100.

Kearl, P. M., Korte, N. E., and Cronk, T. A., 1992, Suggested modifications to ground water sampling procedures based on observations from the colloidal borescope: Ground Water Monitoring Review, v. 12, no. 2, p. 155-161.

Kinzelbach, W., 1986, Groundwater modelling: Amsterdam, Elsevier, 333 p.

Klausing, R. L., 1979a, Ground-water basic data for Dunn County, North Dakota: North Dakota Geological Survey Bulletin 68--Part II, 501 p.

---, 1979b, Ground-water resources of Dunn County, North Dakota: North Dakota Geological Bulletin 68--Part III, 48 p.

Lawson, D. E., 1993, Glaciohydrologic and glaciohydraulic effects on runoff and sediment yield in glacierized basins: U.S. Army Corps of Engineers Cold Regions Research & Engineering Laboratory, Monograph 93-2, 108 p.

LeFever, R. D., Thompson, S. C., and Anderson, D. B., 1987, Earliest Paleozoic history of the Williston basin in North Dakota, *in* Carlson, C. G., and Christopher, J. E., eds., Fifth International Williston Basin Symposium: Regina, Saskatchewan, Saskatchewan Geological Society, p. 22-36.

Lobmeyer, D. H., 1985, Freshwater heads and ground-water temperatures in aquifers of the Northern Great Plains in parts of Montana, North Dakota, South Dakota, and Wyoming: U.S. Geological Survey Professional Paper 1402-D, 11 p.

Mathews, W. H., 1974, Surface profiles of the Laurentide ice sheet in its marginal areas: Journal of Glaciology, v. 13, p. 37-43.

Maughan, E. K., and Perry, J., WJ, 1986, Lineaments and their tectonic implications in the Rocky Mountains and adjacent Plains region, *in* Peterson, J. A., ed., Paleotectonics and sedimentation in the Rocky Mountain Region, United States: Tulsa, Oklahoma, American Association of Petroleum Geologists Memoir 41, p. 41-53.

McGinnis, L. D., 1968, Glaciation as a possible cause of mineral deposition: Economic Geology, v. 63, p. 390-400.

Merlivat, L., and Jouzel, J., 1979, Global climatic interpretation of the Deuterium-Oxygen 18 relationship for precipitation: Journal of Geophysical Research, v. 84, p. 5029-5033.

Mooers, H. D., 1990, Ice-marginal thrusting of drift and bedrock: thermal regime, subglacial aquifers, and glacial surges: Canadian Journal of Earth Science, v. 27, p. 849-862.

Moran, S. R., Arndt, M., Bluemle, J. P., Camara, M., Clayton, L., Fenton, M. M., Harris, K. L., Hobbs, H. C., Keatinge, R., Sackreiter, D. K., Salomon, N. L., and Teller, J., 1976, Quaternary stratigraphy and history of North Dakota, southern Manitoba, and northwestern Minnesota, *in* Mahaney, W.

C., ed., Quaternary stratigraphy of North America: Stroudsburg, PA, Dowden, Hutchinson & Ross, Inc., p. 133-158.

Moser, H., and Stichler, W., 1980, Environmental isotopes in ice and snow, *in* Fritz, P., and Fontes, J. C., eds., Handbook of environmental isotope geochemistry: New York, Elsevier, v. 1, p. 141-178.

Panichi, C., and Gonfiantini, R., 1981, Geothermal waters, *in* Gat, J. R., and Gonfiantini, R., eds., Stable isotope hydrology: Deuterium and Oxygen-18 in the water cycle: Vienna, International Atomic Energy Agency Technical Report Series No. 210, p. 241-272.

Patch, J. C., and Knell, G. W., 1988, The Hydrogeology of the New Rockford Aquifer System in Wells County, North Dakota: North Dakota State Water Commission Ground-Water Studies 95, 178 p.

Paterson, W. S. B., 1981, The physics of glaciers [2nd ed.]: Elmsford, NY, Pergamon Press Inc., 380 p.

Peter, K. D., 1984, Hydrochemistry of Lower Cretaceous sandstone aquifers, Northern Great Plains, *in* Jorgensen, D. G., and Signor, D. C., eds., Proceedings of the Geohydrology Dakota Aquifer Symposium: Worthington, OH, The National Water Well Association, p. 163-174.

Randich, P. G., 1975, Ground-water basic data for Grant and Sioux Counties, North Dakota: North Dakota Geological Survey Bulletin 67--Part II, 303 p.

---, 1979, Ground-water resources of Grant and Sioux Counties, North Dakota: North Dakota Geological Survey Bulletin 67--Part III, 49 p.

Robin, M. J. L., and Gillham, R. W., 1987, Field evaluation of well purging procedures: Ground Water Monitoring Review, v. 7, no. 4, p. 85-93.

Ruhe, R. V., 1983, Depositional environment of Late Wisconsin loess in the midcontinental United States, *in* Porter, S. C., ed., Late-Quaternary environments of the United States. I. The Pleistocene: Minneapolis, Univ. Minnesota Press, p. 130-137.

Shreve, R. L., 1972, Movement of water in glaciers: Journal of Glaciology, v. 11, p. 205-214.

Shurr, G. W., 1979, Lineament control of sedimentary facies in the Northern Great Plains, United States, *in* Podwysocki, M. H., and Earle, J. L., eds., Proceedings of the Second International Conference on Basement Tectonics: Denver, Colorado, Basement Tectonics Committee, Inc., p. 361-370.

Siegel, D. I., 1983, Geochemical evidence for glaciation of the driftless area, southern Wisconsin: Geological Society of America Abstracts with Programs, v. 15, p. 687.

---, 1991, Evidence for dilution of deep, confined ground water by vertical recharge of isotopically heavy Pleistocene water: Geology, v. 19, p. 433-436.

Sloss, L. L., 1963, Sequences in the cratonic interior of North America: Geological Society of America Bulletin, v. 74, p. 93-113.

Thomas, G. E., 1974, Lineament-block tectonics: Williston Blood Creek basin: American Association of Petroleum Geologists Bulletin, v. 58, p. 1305-1322.

---, 1979, Lineament-block tectonics: North American Cordilleran Orogen, *in* Podwysocki, M. H., and Earle, J. L., eds., Proceedings of the Second nternational Conference on Basement Tectonics: Denver, Colorado, Basement Tectonics Committee, Inc., p. 361-370.

Thorstenson, D. C., Fisher, D. W., and Croft, M. G., 1979, The geochemistry of the Fox Hills-basal Hell Creek aquifer in southwestern North Dakota and northwestern South Dakota: Water Resources Research, v. 15, p. 1479-1498.

Trapp, H. J., 1971, Ground-water basic data, Hettinger and Stark Counties, North Dakota: North Dakota State Water Commission County Ground Water Studies 16 -- Part II, 455 p.

Yurtsever, Y., and Gat, J. R., 1981, Atmospheric waters, *in* Gat, J. R., and Gonfiantini, R., eds., Stable isotope hydrology: Deuterium and Oxygen-18 in the water cycle: Vienna, International Atomic Energy Agency Technical Report Series No. 210, p. 103-176.

Zaporozec, A., 1972, Graphical interpretation of water quality data: Ground Water, v. 10, p. 32-43.

MICHIGAN STATE UNIV. LIBRARIES
31293010463457